Topics in Advanced Geoinformatics
Volume 1

Zhenfeng Shao

URBAN REMOTE SENSING

高等教育出版社
HIGHER EDUCATION PRESS

World Scientific

Downloaded from www.worldscientific.com
by fac sciences de la terre universite annaba on 07/30/24. Re-use and distribution is strictly not permitted, except for Open Access articles.

Downloaded from www.worldscientific.com
by fac sciences de la terre universite annaba on 07/30/24. Re-use and distribution is strictly not permitted, except for Open Access articles.

URBAN REMOTE SENSING

TOPICS IN ADVANCED GEOINFORMATICS

Series Editors: Jianya Gong *(Wuhan University, China)*
Huayi Wu *(Wuhan University, China)*

This book series aims to comprehensively cover the theory, methodology and applications of geospatial information science (GIScience), which mainly includes advanced topics on geographic information system (GIS), remote sensing (RS), and global navigation satellite system (GNSS).

The books in this series will include monographs and graduate level textbooks aimed at young researchers and postgraduates specialising in remote sensing, surveying and mapping, geography, urban planning and environmental science, global climate change and related majors.

Published

Vol. 1 *Urban Remote Sensing*
by Zhenfeng Shao (*Wuhan University, China*)

Downloaded from www.worldscientific.com
by fac sciences de la terre universite annaba on 07/30/24. Re-use and distribution is strictly not permitted, except for Open Access articles.

Topics in Advanced Geoinformatics
Volume 1

URBAN REMOTE SENSING

Zhenfeng Shao
Wuhan University, China

高等教育出版社
HIGHER EDUCATION PRESS

World Scientific

Downloaded from www.worldscientific.com
by fac sciences de la terre universite annaba on 07/30/24. Re-use and distribution is strictly not permitted, except for Open Access articles.

Published by

Higher Education Press Limited Company
4 Dewai Dajie, Xicheng District
Beijing 100120, P. R. China

and

World Scientific Publishing Co. Pte. Ltd.

5 Toh Tuck Link, Singapore 596224

USA office: 27 Warren Street, Suite 401-402, Hackensack, NJ 07601

UK office: 57 Shelton Street, Covent Garden, London WC2H 9HE

Library of Congress Cataloging-in-Publication Data
Names: Shao, Zhenfeng, 1976– author.
Title: Urban remote sensing / Zhenfeng Shao, Wuhan University, China.
Description: New Jersey : World Scientific, [2023] | Series: Topics in advanced geoinformatics ; vol. 1 | Includes bibliographical references and index.
Identifiers: LCCN 2022040628 | ISBN 9789811266164 (hardcover) | ISBN 9789811266171 (ebook) | ISBN 9789811266188 (ebook other)
Subjects: LCSH: City planning--Remote sensing. | Land use, Urban--Remote sensing. | Landsat satellites. | Urban geography--Remote sensing.
Classification: LCC HT166 S4623 2023 | DDC 511/.5--dc25/eng/20220914
LC record available at https://lccn.loc.gov/2022040628

British Library Cataloguing-in-Publication Data
A catalogue record for this book is available from the British Library.

B&R Book Program

Copyright © 2023 by Higher Education Press Limited Company and
World Scientific Publishing Co. Pte. Ltd.

All rights reserved. This book, or parts thereof, may not be reproduced in any form or by any means, electronic or mechanical, including photocopying, recording or any information storage and retrieval system now known or to be invented, without written permission from the publishers.

For photocopying of material in this volume, please pay a copying fee through the Copyright Clearance Center, Inc., 222 Rosewood Drive, Danvers, MA 01923, USA. In this case permission to photocopy is not required from the publishers.

For any available supplementary material, please visit
https://www.worldscientific.com/worldscibooks/10.1142/13137#t=suppl

Desk Editors: Balasubramanian Shanmugam/Steven Patt

Typeset by Stallion Press
Email: enquiries@stallionpress.com

Printed in P. R. China

Downloaded from www.worldscientific.com
by fac sciences de la terre universite annaba on 07/30/24. Re-use and distribution is strictly not permitted, except for Open Access articles.

Downloaded from www.worldscientific.com
by fac sciences de la terre universite annaba on 07/30/24. Re-use and distribution is strictly not permitted, except for Open Access articles.

Preface

According to the *World Urbanization Prospects* by United Nations, about 68% of the global population will live in urban areas by 2050. Cities have become the hot spots of production, consumption and waste generation. However, continued urbanization brings many global problems related to waste disposal and air and water pollution. Therefore, it is critical to understand the natural environments of urban areas to improve and foster environmental and human sustainability of cities around the world.

Taking cities as observing objects, urban remote sensing is an important branch of remote sensing. Under the context of global urbanization, urban remote sensing technology has been playing a significant role in urban monitoring, planning, construction and urban management. To meet the growing demand for urban remote sensing observation, we detail advanced remote sensing technologies and methodologies for complicated urban areas in this book, consisting of ten chapters that describe the principles of urban remote sensing and multi-source remote sensing big data acquisition, urban remote sensing image processing methods, urban remote sensing image-specific application in related industries and the prospect of urban remote sensing development. To facilitate readers' understanding, we use a large number of algorithm studies as intuitive materials and provide typical industry solutions or case studies in specific applied research areas. The main contents are as follows:

Chapter 1 introduces an urban spatio-temporal-spectral-angular observation model that applies multi-platform, multi-sensor collaborative observation from space, sky and ground to acquire abundant 3D spatial data. The data obtained by different remote sensing observation platforms serve as a complementary data source.

Chapter 2 describes big data characteristics of urban remote sensing, including urban scene visible light remote sensing images, multi-spectral remote sensing images, hyperspectral remote sensing images, thermal

infrared images, microwave remote sensing images, LiDAR data and luminous remote sensing images, providing a decision-making basis for data selection of specific urban remote sensing applications in subsequent chapters.

Chapter 3 focuses on tasks, objects and mechanisms of urban remote sensing interpretation and interpretation methods by taking visual interpretation, semi-automatic interpretation, full-automatic interpretation and big data interpretation as examples.

Chapter 4 presents selected mainstream methods of cloud detection and shadow detection of urban remote sensing images, mainstream methods of tone adjustment of urban remote sensing images, mainstream methods of super-resolution reconstruction of urban remote sensing images and mainstream methods of image fusion.

Chapter 5 introduces the classification and information extraction methods for urban remote sensing imagery from seven perspectives that include the classification and information extraction demands, unsupervised classification methods, supervised classification methods, new classification methods, urban road extraction, urban buildings extraction and urban lakes extraction.

Chapter 6 describes urban 3D reconstruction methods based on multi-source high-resolution remote sensing imagery.

Chapter 7 presents the change detection methods and applications of urban remote sensing. Change detection is an important means of recognizing and analyzing the changes of targets from different time periods. By comparing remote sensing images from two different phases, the change detection methods own notable advantages in urban land cover change monitoring, urbanization dynamic monitoring, environmental change dynamic monitoring, natural disaster monitoring and crop yield estimation.

Chapter 8 introduces the demands of dynamic urban monitoring, the urban dynamic monitoring process, the urban dynamic monitoring methods and the remote sensing monitoring of urban geological hazards, planning, conditions and geological hazards, providing a comprehensive understanding of remote sensing monitoring.

Chapter 9 focuses on the remote sensing monitoring technologies and practices of the urban ecological environment. This chapter contains three topics: (i) remote sensing monitoring of urban thermal environment, (ii) remote sensing inversion of urban aboveground biomass and (iii) remote sensing quantitative monitoring of cyanobacteria in urban lakes.

Downloaded from www.worldscientific.com
by fac sciences de la terre universite annaba on 07/30/24. Re-use and distribution is strictly not permitted, except for Open Access articles.

Chapter 10 summarizes and envisions the developing directions of urban remote sensing technologies and applications.

This book can serve as a textbook for undergraduate and graduate students and as a reference book for anyone interested in urban remote sensing.

Downloaded from www.worldscientific.com
by fac sciences de la terre universite annaba on 07/30/24. Re-use and distribution is strictly not permitted, except for Open Access articles.

This page intentionally left blank

Downloaded from www.worldscientific.com
by fac sciences de la terre universite annaba on 07/30/24. Re-use and distribution is strictly not permitted, except for Open Access articles.

Downloaded from www.worldscientific.com
by fac sciences de la terre universite annaba on 07/30/24. Re-use and distribution is strictly not permitted, except for Open Access articles.

About the Author

Zhenfeng Shao is a professor at the State Key Laboratory of Information Engineering in Surveying, Mapping and Remote Sensing (LIESMARS) of Wuhan University since 2009, and as an assistant director of LIESMARS and director of the Department of Geo-spatial Information System and Service. He received the PhD degree in photogrammetry and remote sensing at Wuhan University, China. His research interests include high-resolution image processing, pattern recognition and urban remote sensing applications. Since 2019, he has served as an Associate Editor of the journal *Photogrammetric Engineering and Remote Sensing* specializing in smart cities, photogrammetry and change detection. He has authored or co-authored over 100 peer-reviewed articles in international journals. He was the recipient of the Talbert Abrams Award for the Best Paper in image matching from the American Society for Photogrammetry and Remote Sensing in 2014 and the New Century Excellent Talents in University from the Ministry of Education of China in 2012.

This page intentionally left blank

Downloaded from www.worldscientific.com
by fac sciences de la terre universite annaba on 07/30/24. Re-use and distribution is strictly not permitted, except for Open Access articles.

Downloaded from www.worldscientific.com
by fac sciences de la terre universite annaba on 07/30/24. Re-use and distribution is strictly not permitted, except for Open Access articles.

Contents

Preface v

About the Author ix

Chapter 1 Urban Spatio-Temporal-Spectral-Angular Observation Model 1

1.1 Urban Remote Sensing Observation Demand ····· 2
1.1.1 The observation objects of urban remote sensing ····· 3
1.1.2 The demand for urban application services for remote sensing platform····· 7
1.1.3 The demand for sensor diversity in urban remote sensing ····· 11
1.1.4 Remote sensing platform for various urban applications ····· 13
1.2 Multi-platform Multi-sensor Collaborative Network Observation Mode of Space-Air-Ground for Urban Service Demand ····· 15
1.3 Theoretical Model of Urban Spatio-Temporal-Spectral-Angular Observation ····· 18
1.4 Urban Remote Sensing Observation Services····· 21
Questions····· 24
References ····· 24

Chapter 2 Big Data Characteristics of Urban Remote Sensing 27

2.1 Multi-source Heterogeneous Remote Sensing Big Data with Long Time Series ····· 28
2.1.1 Urban satellite imagery····· 28
2.1.2 Urban aerial imagery····· 32
2.1.3 Urban UAV imagery ····· 32
2.1.4 Urban mobile mapping system····· 34

2.1.5 Urban crowdsourcing images ····· 36
2.2 Data Characteristics of Urban Visible Panchromatic Remote Sensing Imagery ····· 37
2.2.1 Image characteristics of urban houses ····· 38
2.2.2 Image characteristics of urban roads ····· 38
2.2.3 Image characteristics of urban green space ····· 39
2.2.4 Image characteristics of urban water bodies ····· 40
2.3 Data Characteristics of Urban Multi-spectral Remote Sensing Images ····· 41
2.3.1 Data characteristics of urban green space ····· 42
2.3.2 Data characteristics of urban water bodies ····· 43
2.4 Data Characteristics of Urban Hyperspectral Imagery ····· 44
2.5 Data Characteristics of Urban Thermal Infrared Images ····· 48
2.6 Data Characteristics of Urban Microwave Remote Sensing Images ····· 49
2.7 Data Characteristics of Urban LiDAR Data ····· 51
2.8 Data Characteristics of Urban Nighttime Light Remote Sensing Imagery ····· 53
2.9 Data Characteristics of Urban Crowdsourcing Images ····· 54
Questions ····· 54
References ····· 55

Chapter 3 Principles and Methods of Urban Remote Sensing Image Interpretation 57
3.1 The Task of Urban Remote Sensing Imagery Interpretation ·· 57
3.2 The Objects of Urban Remote Sensing Imagery Interpretation ····· 59
3.2.1 Image spatial interpretation ····· 59
3.2.2 Interpretation of spectrum space ····· 61
3.2.3 Interpretation of feature space ····· 61
3.3 The Mechanism of Urban Remote Sensing Imagery Interpretation ····· 62
3.3.1 Direct interpretation signs ····· 64
3.3.2 Indirect interpretation signs ····· 69
3.4 Methods of Urban Remote Sensing Imagery Interpretation ·· 71
3.4.1 Visual interpretation ····· 71
3.4.2 Semi-automatic interpretation ····· 73
3.4.3 Automatic interpretation based on machine learning ·· 75

Downloaded from www.worldscientific.com
by fac sciences de la terre universite annaba on 07/30/24. Re-use and distribution is strictly not permitted, except for Open Access articles.

3.4.4 Automatic interpretation based on deep learning ····· 76
3.4.5 Interpretation of remote sensing big data ····· 80
Questions ····· 81
References ····· 81

Chapter 4 Preprocessing Methods of Urban Remote Sensing Imagery 83
4.1 Cloud Detection Methods for Urban Remote Sensing Imagery ····· 84
4.2 Shadow Detection Methods for Urban Remote Sensing Imagery ····· 87
4.3 Image Enhancement Methods for Urban Remote Sensing Imagery ····· 91
4.4 Super-Resolution Reconstruction Methods for Urban Remote Sensing Imagery ····· 94
4.5 Fusion Demands of Urban Remote Sensing Imagery ····· 98
4.5.1 Spatial-spectral fusion methods ····· 99
4.5.2 Spatio-temporal fusion methods ····· 103
Questions ····· 104
References ····· 105

Chapter 5 Classification and Information Extraction Methods for Urban Remote Sensing Imagery 107
5.1 Classification and Information Extraction Demands for Urban Remote Sensing Imagery ····· 107
5.2 Unsupervised Classification Methods for Urban Remote Sensing Imagery ····· 110
5.3 Supervised Classification Methods for Urban Remote Sensing Imagery ····· 113
5.4 New Classification Methods for Urban Remote Sensing Imagery ····· 114
5.5 Urban Road Extraction Methods Based on Remote Sensing Imagery ····· 119
5.5.1 Automatic extraction method of urban roads ····· 120
5.5.2 Road extraction method based on deep learning models ····· 122
5.6 Urban Building Extraction Methods Based on Remote Sensing Imagery ····· 123

Downloaded from www.worldscientific.com
by fac sciences de la terre universite annaba on 07/30/24. Re-use and distribution is strictly not permitted, except for Open Access articles.

5.7 Urban Lake Extraction Methods Based on Remote Sensing Imagery ····· 124
Questions ····· 127
References ····· 127

Chapter 6 Urban 3D Reconstruction Methods Based on Multi-source High-Resolution Remote Sensing Imagery 129
6.1 Urban 3D Reconstruction Demands ····· 130
6.2 Urban 3D Reconstruction Based on Stereo-Pair Image ····· 133
6.3 3D Reconstruction Based on Onboard LiDAR ····· 135
6.4 3D Reconstruction Based on Mobile Mapping Systems ····· 136
6.5 3D Reconstruction of Urban Ancient Buildings Based on Ground LiDAR ····· 137
6.6 Texture Reconstruction of Urban 3D Model ····· 140
6.7 Urban 3D Reconstruction Based on Street View Data ····· 141
6.8 3D Modeling Technology Based on Integrated Aerial-Ground Panoramic Imagery from Indoor and Outdoor ····· 142
6.9 Quality Control Strategy for 3D Reconstruction of the Urban Scene ····· 145
6.10 3D Reconstruction Management Platform of the Urban Scene ····· 146
6.11 The Planning and Construction Practice of Real-Scene 3D in China ····· 148
Questions ····· 150
References ····· 150

Chapter 7 Change Detection Methods and Applications of Urban Remote Sensing 153
7.1 Change Detection Demands of Urban Remote Sensing ····· 153
7.1.1 Urban construction monitoring demands ····· 154
7.1.2 Urban management monitoring needs ····· 156
7.2 Change Detection Process of Urban Remote Sensing ····· 156
7.3 Change Detection Methods of Urban Remote Sensing ····· 158
7.3.1 2D change detection methods ····· 158
7.3.2 3D change detection methods ····· 169
7.4 Change Detection Practice of Urban Remote Sensing ····· 171
7.4.1 Urban land cover/use change detection methods ····· 172

Downloaded from www.worldscientific.com
by fac sciences de la terre universite annaba on 07/30/24. Re-use and distribution is strictly not permitted, except for Open Access articles.

7.4.2 Urban impervious surface change detection methods 172
7.4.3 Urban cultivated land change detection methods 175
Questions 177
References 177

Chapter 8 Dynamic Monitoring Methods and Applications through Urban Remote Sensing 179
8.1 Demands of Dynamic Urban Monitoring 179
8.2 Urban Dynamic Monitoring Process 181
8.3 Urban Dynamic Monitoring Methods 182
8.3.1 Urban dynamic monitoring based on time series remote sensing imagery 183
8.3.2 Urban dynamic monitoring based on the integration of earth observation sensor network 184
8.4 Remote Sensing Monitoring Applications of Urban Natural Resources 185
8.4.1 Remote sensing monitoring of urban lake changes 186
8.4.2 Remote sensing monitoring of urban impervious surface 188
8.4.3 Remote sensing monitoring of urban cultivated land 190
8.5 Remote Sensing Monitoring of Urban Planning 191
8.6 Remote Sensing Monitoring of Urban Conditions 194
8.6.1 Difficulties of remote sensing monitoring of urban situations 194
8.6.2 Urban area extraction method based on progressive learning models 195
8.7 Remote Sensing Monitoring of Urban Geological Hazards 197
Questions 199
References 199

Chapter 9 Remote Sensing Monitoring Technology and Practice of Urban Ecological Environment 201
9.1 Remote Sensing Monitoring Demands of Urban Ecological Environment 202

Downloaded from www.worldscientific.com
by fac sciences de la terre universite annaba on 07/30/24. Re-use and distribution is strictly not permitted, except for Open Access articles.

9.1.1 The concept of urban heat island and the remote sensing monitoring demands of the urban thermal environment 202
9.1.2 Application demands for remote sensing inversion of urban aboveground biomass 204
9.2 Remote Sensing Monitoring Methods and Practice of Urban Heat Island Effect 207
9.3 Remote Sensing Inversion and Application of Urban Aboveground Biomass 211
9.4 Innovative Models and Methods in Remote Sensing Quantitative Monitoring of Cyanobacteria from Urban Lakes with Eutrophication 215
Questions 218
References 218

Chapter 10 Prospects of Urban Remote Sensing Technologies and Applications 221
10.1 The Developing Directions of Urban Remote Sensing Sensors 221
10.2 New Application Fields of Urban Remote Sensing 222
10.3 The Future Directions of Urban Remote Sensing 233
Questions 235
References 236

Index 237

Downloaded from www.worldscientific.com
by fac sciences de la terre universite annaba on 07/30/24. Re-use and distribution is strictly not permitted, except for Open Access articles.

Downloaded from www.worldscientific.com
by fac sciences de la terre universite annaba on 07/30/24. Re-use and distribution is strictly not permitted, except for Open Access articles.

Chapter 1

Urban Spatio-Temporal-Spectral-Angular Observation Model

Taking a city as a study entity, urban remote sensing has played an important role in urban planning, construction and management. Scholars have applied remote sensing sciences and technologies to support urban scenes and to solve a series of problems in urban development and management. Remote sensing techniques have been widely used to describe and monitor the urban environment from various aspects that include patterns, elements, functions and evolutions. Such techniques provide essential situation awareness for urban environmental assessment, planning, simulation and prediction. The applications of remote sensing images include classifying urban land cover and land use, extracting urban information and discovering urban changing dynamics. It has transformed from a pure sensing technique to a service that promotes high-quality human activities.

However, the urban scene is a highly heterogeneous scene, and ground objects in urban settings are rich in types, densely distributed and seriously fragmented according to a high-resolution remote sensing image of urban scenes (as shown in Figure 1.1). And due to the occlusion of high-rise buildings and trees, the information of urban ground objects is seriously missing. Besides, under the influence of both human activities and natural processes, urban land cover changes rapidly and the change trajectory is complex. Therefore, urban remote sensing is faced with the following problems:

1. How to construct an effective remote sensing observation model for urban complex scenes?

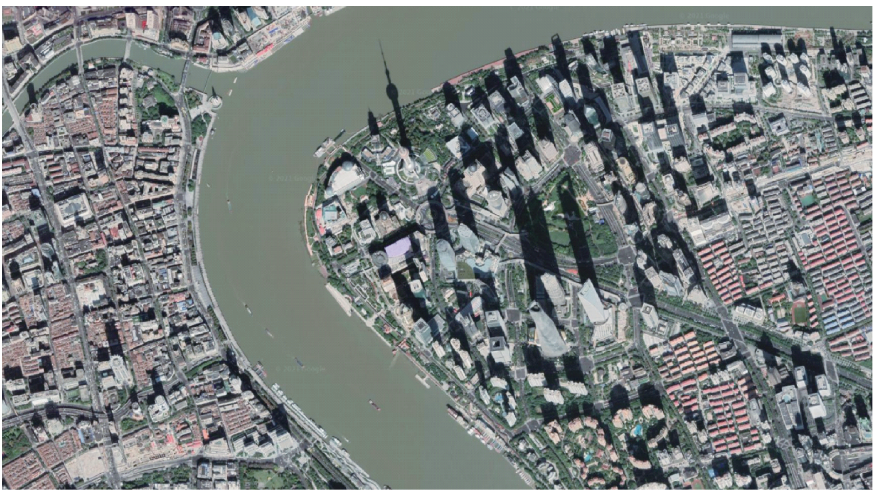

Figure 1.1 A high spatial resolution Google Earth remote sensing image of Shanghai.

2. How to improve the level of automatic extraction of shaded city information?
3. How to extract the rapidly changing information of a city (including time-sensitive targets)?

This chapter first introduces the requirements of urban remote sensing from four aspects: observation objects, application services, sensors and remote sensing platforms. Then this chapter analyzes the multi-platform multi-sensor collaborative network observation mode of space-air-ground for urban service demand and constructs the urban spatio-temporal-spectral-angular observation model. Finally, the main content of urban remote sensing is briefly introduced.

1.1 Urban Remote Sensing Observation Demand

This section introduces mainly observation objects, demand-oriented urban remote sensing observation platform and sensors. Compared with other thematic remote sensing techniques, the diversity of urban remote sensing observation objects brings difficulties to urban remote sensing observation. Therefore, we first briefly introduce observation objects of urban remote sensing. Remote sensing platforms refer to the carrier of sensors, e.g., ground

Downloaded from www.worldscientific.com
by fac sciences de la terre universite annaba on 07/30/24. Re-use and distribution is strictly not permitted, except for Open Access articles.

Downloaded from www.worldscientific.com
by fac sciences de la terre universite annaba on 07/30/24. Re-use and distribution is strictly not permitted, except for Open Access articles.

motion measurement systems, stratospheric airships, detection balloons, unmanned air vehicles, satellites and spacecraft, for monitoring purposes. Here, we introduce two main types of sensors in urban remote sensing, namely, active sensors and passive sensors. Passive sensors measure emissions produced by constituents of objects, such as multi-spectral scanners and thermal infrared scanners. In comparison, active sensors measure signals transmitted by the sensor that were reflected, refracted or scattered by objects, such as Radar, LiDAR and Sonar. The types of sensors and platforms determine the characteristics of remote sensing image. Given the requirements on resolution, data type, time and budget of urban remote sensing data, users are expected to determine the most suitable image type.

1.1.1 The observation objects of urban remote sensing

The objects in urban remote sensing observation are generally characterized by multi-dimension, multi-scale and multi-mode. For multi-dimension, horizontal and vertical observations are both required in urban remote sensing observations (Shao *et al.*, 2021b). For example, the land cover classification might require only horizontal observation (Guan *et al.*, 2017), but energy demand estimation, aiding positioning and other similar applications demand vertical observation (Biljecki *et al.*, 2015). Beyond that, when exploring the effect of urban structure on urban biophysical processes, horizontal and vertical observations are both required (Zhu *et al.*, 2019). For multi-scale, objects in urban remote sensing observation can be divided into three scales, point, line and plane, among which the image feature points belong to the point scale (Shao *et al.*, 2015), roads are line objects (Zhai *et al.*, 2015) and impervious surfaces are plane objects (Shao *et al.*, 2016). For multi-mode, the observed objects can be divided into two modes, static and time-sensitive objects, among which buildings belong to static targets (Shao *et al.*, 2020) and vehicles belong to time-sensitive objects. Moreover, due to the rapid urbanization process, urban land cover and land use are interchanging in a dynamic manner, especially in developing countries (e.g., China and India (Zhang *et al.*, 2017)). In fact, dynamic land cover and land use in urban fabrics also belong to time-sensitive objects. To sum up, urban remote sensing observation mainly includes the following five aspects.

Downloaded from www.worldscientific.com
by fac sciences de la terre universite annaba on 07/30/24. Re-use and distribution is strictly not permitted, except for Open Access articles.

1.1.1.1 Observation of urban land cover and land use

Land cover and land use are the most important observation objects of urban remote sensing. Land cover and land use classifications are of great significance to global climate warming (Zhou *et al*., 2021), urban ecological environment (Firozjaei *et al*., 2021) and urban sprawl (Gong *et al*., 2019), to list a few. Figure 1.2 shows the typical land cover and land use types including buildings, roads, parking lots, water bodies, vegetation and bare soils in the urban scene. Urban land cover and land use can be very complex with detailed classes of different materials, such as concrete, asphalt, various types of vegetation, base soil and various types of water surfaces. Generally, the selected classification scheme depends on the requirements of the applications and the resolution of remote sensing data. Therefore, accurate urban land cover and land use classification remains to be a challenging task.

Figure 1.2 Typical land cover and land use types in urban.

1.1.1.2 Observe city information at different heights from multi-angles in three-dimensional space

In terms of space, horizontal and vertical observations should be carried out simultaneously in urban remote sensing observation. In horizontal

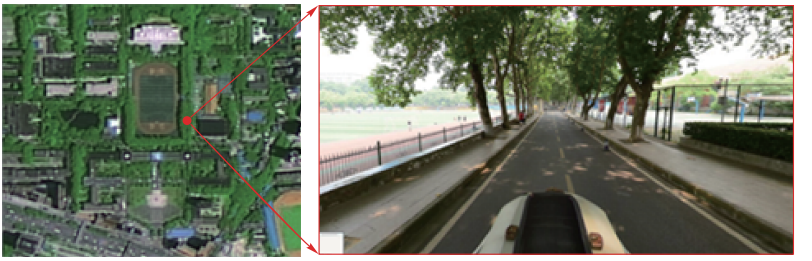

Figure 1.3 Cooperative data acquisition of air-ground remote sensing platform.

space, there are abundant types of ground objects and compact elements. In terms of three-dimensional (3D) space observation, due to the occlusion of high-rise buildings and vegetation in urban space dimension, multi-platform, multi-sensor and multi-angle collaborative observations should be carried out at the same time to effectively obtain the data of urban targets of different heights. Figure 1.3 shows the process of cooperative data acquisition of an air-ground remote sensing platform. Its purpose is to make up for the information loss caused by vegetation occlusion in aerial remote sensing images by using a vehicle remote sensing platform. In addition a large number of shadows in high-resolution images affect the subsequent applications. Observing at different heights from multi-angles in three-dimensional space is also an effective way to solve this problem.

1.1.1.3 Monitoring the change information of urban land use and land cover on time scale

Urban land expansion is one of the most obvious, irreversible and rapid types of land cover and land use change in contemporary human history, and it is the key driving factor of many cross-scale environmental and social changes. Monitoring the status of land cover and land use can provide data support for urban planners, analyze the driving force of urbanization and its interaction and coupling effect with the urban ecological environment. Figure 1.4 shows the remote sensing images of Shiqiao Town and Guangzhou city, Guangdong province, in 1976 and 1995, respectively. Shiqiao Town was still an agricultural town in 1976, but in 1995, after 20 years of development, it became a part of the modern metropolis, and a large amount of farmland was turned into construction land. Therefore, the change information of urban land use and land cover on a time scale is also an important object of urban remote sensing observations.

Downloaded from www.worldscientific.com
by fac sciences de la terre universite annaba on 07/30/24. Re-use and distribution is strictly not permitted, except for Open Access articles.

Figure 1.4 Remote sensing images of Shiqiao Town, Guangzhou in 1976 (a) and 1995 (b).

1.1.1.4 Remote sensing detection and tracking observation of time-sensitive targets in cities

The sustainable development of cities is to realize the harmony between cities and human beings. Therefore, human and vehicle behavior monitoring to maintain the safety of urban traffic and the health of residents is also an important purpose of urban remote sensing. Figure 1.5 shows the remote sensing image of an airport taken by Jilin-1 satellite. As can be seen from this figure, it is possible to see time-sensitive objects such as planes and cars in remote sensing images as long as the resolution is high enough. It is

Figure 1.5 Remote sensing image of an airport taken by Jilin-1 satellite.

Downloaded from www.worldscientific.com
by fac sciences de la terre universite annaba on 07/30/24. Re-use and distribution is strictly not permitted, except for Open Access articles.

worth noting that for such observation objects, urban remote sensing needs to consider the temporal resolution of the images used.

1.1.1.5 Observation of social and economic activities

Cities are the most frequent places of human activity. The proportion of the world's population living in cities has risen from 5% in 1900 to 55% in 2018 (Maktav *et al.*, 2005; Hoole *et al.*, 2019). The United Nations (UN) *World Urbanization Prospects* estimated that more than two-thirds of the world population (close to 7 billion) would live in cities by 2050 (Ritchie *et al.*, 2018). Human activities will affect urban environment, ecology and land cover. Therefore, urban remote sensing should not only observe the natural land cover but also observe the social and economic activities of human beings. For example, in 2019, COVID-19 wreaked havoc around the world, posing a grave threat to human life and security. Controlling the size of crowds is the most effective means of epidemic prevention and control. Figure 1.6 shows an example of crowd monitoring using an unmanned aerial vehicle (UAV) during the period of COVID-19 prevention and control.

Figure 1.6 Monitoring crowds using unmanned aerial vehicle (UAV) during the period of COVID-19 prevention and control.

1.1.2 The demand for urban application services for remote sensing platform

Under the context of global urbanization, remote sensing technology can play a significant role in urban monitoring, planning and supervision given

Downloaded from www.worldscientific.com
by fac sciences de la terre universite annaba on 07/30/24. Re-use and distribution is strictly not permitted, except for Open Access articles.

Downloaded from www.worldscientific.com
by fac sciences de la terre universite annaba on 07/30/24. Re-use and distribution is strictly not permitted, except for Open Access articles.

its short revisiting cycle, low cost and high effectiveness. According to different needs, we can choose appropriate remote sensing platforms and the corresponding sensors. The following is a brief introduction of example applications of urban remote sensing platforms.

Water pollution is a widely acknowledged urban environmental problem. Conventional monitoring methods usually fail to meet the requirements of timely and large-scale monitoring and evaluation of water quality. In comparison, remote sensing monitoring can help authorities promptly respond to water quality changes in a timely manner. Long-term and dynamic remote sensing observation can provide essential knowledge on changing dynamics of water quality, benefiting the formation of specific plans to control water pollution. Numerous efforts have been made to leverage satellite images, aiming to monitor water pollution in urban water environment. Remote sensing models of water pollution prediction can be established, facilitating the effective monitoring of the status of urban water pollution. Figure 1.7 shows an example of water quality monitoring based on the Beijing-2 satellite remote sensing observations. In this figure, the region circled in red is the black smelly water.

With the rapid expansion of cities, urban land cover and land use, such as illegal construction, private construction and disorderly construction,

Figure 1.7 Water quality monitoring of city based on Beijing-2 satellite. The region circled in red is the black smelly water.

change rapidly and the change trajectory is complex under the influence of both human activities and natural processes. The change can be identified through the differences from bi-temporal images that cover the same area. Figures 1.8 and 1.9 show the GF-2 images of Wuhan in 2019 and 2020, respectively, and we can find that land cover has obviously changed. Detecting these changes can benefit the understanding of the changing process of the earth's surface and provide scientific data reference for land planning, government management and ecological-environmental protection. The traditional change detection methods are not efficient, usually with time lags, and consume a large amount of manpower and resources. With the continuous progress of earth observation technology, more and more high-resolution (HR) and very high-resolution (VHR) optical sensors have been designed and put into operation (such as QuickBird, WorldView-3, GF-2, ZY, Pleiades). These sensors with improved spatial resolution have greatly enriched the available data sources for change detection. Compared with medium-resolution and low-resolution images, HR/ VHR images contain more detailed information regarding the texture, shape, structure and neighborhood relationship of ground objects and are one of the ideal data sources for change monitoring. Compared with the traditional manual verification method, the change detection based on remote sensing images is less time- and labor-consuming and error-prone.

Figure 1.8 GF-2 image of Wuhan on October 29, 2019.
Source: China Land Observation Satellite Data Center.

Downloaded from www.worldscientific.com
by fac sciences de la terre universite annaba on 07/30/24. Re-use and distribution is strictly not permitted, except for Open Access articles.

Figure 1.9 GF-2 image of Wuhan on January 31, 2020.
Source: China Land Observation Satellite Data Center.

Global climate change and the rapid urbanization process can lead to an increased occurrence of urban floods, which are responsible for great economic and human losses in China. In view of this situation, various sensors have been adopted to obtain urban surface information, aiming to provide data support for urban flood simulation. The applications of remote sensing technology in flood simulation mainly include the following:

1. providing meteorological and hydrological knowledge from remote sensing observations, including quantitative rainfall prediction, soil water inversion and information regarding the evapotranspiration inversion;
2. providing detailed surface information, such as 3D construction (Figure 1.10), land use and land cover, digital rivers and basins, as well as hydrologic and hydraulic parameters extracted from the above information.

For coastal cities, remote sensing platforms, e.g., ship-borne monitoring platforms, can also provide essential support. Numerous sea-based or river-based remote sensing platforms have been established in cities along the coastline and in large inland cities. For example, the Hengqin New District of Zhuhai City in China has established a remote sensing platform of island electronic purse seine on the sea. Through infrared detection, radar monitoring, UAV inspection, vehicle inspection, satellite

Downloaded from www.worldscientific.com
by fac sciences de la terre universite annaba on 07/30/24. Re-use and distribution is strictly not permitted, except for Open Access articles.

Figure 1.10 The integrated 3D point cloud that combines the UAV point cloud and the mobile mapping system point cloud.

positioning, automatic ship identification system and other technologies, an all-weather monitoring framework has been established in Hengqin and its surrounding areas, featuring all-time visibility and comprehensive information acquisition.

1.1.3 The demand for sensor diversity in urban remote sensing

Urban scenes are complex, with various types of shelters and fragile environments that are susceptible to natural and sudden man-made disasters, which demand innovative monitoring techniques. The refined management of cities requires high spatial resolution remote sensing images. There are some satellites that can collect such data, e.g., GF-2, Beijing-2, GF-1, ZY-3, WorldView Series, GeoEye-1, QuickBird, IKONOS, Pleiades and SPOT 6, 7.

Urban land uses are rather diverse with complex materials within urban environments. Urban production can also lead to water pollution, which requires timely monitoring by various multi-spectral and hyperspectral remote sensing platforms, such as AIS, AVRIS, WIS, PROBE, TEEMS, MODIS, Hyperion, FTHSIAHI, SEBASS satellite, Australian Hymap, ARIES, TIPS satellites, Canadian CAS satellites, German ROSIS satellites, French IMS satellites, Finnish AISA satellites, ESA CHRIS satellites, Japanese

Downloaded from www.worldscientific.com
by fac sciences de la terre universite annaba on 07/30/24. Re-use and distribution is strictly not permitted, except for Open Access articles.

Downloaded from www.worldscientific.com
by fac sciences de la terre universite annaba on 07/30/24. Re-use and distribution is strictly not permitted, except for Open Access articles.

GLI satellites and Chinese MAIS, PHI, OMIS-1, CMODIS and Env-DD satellites, to list a few. Many cities have complex geological conditions. Urban subsidence, e.g., has been a widely noted issue that needs to be monitored and addressed. Large-scale land subsidence monitoring generally uses GPS measuring methods and InSAR monitoring methods. As for urban land covers, urban gardens are different from forests and grasslands as the contradictions between people and land are usually fragmented, and it is difficult to distinguish them from shadows and water bodies. For urban heat, the increase of impervious surfaces in cities leads to the emergence of the urban heat island effect that requires thermal infrared sensors, such as NOAA/AVHRR sensors, MODIS and Landsat TM6 sensors, to list a few. Laser scanners can be used for geological surveys, architectural design, cultural relic restoration and volume measurement. SAR sensors that include Synthetic Aperture Radar (EOS-SAR) of the Earth Observation System (EOS), SIR-C/X-SAR of NASA, Advanced Synthetic Aperture Radar (ASAR) of ESA and the HJ-1C satellite of China that can benefit disaster monitoring, environmental monitoring, surveying, as well as other monitoring applications.

The measurement of electromagnetic energy in remote sensing technology is realized by sensors mounted on a stationary or moving remote sensing platform. In order to adapt to different applications, different types of sensors have been developed. Sensors are devices that measure and record electromagnetic energy, which can be divided into passive sensors, active sensors and complex sensor systems that integrate active and passive sensors. Passive sensors rely on external energy sources, while active sensors have their own energy source.

1. *Passive sensors*: sensors that rely on an external source of energy, usually the sun and sometimes the Earth itself. Current passive sensors cover the electromagnetic spectrum in the wavelength range from less than 1 pm to more than 1 m (microwave).
2. *Active sensors*: sensors with their own energy source. Since active sensors are not dependent on lighting conditions, their measurements are subject to control requirements. Active sensor types include Radar, LiDAR and Sonar, all of which can be used for altitude measurement and imaging.
3. *Active and passive integrated sensor systems*: an integrated system that incorporates active sensors and passive sensors. Typical examples are

the multi-spectral LiDAR sensor system and hyperspectral LiDAR sensor system that simultaneously acquires three-dimensional spatial information and extracts multi-/hyperspectral information from ground features.

1.1.4 Remote sensing platform for various urban applications

1.1.4.1 Urban space remote sensing platform

A space remote sensing platform mainly refers to an artificial satellite, space shuttle and space station. The monitoring of sensors needs to know the orbit para-meters of satellites. In order to introduce the application of remote sensing, the following are related knowledge of orbital parameters:

1. *Orbital altitude*: the orbital altitude is defined as the distance from the satellite to the surface of the area, usually in kilometers. Usually, remote sensing satellites fly 150 km to 36,000 km above the ground. Flight altitude affects the range and detail of the ground and also affects the spatial resolution of the satellite.
2. *Orbital inclination*: the angle between the plane of flight of the satellite and the equatorial plane. The inclination of the satellite's orbit, the field of view of the sensor and the altitude to the ground can be observed.
3. *Orbital period*: the time required to complete a complete flight.
4. *Repeat flight cycle*: the time difference between two successive passes through the same place, usually recorded in days.
5. Satellite sensors need to send remote sensing image data to the ground for analysis and processing. The obtained high-resolution panchromatic images and imaging spectrometer data will be able to provide services for the rapid update of urban spatial data. The multi-band and multi-polarization radar data will be able to solve the all-weather and all-time earth observation in rainy and foggy conditions.

Here are several satellite remote sensing platforms commonly used in urban applications, including QuikBird and WorldView satellites of the United States, Sentinel-2 satellite of ESA, SPOT satellite of France and ZY-3 satellite of the China high-resolution earth observation system.

Downloaded from www.worldscientific.com by fac sciences de la terre universite annaba on 07/30/24. Re-use and distribution is strictly not permitted, except for Open Access articles.

Downloaded from www.worldscientific.com
by fac sciences de la terre universite annaba on 07/30/24. Re-use and distribution is strictly not permitted, except for Open Access articles.

1.1.4.2 Urban aerial remote sensing platform

The realization of the aerial remote sensing platform has several types of aircraft according to the operation requirements. The altitude and flight attitude of the aircraft have an impact on the scale and the acquired images. The flight attitude of an aircraft is affected by the wind, and its relative flight orbit can be expressed by three different rotation angles, namely, the lateral inclination angle, the heading inclination angle and the photo rotation angle. The airborne satellite positioning system and navigation system can measure the azimuth and three rotation angles of the aircraft at regular intervals to correct the geometric deformation of the remote sensing data caused by the altitude and azimuth errors of the aircraft.

In aerial photogrammetry, images are recorded on hard-copy materials or with digital cameras. For digital sensors, such as multi-spectral scanners, the acquired data can be stored on tape and other mass storage devices or directly transmitted to the receiving station. The aerial remote sensing platform mainly includes a manned aerial remote sensing platform and an unmanned aerial vehicle (UAV) platform. The manned aerial remote sensing platform can integrate the remote sensing mission payload, airborne satellite communication system, operation management system, high-precision stable platform, position and attitude measurement system, and other equipment to form an advanced Earth observation system and realize powerful aerial remote sensing information acquisition, data comprehensive processing and management functions. At present, although oil-powered and electric fixed-wing aircraft have been used in large-scale aerial survey, the professional mapping UAV is limited in the actual project application because of its high price. With the development of UAV and computer vision technology in recent years, a variety of small and portable UAVs have begun to enter the field of surveying, mapping and remote sensing, and their application scope is wider, with obvious advantages.

1.1.4.3 Urban ground remote sensing platform

The ground mobile remote sensing platform mainly includes a mobile measurement system serving for measurable image data acquisition, a road detection system serving for urban intelligent transportation and various remote sensing monitoring platforms serving for urban pollution monitoring with tower-mounted sensors.

Downloaded from www.worldscientific.com
by fac sciences de la terre universite annaba on 07/30/24. Re-use and distribution is strictly not permitted, except for Open Access articles.

The mobile road measurement platform is a typical representative of ground remote sensing platform. The mobile road measurement platform generally is equipped with GNSS (Global Navigation Satellite System), CCD (imaging system), INS/ DR (inertial navigation system or dead reckoning system) and other sensors and equipment on the motor vehicle to quickly collect the digital measurable image (DMI) of the road and the ground objects on both sides when the vehicle is moving at high speed. These DMIs have the function of photogrammetry analysis. The required exterior orientation position elements and attitude elements, with precise time parameters, under the support of strict photogrammetric calibration parameters, realize the formation of stereo image pairs by DMIs in any space and time series, realize the seamless fusion of multi-level measurement and database, and any on-demand measurement at any time.

1.2 Multi-platform Multi-sensor Collaborative Network Observation Mode of Space-Air-Ground for Urban Service Demand

According to the above descriptions regarding observation objects, demand-oriented urban remote sensing observation platforms and sensors, urban remote sensing needs to thoroughly consider information from three dimensions: temporal dimension, spatial dimension and spectral dimension. Ideally, urban remote sensing observation requires data with a high temporal resolution, high spatial resolution and high spectral resolution. To the best of our knowledge, however, no satellite owns all the above characteristics. Thus, it is necessary to coordinate data from existing remote sensing satellites to meet the needs of urban observation.

Observations captured by a single remote sensing platform have some limitations, especially for collecting and updating 3D spatial data. Observations taken from a single angle can only obtain the effective data covering the local area, resulting in data insufficiency. Although aerial photogrammetry and remote sensing platforms can provide the spatial information and texture features of the target, they only obtain the building surface information and omit a large amount of geometric and texture data of the building facades. In addition, occlusion widely occurs in dense

urban areas. In comparison, the ground photogrammetry platform is able to obtain the facade information of the building, and the vehicle mobile measurement platform can provide 3D scene descriptions. However, data from vehicle mobile measurement platforms contain a lot of noise, leading to difficulty in extracting the shape information and topological relationship. In addition, mobile vehicles usually fail to collect data in narrow areas. The data obtained by different remote sensing observation platforms can serve as a complementary data source. Thus, abundant data can be collected using multi remote sensing platform cooperative observations.

As shown in Figure 1.11, the cooperative observation of the UAV platform and ground mobile measurement vehicle acquisition platform can mitigate the problems of a lack of mobile measurement vehicle acquisition data due to road obstruction and UAV imaging information due to occlusion issues in complex urban environments (Shao *et al.*, 2021a). Through collaborative observation and information complementation, the integration of urban 3D seamless holographic spatio-temporal data and aerial-ground collaborative observation is realized.

Figure 1.12 shows the data collected by the cooperative observation platform of UAV and vehicle-mounted mobile measurement vehicle from the Department of Information Science, Wuhan University. Due to the occlusion of trees, the UAV cannot obtain the ground information under the leaves,

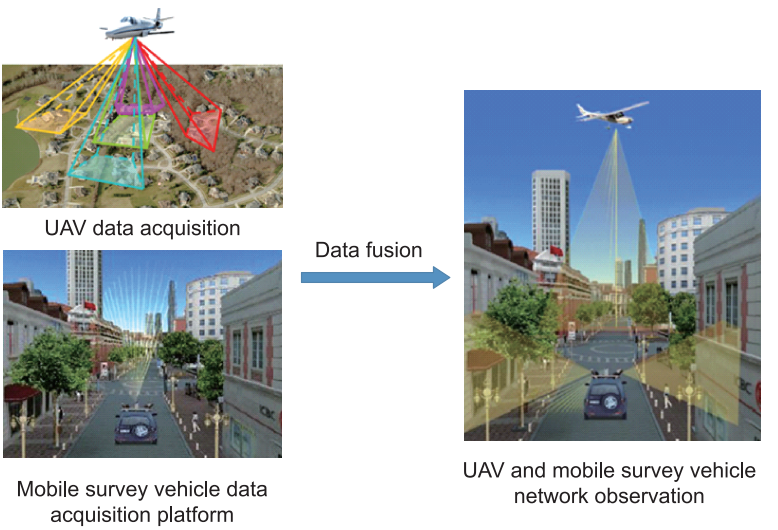

Figure 1.11 Example of cooperative observation between UAV platform and ground mobile survey vehicle acquisition platform.

Downloaded from www.worldscientific.com by fac sciences de la terre universite annaba on 07/30/24. Re-use and distribution is strictly not permitted, except for Open Access articles.

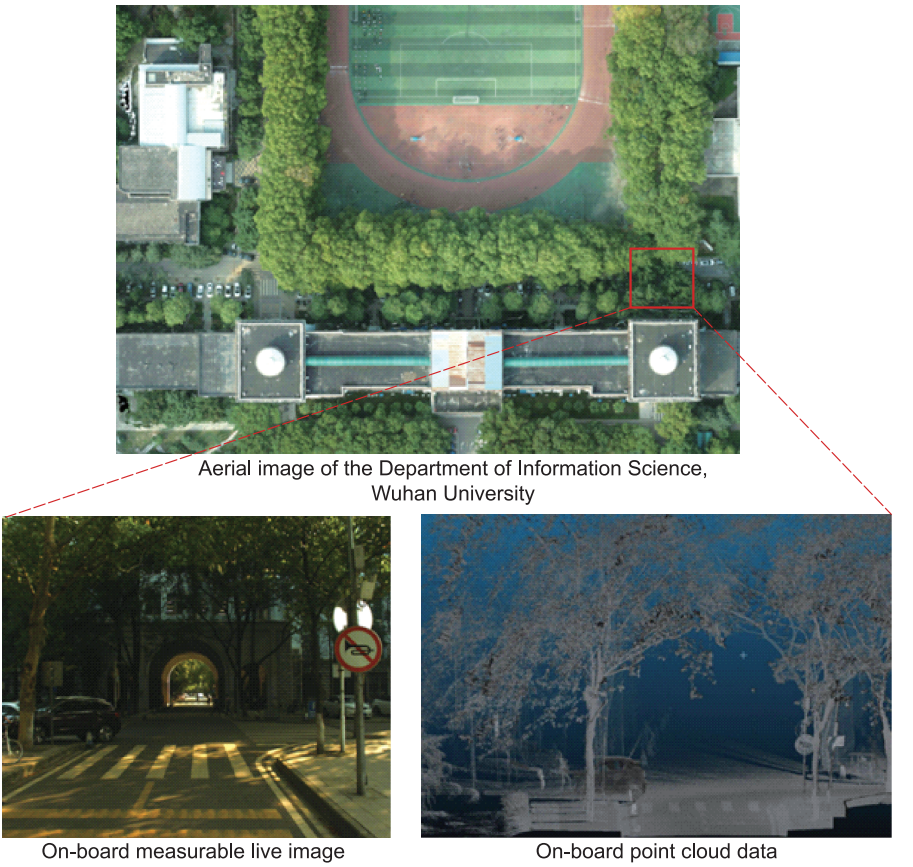

Figure 1.12 Data collected by the cooperative observation platform of UAV and mobile measurement vehicle.

resulting in data insufficiency. The mobile survey vehicle can obtain the elevation information of the ground, including elevation image and 3D point cloud data, complementing data collected from UAV platforms.

Hengqin New District of Zhuhai City, a coastal city in China, has built a multi-platform collaborative intelligent urban monitoring system based on big video data. According to different video acquisition platforms and data characteristics, corresponding technologies are established, as shown in Figure 1.13.

1. *Acquisition and processing of space-based satellite video data*: according to the characteristics of observation angle time change of video satellite data, a fast preprocessing and classification technology of space-based video

Downloaded from www.worldscientific.com by fac sciences de la terre universite annaba on 07/30/24. Re-use and distribution is strictly not permitted, except for Open Access articles.

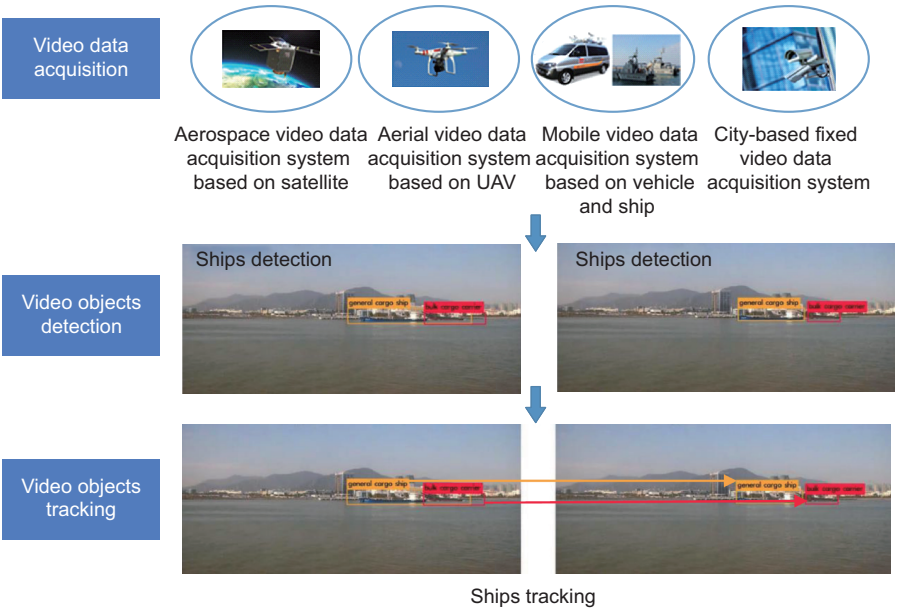

Figure 1.13 Urban video big data spatio-temporal intelligent system based on multi-platform cooperation.

is established, aiming to quickly process, analyze and apply space-based video data.

2. *Space-based UAV video acquisition and processing technology*: the efficient target extraction and processing technologies of UAV video data are realized, aiming to quickly identify and track targets (e.g., ships) and calculate the moving position of targets in a real-time manner.
3. *Ground fixed and mobile video acquisition and processing technology*: the system of automatic recognition and early warning of abnormal behavior based on ground monitoring video big data is established, aiming to realize the functions of intelligent spatio-temporal analysis of big video data.

1.3 Theoretical Model of Urban Spatio-Temporal-Spectral-Angular Observation

In remote sensing images, image spatial characteristics reflected by spectral differences play a very important role in information extraction, especially in high spatial resolution images. In practical applications, spatial resolution is

Downloaded from www.worldscientific.com by fac sciences de la terre universite annaba on 07/30/24. Re-use and distribution is strictly not permitted, except for Open Access articles.

Downloaded from www.worldscientific.com
by fac sciences de la terre universite annaba on 07/30/24. Re-use and distribution is strictly not permitted, except for Open Access articles.

usually the first feature to be considered. Commonly used spatial features include edge, shape, texture, height and semantic features, to list a few. Therefore, the set of empty features I_{spatial} can be expressed as follows:

$$I_{\text{spatial}} = \left\{h_{\text{edge}}, h_{\text{shape}}, h_{\text{texture}}, h_{\text{height}}, \ldots, h_{\text{semantic}}\right\} \tag{1.1}$$

where h_{edge}, h_{shape}, h_{texture}, h_{height} and h_{semantic} represent edge, shape, texture, height and semantics, respectively. Required spatial characteristics can be carefully selected according to the specific needs of urban remote sensing observations. It should be noted that mixing of pixel issues needs to be considered for images with coarse spatial resolution.

Spectral characteristics are also important features in remote sensing images, which can fully reflect the biochemical characteristics of the observation object. Different observation objects have different spectral responses, which is the physical basis of remote sensing observation. However, for images with fewer bands and lower spectral resolution, the phenomenon of same objects with different spectrum and different objects with same spectrum is more obvious. At this time, hyperspectral remote sensing is needed to alleviate this problem. Hyperspectral remote sensing can obtain continuous and fine spectral curves of ground objects within a certain range, which greatly improves the ability in Earth observations. At present, the commonly used spectral characteristics can be shown by the following formula:

$$I_{\text{spectral}} = \{h_{\text{bands}}, h_{\text{indexes}}, h_{\text{SD}}, h_{\text{SA}}, h_{\text{SID}}, \ldots, h_{\text{CC}}\} \tag{1.2}$$

where h_{bands} represents the spectral reflectance of ground features, and h_{indexes} represents the index characteristics obtained by calculation between bands, such as normalized vegetation index (NDVI) and normalized water index (NDWI). These two features are usually extracted from multi-spectral images. h_{SD}, h_{SA}, h_{SID} and h_{CC} represent spectral derivative, spectral angle, spectral information divergence and correlation coefficient of the hyperspectral image, respectively. Although hyperspectral images contain a large number of spectral features, there exists a strong correlation between the features, resulting in a large amount of information redundancy. In addition, the spatial resolution of hyperspectral remote sensing is generally low.

In urban remote sensing, similar to the observation tasks that need to detect the changing information of ground features, e.g., land use update and disaster assessment, certain requirements need to be met from a temporal perspective. In addition, for some targets with strong temporal

Downloaded from www.worldscientific.com
by fac sciences de la terre universite annaba on 07/30/24. Re-use and distribution is strictly not permitted, except for Open Access articles.

characteristics, many temporal characteristics that are helpful for target observation can be mined through multi-temporal observations. These characteristics can be shown by the following formula:

$$I_{\text{temporal}} = \left\{h_{\text{spatial}}(t_1, t_2, \ldots, t_n), h_{\text{spectral}}(t_1, t_2, \ldots, t_n), h_{\text{DTW}}, \ldots, h_{\text{statistics}}\right\} \tag{1.3}$$

where $h_{\text{spatial}}(t_1, t_2, \ldots, t_n)$ represents the spatial characteristics of different times, $h_{\text{spectral}}(t_1, t_2, \ldots, t_n)$ represents the spectral characteristics of different times, h_{DTW} represents the dynamic time warp distance (DTW) characteristics and $h_{\text{statistics}}$ represents the statistical characteristics such as the mean value and variance of the time series image.

In urban scenes, high-rise buildings and tall street trees can block the ground surface, posing challenges to accurately extract ground objects. Therefore, multi-angle remote sensing images should be considered. The angular features can be expressed by the following formula:

$$I_{\text{angular}} = \left\{h_{\text{spatial}}(ang_1, ang_2, \ldots, ang_n), h_{\text{spectral}}(ang_1, ang_2, \ldots, ang_n)\right\} \tag{1.4}$$

where $h_{\text{spatial}}(ang_1 ang_2, \ldots, ang_n)$ represents the spatial characteristics of different imaging angles and $h_{\text{spectral}}(ang_1 ang_2, \ldots, ang_n)$ represents the spectral characteristics of different imaging angles.

By comprehensively considering the characteristics of the four dimensions, i.e., space, spectrum, time and angular, we abstract the urban remote sensing process and propose an urban spatio-temporal-spectral-angular observation model. The inputs of the model are temporal, spatial, spectral and angular features. According to the output of the model, the model can be divided into two types: (i) data quality improvement model and (ii) information extraction model. The data quality improvement model refers to the fusion of different resolutions, different platforms and different types of multi-source data to obtain high-quality images with higher spatial, temporal and spectral resolution. This type of model can be modeled by the following formula:

$$I = O\left(I_1, I_2, I_3, \ldots, I_K\right) \tag{1.5}$$

where $I_1, I_2, I_3, \ldots, I_K$ is a multi-source image, O a fusion model and I the output of the model, that is, a higher-quality image.

Generally speaking, multi-source remote sensing images mainly contain four types of features, namely, spatial, spectral, temporal and angular features.

Downloaded from www.worldscientific.com
by fac sciences de la terre universite annaba on 07/30/24. Re-use and distribution is strictly not permitted, except for Open Access articles.

The fused high-quality image can be modeled via the following formula:

$$I = F\left(\left\{I_{i,\text{spatial}}\right\}_{i=1}^{K}\right) \oplus F\left(\left\{I_{i,\text{temporal}}\right\}_{i=1}^{K}\right) \oplus F\left(\left\{I_{i,\text{spectral}}\right\}_{i=1}^{K}\right) \oplus F\left(\left\{I_{i,\text{angular}}\right\}_{i=1}^{K}\right) \tag{1.6}$$

where $F(\cdot)$ is the fusion function of each image.

In addition, the spatio-temporal-spectral-angular observation model is able to extract information from the image according to different tasks. This task-specific observation model can be abstracted as follows:

$$Y = O\left(I_1, I_2, I_3, \ldots, I_K; T\right) \tag{1.7}$$

Similarly, under the constraints of the task T, features can be extracted from four aspects of spatial, spectral, temporal and angular, and useful information can be derived. This process can be expressed by the following formula:

$$Y = H\begin{pmatrix} F\left(\left\{I_{i,\text{spatial}}\right\}_{i=1}^{K}; T\right) \oplus F\left(\left\{I_{i,\text{temporal}}\right\}_{i=1}^{K}; T\right) & \oplus \\ F\left(\left\{I_{i,\text{spectral}}\right\}_{i=1}^{K}; T\right) \oplus F\left(\left\{I_{i,\text{angular}}\right\}_{i=1}^{K}; T\right) & \end{pmatrix} \tag{1.8}$$

where $H(\cdot)$ is the information extraction function.

Although remote sensing images contain a large number of spatial, spectral, temporal and angular features, not all features are required at the same time. We need to prioritize important features according to the purposes of the observation tasks. The proposed model, although in a conceptual stage, can largely benefit urban observation by providing a new data fusion paradigm and guide the selection of satellites for collaborative observation based on urban observation needs.

1.4 Urban Remote Sensing Observation Services

The applications of urban remote sensing cover a wide range of industries. In this session, we present applications of urban remote sensing technology, including urban natural resources, landscape, environmental protection and geological management.

Information extraction of typical urban elements: Typical urban elements mainly include roads, green spaces, buildings and lakes. Urbanization is

Downloaded from www.worldscientific.com
by fac sciences de la terre universite annaba on 07/30/24. Re-use and distribution is strictly not permitted, except for Open Access articles.

accompanied by increasingly prominent urban environmental problems. Remote sensing techniques largely facilitate the extraction of urban elements in a timely manner, benefiting the effective monitoring of urban fabrics (Shi *et al*., 2019; Sun *et al*., 2019).

Urban remote sensing image retrieval: Urban is a complex entity with intensive human activities. Remote sensing image retrieval technology can be applied to quickly and accurately identify areas and objects that need our attention.

Urban 3D reconstruction: The construction of the digital 3D model of urban environments is an important task of urban informatization. The three-dimensional modeling results can better reflect the three-dimensional landscape of cities from multiple angles, restore the urban landscape in a more intuitive manner and better serve urban planning policymaking.

Urban change detection: Remote sensing image change detection algorithms can be applied to monitor the dynamics of urban development and ecological environments, greatly assisting urban management. It is of great importance to investigate the interaction between humans and natural environments, as a better knowledge of human-environment dynamics largely benefits urban management decision-making.

Remote sensing monitoring of urban natural resources: The advantages of remote sensing technology include a wide observation range, a fast update speed and a strong data integration capability. The applications of digital technologies such as remote sensing image comparison and analysis, automatic extraction of pattern, planning management rules and others can promote urban planning supervision.

Remote sensing extraction and monitoring of urban impervious surfaces: Urban impervious surfaces include typical urban objects such as buildings, roads and parking lots. It is an important indicator that measures the level of urbanization and environmental quality and has been widely used in urban land use classification, urban population density assessment, urban planning, urban environmental assessment, heat island effect analysis and hydrological simulation studies.

Urban heat island remote sensing monitoring: The urban heat island effect caused by urbanization has a significant impact on the urban climate. Remotely sensed imagery is generally with extensive spatial coverage that benefits large-scale investigations. With the current development of high-resolution satellite thermal infrared remote sensing sensors, remote sensing observations play an important role in monitoring urban heat island effects.

Downloaded from www.worldscientific.com
by fac sciences de la terre universite annaba on 07/30/24. Re-use and distribution is strictly not permitted, except for Open Access articles.

Urban aboveground biomass monitoring: Remote sensing technology can quickly and accurately obtain information on the spatial distribution of urban green space, providing essential knowledge of the compositions, types and layouts of urban green landscapes. Carrying out remote sensing inversion of the aboveground biomass of urban vegetation is conducive to the rational use of land resources, promoting the integrity of the ecosystem.

Urban geological disaster monitoring: Geological disasters such as landslides, mudslides, rockslides, road subsidence and ground subsidence have posed great threats to the sustainable development of cities. Taking advantage of remote sensing technologies, we can carry out investigations on inducing factors, perform disaster interpretation and cataloging, early disaster identification, long-term monitoring and post-disaster assessment of hidden geological hazards, greatly supporting the assessment of susceptibility and risk of geological hazards and providing important situational awareness for disaster relief and disaster reduction decision-making.

Three-dimensional real-scene management: With the development of remote sensing technology, orthophotos and measurable real object images have become important digital products. The refined management of urban municipalities based on electronic maps is shifting to urban grid management and services based on remote sensing images. Taking advantage of urban management using remote sensing technology, we can apply real-life images to digital city management and promote the scientific and efficient participation of relevant departments and personnel in urban management and decision-making.

Monitoring urban air quality: Urban air quality is affected by various factors, such as the exhaust of vehicles, ships and airplanes, the emissions of industrial enterprises, residents' heating, garbage incineration and urban constructions. Remote sensing technology establishes a valuable venue where urban air quality can be monitored in a timely manner with extensive spatial coverage, providing essential knowledge that benefits the improvement of urban air quality and the development of sustainable cities.

Monitoring urban water environment: Remote sensing techniques have been widely adopted in monitoring urban water resources in terms of their spatial coverage and quality. Assisted by remote sensing images, we can quickly and accurately monitor the total amount of water resources, investigate urban wastewater pollution and identify pollution sources, scope and concentration in a real-time manner with extensive spatial coverage.

Questions

1. What are the challenges of airborne remote sensing platforms in urban observation?
2. What difficulties do urban remote sensing observation platforms encounter in various urban applications?
3. What observation requirements need to be considered for urban remote sensing data acquisition?
4. What are the examples of the time, space, spectrum and angle requirements of remote sensing images for specific applications in urban monitoring?
5. What are the major challenges and solutions of urban remote sensing?
6. What are the applications of urban remote sensing?

References

Biljecki F, Stoter J, Ledoux H, Zlatanova S, Çöltekin, A. 2015. Applications of 3D city models: State of the art review. *ISPRS International Journal of Geo-Information*, 4: 2842–2889.

Firozjaei M K, Kiavarz M, Homaee M, Arsanjani J J, Alavipanah S K. 2021. A novel method to quantify urban surface ecological poorness zone: A case study of several European cities. *Science of the Total Environment*, 757: 143755.

Gong P, Li X C, Zhang W. 2019. 40-year (1978–2017) human settlement changes in China reflected by impervious surfaces from satellite remote sensing. *Science Bulletin,* 64(11): 756–763.

Guan X H, Liao S, Bai J, Wang F, Li Z X, Wen Q, He J J, Chen T. 2017. Urban land-use classification by combining high-resolution optical and long-wave infrared images. *Geo-spatial Information Science*, 20: 299–308.

Hoole C, Hincks S, Rae A. 2019. The contours of a new urban world? Megacity population growth and density since 1975. *Town Planning Review*, 90(6): 653–678.

Maktav D, Erbek F S, Jürgens, C. 2005. Remote sensing of urban areas. *International Journal of Remote Sensing,* 26: 655–659.

Shao Z F, Chen M, Liu C. 2015. Feature matching for illumination variation images. *Journal of Electronic Imaging*, 24(3): 033011.

Shao Z F, Cheng G, Li D R, Huang X, Lu Z P, Liu J. 2021a. Spatio-temporal-spectral-angular observation model that integrates observations from UAV and mobile mapping vehicle for better urban mapping. *Geo-spatial Information Science*, 24(4): 615–629.

Shao Z F, Fu H Y, Fu P, Yin L. 2016. Mapping urban impervious surface by fusing optical and SAR data at the decision level. *Remote Sensing*, 8(11): 945.

Downloaded from www.worldscientific.com by fac sciences de la terre universite annaba on 07/30/24. Re-use and distribution is strictly not permitted, except for Open Access articles.

Shao Z F, Tang P H, Wang Z Y, Saleem N, Yam S, Sommai C. 2020. BRRNet: A fully convolutional neural network for automatic building extraction from high-resolution remote sensing images. *Remote Sensing*, 12(6): 1050.

Shao Z F, Wu W W, Li D R. 2021b. Spatio-temporal-spectral observation model for urban remote sensing. *Geo-spatial Information Science,* 24(3): 327–386.

Shi L F, Taubenbock H, Zhang Z X, Liu F, Michael W. 2019. Urbanization in China from the end of 1980s until 2010 — spatial dynamics and patterns of growth using EO-data. *International Journal of Digital Earth*, 12(1): 78–94.

Sun Z C, Xu R, Du W J, Wang L, Lu D S. 2019. High-resolution urban land mapping in China from Sentinel 1A/2 imagery based on google earth engine. *Remote Sensing*, 11(7): 752.

Zhai K, Wu X Q, Qin Y W, Du P P. 2015. Comparison of surface water extraction performances of different classic water indices using OLI and TM imageries in different situations. *Geo-spatial Information Science,* 18(1): 32–42.

Zhang L, Weng Q H, Shao Z F. 2017. An evaluation of monthly impervious surface dynamics by fusing Landsat and MODIS time series in the Pearl River Delta, China, from 2000 to 2015. *Remote Sensing of Environment*, 201: 99–114.

Zhou D C, Xiao J F, Frolking S, Liu S G, Zhang L X, Cui Y P, Zhou G Y. 2021. Croplands intensify regional and global warming according to satellite observations. *Remote Sensing of Environment*, 264: 112585.

Zhu Z, Zhou Y Y, Seto K C, Stokes E C, Deng C B, Pickett S T A, Taubenböck H. 2019. Understanding an urbanizing planet: Strategic directions for remote sensing. *Remote Sensing of Environment*, 228: 164–182.

Downloaded from www.worldscientific.com
by fac sciences de la terre universite annaba on 07/30/24. Re-use and distribution is strictly not permitted, except for Open Access articles.

This page intentionally left blank

Downloaded from www.worldscientific.com
by fac sciences de la terre universite annaba on 07/30/24. Re-use and distribution is strictly not permitted, except for Open Access articles.

Downloaded from www.worldscientific.com
by fac sciences de la terre universite annaba on 07/30/24. Re-use and distribution is strictly not permitted, except for Open Access articles.

Chapter 2

Big Data Characteristics of Urban Remote Sensing

Cities are the epitome of a concentration of human activity and are constantly undergoing rapid changes that require timely monitoring. Urban remote sensing technology can be applied to characterize the regional environment of the urban surface, and describe the geometric and spectral characteristics of the complex urban artificial features, a variety of artificial and natural vegetation types, as well as easy eutrophication and pollution of urban lakes. Expert knowledge and computer technology in remote sensing image interpretation of image feature information, and comprehensive analysis of remote sensing image spectral characteristics (Nasarudin and Shafr, 2021), polarization, time, spatial characteristics and related information, can render reliable data and technical support for better urban management and sustainable development.

Different sensor-platform systems differ in the characteristics of urban remote sensing data. Users can obtain urban-specific space-spectrum-time remote sensing data given observation requirements. In this chapter, we introduce the data characteristics of the urban scene visible light remote sensing images, multi-spectral remote sensing images, hyperspectral remote sensing images, thermal infrared images, microwave remote sensing images, LiDAR data and luminous remote sensing images, aiming to provide decision-making basis for the data selection of specific urban remote sensing applications.

2.1 Multi-source Heterogeneous Remote Sensing Big Data with Long Time Series

2.1.1 Urban satellite imagery

In order to strengthen the scientific research on the Earth's surface, NASA initiated the Earth observation system program in 1991 and launched the Terra satellite in December 1999. This satellite carries Clouds and the Earth's Radiant Energy System (CERES) and Moderate-resolution Imaging Spectroradiometer (MODIS), Multiangle Imaging Spectroradiometer (MISR), Advanced Spaceborne Thermal Emission and Reflection Radiometer (ASTER), and Measurements of Pollution in the Tropism (MOPITT).

Since the launch of the Landsat-1 satellite in 1972, Landsat series satellites data with a history of 40 years have become the most widely used satellite data, which have made a great contribution to the monitoring of the Earth's surface. These are also one of the important data sources in the field of urban remote sensing. Following the failure of Landsat-1–4 satellites, Landsat-5 was retired in 2013, and Landsat-8 was launched in 2013, becoming the main force of Landsat series. Landsat-8 is equipped with two sensors: Operational Land Imager (OLI) and Thermal Infrared Sensor (TIRS). OLI has 9 bands. Except that the spatial resolution of panchromatic band is 15 m, the spatial resolution of the other bands is 30 m, and the thermal infrared sensor TIRS has two bands with a resolution of 100 m. The return period of Landsat-1–3 satellites is 18 days, and that of Landsat-4–8 satellites (except Landsat-6 with launch failure) is 16 days. Considering the 15–100-m spatial resolution and relatively short return period of Landsat data, the data are widely used in the dynamic monitoring of interannual changes of urban remote sensing.

For a long time, WorldView series satellites, a commercial imaging satellite system of Digital Globe, have been considered the commercial imaging satellites with the highest resolution and the fastest response in the world. WorldView-1 was launched in 2007, and provides panchromatic images with 0.5-m spatial resolution. WorldView-2 was launched in 2009, and provides panchromatic images with a spatial resolution of 0.5 m as well as multi-spectral images with a spatial resolution of 1.8 m. WorldView-3 was launched in 2014, and collects images with a spatial resolution of 0.31 m. Given that the US government prohibits commercial companies from marketing satellite images with spatial resolution better than 0.5 m, the

Downloaded from www.worldscientific.com
by fac sciences de la terre universite annaba on 07/30/24. Re-use and distribution is strictly not permitted, except for Open Access articles.

original data have been resampled to 0.5-m resolution. WorldView-4 satellite was launched in 2016, and captures images with a panchromatic resolution of 0.3 m and multi-spectral resolution of 1.24 m, similar to WorldView-3. Figure 2.1 shows examples of WorldView-4 satellite images in urban areas.

In recent years, China has seen rapid development in high-resolution satellites, evidenced by the launch of a series of high-resolution satellites (GF satellite series, Table 2.1). At present, the high-resolution series of satellites cover many types, from panchromatic, multi-spectral to hyperspectral, from optics to radar, from solar synchronous orbit to geosynchronous orbit, forming an earth observation system with high spatial resolution, high temporal resolution and hyperspectral resolution.

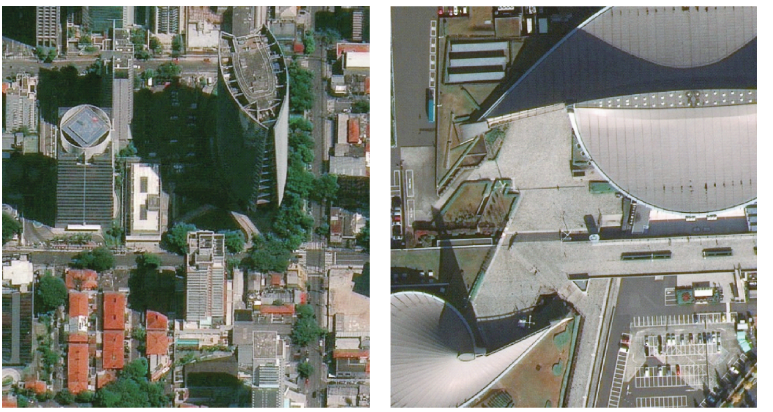

Figure 2.1 WorldView-4 satellite images in urban areas.

Table 2.1 The parameters of GF series satellites.

Satellite	Launch time	Resolution (m)	Bands
GF-1	2013	Panchromatic: 2, multi-spectral: 8	Panchromatic, blue, green, red, near-infrared
GF-2	2014	Panchromatic: 0.8, multi-spectral: 3.2	Panchromatic, blue, green, red, near-infrared
GF-3	2016	1–500	C-band SAR
GF-4	2015	50–400	Visible light, near-infrared, medium-wave infrared
GF-5	2018	30	Visible to short-wave infrared, full-spectrum
GF-6	2018	Panchromatic: 2, multi-spectral: 8, multi-spectral: 16	Panchromatic, blue, green, red, near-infrared

Downloaded from www.worldscientific.com
by fac sciences de la terre universite annaba on 07/30/24. Re-use and distribution is strictly not permitted, except for Open Access articles.

Downloaded from www.worldscientific.com
by fac sciences de la terre universite annaba on 07/30/24. Re-use and distribution is strictly not permitted, except for Open Access articles.

The GF-1 satellite provides panchromatic images with 2-m spatial resolution and multi-spectral images with 8-m spatial resolution. GF-2 is equipped with two high-resolution 1-m panchromatic and 4-m multi-spectral cameras. The spatial resolution of points under the satellite can reach 0.8 m, providing panchromatic images with 1-m spatial resolution and multi-spectral images with 4-m spatial resolution. Launched in 2018, the GF-6 satellite is a low-orbit optical remote sensing satellite, equipped with a 2-m panchromatic camera, an 8-m multi-spectral high-resolution camera and a 16-m multi-spectral medium-resolution wide-band camera. The 2-m panchromatic camera and 8-m multi-spectral camera have an observation width of 90 km, and 16-m multi-spectral camera has an observation width of 800 km (Figure 2.2). The network composed of the GF-6 satellite and GF-1 satellite greatly benefits the observation of China's land areas. The temporal resolution has greatly improved, effectively making up for the shortage of existing medium and high spatial resolution multi-spectral satellite resources and improving the self-sufficiency rate and application scope of China's remote sensing satellite data.

Figure 2.2 GF-6 panchromatic, multi-spectral fusion image.

The GF-3 satellite, China's first C-band multi-polarization synthetic aperture radar (SAR) imaging satellite with a resolution of 1 m, was launched in 2016. GF-3 has 12 imaging modes. It covers the traditional strip and scanning imaging modes and also realizes free switching under a variety of imaging modes, e.g., bunching, strip, scanning, wave, global observation, and high and low incident angles. Figure 2.3 is an image obtained by GF-3.

Synthetic aperture radar (SAR) is an active microwave imaging sensor. By transmitting broadband signals and combining synthetic aperture technology, SAR can obtain two-dimensional (2D) high-resolution images in range and azimuth at the same time. Compared with optical remote sensing and hyperspectral remote sensing, SAR has numerous advantages, e.g., all-weather, all-time imaging ability and high penetration. Being able to reflect the characteristics of surface microwave scattering, SAR has been widely used in various fields that include natural resource surveys and natural disaster monitoring. SAR is also an important data source for urban remote sensing research. The surface subsidence caused by overexploitation of underground mineral resources or groundwater resources is one of the most serious geological disasters in China. Urban surface subsidence is a slow process. Some researches demonstrate the great potentials of

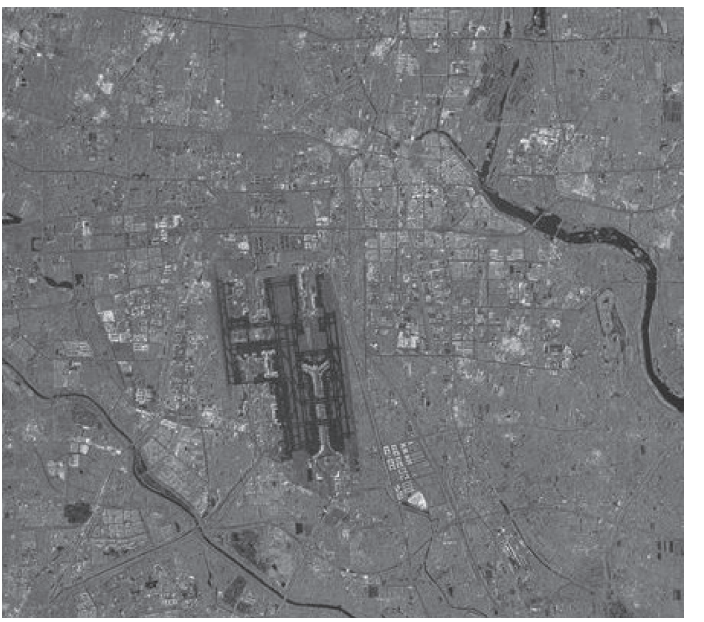

Figure 2.3 An example of GF-3 image.

Downloaded from www.worldscientific.com
by fac sciences de la terre universite annaba on 07/30/24. Re-use and distribution is strictly not permitted, except for Open Access articles.

SAR interferometric point target technology in urban surface deformation monitoring.

2.1.2 Urban aerial imagery

Aerial imagery refers to the techniques that install cameras on the aircraft for automatic continuous photography on the ground. The aerial cameras have a complex structure and have a precision fully automatic optical and electromechanical system. In recent years, digital aerial cameras have gradually replaced optical aerial cameras, becoming the mainstream sensor of aerial images. Digital aerial cameras can be mainly divided into three categories: (i) single-sided array aerial digital camera, (ii) multi-array aerial digital camera, and (iii) line-array aerial digital camera.

Aerial remote sensing serves as an important approach to collecting spatial data via photogrammetry and producing 4D products: digital elevation model (DEM), digital surface model (DSM), digital orthophoto model (DOM) and digital line graph (DLG).

2.1.3 Urban UAV imagery

UAV is a new remote sensing platform, which owns the advantages of simple structure, low cost, low risk, high mobility and strong real-time performance. UAV as a remote sensing platform to obtain real-time high-resolution remote sensing image data can overcome the shortcomings of traditional aerial remote sensing subject to flight time and meteorological conditions. UAVs can also provide regular monitoring for areas that are not covered by other satellite and aerial remote sensing sensors. In addition, they avoid factors such as small working range, narrow field of vision and large workload of ground remote sensing and have low technical requirements for operators. Due to the characteristics of high mobility, flexibility and speed of the UAV photography platform, UAV tilt photogrammetry plays an essential role in aerial photogrammetry and largely supplements the national aerial remote sensing monitoring system. The UAV is able to obtain the vertical information of urban buildings with high image resolution in a rapid manner

Downloaded from www.worldscientific.com
by fac sciences de la terre universite annaba on 07/30/24. Re-use and distribution is strictly not permitted, except for Open Access articles.

and improves the acquisition ability of fine three-dimensional data, greatly promoting the development of 3D modeling of tilt photogrammetry.

UAVs play an irreplaceable role in natural disaster monitoring. UAV aerial photography makes up for the shortcomings of low observation accuracy and poor timeliness of earth observation means such as satellite remote sensing and aerial remote sensing. A large number of real-time high-resolution images can provide reliable, comprehensive and timely disaster information for urban emergency disaster relief decision-making and command. After the Wenchuan earthquake on May 12, 2008, the disaster area was devastated and the traffic was paralyzed. In order to understand the disaster situation in the disaster area in a timely manner, the rescue personnel used the UAV remote sensing system to take aerial photos of the disaster area, processed the acquired images and evaluated the disaster situation, which provided effective decision support for earthquake relief. On August 8, 2017, a magnitude 7.0 earthquake occurred in Jiuzhaigou County, Aba Tibetan and Qiang Autonomous Prefecture, Sichuan Province. The emergency department of State Grid Sichuan Electric Power Company used UAV aerial photography to conduct three-dimensional modeling of the disaster area, obtain the information of power facilities and real-time information of geological disasters in the disaster area, and provide reliable data support for technicians to carry out power emergency repair in the disaster area.

Figure 2.4 shows the UAV remote sensing platform and Figure 2.5 shows an example of a UAV image. The data location is the South Trunk Canal Garden in Qingshan District, Wuhan. The UAV image is an orthophoto remote sensing image with a spatial resolution of 0.03 m.

Figure 2.4 UAV remote sensing platform.

Downloaded from www.worldscientific.com
by fac sciences de la terre universite annaba on 07/30/24. Re-use and distribution is strictly not permitted, except for Open Access articles.

Figure 2.5 UAV aerial remote sensing image of South Trunk Canal Garden in Qingshan District, Wuhan.

2.1.4 Urban mobile mapping system

Satellite remote sensing and aerial remote sensing platforms are able to obtain a wide range of urban surface information. However, due to the existence of dense urban buildings and complex components, it is challenging to obtain complete information on ground objects. The high cost and poor situation of aerospace and aerial remote sensing also restrict the development of urban remote sensing. The emergence of vehicle mobile measurement systems largely makes up for these shortcomings and presents great applicable potentials in the fields of smart city, traffic management and public safety.

The data obtained by the onboard mobile measurement system mainly includes image sequence and three-dimensional point cloud. The image has high resolution and contains rich color and texture information. The point cloud data directly obtains the three-dimensional coordinates of object surface points, but its spatial resolution is low and the effective measurement distance is limited. At present, the commonly used street view map is obtained by directly displaying the image sequence after processing. The combination of the two kinds of data for three-dimensional reconstruction of urban buildings has been a research hotspot in recent years. The basic steps of building 3D reconstruction based on point cloud data and image

Downloaded from www.worldscientific.com
by fac sciences de la terre universite annaba on 07/30/24. Re-use and distribution is strictly not permitted, except for Open Access articles.

Downloaded from www.worldscientific.com
by fac sciences de la terre universite annaba on 07/30/24. Re-use and distribution is strictly not permitted, except for Open Access articles.

data are point cloud data acquisition, building point cloud recognition, geometric model reconstruction and texture mapping. Although the onboard mobile measurement system is extremely efficient and quick to provide data, this acquisition method still has limitations. It cannot obtain the data on the back of a building or an area where vehicles cannot drive into. The mobile measurement system can be combined with other data sources. For example, the multi-source images with geographical coordinates taken by mobile phones or ordinary cameras are used to supplement the onboard mobile measurement data.

Figure 2.6 shows an onboard mobile measurement system composed of a high-precision optical fiber or laser inertial navigation system (INS), a panoramic camera (CCD), a 920-m ultra-long-distance laser scanner (LiDAR) and a high-grade protective cover. During high-speed travel, it is able to quickly collect spatial position data and attribute data, synchronously store them in the computer and form a street view after editing and processing using a special software advanced geographic information acquisition system for laser point cloud and various thematic data results.

Figure 2.7 shows the data acquisition process of the onboard mobile measurement system. In the process of data acquisition, it is necessary to initialize the mobile measurement system, adjust the GPS/ INS signal and then drive according to the route set in advance to continuously scan and obtain continuous images. The images obtained by CCD need stereo matching and then are combined with INS attitude information and GPS position information. We can further build the image index database and eventually establish the database and electronic map.

(a) (b) (c)

Figure 2.6 An onboard mobile measurement system: (a) Mobile measuring vehicle; (b) Panoramic camera (CCD); (c) INS LiDAR.

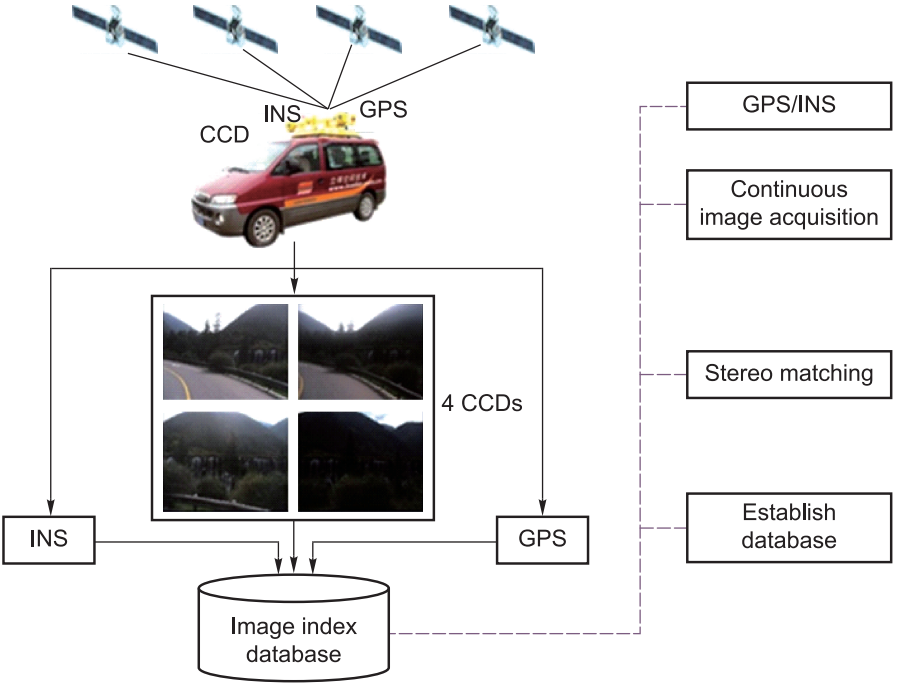

Figure 2.7 Data acquisition process of onboard mobile measurement system.

2.1.5 Urban crowdsourcing images

Multi-source geographic data refer to open geospatial data voluntarily obtained by a large number of non-professionals. It has been a research hotspot in the field of Geographic Information Science in recent years. Crowdsourcing geographic data are characterized by their large volume, low acquisition cost and timeliness. Representative crowdsourcing geographic data include GPS route data (e.g., OpenStreetMap), map data marked and edited by users (e.g., Wikimapia), various social networking website data (e.g., Twitter and microblog) and interest point data signed in by street users, to list a few.

Urban crowdsourcing images are a part of crowdsourcing geographic data. Users use smartphones, tablets, UAVs and other devices to take images and become information publishers after publishing them through the Internet. Figure 2.8 is a picture taken by a student of Wuhan University with a UAV. Social media platforms, e.g., microblog and WeChat, provide functions of

Downloaded from www.worldscientific.com
by fac sciences de la terre universite annaba on 07/30/24. Re-use and distribution is strictly not permitted, except for Open Access articles.

Figure 2.8 Image of Wuhan University taken by UAV.

uploading photos and associating them with the actual geographical location on the map. For the purpose of urban public security management, there are a large number of surveillance cameras throughout the city, and the full coverage of surveillance cameras is realized in key areas, such as the bright project implemented by many cities in recent years. Data from this public networked surveillance can also be used as a part of urban multi-source image data, serving as a supplementary means for aerospace, aviation and ground vehicle-mounted remote sensing platforms.

2.2 Data Characteristics of Urban Visible Panchromatic Remote Sensing Imagery

In urban remote sensing, the most widely used data include visible remote sensing image data. Urban visible full-color remote sensing data are commonly used in the extraction of urban artificial features, vegetation, water systems and other typical elements. In the following sub-sessions, the characteristics of urban houses, roads, green spaces and water are introduced.

Downloaded from www.worldscientific.com
by fac sciences de la terre universite annaba on 07/30/24. Re-use and distribution is strictly not permitted, except for Open Access articles.

2.2.1 Image characteristics of urban houses

In visible light remote sensing images (as shown in Figure 2.9), the houses tend to have a lighter tone compared to their background with strongly regulated shapes and textures. High-height houses usually form shadows on the image, and the outline of the shadows reflects the height and shape of the house. Given the extensive coverage of remote sensing images, we are able to see the entire built-up area of a city, which is conducive to a complete survey of the built-up area of the entire city. The urban roads, squares and newly built areas have brighter tones, while general urban buildings have lighter tones.

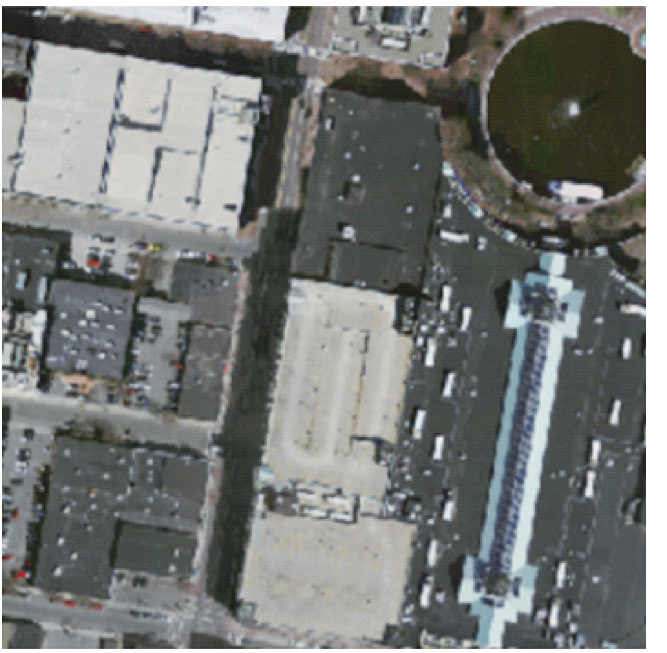

Figure 2.9 Visible light remote sensing image of urban houses.

2.2.2 Image characteristics of urban roads

Urban roads appear as bright-toned network lines on the visible light remote sensing image (as shown in Figure 2.10). Usually, their geometric forms are vertical and horizontal roads and multi-directional roads with straight-edge shapes and circular or gentle curves. The tones of roads are highly dependent

Downloaded from www.worldscientific.com
by fac sciences de la terre universite annaba on 07/30/24. Re-use and distribution is strictly not permitted, except for Open Access articles.

on the paving materials. On the high-resolution optical remote sensing image, the flow of people, traffic and auxiliary transportation facilities is clearly visible, providing auxiliary information for road extraction, but leading to the introduction of noises.

Figure 2.10 Visible light remote sensing image of urban road.

2.2.3 Image characteristics of urban green space

Urban green space, referring to urban land with natural vegetation and artificial vegetation, has obvious phenological characteristics under the influence of the geographic location of the city. The main vegetation types of urban green space include grassland and trees. Grassland is mainly located in recreational park or landscape land in communities. The trees in the city include small-scale forests, parks, street trees and independent old and famous trees. In the visible light remote sensing image (as shown in Figure 2.11), the urban green space appears green, with lush woodland having a darker tone and grassland having a lighter tone. Urban green space is also characterized by notable shape and location characteristics. Street trees are distributed on both sides of the road, and urban green areas such as parks are

Downloaded from www.worldscientific.com
by fac sciences de la terre universite annaba on 07/30/24. Re-use and distribution is strictly not permitted, except for Open Access articles.

arranged in a regular shape. In terms of texture characteristics, grass tends to have a texture with higher intensity than trees.

Figure 2.11 Visible light remote sensing image of urban green space.

2.2.4 Image characteristics of urban water bodies

Urban water bodies include rivers, lakes, reservoirs, reeds, beaches and channels, to list a few. Coastal cities also include offshore waters.

In visible light remote sensing images, the texture of the water body on the remote sensing image is relatively uniform, but with a complex color tone (as shown in Figures 2.12 and 2.13), due to the varying depths of the water body, the amount of sand, the degree of pollution and the flow rate of the river, among other factors. Under normal circumstances, the deeper the water body, the darker the color tone; the greater the sand content of the water body, the lighter the color tone; the more polluted the water body, the darker the color tone. Still water bodies have a relatively darker color tone, while rushing rivers have a relatively light tone.

Downloaded from www.worldscientific.com
by fac sciences de la terre universite annaba on 07/30/24. Re-use and distribution is strictly not permitted, except for Open Access articles.

Figure 2.12 Visible light remote sensing image of urban lakes.

Figure 2.13 Visible light remote sensing image of urban rivers.

2.3 Data Characteristics of Urban Multi-spectral Remote Sensing Images

Urban vegetation and water bodies tend to present unique spectral characteristics in multi-spectral remote sensing images. The spectral

Downloaded from www.worldscientific.com
by fac sciences de la terre universite annaba on 07/30/24. Re-use and distribution is strictly not permitted, except for Open Access articles.

characteristics of vegetation can be effectively distinguished from other ground features on remote sensing images. At the same time, different vegetation types have their own spectral characteristics, establishing the foundation for the distinguishment of vegetation types, growth conditions and whether there are diseases and insect pests. The spectral characteristics of the water bodies are beneficial for the determination of water body boundaries, the determination of water body suspended matter, and the detection of water temperature, water pollution and water depth.

2.3.1 Data characteristics of urban green space

In different urban areas, the color, tone, shape and other characteristics of vegetation on the color infrared image are different (as shown in Figure 2.14). The urban forest park is usually presented as dark red strips, dark red or black blocks; the green space of the park is usually presented as a red block located inside the city on the image with regular shapes (mostly squares); the community green space is generally around the building, dot-shaped trees arranged in surface-shaped grass; the greening of the traffic road is elongated

Figure 2.14 The color infrared images of different urban green spaces.

Downloaded from www.worldscientific.com
by fac sciences de la terre universite annaba on 07/30/24. Re-use and distribution is strictly not permitted, except for Open Access articles.

in the image, connected with the road. Due to the large distance between the street trees, the tree shadows can be clearly observed; paddy fields are generally regular dark red plots on the periphery of cities; dry land is generally irregular red plots. A better understanding of the distribution of various vegetation types in different urban areas facilitates the construction of forest, garden and ecological cities.

Different vegetation types tend to have different spectral, morphological and environmental characteristics due to differences in organizational structure, seasonal phases and ecological conditions, which can be expressed in remote sensing images. Considering the spectral characteristics of vegetation, we can select multi-spectral remote sensing data through analysis and calculation of linear or nonlinear combination methods such as addition, subtraction, multiplication and division to generate some numerical values that have certain indications for vegetation growth, biomass, etc., namely, the vegetation index. The vegetation index represents simple and effective form-only spectral signals to achieve the expression of plant state information.

2.3.2 Data characteristics of urban water bodies

When sunlight shines on the water surface, a small part of it is reflected back into the air by the water surface, but most of it is incident on the water body. Most of the light incident on the water body is absorbed by the water body, a proportion is reflected by the suspended matter in the water and a small proportion is transmitted to the bottom of the water, absorbed and reflected by the water bottom. The radiation reflected by suspended objects and by the bottom of the water partly returns to the surface of the water and folds back into the air. Therefore, the radiation received by the sensor contains the reflected light from the water surface, from suspended objects and from the water bottom, as well as the scattered light from the sky. The discrepancies in surface properties of different water bodies, the nature and contents of suspended solids in water bodies, water depth and bottom characteristics lead to the differences in the characteristics of the reflection spectrum received on the sensor, providing a basis for remote sensing-based water body monitoring.

Downloaded from www.worldscientific.com
by fac sciences de la terre universite annaba on 07/30/24. Re-use and distribution is strictly not permitted, except for Open Access articles.

Figure 2.15 The color infrared images of different urban water body.

In color infrared remote sensing images, water bodies can be distinguished by color and texture (as shown in Figure 2.15). Water bodies are generally represented by blue, while heavily polluted water bodies are black. Some rivers and other large water bodies present light green tones.

The interpretation of the spectral characteristics of the water system is of great importance to the determination of the water body boundary, the determination of the suspended matter in the water body, the detection of water temperature, water pollution and water depth, according to the study of the spectral characteristics of the above-mentioned related factors, for different geological environments and geological disasters.

2.4 Data Characteristics of Urban Hyperspectral Imagery

Urban features are complex and diverse. The spectral characteristics of different types of artificial surfaces are complex with strong heterogeneity, posing challenges in applications of urban remote sensing. Commonly used high-resolution remote sensing images contain objects hidden from street trees and shadows. There are large errors in the classification of scenes, such as the confusion of shadows and water bodies. Hyperspectral data can acquire

Downloaded from www.worldscientific.com
by fac sciences de la terre universite annaba on 07/30/24. Re-use and distribution is strictly not permitted, except for Open Access articles.

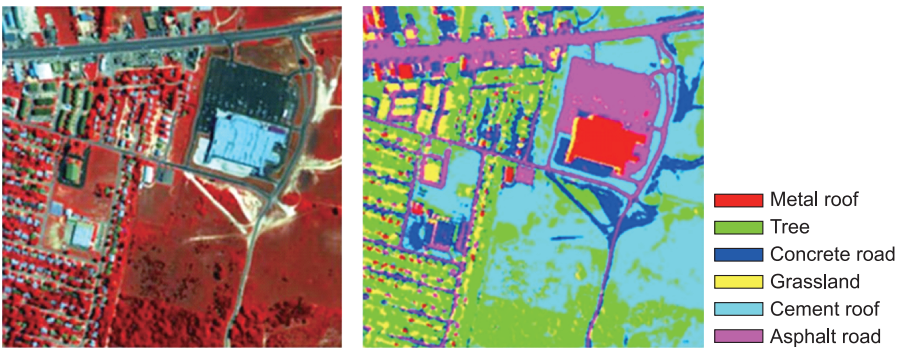

Figure 2.16 Urban hyperspectral remote sensing images and corresponding image classification results.

the spectral features and differences of features in a more comprehensive and detailed manner, thereby greatly improving the feature classification accuracy and leading to the fine classification of urban features (Heiden *et al.*, 2007). Figure 2.16 shows the fine classification results of urban hyperspectral images. Hyperspectral remote sensing can better distinguish roofs and road types of different materials compared to multi-spectral remote sensing.

Hyperspectral remote sensing images benefit the accuracy of vegetation classification. The applications of hyperspectral remote sensing images in the retrieval of urban vegetation parameters mainly include the following: (i) inversion of biochemical component parameters (e.g., chlorophyll, carotenoids and nitrogen); (ii) inversion of biophysical parameters (e.g., leaf area index (LAI)); and (iii) inversion of environmental interaction factors (e.g., fraction of photosynthetically active radiation (FPAR)). The advancement of remote sensing technology to measure and analyze the changes in time and space of the biochemical information of leaves and even the canopy facilitates our understanding of the productivity of plants, the decomposition rate of litter and the effectiveness of nutrients. In addition, the growth of vegetation can be evaluated according to the changes in the concentration of various chemical components. The effect of the urban heat island on vegetation phenology can be further studied through the parameter difference of urban and rural vegetation.

The development of hyperspectral small-satellite constellations ushered in new opportunities with the launch of the Zhuhai-1 satellite. The Zhuhai-1 hyperspectral satellite is designed to transmit 32 bands, with a spatial resolution of up to 10 m and a scanning bandwidth of up to 150 km.

Downloaded from www.worldscientific.com
by fac sciences de la terre universite annaba on 07/30/24. Re-use and distribution is strictly not permitted, except for Open Access articles.

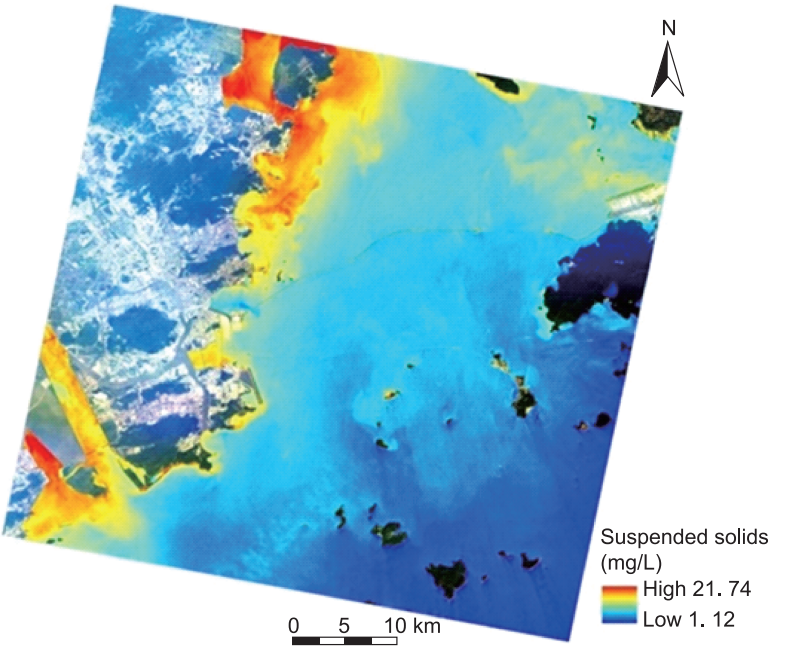

Figure 2.17 The concentration distribution of suspended solids in the offshore waters of Zhuhai City.

It has unique advantages: high spatial resolution, large amplitude, large constellation scale and short revisit period (Weng, 2012). Data collected from Zhuhai-1 have great prospects in the application of urban remote sensing. Figure 2.17 shows the concentration distribution of suspended solids in the offshore waters of Zhuhai City based on the Zhuhai-1 satellite.

The most important feature of hyperspectral database data is the following: the traditional image dimension information and spectral dimension information are integrated, and the continuous spectral information of each feature is obtained while acquiring the spatial image of the surface so as to realize the land based on the spectral characteristics' object composition information inversion and feature recognition. Taking urban permeable pavement as an example, the measurement of the spectral library of different permeable pavements is of great importance in analyzing the permeable characteristics of different materials. Figure 2.18 presents the material map of permeable pavements in Qingshan District, Wuhan, and Figure 2.19 shows the spectrum curves of the corresponding permeable materials.

Downloaded from www.worldscientific.com
by fac sciences de la terre universite annaba on 07/30/24. Re-use and distribution is strictly not permitted, except for Open Access articles.

Downloaded from www.worldscientific.com
by fac sciences de la terre universite annaba on 07/30/24. Re-use and distribution is strictly not permitted, except for Open Access articles.

Figure 2.18 Permeable pavement material in the Sponge City Demonstration Zone in Qingshan District, Wuhan.

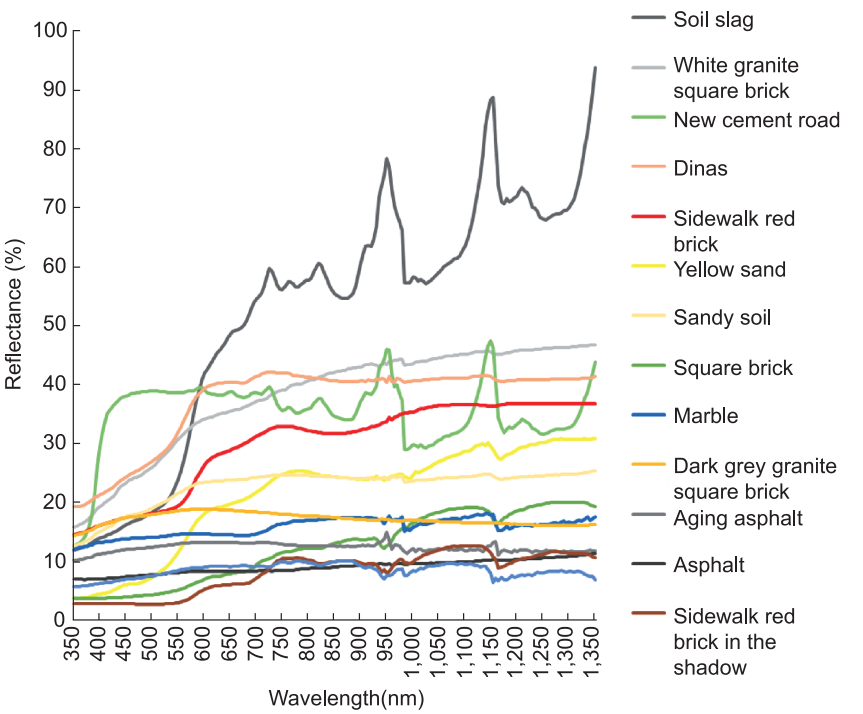

Figure 2.19 The spectrum curve of permeable material in the sponge city demonstration area in Qingshan District, Wuhan.

2.5 Data Characteristics of Urban Thermal Infrared Images

Thermal infrared images (Nagumo *et al.*, 2021) record the radiant temperature distribution of ground objects and describe the thermal contrast of ground objects with changes in tones. Generally speaking, light tones on thermal infrared images (positive film) represent strong radiators, indicating high surface temperature; dark tones otherwise. Due to the effect of thermal diffusion, thermal infrared images usually fail to reflect the exact shape of objects. The water in the thermal infrared image appears notably different from other land covers, and it is sensitive to the inversion of information, e.g., the moisture content in the environment.

Generally, ground objects are exposed to solar radiation at a higher temperature during the day and have a warm color; at night, the heat dissipation temperature of the material is lower, showing a cool color, especially in soil and rocks.

The roads, parking lots and other artificially paved features in the city are heated higher during the day than the surrounding area, and heat dissipation is slower at night, and still maintains a higher temperature than the surrounding area. Therefore, the day and night thermal infrared images appear brighter than the surrounding area.

The specific heat capacity and thermal inertia of the water body are large, the infrared wave band is almost completely absorbed, the self-radiation emissivity is high and the temperature inside the water body is transferred by heat convection, so that the surface temperature of the water body is relatively uniform, and the temperature change during day and night is slow and small. During the day, the water heat capacity is large and the temperature rises slowly, which is lower than the surrounding soil and rock temperature, showing a dark color; at night, the heat loss of the water is slow, and the temperature is higher than the surrounding soil and rock temperature, showing a light color. Water can be used as a reliable indicator for judging the time of thermal infrared imaging. If the water has a warmer mark than nearby objects, the imaging time is night; otherwise, it is daytime.

The radiant temperature of vegetation such as trees is relatively high, and the thermal infrared image at night presents a warm color. Although the vegetation is irradiated by sunlight during the day, the temperature of the leaf surface is lowered by the effect of water transpiration, making the vegetation lower than the surrounding soil temperature, so the color tone on the thermal

Downloaded from www.worldscientific.com
by fac sciences de la terre universite annaba on 07/30/24. Re-use and distribution is strictly not permitted, except for Open Access articles.

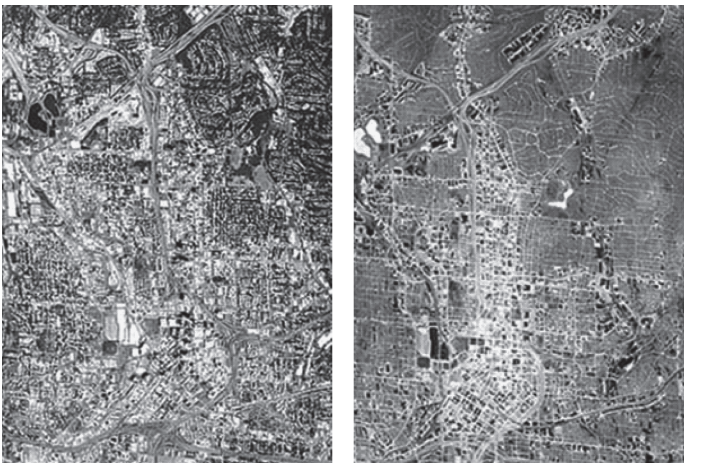

Figure 2.20 Thermal infrared remote sensing images of Atlanta, USA, at daytime (a) and night (b).

infrared image is darker than the surrounding ground objects. However, coniferous forests have a slight exception, which is due to the high synthetic emissivity of the coniferous forest canopy.

The image characteristics of urban aerial thermal infrared images during the day are similar to optical aerial remote sensing images, with thermal buildings appearing bright white, roads appearing light gray and water bodies appearing black. Figure 2.20 shows infrared images of Atlanta, USA, at day and night. In the night image, the water body appears bright white, and the overall temperature difference is significantly reduced; although the building complex has a brighter tone due to the local heat island effect, shadow and three-dimensional effects are reduced, with weakened temperature difference; the asphalt street absorbs more heat during the day, while the excess heat remains at night, leading to their brighter tone.

2.6 Data Characteristics of Urban Microwave Remote Sensing Images

Radar images and optical images differ in imaging mechanism and the information reflected on the images. The optical image mainly reflects

Downloaded from www.worldscientific.com
by fac sciences de la terre universite annaba on 07/30/24. Re-use and distribution is strictly not permitted, except for Open Access articles.

the difference in spectral characteristics caused by the composition and moisture content of the surface material; the radar image mainly reflects the difference in the backscattering characteristics of the surface objects' dielectric constant, humidity and surface roughness. Radar images essentially record the intensity and phase of the echo scattered by the ground target on the radar signal. Thus, the study of the scattering characteristics of ground objects is the basis for the interpretation of radar images, as well as the basis for the quantitative research of imaging radar microwave remote sensing. The scattering characteristics of ground objects are usually described by the scattering coefficient.

For artificial buildings, e.g., residential areas, the shape of features has a significant impact on the direction and intensity of microwave reflection. The wall of houses produces angular reflection effects, similar to the ground composed of two-sided or multi-sided reflectors, which causes radar beams to present double-image or multiple-angle reflections, leading to enhanced echoes. Objects that include houses contain metal structures, leading to an increased dielectric constant and strong radar backscattering. Therefore, the houses on the microwave remote sensing image often show notable bright spots, and the residential areas tend to present scattered bright white spots, leading to their easy identification.

As for smooth artificial surfaces, e.g., cement roads and asphalt plazas, microwaves are reflected specular, and the radar antenna cannot receive the echo signal, leading to dark and black images. Signals are strong only when it is close to vertical incidence. Figures 2.21 and 2.22 show the comparison

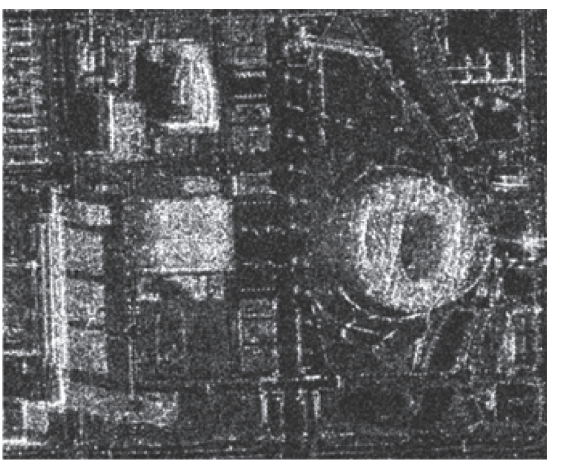

Figure 2.21 Radar image in an urban setting.

Downloaded from www.worldscientific.com
by fac sciences de la terre universite annaba on 07/30/24. Re-use and distribution is strictly not permitted, except for Open Access articles.

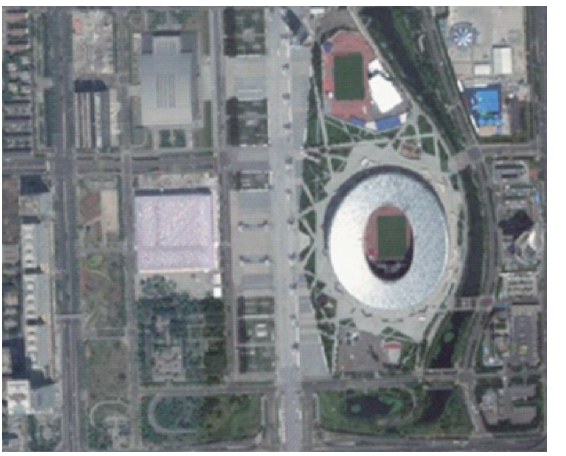

Figure 2.22 Optical image in an urban setting.

between the radar image and the optical image near the Beijing Olympic Park National Stadium.

2.7 Data Characteristics of Urban LiDAR Data

LiDAR refers to a system that integrates three major technologies: laser, global positioning system (GPS) and inertial navigation system (INS). The LiDAR system can be used in cities to obtain point cloud data and generate accurate digital three-dimensional models. The LiDAR system has been widely applied to urban remote sensing, thanks to its unique characteristics that include high speed, high performance, high precision and long-distance aerial measurement equipment.

Since LiDAR data are discrete points, it is usually necessary to obtain the elevation feature and intensity feature map of the LiDAR point cloud when applied within urban areas and distinguish typical features (e.g., buildings and roads) based on different strength and elevation features. The elevation feature map of LiDAR data is expressed by the normalized digital surface model (nDSM). The nDSM can be generated according to the following steps: (i) the digital surface model (DSM) is obtained by interpolating the first echo point in the laser point cloud, and then the progressive triangulation filtering method is used to first extract the ground points from the LiDAR data (via interpolating approaches, digital elevation model (DEM) can be obtained);

Downloaded from www.worldscientific.com
by fac sciences de la terre universite annaba on 07/30/24. Re-use and distribution is strictly not permitted, except for Open Access articles.

(ii) subtract the two to derive nDSM. Building roofs and vegetation usually have higher normalized heights compared to other features. Figure 2.23 shows the aerial image. Figure 2.24 shows the extraction results of aerial images and nDSM.

Figure 2.23 Aerial images of urban areas.

Figure 2.24 nDSM extracted from LiDAR.

Downloaded from www.worldscientific.com
by fac sciences de la terre universite annaba on 07/30/24. Re-use and distribution is strictly not permitted, except for Open Access articles.

2.8 Data Characteristics of Urban Nighttime Light Remote Sensing Imagery

Luminous remote sensing images can reflect the lighting conditions of towns at night under cloud-free conditions. The artificial buildings and road networks that are used by human activities and lights can be clearly presented (Li and Li, 2015). Figure 2.25 shows the luminous remote sensing image of Abu Dhabi and Dubai in the United Arab Emirates (UAE) sent back by Wuhan University's Luminous Remote Sensing Experiment Star Luojia-1. The city structures and road networks can be clearly observed. Compared with ordinary remote sensing satellite images, luminous remote sensing images are able to reflect human activity intensities. Luminous remote sensing has been widely used in various applications in the fields of socio-economic parameter estimation, urbanization detection and assessment, major event assessment, and environmental and health effects research, to list a few.

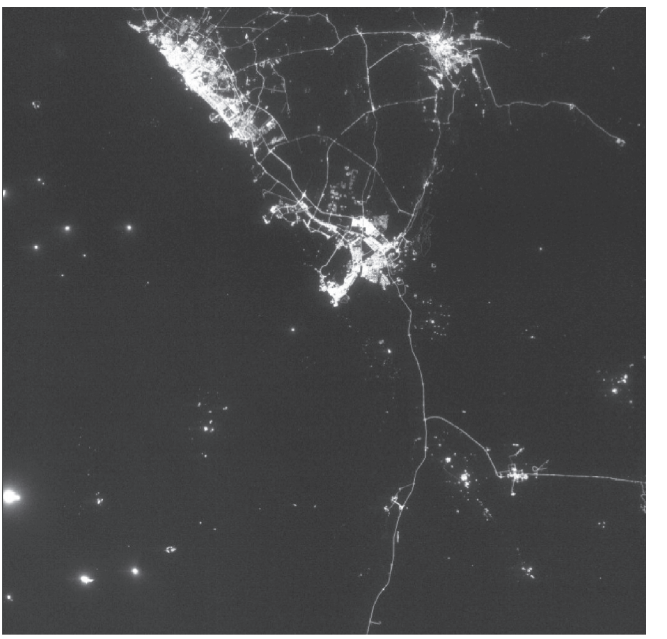

Figure 2.25 Luminous remote sensing image.

Downloaded from www.worldscientific.com
by fac sciences de la terre universite annaba on 07/30/24. Re-use and distribution is strictly not permitted, except for Open Access articles.

2.9 Data Characteristics of Urban Crowdsourcing Images

Urban crowdsourcing data refer to open geographic data obtained by a large number of non-professionals and provided to the public through the Internet in a voluntary manner. Multi-source geographic data have the following characteristics:

1. *Large volume*: The multi-source geographic data mainly come from the geographic data spontaneously obtained and uploaded by network users, characterized by their large volume.
2. *Low cost*: Except for the geographic data provided by a few government agencies or organizations, most multi-source geographic data can be collected spontaneously by users and volunteers.
3. *Rich information*: Compared with traditional spatial geographic data, multi-source geographic data contain rich contextual and semantic information.
4. *Timeliness*: Multi-source geographic data can provide timely situational awareness on urban fabrics.
5. *Varying data quality*: As the basis of various applications and research in the field of geographic information, the quality of spatial data has a profound impact on the reliability and accuracy of final results and decision-making. As the multi-source geographic data are collected and uploaded spontaneously by untrained non-professional users, its production process is relatively independent and the accuracy of the data collection equipment is inconsistent, leading to great disparity in the data quality.

Questions

1. Briefly describe the differences in characteristics of urban houses, roads, green spaces and water bodies in visible light panchromatic remote sensing images.
2. Considering the difference in the characteristics of urban residential areas and vegetation in visible light, infrared, thermal infrared and microwave images, how can one choose remote sensing data when extracting urban residential areas and vegetation?

Downloaded from www.worldscientific.com
by fac sciences de la terre universite annaba on 07/30/24. Re-use and distribution is strictly not permitted, except for Open Access articles.

3. Considering the image characteristics of urban houses and roads, how can one extract the range of urban built-up areas?
4. What are the characteristics of urban buildings, roads, water bodies and vegetation based on the urban day and night thermal infrared images in Figure 2.20?
5. Factors such as organic matter, suspended sediment, water depth and water temperature in urban water bodies tend to affect the spectral characteristics. What are the potential uses of urban water spectral characteristics in conjunction with the characteristics of remote sensing data?

References

Heiden U, Segl K, Roessner S, Kaufmann H. 2007. Determination of robust spectral features for identification of urban surface materials in hyperspectral remote sensing data. *Remote Sensing of Environment*, 111: 537–552.

Li D R, Li X. 2015. On luminous remote sensing data mining. *Journal of Surveying and Mapping*, 44: 591–601.

Nasarudin N, Shafr H. 2021. Development and utilization of urban spectral library for remote sensing of urban environment. *Journal of Urban and Environmental Engineering*, 51: 44–56.

Nagumo K, Kobayashi T, Oiwa K, Nozawa A. 2021. Face alignment in thermal infrared images using cascaded shape regression. *International Journal of Environmental Research and Public Health*, 18: 1776.

Weng Q H. 2012. Remote sensing of impervious surfaces in the urban areas: Requirements, methods, and trends. *Remote Sensing of Environment*, 117: 34–49.

Downloaded from www.worldscientific.com
by fac sciences de la terre universite annaba on 07/30/24. Re-use and distribution is strictly not permitted, except for Open Access articles.

This page intentionally left blank

Downloaded from www.worldscientific.com
by fac sciences de la terre universite annaba on 07/30/24. Re-use and distribution is strictly not permitted, except for Open Access articles.

Downloaded from www.worldscientific.com
by fac sciences de la terre universite annaba on 07/30/24. Re-use and distribution is strictly not permitted, except for Open Access articles.

Chapter 3

Principles and Methods of Urban Remote Sensing Image Interpretation

Remote sensing image interpretation theory is a basic theory of obtaining ground object information from remote sensing images. The image interpretation process completes the transmission of ground object information and plays the role of interpreting the content of remote sensing images. Remote sensing image interpretation is a comprehensive technology that involves digital image processing, physics, geoscience, biology, etc. According to its purpose and task, remote sensing image interpretation can be divided into general geoscience interpretation and professional interpretation. In this chapter, we mainly introduce the task, object and mechanism of urban remote sensing interpretation and the interpretation methods by taking visual interpretation, semi-automatic interpretation, full-automatic interpretation and big data interpretation as examples.

3.1 The Task of Urban Remote Sensing Imagery Interpretation

In recent years, more and more attention has been paid to the development of satellite remote sensing, and independent and controllable earth observation systems have been established. At the same time, the commercial satellite market continues to grow, with more and more diversified observation platforms being launched.

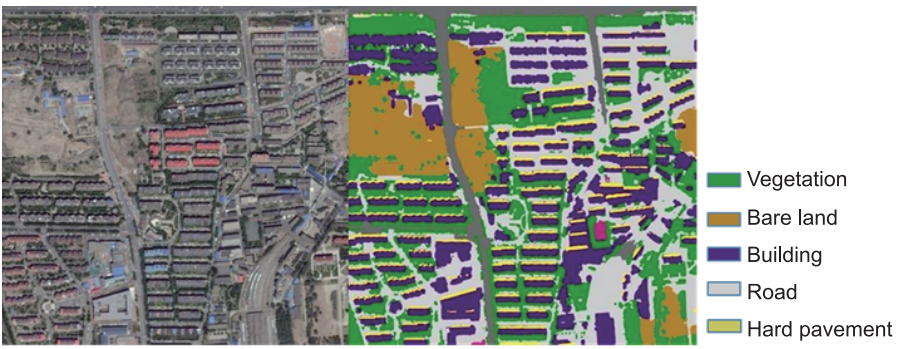

Figure 3.1 Urban remote sensing interpretation.

At present, many special plans related to urban remote sensing information extraction have been carried out, and many sets of global land cover/use data products have been produced and released. China has launched the global mapping project and is currently conducting the national land survey, geographical market survey and monitoring, urban impervious surface survey and sponge city remote sensing monitoring on a yearly basis. These surveying and mapping projects include global land cover maps geographic national conditions monitoring and survey, global urban built-up area information monitoring, urban impervious surface remote sensing census and sponge city remote sensing monitoring. Figure 3.1 shows an example of remote sensing interpretation in an urban scene.

A city is a complex mixture of various natural and human phenomena. From the characteristics of the city as a special research object and the basic principle of remote sensing, the special needs of urban remote sensing interpretation are mainly reflected in the following three aspects:

1. The composition, structure, state and change trend of urban geospatial and land cover/ use are closely related to a certain surface state or geographical process, with obvious spectral or temporal characteristics and specific image characteristics in remote sensing images. Using these spectral, texture, structure and spatial features, we can realize the recognition, monitoring, analysis and evaluation of cities. This is also the theoretical and methodological basis of urban remote sensing application.
2. Although urban socio-economic information does not directly have obvious remote sensing image signs or characteristics, it often has a specific relationship with the information obtained from remote sensing images. Therefore, remote sensing application can be realized through

Downloaded from www.worldscientific.com
by fac sciences de la terre universite annaba on 07/30/24. Re-use and distribution is strictly not permitted, except for Open Access articles.

image information, correlation, knowledge reasoning and statistical analysis. The key is to establish the correlation mechanism between remote sensing observable factors and urban human, social and economic phenomena.

3. The remote sensing applications of urban resources, ecology, environment and land not only have the characteristics of resource remote sensing, ecological environment remote sensing and land remote sensing but also have their unique spatial and spectral characteristics because they are in the special system of the city. Urban remote sensing can draw on the experience and achievements of remote sensing applications in relevant fields, and further deepen and improve according to the particularity of the city.

3.2 The Objects of Urban Remote Sensing Imagery Interpretation

At present, various image data have been acquired by multiple platforms and on-ground and airborne sensors. Urban remote sensing images, which belong to the big data category, are characterized by their multi-source and heterogeneous nature. The interpretation of big remote sensing data of urban time series can assist in revealing the laws of urban development and support the sustainable development of cities.

3.2.1 Image spatial interpretation

Regarding remote sensing data as images is the closest approach to human cognitive habits. Each pixel in the image is connected with the ground objects in the ground landscape in the corresponding range. Thus, the geometric relationship between the pixels reflects the spatial relationship between the real ground objects, allowing people to interpret images in an intuitive manner. Figure 3.2 presents a schematic diagram of the image, which provides true-color and false-color images of urban areas. In fact, a common method for sample acquisition in remote sensing image classification is to draw directly from the image using the prior knowledge of the study area

Downloaded from www.worldscientific.com
by fac sciences de la terre universite annaba on 07/30/24. Re-use and distribution is strictly not permitted, except for Open Access articles.

(a)

(b)

Figure 3.2 The characteristics of a true-color image (a) and a false-color image (b). Combination of near infrared, red and green bands.

that has been captured by the image. In addition, the spatial information provided by the image space can be used as important classification auxiliary information (often referred to as contextual information). Context information is particularly important in the classification of remote sensing

Downloaded from www.worldscientific.com
by fac sciences de la terre universite annaba on 07/30/24. Re-use and distribution is strictly not permitted, except for Open Access articles.

Downloaded from www.worldscientific.com
by fac sciences de la terre universite annaba on 07/30/24. Re-use and distribution is strictly not permitted, except for Open Access articles.

data, especially for images with a higher spatial resolution. The biggest shortcoming of this image space expression is that the image is usually a single-band grayscale image or a three-band true-color (false-color) image. The human visual system fails to fully perceive all the information of the spectral remote sensing data, leading to misinterpretation of hyperspectral images when conducting manual image interpretation.

3.2.2 Interpretation of spectrum space

The spectrum space can be regarded as a two-dimensional coordinate space, where the abscissa represents different wavebands and the ordinate represents the radiation intensity. Different ground objects vary in band-wise electromagnetic wave reflection and absorption characteristics, manifested as different radiation intensities in remote sensing data. In theory, if the spectral range of the sensor is wide enough with sufficient sensitivity and resolution, different ground objects present separable spectral curves. Therefore, using the expression of spectral space, people can intuitively analyze the differences in their intrinsic physical properties based on the spectral curves of different ground objects. In addition, the best band for interpretation according to the different physical characteristics of the ground objects can be found.

In cities, artificially constructed urban surfaces are rich and diverse in type with different materials, leading to their good distinguishment in the spectral space. Taking typical urban underlying surfaces as an example, their spectral space is shown in Figure 2.19.

3.2.3 Interpretation of feature space

Via the plotting of the radiation intensity values of different objects in the two bands on a two-dimensional plane, a two-dimensional feature space can be obtained. Each pixel, expressed as a point in the two-dimensional feature space, corresponds to the radiation value of two bands. If there are 10 bands in the multi-spectral remote sensing data, the 10 radiation values of each pixel can be expressed as a 10-dimensional vector, i.e., a 10-dimensional feature space.

However, such a way for image understanding is not intuitive enough, as it is difficult for people to imagine how data is distributed in a high-dimensional space. In mathematical processing, however, this way of expression is very easy to process and can make full use of the pixel-wise information in all spectrums. Most pattern recognition methods first determine the distribution area of different types of samples in the feature space and then determine their type according to which area the unknown sample falls in the feature space.

Many pattern recognition methods do not directly classify in the above-mentioned feature space but map the data to another feature space for category judgment. At this time, the initial feature space is usually called the input space, and the feature space after the mapping changes is called the feature space.

3.3 The Mechanism of Urban Remote Sensing Imagery Interpretation

Urban remote sensing image interpretation aims to understand the urban remote sensing image from the image space, spectral space and feature space of the data and use the difference of remote sensing image spectrum, radiation, space and time characteristics to identify city-related targets. It is the process of qualitatively and quantitatively extracting the target's distribution, structures, functions, etc. Urban remote sensing image interpretation has different processes and methods depending on different purposes. For example, the interpretation of urban land use first identifies land use types on the image and then calculates various types of land areas on the map. Since urban remote sensing imagery is a comprehensive reflection of complex urban fabrics, its corresponding geographic environment is a complex, multi-element, multi-layered open system with dynamic structures and notable regional differences. The urban surface environment is affected by various factors that involve geology, landform, water temperature, soil, vegetation, man-made elements and social ecology. Therefore, the interpretation of urban remote sensing images often requires a combination of manual interpretation and automatic interpretation, thus demanding expert knowledge. Urban remote sensing

Downloaded from www.worldscientific.com
by fac sciences de la terre universite annaba on 07/30/24. Re-use and distribution is strictly not permitted, except for Open Access articles.

Downloaded from www.worldscientific.com
by fac sciences de la terre universite annaba on 07/30/24. Re-use and distribution is strictly not permitted, except for Open Access articles.

image interpretation uses knowledge bases and model libraries based on remote sensing image processing technology to achieve rapid and accurate identification and classification of ground objects. The main steps include image denoising, image enhancement, image classification, image mosaic and image interpretation. Through comprehensive analysis, comparison, reasoning and judgment of a diversity of features from remote sensing images, the information of interest is finally extracted.

According to this interpretation principle, the basic process of urban remote sensing image interpretation includes the following steps: (i) radiation correction and geometric correction on the image that needs to be interpreted are performed; (ii) appropriate image denoising according to the image quality is conducted, followed by image enhancement processing and image segmentation to selected ROI (region of interest); and (iii) the image human–computer interaction interpretation is completed based on image segmentation, followed by the image digital interpretation based on the interpretation result.

The spectrum, radiation, space and time characteristics of remote sensing images determine the visuals of the image, thus causing the differences of objects in the image (i.e., the interpretation of the sign). The urban remote sensing interpretation sign gives the possibility of distinguishing objects or phenomena in urban remote sensing images.

In remote sensing image interpretation, the signs of remote sensing image interpretation include direct interpretation signs and indirect interpretation signs. Direct interpretation signs are inherent to the features themselves and remote sensing images and can be determined by simpler observation or measurement methods. In general, the more direct an interpretation of signs that can be obtained, the more reliable the interpretation results. Indirect interpretation signs, not directly related to the object, can assist in the obtaining of the supplementary characteristics of the object and in the elimination of the ambiguity of the conclusion drawn by the direct analysis. Direct interpretation signs include image tone and color, shape, size, texture, pattern, shadow and three-dimensional appearance. In cities, direct interpretation signs with distinctive features mainly include hue and color, shape, shadow and texture. Indirect interpretation signs include topography, soil and soil quality, the relationship among features, vegetation type, climate and location.

Downloaded from www.worldscientific.com
by fac sciences de la terre universite annaba on 07/30/24. Re-use and distribution is strictly not permitted, except for Open Access articles.

3.3.1 Direct interpretation signs

3.3.1.1 Hue and color of urban features

Single-band satellite images and black-and-white aerial images are grayscale images that can be expressed by tone. In cities, artificial buildings tend to have a lighter tone, while the surrounding green areas and water bodies tend to have a darker tone.

In the color image, different targets differ in colors, manifested as different brightness (I), hue (H) and saturation (S) values. In cities, the color feature of man-made buildings is determined by the color of their roofs, which are usually light gray, red or blue (Figure 3.3). In the standard false-color infrared image, the vegetation is generally red, with the lush vegetation being bright red and the vegetation that is in a poor growth state or infested with pests being in dark red or pink. The purified water appears dark blue or black on the color infrared image. However, water bodies turn to light blue when they contain suspended substances.

Figure 3.3 Hue features of gray image and color features of color image.

3.3.1.2 The shape of urban features

The shape, as the most intuitive mark, suggests the appearance of objects by the combination of external surfaces or lines. For example, telephone poles are point-shaped, roads are linear and lakes are planar. The edge extraction operator can be used to extract the edge shape features for

semi-automatic interpretation, as shown in Figure 3.4. The classical edge extraction operator Canny method is used to extract the road edge and assist the road interpretation.

Based on a certain shape descriptor, the object can be interpreted automatically. As shown in Figure 3.5, the ship has typical shape features. Under the top view imaging, the ship is a combination of rectangle and arrow shape. Based on the shape operator, the cruise ship can be automatically extracted. The shape characteristics of roads are obvious and the topological relationship is fixed, which is reflected in the following: (i) a continuous

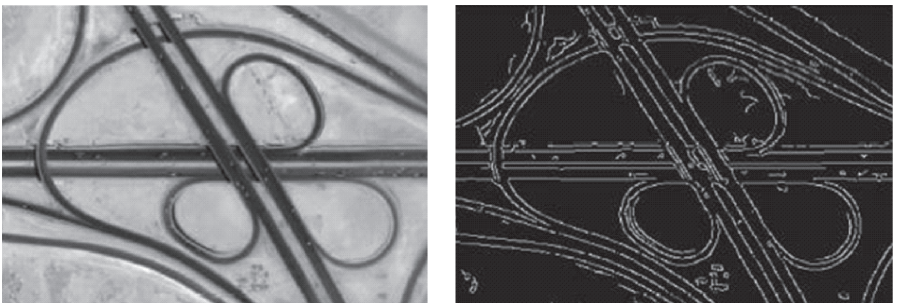

Figure 3.4 Semi-automatic interpretation based on the shape detection operator.

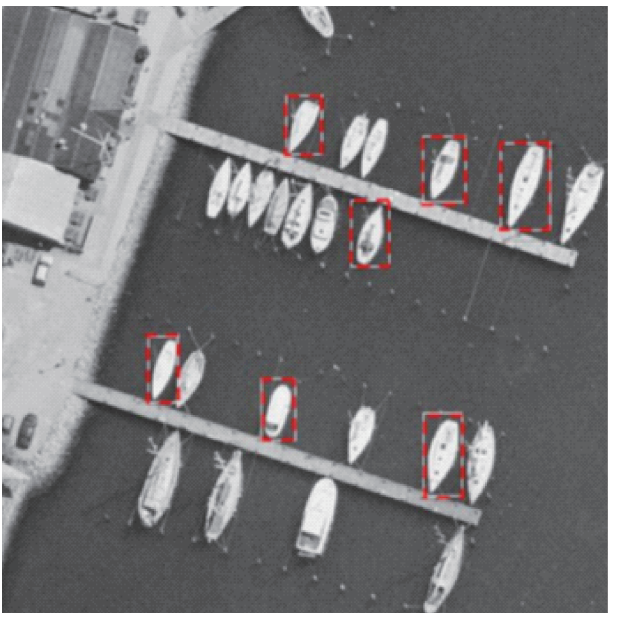

Figure 3.5 Automatic interpretation of cruise ships based on certain shape descriptors.

Downloaded from www.worldscientific.com
by fac sciences de la terre universite annaba on 07/30/24. Re-use and distribution is strictly not permitted, except for Open Access articles.

section of roads presents the same attributes in shape, size, orientation, width, curvature and mode; (ii) the topological relationship of road connection presents cross shape, T shape and Y shape. Based on the shape description of the road, the automatic or semi-automatic extraction of the road can be realized.

For man-made buildings, the typical shape relationship of man-made buildings makes the residential area show typical significance on the remote sensing image. The building monomer in the same building area usually has the same or similar shape and structure (Figure 3.6). In the planning and construction process of the building area, considering the full use of land resources and better lighting and ventilation effects, all buildings often adopt the same orientation, and the arrangement methods

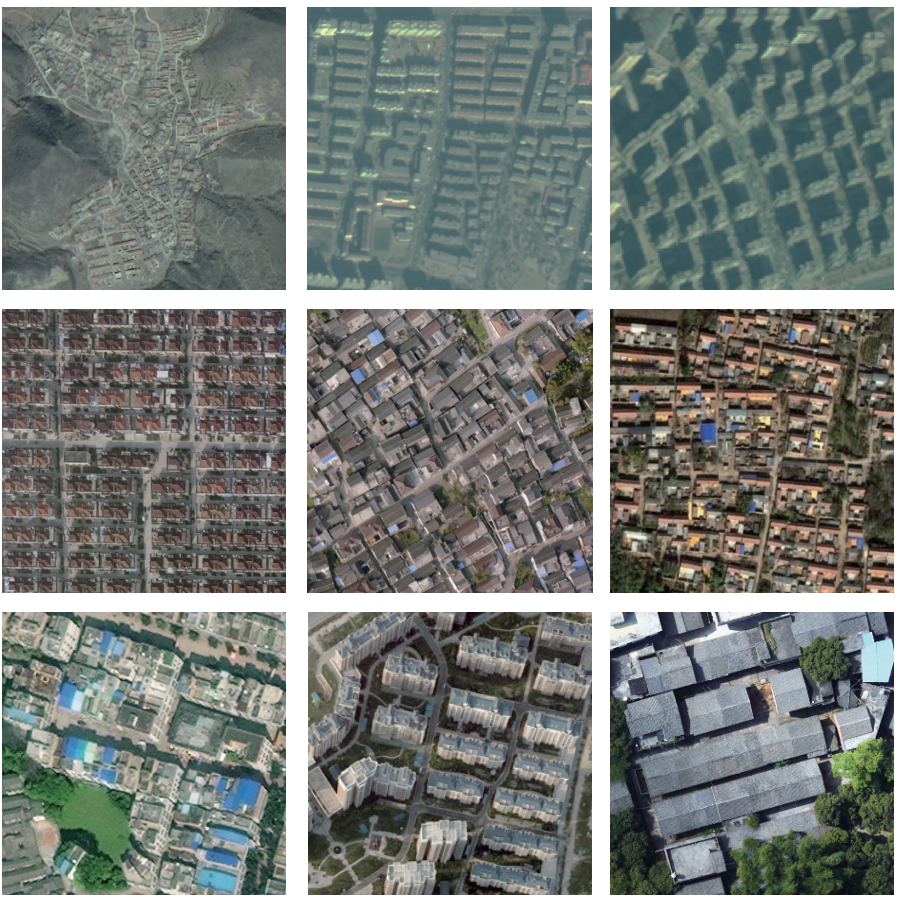

Figure 3.6 Building area under different scenes.

Downloaded from www.worldscientific.com
by fac sciences de la terre universite annaba on 07/30/24. Re-use and distribution is strictly not permitted, except for Open Access articles.

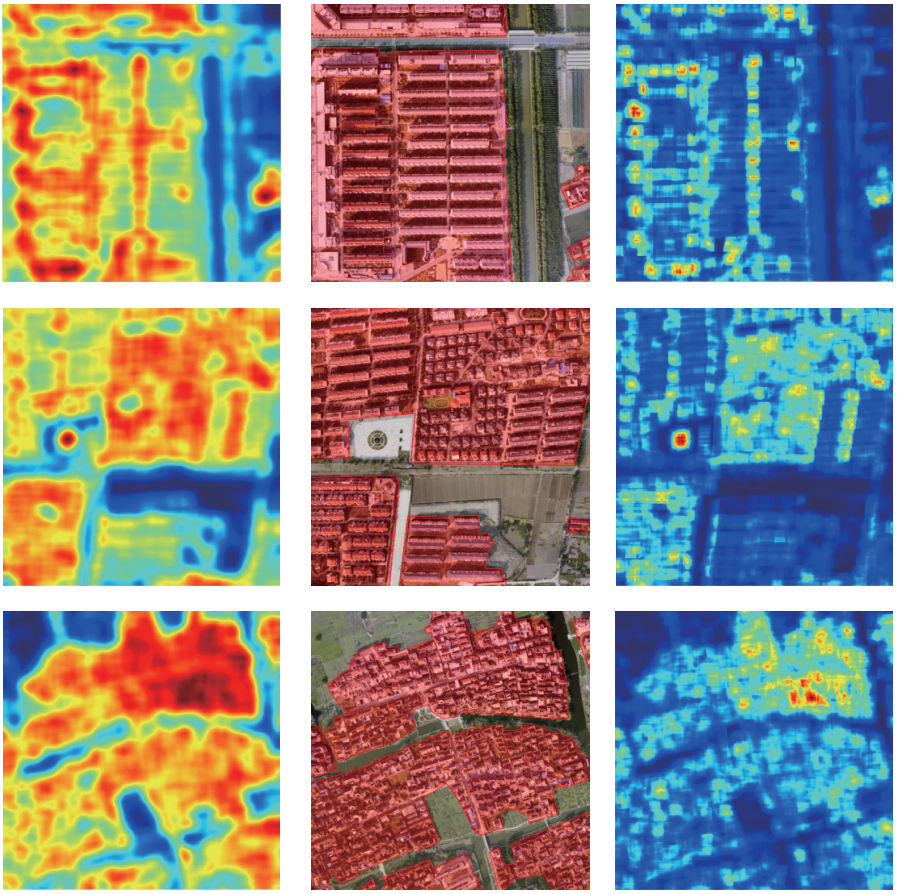

Figure 3.7 Building extraction based on Pantex index.

are mostly determinant, peripheral and point group, so the regular repetition of building units is formed. Based on the feature description of shape texture, e.g., the construction area index is constructed by using edge, shape and other features, such as Pantex and the improved Pantex index, one can realize the automatic extraction of construction area, as shown in Figure 3.7.

3.3.1.3 The shadow of urban features

Due to the occlusion of buildings and other structures in urban areas, shadows are commonly used interpretation signs for urban remote sensing images, as shown in Figure 3.8. Shadows in different types of remote

Downloaded from www.worldscientific.com
by fac sciences de la terre universite annaba on 07/30/24. Re-use and distribution is strictly not permitted, except for Open Access articles.

Figure 3.8 Examples of building shadows.

sensing images tend to have different meanings. Shadows in the visible light range are divided into the umbra, referring to areas where ground objects are not directly exposed to sunlight, and falling shadows, referring to the shadows cast by targets on the ground. In urban environments, shadows of the building benefit the judgment of the height and shape of buildings.

3.3.1.4 The texture of urban features

The texture is composed of repeated tones of many small features. Texture analysis can be carried out from two levels: the first level is from the perspective of the physical meaning of the texture, including texture strength, density, direction, length and width, and the second level is related to the geographical meaning. In urban areas, the texture features of urban grassland and woodland are usually represented as irregular dots, grids or blocks. Figure 3.9 shows examples of urban grassland and trees. The difference between the two texture features can be helpful. For example, the intensity of grass texture is generally higher than that of trees, leading to their distinguishment from images.

Downloaded from www.worldscientific.com
by fac sciences de la terre universite annaba on 07/30/24. Re-use and distribution is strictly not permitted, except for Open Access articles.

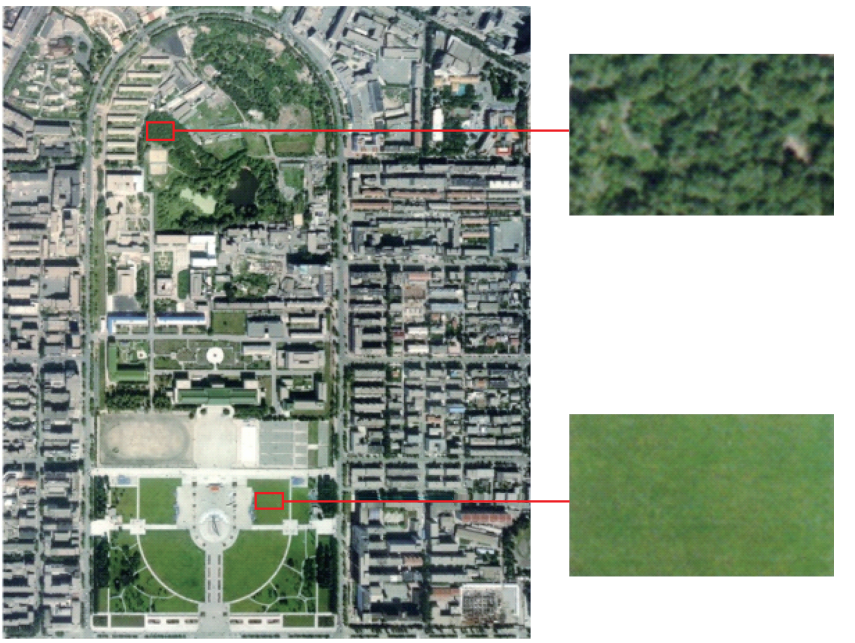

Figure 3.9 Texture characteristics of urban grassland and trees.

3.3.2 Indirect interpretation signs

The indirect interpretation signs include the city's unique topography, soil and soil quality, the relationship among features, vegetation, climate and location. In cities, indirect interpretation signs with distinctive features mainly include the locations of objects and the relationship between objects.

3.3.2.1 Locations of urban objects

Locations represent the geographic environments of features from images, providing information regarding the relationships between the target feature and the background environment, thereby facilitating image interpretation. Figure 3.10 shows the remote sensing image of Yichang City, and the box in the figure is Gezhouba, a water conservancy engineering facility. Given its location across the river combined with its shape feature, it can be easily identified.

Downloaded from www.worldscientific.com
by fac sciences de la terre universite annaba on 07/30/24. Re-use and distribution is strictly not permitted, except for Open Access articles.

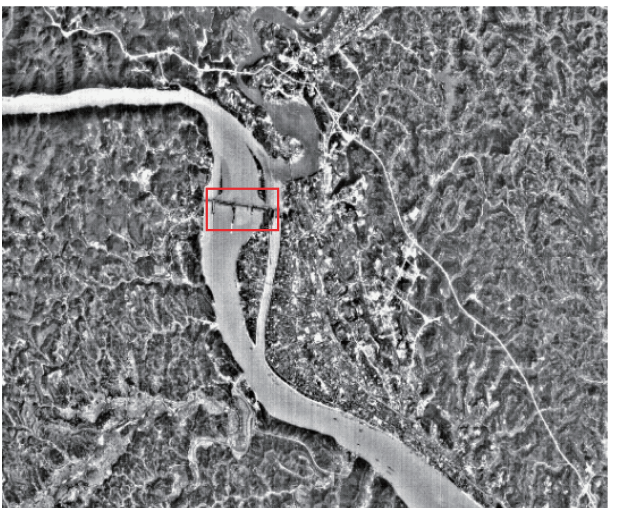

Figure 3.10 Gezhouba in remote sensing image.

3.3.2.2 Interrelationships between urban objects

Urban scenes are complex. The interrelationship between objects usually refers to the spatial configuration between multiple feature targets. For easily recognizable feature targets, they tend to have clear indications of surrounding features. For example, for an airport scene in Figure 3.11, the easy-to-recognize aircraft in the figure helps to identify the bright white linear objects as boarding bridges.

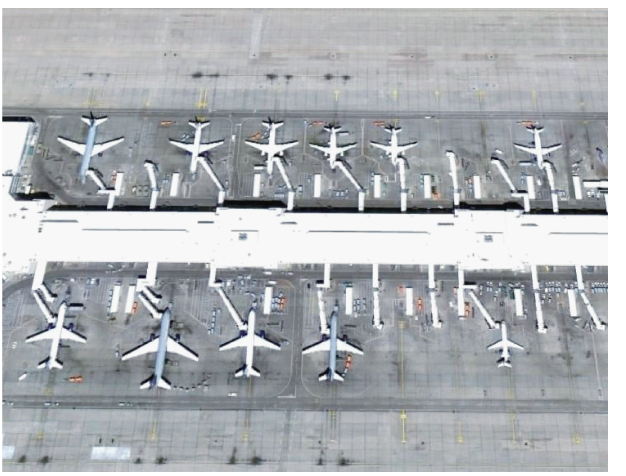

Figure 3.11 Remote sensing image of an airport.

Downloaded from www.worldscientific.com
by fac sciences de la terre universite annaba on 07/30/24. Re-use and distribution is strictly not permitted, except for Open Access articles.

3.4 Methods of Urban Remote Sensing Imagery Interpretation

3.4.1 Visual interpretation

Visual interpretation is a method that relies on human experience and relevant data to extract useful information. The process of manual visual interpretation can be generally divided into the following steps:

1. *Find the targets*: According to various characteristics and interpretation signs, the identification steps follow "from large to small, from easy to difficult, from known to unknown, from high contrast and to small contrast, from macro-observation to microanalysis, etc." For targets with small visual differences, optical or digital enhancement methods can be used to improve image quality and enhance visual effects.
2. *Describe the targets*: Describe the discovered targets in terms of spectral characteristics, spatial characteristics, time characteristics, etc., and establish a list of characteristic target interpretations as the basis for interpretation.
3. *Identify the targets*: Combining existing data with the experience of the interpreter, targets can be identified by reasoning and analysis. The judged targets can only be confirmed after identification. Among the identification methods, field identification is the most reliable approach. After identification, a comparison table of correct and wrong interpretations should be listed so that credibility levels of interpretation can be obtained.
4. *Clear and evaluate the targets*: After the various targets on the map are confirmed, thematic maps can be used to calculate the area of various features. After evaluation, the management, development, planning and other aspects can be proposed. Under normal circumstances, the quality of the visual interpretation of urban remote sensing images depends on the basic knowledge level, the experience accumulation and the understanding of the work area of the interpreter, the remote sensing imaging period and imaging quality, and the work area complexity of the situation.

Downloaded from www.worldscientific.com
by fac sciences de la terre universite annaba on 07/30/24. Re-use and distribution is strictly not permitted, except for Open Access articles.

In the current urban remote sensing studies, human visual interpretation still plays an irreplaceable role. For example, the image classification of supervised learning requires manual sample labeling. The applications of popular deep learning algorithms for remote sensing image analysis also rely on manual labels. The outline of the sample and the annotation of the image are often obtained utilizing manual visual interpretation. Figure 3.12 shows the sample types of bare soil, building, road, pavement, road, vegetation and water bodies in a remote sensing image.

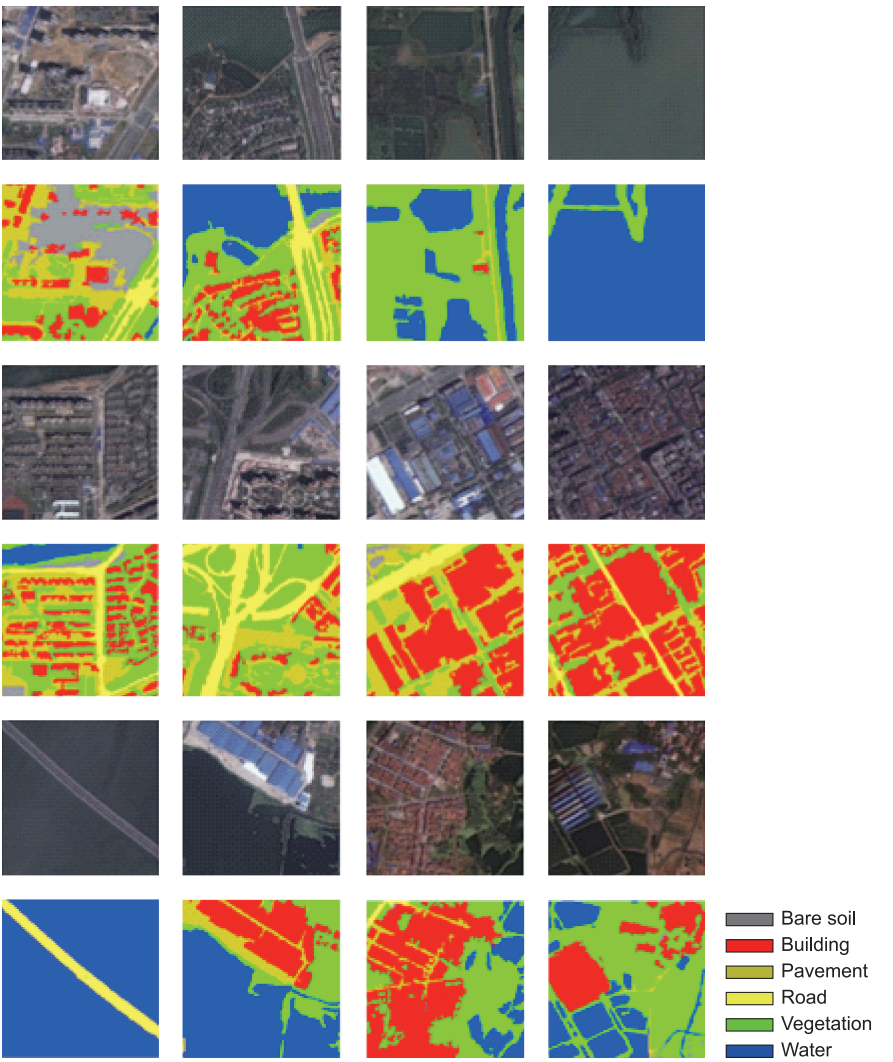

Figure 3.12 Example of labels on a remote sensing image.

Downloaded from www.worldscientific.com
by fac sciences de la terre universite annaba on 07/30/24. Re-use and distribution is strictly not permitted, except for Open Access articles.

Downloaded from www.worldscientific.com
by fac sciences de la terre universite annaba on 07/30/24. Re-use and distribution is strictly not permitted, except for Open Access articles.

3.4.2 Semi-automatic interpretation

The essence of remote sensing image interpretation is to classify remote sensing images, delineate their distribution range and extract useful information. Given that the spectral features of urban remote sensing images are generally complex and given the existence of "the same spectrum of foreign objects and different spectrums of the same objects", it is generally difficult to achieve satisfactory interpretation accuracy for automatic classification. While manual visual interpretation has great flexibility and adaptability, it is labor intensive. In the interpretation process, automatic supervision and classification are used for image areas with obvious features and consistent geological conditions, and for image areas with complex features that are not suitable for automatic classification, manual interpretation is used to extract thematic information. Without increasing the complexity of the system, the respective advantages of the human brain and the computer can be fully utilized to improve the speed and accuracy of interpretation.

Urban human–computer interaction interpretation requires a combination of manual visual interpretation and digital image processing, remote sensing and geographic information systems, geoscience knowledge and information technology. Common human–computer interaction interpretation processes include a manual selection of interpretation scope, image preprocessing, automatic image classification, fragment synthesis, line drawing filling and image editing. A few application examples are briefly introduced below.

3.4.2.1 Large-scale scene interpretation of urban remote sensing images

Urban remote sensing applications usually require the image tiling process that divides images into small and different scenes. Scene interpretation can refer to dividing the city into different functional areas according to social and cultural attributes. It can also refer to the process of dividing a city into densely built areas according to the natural attributes of features. Urban remote sensing image scene interpretation can be conducted by first using a computer automatic segmentation algorithm to segment the image into homogenous block regions in large-scale scenes and then visually interpreting and classifying the scenes of these homogenous regions.

Downloaded from www.worldscientific.com
by fac sciences de la terre universite annaba on 07/30/24. Re-use and distribution is strictly not permitted, except for Open Access articles.

3.4.2.2 *Manually assisted interpretation of urban street scene images*

Due to the complexity of urban remote sensing image scenes, resulting from shadows and occlusions, to list a few, misclassifications occur after the automatic interpretation by computers. Thus, manual corrections should be made after automatic interpretation. For urban shadows and occluded areas, manual judgments can be made in conjunction with urban street scene images, thus correcting the interpretation results. Figure 3.13 shows the street view image under the occluded street trees and the street view image in the shadow area. The use of street view maps for manual interpretation and computer interpretation can make up for the lack of information in remote sensing images.

Figure 3.13 An example of the manual interpretation of urban street scene images.

3.4.2.3 *City interactive interpretation guided by vector features*

For images with inconspicuous road features, road interpretation often adopts human–computer interaction, requiring manual selection of seed points, centerlines or planar areas for guidance, followed by automatic interpretation through area growth algorithms. Figure 3.14 shows an example of the interpretation of urban roads in an interactive manner.

Figure 3.14 Guidance methods in urban road interpretation: (a) Edge guidance; (b) Road width guidance.

3.4.3 Automatic interpretation based on machine learning

Machine learning-based urban remote sensing image interpretation needs to extract and optimize the spectral information and spatial information via feature mining techniques to better represent the pattern information of the samples in the spectral image. The mined features are later used for pattern recognition or pattern classification. Given the necessity of training samples, common classification methods include unsupervised classification methods, supervised classification methods and semi-supervised classification methods.

Unsupervised classification methods, relying on pattern mining from samples, do not require prior knowledge. Given the fact that they do not need field marking, they are easy to implement. The supervised classification methods use prior information in the labeled training samples to train the classifier in order to obtain the parameters of the classifier. The well-trained classifiers are later used to classify the data of unknown categories.

Random forest (RF) and support vector machine (SVM) are the most commonly used machine learning methods. RF belongs to the decision tree algorithm, which constructs multiple decision trees and combines them to obtain a more accurate and stable prediction. Compared with a single decision tree, the random forest algorithm obtains the classification results of each decision tree for the final classification, leading to its higher stability and

Downloaded from www.worldscientific.com
by fac sciences de la terre universite annaba on 07/30/24. Re-use and distribution is strictly not permitted, except for Open Access articles.

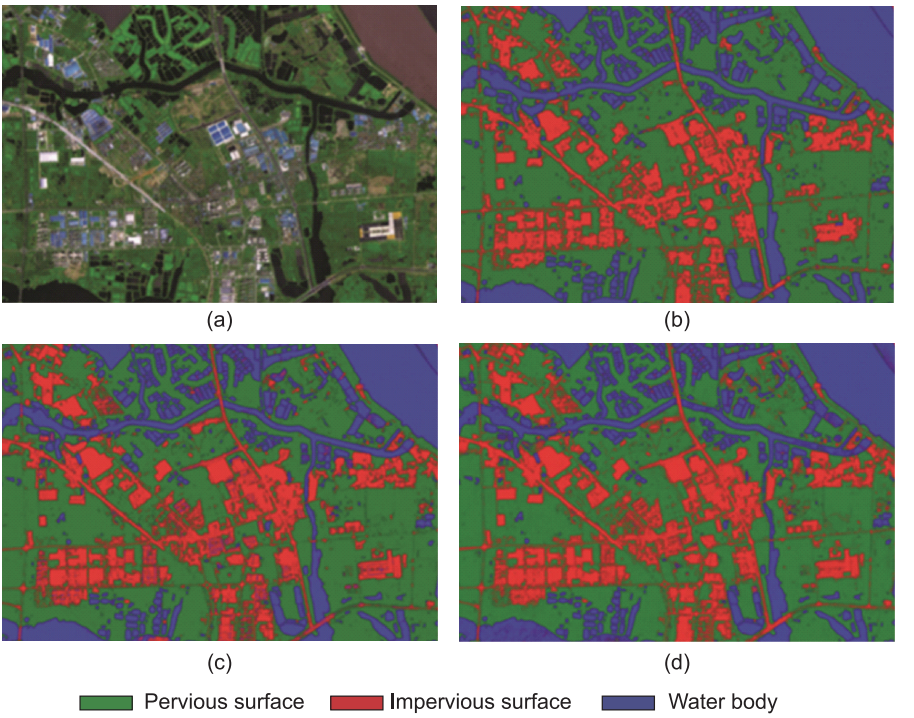

Figure 3.15 Comparison example of impervious surface extraction results from RF, SVM and deep learning: (a) Original image; (b) Deep learning; (c) Random forest; (d) Support vector machine.

accuracy. The main idea of SVM is to establish a decision surface to maximize the classification interval between positive and negative examples. General SVM is effective for two kinds of sample problems. Figure 3.15 shows the examples of impervious surface extraction results from RF and SVM.

3.4.4 Automatic interpretation based on deep learning

Recent years have seen great progress in the development of smart sensors. Early automatic interpretation refers to the use of content-based image retrieval and other methods, as well as simpler template-matching methods. According to the geometric characteristics or unique texture characteristics of the target, the integration of multiple criteria can be considered through automatic interpretation. The emerging algorithms that include neural

Downloaded from www.worldscientific.com
by fac sciences de la terre universite annaba on 07/30/24. Re-use and distribution is strictly not permitted, except for Open Access articles.

networks and deep learning can take advantage of the massive training samples, thus leading to automatic interpretation. According to different tasks, the applications of deep learning to the automatic interpretation of remote sensing images are mainly reflected in image retrieval and semantic segmentation, object detection and instance segmentation.

3.4.4.1 Applications in image automatic retrieval

The production capacity of remote sensing images has been greatly improved in recent years. The automatic retrieval of remote sensing images is very important for the management and applications of urban remote sensing images. As remote sensing images usually cover extensive areas with complex features, they are usually divided into fixed-size tiles (Zhou *et al.*, 2017). These tiles are further classified. Figure 3.16 shows an example of single-tag retrieval of remote sensing image tiles.

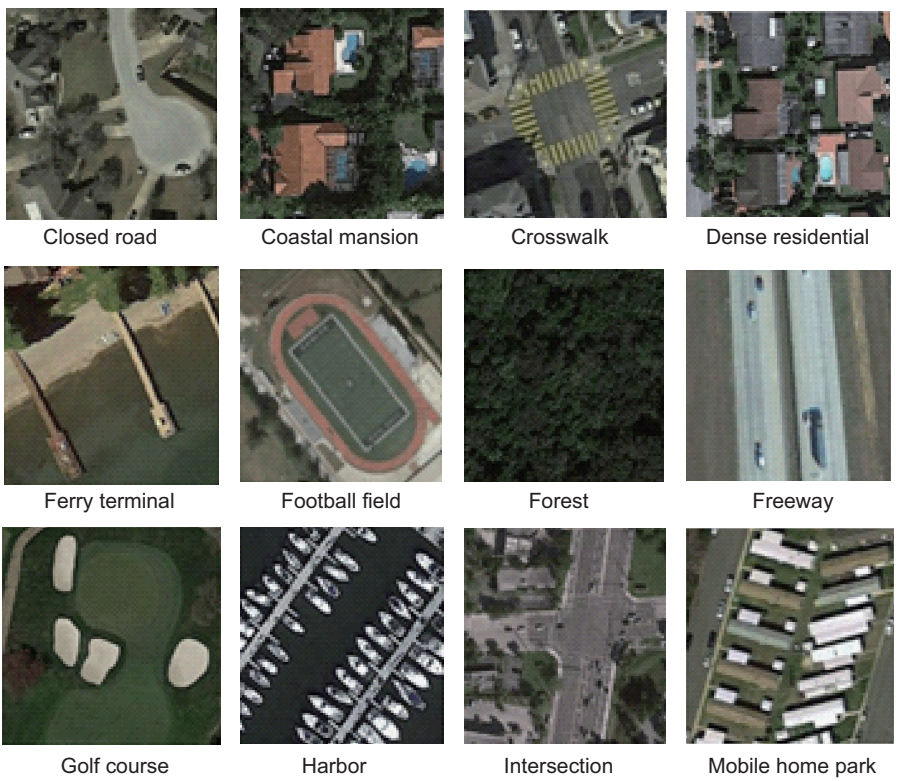

Figure 3.16 An example of single-label retrieval of urban remote sensing image.

Downloaded from www.worldscientific.com
by fac sciences de la terre universite annaba on 07/30/24. Re-use and distribution is strictly not permitted, except for Open Access articles.

Downloaded from www.worldscientific.com
by fac sciences de la terre universite annaba on 07/30/24. Re-use and distribution is strictly not permitted, except for Open Access articles.

3.4.4.2 *The applications of semantic segmentation*

Semantic segmentation of urban remote sensing images refers to the segmentation of one or more types of urban scenes at the pixel level, e.g., segmenting the image into artificial buildings, roads, vegetation and water bodies. The meaning of semantic segmentation is closer to traditional remote sensing image classification. Taking the single-target segmentation as an example, the label of the target pixel set is set to 1 as a positive sample, and other image regions are set to 0 as a negative sample. The segmentation task aims to learn the feature expression from the original image, aiming to complete the binary segmentation of images. Figure 3.17 shows an example of the interpretation of the results of road semantic segmentation.

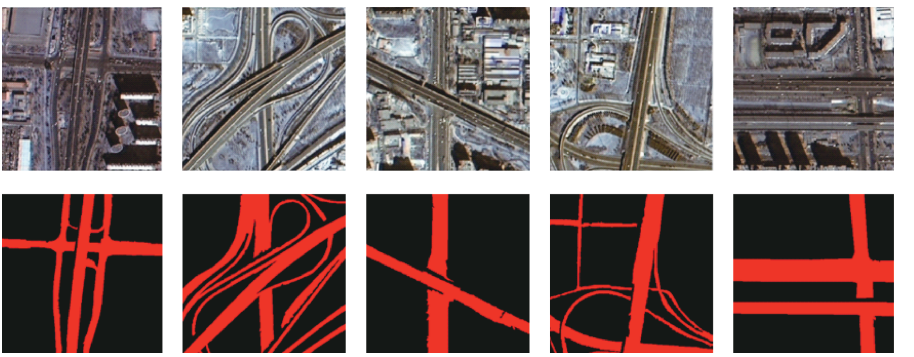

Figure 3.17 Road semantic segmentation results.

3.4.4.3 *The applications in urban object automatic detection*

Automatic detection of urban objects is similar to image retrieval and semantic segmentation, however, with notable differences. Remote sensing image retrieval represents a probabilistic ranking of the categories of objects found in image blocks without identifying the number and precise location of objects. Semantic segmentation is a pixel-level operation, not at the target or object level. Target detection refers to identifying and locating "an instance of a certain type of object", e.g., a certain house in the building category. Fully automatic target recognition is usually achieved by the detection of the optimal containment box. If the target to be retrieved is an airplane or a building, the circumscribed rectangle of its outline is its containment box.

Containment box detection is also called containment box regression. As described above, image retrieval, semantic segmentation and category labels are all discrete quantities, which can be summarized as a classification problem. In comparison, the labels that correspond to the containment box regression are continuous quantities, i.e., values in the four coordinates. Regression techniques can be used to obtain the optimal estimates of these continuous quantities (Xia *et al.*, 2018). Figure 3.18 shows examples of ship target detection from remote sensing images, where red boxes are the obtained containment boxes.

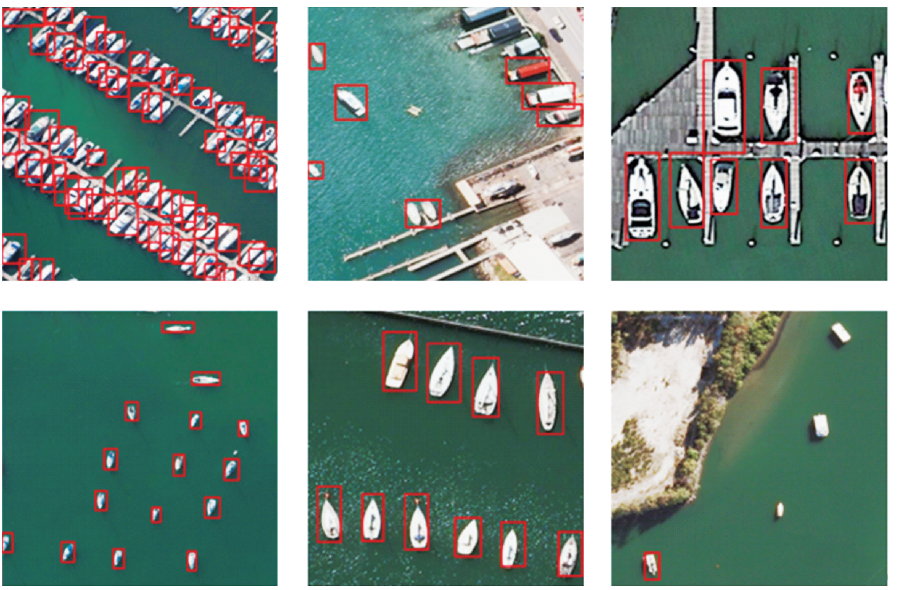

Figure 3.18 Examples of ship detection from remote sensing images.

3.4.4.4 The applications of automatic segmentation of urban building entities

The applications of automatic segmentation of urban building entities are higher tasks compared to target recognition, as they require not only precise positioning of each target (Hafiz and Bhat, 2020) but also foreground segmentation of objects in the containment box. Figure 3.19 shows an example of city instance segmentation.

Downloaded from www.worldscientific.com
by fac sciences de la terre universite annaba on 07/30/24. Re-use and distribution is strictly not permitted, except for Open Access articles.

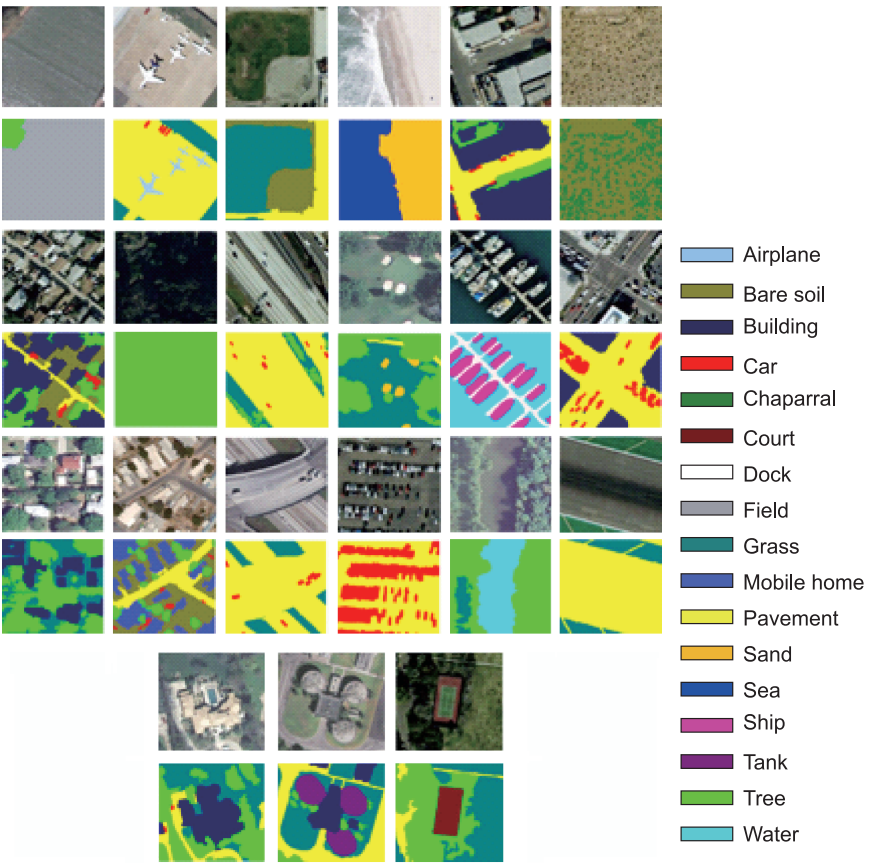

Figure 3.19 An example of automatic segmentation of urban building instances.

3.4.5 Interpretation of remote sensing big data

The rapid development of earth observation systems and intelligent computing technology with the integration of heaven and earth establishes a great venue for the progress of remote sensing science and technology. Remote sensing technology has entered a big data era, characterized by data model-driven and big data intelligent analysis. The developing trend of big data remote sensing interpretation includes the construction of an object-oriented remote sensing knowledge base, the big data intelligent information extraction strategy integrating remote sensing knowledge and deep learning algorithm, the construction of a spatio-temporal spectral angle

Downloaded from www.worldscientific.com
by fac sciences de la terre universite annaba on 07/30/24. Re-use and distribution is strictly not permitted, except for Open Access articles.

model and the integrated application of multi-source data. Remote sensing applications are expected to be quantitative, real time and intelligent.

Downloaded from www.worldscientific.com
by fac sciences de la terre universite annaba on 07/30/24. Re-use and distribution is strictly not permitted, except for Open Access articles.

Questions

1. Give examples of interpretation needs for urban remote sensing images.
2. What are the signs of direct interpretation and indirect interpretation of urban remote sensing images? What are the similarities and differences between these two?
3. Please draw a flow chart of urban remote sensing image interpretation based on a practical application.
4. What are the characteristics of the three interpretation methods, i.e., manual interpretation, human–computer interaction interpretation and fully automatic interpretation of urban remote sensing images? What are the practical applications of these three methods with examples?
5. What are the connections and differences between remote sensing image interpretation and information extraction, classification, change detection and other tasks?

References

Hafiz A M, Bhat G M. 2020. A survey on instance segmentation: State of the art. *International Journal of Multimedia Information Retrieval*, 9: 171–189.

Xia G S, Bai X, Ding J, Zhu Z, Belongie S, Luo J B, Datcu M, Pelillo M, Zhang L P. 2018. DOTA: A large-scale dataset for object detection in aerial images. *IEEE Conference on Computer Vision and Pattern Recognition*. Salt Lake City, UT, USA.

Zhou W, Newsam S, Li C M, Shao Z F. 2017. PatternNet: A benchmark dataset for performance evaluation of remote sensing image retrieval. *ISPRS Journal of Photogrammetry and Remote Sensing*, 145(A): 197–209.

This page intentionally left blank

Downloaded from www.worldscientific.com
by fac sciences de la terre universite annaba on 07/30/24. Re-use and distribution is strictly not permitted, except for Open Access articles.

Downloaded from www.worldscientific.com
by fac sciences de la terre universite annaba on 07/30/24. Re-use and distribution is strictly not permitted, except for Open Access articles.

Chapter 4

Preprocessing Methods of Urban Remote Sensing Imagery

The continuous development of modern remote sensing technology has led to an increasing amount of remote sensing images with improved spatial resolution, providing new applicable directions. There are several high-resolution platforms including IKONOS, QuickBird and WorldView-2. Due to the influence of external factors such as sensor performance, bad weather and uneven illumination, the obtained images often have certain issues, such as edge blur, color distortion, noise pollution, low contrast and shadow occlusion, resulting in poor image quality and seriously affecting downstream tasks, such as image interpretation and image information extraction. Therefore, to improve image quality and extract more available information, image preprocessing algorithms (e.g., cloud detection, shadow detection, tone adjustment, super-resolution reconstruction and image fusion) have become essential components contents for image analysis and understanding.

In this chapter, several methods of cloud detection and shadow detection of urban remote sensing images, several main methods of tone adjustment of urban remote sensing images, the main methods of super-resolution reconstruction of urban remote sensing images and the mainstream methods of image fusion are introduced. There exist many kinds of image quality issues. Therefore, before image enhancement, we should analyze the existing images problems and select appropriate image preprocessing methods.

The image preprocessing algorithm is an important part of image analysis and understanding. This chapter introduces the principles and main methods of cloud detection, shadow detection, image enhancement, super-resolution reconstruction and fusion of urban remote sensing images.

These methods are mainly to improve the image quality of urban remote sensing information extraction and other applications. Combined with the image quality characteristics and application requirements, the required image enhancement methods should be selected.

4.1 Cloud Detection Methods for Urban Remote Sensing Imagery

According to the statistical results of international satellite cloud climate flux data, the proportion of annual average cloud coverage on the global surface is as high as 66%. Due to the impact of cloud cover, a large amount of surface information in remote sensing images is attenuated or even lost, posing challenges for many data processing steps such as image registration and image fusion. Cloud pollution often leads to poor quality and low utilization of remote sensing data, which eventually brings difficulties to the analysis and application of remote sensing images (Figure 4.1). Therefore, cloud detection plays a vital role in remote sensing image processing.

Many cloud detection methods have been proposed, which can be categorized into physical methods, detection methods (based on cloud texture and spatial characteristics), pattern recognition detection methods, and comprehensive optimization methods. Among them, the most widely used method is the physical threshold method, notably an algorithm

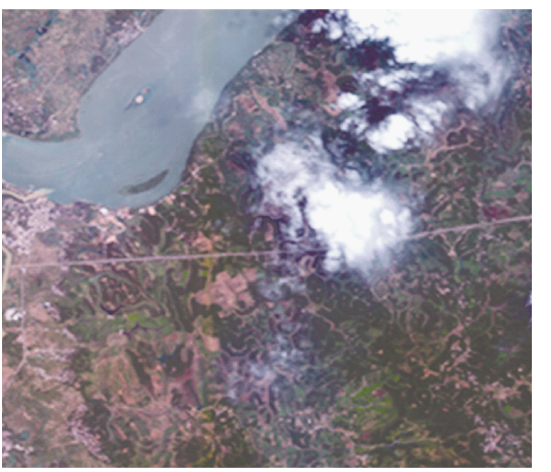

Figure 4.1 Cloud occlusion in urban remote sensing images.

Downloaded from www.worldscientific.com
by fac sciences de la terre universite annaba on 07/30/24. Re-use and distribution is strictly not permitted, except for Open Access articles.

Downloaded from www.worldscientific.com
by fac sciences de la terre universite annaba on 07/30/24. Re-use and distribution is strictly not permitted, except for Open Access articles.

proposed by Saunders and Kriebel (1988), which selects a group of physical thresholds for cloud detection. The cloud detection method proposed by Ackerman *et al.* (1998) is applied to MODIS data, which comprehensively considers the threshold detection results of several spectral bands and further judges whether a given pixel belongs to the cloud or not. Compared with the physical threshold method, this method is more accurate. Under some specific conditions (e.g., when the underlying surface is a desert area at night or and when the underlying surface is a coastline, river or inland lake), however, it fails to make the right prediction, given the similarity in reflectivity of cloud and other objects.

As the physical threshold method is based on the data of certain spectral bands, it can be limited to specific remote sensors and has poor universality. Some cloud detection methods only work on local geographical areas or background areas, as mentioned by Ebert and Elizabeth (1987), Key *et al.* (1989), and Welch *et al.* (1992). These cloud detection methods face difficulties when dealing with the distinction between clouds and surfaces in polar areas; Garand (2009) proposed an automatic cloud pattern classification method based on height, albedo, shape, cloud layered features and two-dimensional power spectrum features of images. However, it is only applicable to a situation with an ocean background. The development of artificial intelligence technology offers a new solution, but most of them rely on auxiliary data for threshold settings. For example, the full probability Bayesian method of Merchant *et al.* (2010) uses the prediction data of climatology and digital weather forecast to establish a priori knowledge. The fuzzy logic classification method proposed by Baum *et al.* (1997) is able to distinguish clear sky and is cloud based on the type of air mass. For thin and low clouds, due to the low brightness contrasting with the underlying surface, it is difficult to establish reliable training data or set optical thresholds. Therefore, remote sensing image cloud detection is a challenging task.

As different features have different cloud detection capabilities, how to extract and optimize cloud features is the key problem of cloud detection. The types and shapes of clouds are diverse, leading to difficulty in describing them with a single shape and size feature. The physical properties of clouds include high reflectivity and natural crystal shape. Imaging attributes can be summarized as large-scale and unique spatial distribution. The characteristics of high reflectivity and large scale are spectral characteristics, the characteristics of natural crystal are fractal geometric characteristics, and the unique spatial distribution is texture characteristics.

Downloaded from www.worldscientific.com
by fac sciences de la terre universite annaba on 07/30/24. Re-use and distribution is strictly not permitted, except for Open Access articles.

The cloud layer scatters in the visible light range of 0.3–0.7 μm, and the near-infrared spectrum ranges from 0.7 μm to 2.5 μm with high reflectivity in this band range. However, if the wavelength decreases, the spectral reflectivity of the cloud tends to increase. When the wavelength decreases to 0.7 μm, the reflectivity of the cloud is close to 1. In the range of 0.58–0.68 μm, ground objects in the clear sky and cloudless area present lower reflection, while the reflection of snow is higher, with a reflectivity of 0.6. The wavelength of 1.38 μm is the strong water vapor absorption band because the water vapor affects the reflection of the surface, making it difficult to penetrate the previous vapor and then reach the sensor inlet, leading to the low reflectivity of the low cloud layer and high reflectivity of the high cloud layer.

Texture features, as one of the three significant visual features, can take into account the image structure from the macro and describe the image characteristics from the micro level. The texture characteristics in a pixel block on the image are closely related to its gray distribution. As clouds present varying shapes and sizes, their texture is random but very different from the underlying surface features. The grayscale of the cloud is concentrated, distributed in a certain range, and the gray value is generally higher than the underlying surface features. For the three texture features of the cloud, i.e., gray level co-occurrence matrix, Fourier power spectrum and wavelet, the classification ability of the wavelet feature is the best, followed by gray-level co-occurrence matrix feature and the Fourier power spectrum feature. In the gray-level co-occurrence matrix, the contrast, mean, variance, the sum of squares, correlation, homogeneity (angular second-order moment) and entropy can be selected, among which entropy has the best classification ability, followed by homogeneity. For the three common texture feature extraction methods, i.e., wavelet transform (WT), singular value decomposition (SVD) and gray level-based co-occurrence matrix (GLCM), these feature extraction methods can be applied to neural network for comparison. Results suggest that the accuracy of the three-features cloud classification is close. From the classification effect, however, SVD and GLCM are slightly better than WT. In addition, GLCM requires large computational power. Therefore, SVD is regarded as an efficient and effective method.

In addition, the maturity of pattern recognition, machine learning and computer vision technology has led to a series of breakthroughs in the field of image classification. The cloud detection method based on classifiers without determining large-scale threshold or optimal eigenvalue has become

Downloaded from www.worldscientific.com
by fac sciences de la terre universite annaba on 07/30/24. Re-use and distribution is strictly not permitted, except for Open Access articles.

popular. Movia *et al.* (2016) used different bands to calculate exponential features. Combined with the unsupervised classification method, it realizes shadow detection and removal of RGB-VHR images for land use analysis. Surya and Simon (2015) applied spectral image matching technology to transform color and generate ratio images and further applied the fuzzy *C*-means clustering method for cloud detection. Tian *et al.* (2000) designed a probabilistic neural network classifier that uses temporal context information to track changes in image sequences with the maximum likelihood (ML) criterion in training and updating schemes. Vivone *et al.* (2014) introduced a new penalty term in the classical maximum a posteriori probability Markov random field (MAP-MRF) method to reduce the misclassification of pixels close to the edges of the cloud. To realize automatic feature extraction, a large number of deep learning models have been applied to target detection with pixels or segmented superpixels as the research object in recent years. These models mainly focus on convolution and pooling operations to achieve cloud classification. Some examples of cloud detection results based on a convolutional neural network are shown in Figure 4.2. Figures 4.2(a)–(d) represent the original cloud detection images in different scenes and (e)–(h) represent the corresponding cloud detection results.

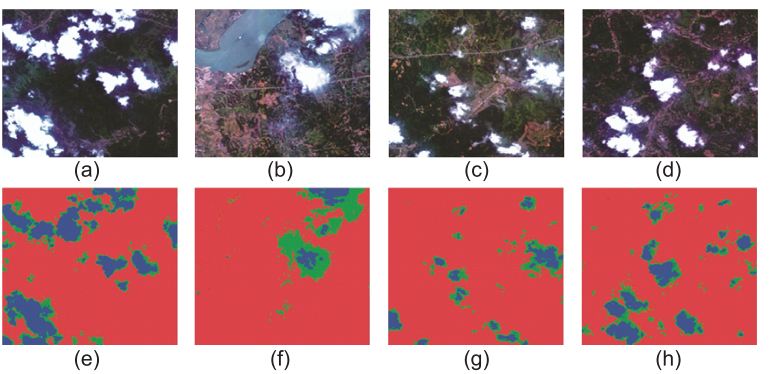

Figure 4.2 An example of cloud detection based on a convolutional neural network.

4.2 Shadow Detection Methods for Urban Remote Sensing Imagery

With the development of remote sensing technology, the spatial resolution of satellite sensors has been greatly improved. High-resolution remote sensing

Downloaded from www.worldscientific.com
by fac sciences de la terre universite annaba on 07/30/24. Re-use and distribution is strictly not permitted, except for Open Access articles.

images provide us with more detailed information, creating a new venue where many advanced remote sensing applications are possible. However, the ground object information in remote sensing images is relatively complex. Realizing the automatic judgment and extraction of ground object information has always been challenging in many fields, such as remote sensing image processing, pattern recognition and computer vision, to list a few. Due to the low orbit of a high-resolution satellite, ground object shadow is inevitable, and shadows in images have a greater and greater impact on image analysis and processing. With the development of urbanization, in the high-density urban environment, the imaging light source can be blocked by buildings, thus producing shadows, weakening the optical feature information in the image and affecting the hue, shape and other features of the shadow coverage area and leading to information loss and the degradation of image quality.

On the one hand, shadows can affect image matching, pattern recognition, feature extraction and digital photogrammetry. In image matching, due to the blur of shadow noises, the ground feature in the image becomes inconspicuous which affects the accuracy and speed of image pair matching. In pattern recognition, shadows can be confused with surface objects with low gray value, increasing the error rate of pattern recognition. In the process of feature extraction, shadows can block the surface information and destroy the continuity of the edge of the feature, negatively affecting the feature extraction of the digital images. In digital photogrammetry, shadows can affect automatic triangulation and orthophoto map generation. On the other hand, shadows are able to provide some additional information. The shapes and sizes of shadows can be used to determine the intensity and position of the light source and infer the spatial information of the light source. The length and width of the shadow can reflect the height of the building and the area projection of the building plane in the sun direction, so as to estimate the height and plot ratio of buildings. At the same time, in the three-dimensional modeling of Digital City Engineering, shadows are able to increase the three-dimensional and spatial sense of the observer (Figure 4.3).

Studies on shadow detection were initially carried out in the field of computer vision. With the rapid development of digital images in the past ten years, more and more attention is being paid to shadow detection in video stream information processing. The specific applications are reflected in fields of video surveillance, traffic control and pedestrian navigation. Shadow

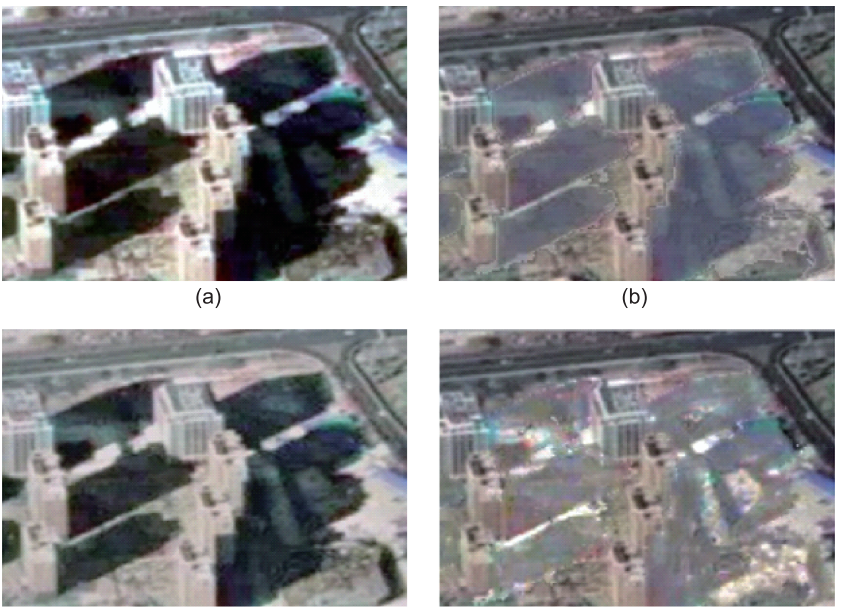

Figure 4.3 Shadow detection and removal in urban remote sensing images.

detection in remote sensing can be divided into feature-based detection method and model-based method.

Feature-based shadow extraction generally uses the geometric and optical properties of shadows (e.g., color, shadow structure, boundary). It performs shadow segmentation relying on the fact that the brightness of the shadow region on the image is lower than that of the surrounding pixels. For example, HSI, HSV, YCBCR and other invariant color spaces can be used for shadow attribute analysis on high spatial resolution aerial images. Salvador *et al.* (2001) first extracted the candidate shadow region using the photometric color invariant feature and then compared the edge detection results of the luminance image and photometric color invariant image according to the assumed conditions to obtain the shadow region.

Model-based shadow detection methods usually use simple shadow features combined with a priori knowledge of the illumination of the target scene to extract shadows. As the prior model of the illumination of the target scene is not easy to obtain, model-based shadow detection methods are suitable only in specific scenes. Stevens (2001) proposed a technical method for shadow detection based on light direction, target building height and digital topographic map. Jiang and Ward (1992) used the light

Downloaded from www.worldscientific.com
by fac sciences de la terre universite annaba on 07/30/24. Re-use and distribution is strictly not permitted, except for Open Access articles.

direction combined with the geometric model to detect the shadow in a simple environment. An example of shadow detection results of continuous threshold is shown in Figure 4.4.

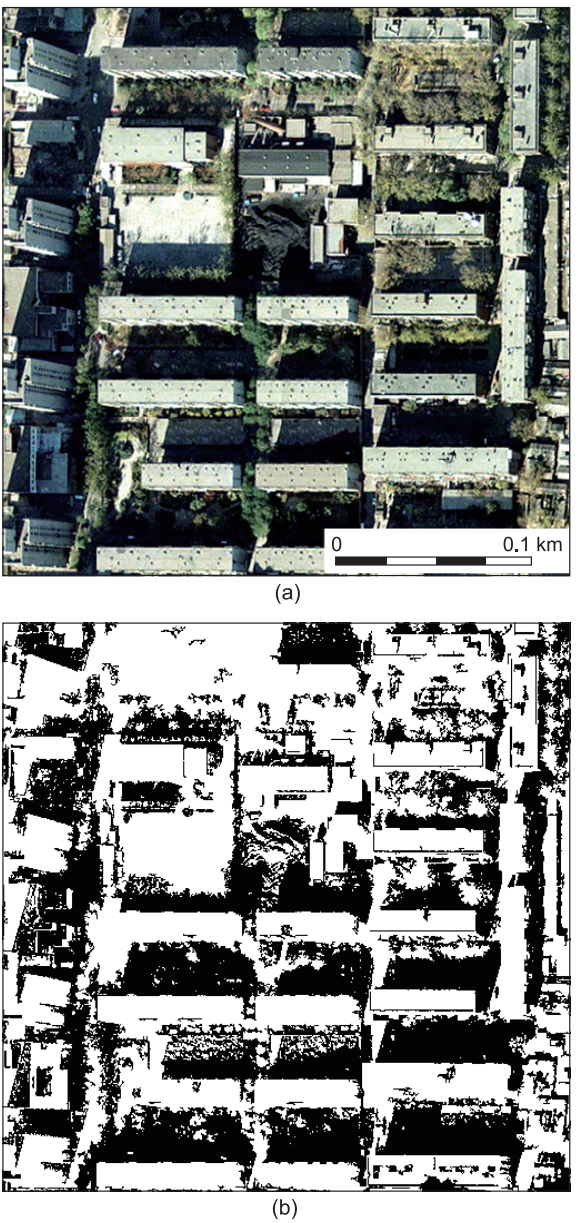

Figure 4.4 An example of shadow detection results of the continuous threshold: (a) Original image; (b) Shadow detection results.

Downloaded from www.worldscientific.com
by fac sciences de la terre universite annaba on 07/30/24. Re-use and distribution is strictly not permitted, except for Open Access articles.

Downloaded from www.worldscientific.com
by fac sciences de la terre universite annaba on 07/30/24. Re-use and distribution is strictly not permitted, except for Open Access articles.

4.3 Image Enhancement Methods for Urban Remote Sensing Imagery

The main purpose of image enhancement is to improve the image quality and visual effect, making images more suitable for visual observation or machine analysis and recognition. Image enhancement is closely related to object characteristics and processing purposes. Although many processing methods have been proposed, they tend to have strong pertinence, and there is no general image enhancement method suitable for all kinds of situations. To meet the demands of different applications, many classical image enhancement methods have been developed. The existing image enhancement methods can be divided into traditional spatial domain and frequency domain image enhancement methods, and image enhancement methods based on fuzzy set theory, and based on visual characteristics.

Spatial image enhancement methods directly processes image pixels and are mainly divided into two categories: spatial transformation enhancement methods and spatial filter enhancement methods.

Frequency domain image enhancement transforms the original image into frequency domain space in some form, uses the feature characteristics of this space to modify different frequency components and finally transforms it back into the original image space. Common image transformation methods include Fourier transform, discrete cosine transform (DCT), wavelet transform, Hotelling transforms, Radon transform, Walsh and Hadamard transform. Frequency domain image enhancement is achieved by the application of filters. Different filters drop and retain different frequencies, leading to filtered enhancement effects. Commonly used filters include low-pass filter, high-pass filter, homomorphic filter, band-pass filter and band-stop filter.

Due to the complexity of urban remote sensing image scenes and the correlation among pixels, the distribution of gray value and color value of the image is uncertain and inaccurate, i.e., fuzziness. The fuzzy set theory can be used to solve the problem of fuzziness and can be introduced into the field of image enhancement. The basic steps of the image enhancement method based on fuzzy set theory are as follows: (i) images are transformed from spatial domain to fuzzy domain; (ii) fuzzy enhancement is carried out through some transformation function in the fuzzy domain; and (iii) after the transformation, images are inversely transformed from fuzzy domain to

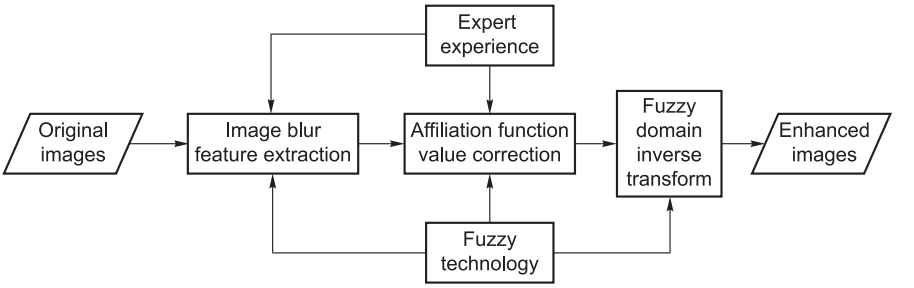

Figure 4.5 Basic framework of fuzzy enhancement.

spatial domain, and the enhanced images are obtained. The performance of the image enhancement method based on fuzzy set theory largely depends on the enhancement transform function. Thus, one of the essential steps is to select the appropriate an enhancement transform function in the fuzzy domain. The basic framework of fuzzy enhancement is shown in Figure 4.5.

Image enhancement methods based on visual characteristics can be mainly divided into two categories. One is the enhancement algorithm based on Retinex theory; the other is to transform only the brightness component in the color space model, keeping the tone unchanged to ensure that no color offset occurs. Figure 4.6 shows the effect of the multi-scale Retinex image enhancement algorithm.

Based on Retinex theory, the enhancement algorithm can improve the color constancy, compress the dynamic range of the image and improve the image contrast. However, on the premise of meeting the characteristics of visual perception, the color and brightness information are mixed, which changes the hue and leads to different degrees of color distortion.

In the color space model, the enhancement method that only transforms the brightness component while keeping the tone unchanged is usually to convert the image from RGB space to HSI or HSV space to eliminate the correlation of color components, where "H" represents hue, "S" represents saturation, and "I" or "V" represents brightness. In the process of image enhancement, the color is constant by adjusting the S, I or V component and keeping the H component unchanged. This kind of algorithm needs to convert the color space, which is time-consuming and cannot realize the real-time image enhancement.

Downloaded from www.worldscientific.com
by fac sciences de la terre universite annaba on 07/30/24. Re-use and distribution is strictly not permitted, except for Open Access articles.

Downloaded from www.worldscientific.com
by fac sciences de la terre universite annaba on 07/30/24. Re-use and distribution is strictly not permitted, except for Open Access articles.

(a)

(b)

Figure 4.6 Rendering of multi-scale Retinex image enhancement algorithm: (a) Original image; (b) MSR_HSI algorithm-enhanced image.

Downloaded from www.worldscientific.com
by fac sciences de la terre universite annaba on 07/30/24. Re-use and distribution is strictly not permitted, except for Open Access articles.

The spatial domain enhancement methods and frequency domain enhancement methods of urban remote sensing images are relatively simple, but these methods have great limitations. They do not consider the fuzziness of the image, but simply stretch the contrast of the whole image or eliminate noise. However, while eliminating noise, it also leads to the loss of image detail information, color distortion and so on.

The urban remote sensing image enhancement method based on fuzzy set theory has a good image enhancement effect on certain occasions. The key of this method is to select the appropriate enhancement transform function in the fuzzy domain, but the enhancement transform function largely depends on the characteristics of the original image, and the image itself is complex, so this method has not been widely used.

The urban remote sensing image enhancement method based on artificial neural network has a complex model and many parameters. When processing different types of images, different parameter selections will produce different processing effects. It often needs manual intervention to select parameters to achieve better enhancement effect.

The urban remote sensing image enhancement method based on visual characteristics is a new research trend, but the theory is not mature enough. People neither have a full understanding of visual characteristics nor use general standards, mainly based on visual experience knowledge and subjective judgment.

4.4 Super-Resolution Reconstruction Methods for Urban Remote Sensing Imagery

Urban areas contain complex environments and ground objects with the existence of mixed pixels (Figure 4.7). It is difficult to meet the demands of high-precision classification and intelligent analysis of urban remote sensing due to the low spatial resolution of remote sensing images. At the same time, due to the limitations of the existing technology, the cost of directly improving the spatial resolution of remote sensing images through the hardware level is considerably high. In comparison, super-resolution reconstruction technology can improve the spatial resolution of images in a cost-efficient manner.

Figure 4.7 Urban remote sensing images requiring super-resolution processing.

Super resolution technology has its rigorous mathematical and physical basis. From a mathematical point of view, if two analytical functions are completely consistent in any given interval, they must be completely consistent as a whole, that is, they are the same function. For an urban remote sensing image, because its airspace is bounded, its spectral function must be analyzed. According to the analytical continuation theory, the information above the cut-off frequency can be reconstructed by using the information below the cut-off frequency, so as to realize the super-resolution processing of urban remote sensing images.

Urban image super-resolution reconstruction is a technology that uses single or multiple low-resolution image sequences of the same target to reconstruct a high-resolution image (Park *et al*., 2003). Super-resolution is able to break through the optical diffraction limit of the imaging system itself to obtain higher-resolution remote sensing images. Compared with directly improving the hardware of the imaging system, super-resolution is achieved by a software system characterized by low cost and high flexibility. Therefore, investigations on super-resolution reconstruction have important theoretical significance and practical value.

At present, the typical urban remote sensing image super-resolution reconstruction methods can be generally divided into three categories: (i) interpolation-based image super-resolution reconstruction methods;

Downloaded from www.worldscientific.com
by fac sciences de la terre universite annaba on 07/30/24. Re-use and distribution is strictly not permitted, except for Open Access articles.

(ii) reconstruction-based image super-resolution reconstruction methods; and (iii) learning-based image super-resolution reconstruction methods.

The interpolation-based algorithm, as the most intuitive and simple super-resolution reconstruction method, uses the known gray values of adjacent pixels to generate the gray values of pixels to be interpolated. Commonly used interpolation methods include nearest-neighbor interpolation, bilinear interpolation, bicubic interpolation and improved interpolation methods.

The reconstruction-based method aims to solve the mathematical model of the imaging process. However, the solution of the image degradation model is an ill-conditioned inverse problem, and there are countless qualified solutions. To obtain a reasonable solution, it is necessary to introduce the actual prior knowledge in the image to establish the regular term, to obtain the feasible solution of the ill-conditioned inverse problem, and recover the high-frequency detail information lost in the degradation process. Reconstruction-based super-resolution approaches can be divided into frequency domain methods and spatial domain methods. And the learning-based method (Freeman, 2002) is becoming the main research hotspot of image super-resolution reconstruction algorithms in recent years. The general goal is to learn the mapping relationship between high-resolution and low-resolution images through a large number of samples, i.e., extracting the prior knowledge of super-resolution reconstruction from samples through learning, to recover the missing high-frequency information on low-resolution images. It is necessary to construct the corresponding high-resolution and low-resolution image library. The low-resolution image is used as the model input, and the high-resolution image is used as the model output. To ensure the training efficiency and reconstruction quality, it is necessary to divide images into small blocks, and the internal mapping relationship between input and output is obtained through the learning of training samples. The learning-based image super-resolution process is shown in Figure 4.8.

The development of deep learning algorithms has led to significant improvement in the image super-resolution domain, with various modeling being proposed, such as SRCNN (Kim *et al.*, 2016) and ESPCN (Shi *et al.*, 2016). SRCNN is a pioneering work of deep learning in super-resolution reconstruction with a simple structure. SRCNN first uses bicubic interpolation to enlarge the low-resolution image into the target size, then fits the nonlinear mapping through the three-layer convolution

Downloaded from www.worldscientific.com
by fac sciences de la terre universite annaba on 07/30/24. Re-use and distribution is strictly not permitted, except for Open Access articles.

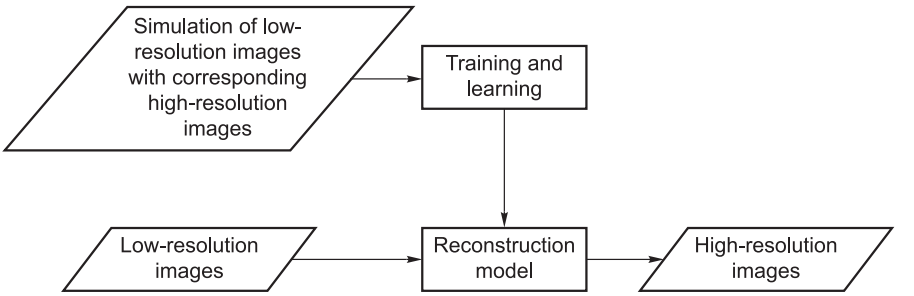

Figure 4.8 The workflow of learning-based image super-resolution process.

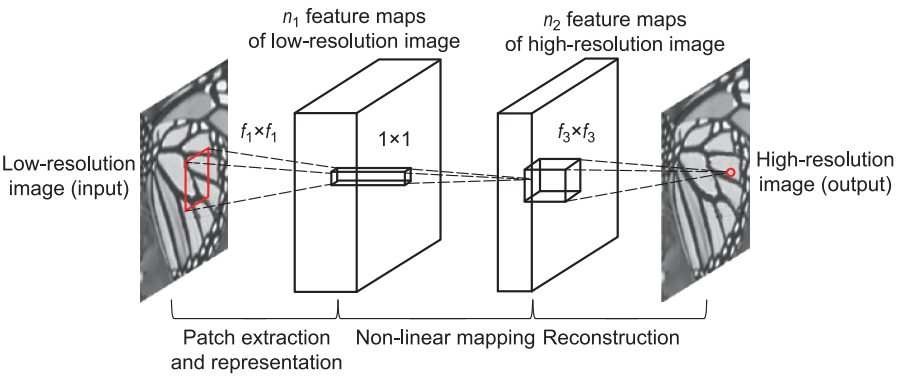

Figure 4.9 The network structure of SRCNN (Kim *et al.*, 2016).

network, and finally outputs the high-resolution image results (Figure 4.9). For a low-resolution image, bicubic interpolation is used to enlarge it to the target size, and then the nonlinear mapping is performed through a three-layer convolution network. The structure of three-layer convolution is interpreted into three steps, corresponding to the traditional super-resolution (SR) method, i.e., (i) image block extraction and feature representation; (ii) feature nonlinear mapping; and (iii) final reconstruction (Kim *et al.*, 2016).

Urban remote sensing image platforms are diverse with many types of images and sensors, such as optical satellite remote sensing images, ground camera images, satellite video images, UAV video images and ground video images. According to different data sources, the application scenarios of remote sensing image super-resolution reconstruction include single-image super-resolution reconstruction and sequence-image (video) super-resolution reconstruction.

Downloaded from www.worldscientific.com by fac sciences de la terre universite annaba on 07/30/24. Re-use and distribution is strictly not permitted, except for Open Access articles.

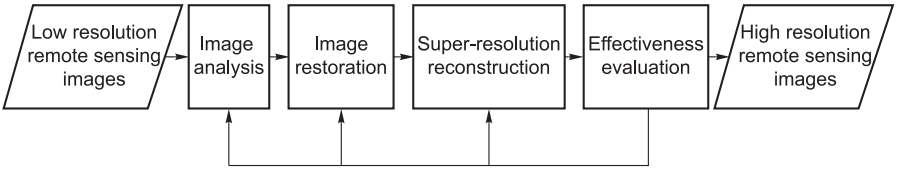

Figure 4.10 The flowchart of super-resolution processing technology for single remote sensing image.

Figure 4.11 An example of processing result a test image with 1-m resolution.

Single-image super-resolution reconstruction uses only the currently observed low-resolution image to reconstruct the high-frequency detail information lost in the process of image degradation. Due to the complexity of urban remote sensing images, the complete single-image super-resolution reconstruction process should include image data acquisition, image analysis, image restoration, super-resolution reconstruction and effect evaluation. Figure 4.10 details the processing steps of image super-resolution processing. An example of a super-resolution result is shown in Figure 4.11.

4.5 Fusion Demands of Urban Remote Sensing Imagery

Compared with non-urban areas, urban areas have complex scenes with rapid changes. According to the source of remote sensing images, the research direction of remote sensing image fusion technology can be roughly divided into two categories: spatial-spectral fusion and spatio-temporal fusion.

Downloaded from www.worldscientific.com
by fac sciences de la terre universite annaba on 07/30/24. Re-use and distribution is strictly not permitted, except for Open Access articles.

Downloaded from www.worldscientific.com
by fac sciences de la terre universite annaba on 07/30/24. Re-use and distribution is strictly not permitted, except for Open Access articles.

The purpose of spatial-spectral fusion is to integrate the spatial resolution and spectral resolution of multi-scene images, eventually obtaining the fusion image with high spatial and hyperspectral resolution. Note that if images belong to multi-spectral images and panchromatic images of high-resolution satellites, the results obtained from spatial spectrum fusion have high spatial resolution and can be used for small-scale fine observation and key target detection.

In contrast, spatio-temporal fusion aims to address different images acquired by different sensors in different areas at different times. The purpose of these fusion methods is to improve the spatial resolution of images with high temporal resolution so that the fused images can reflect the dynamic changes of target objects.

In spatial-spectral fusion and spatial-temporal fusion, the input data types and the focus of output results are largely different. Specifically, spatial-spectral fusion focuses on the improvement of spatial resolution and the retaining of spectral information. As input data contain only one panchromatic image and one multi-spectral image, the fusion algorithm needs to consider the respective characteristics of the two images to obtain a better fusion result. On the other hand, spatio-temporal fusion also focuses on improving spatial resolution. However, due to the different data acquisition times from different sensors, the changing dynamics of surface types should be taken into account. The number of available images is often more than spatial-spectral fusion and single temporal data fusion, given the additional temporal dimension.

4.5.1 Spatial-spectral fusion methods

Spatial-spectral fusion of remote sensing images mainly targets multi-spectral images and panchromatic images from the same satellite. Multi-spectral images often have high spectral resolution and low spatial resolution, while panchromatic images are just the opposite. Therefore, by fusing these two kinds of images, we can obtain images with high spatial resolution and spectral resolution.

Traditional methods of spatial-spectral fusion of remote sensing images can be divided into three categories: methods based on component replacement, methods based on multi-resolution analysis and methods based

on a sparse expression. Given the advantages of deep learning ability and high flexibility, the spatial spectrum fusion methods based on deep learning and convolution neural networks have gradually become a hotspot. This chapter focus on component replacement and multi-resolution analysis methods.

The main idea of the fusion algorithm based on component replacement is to establish a mapping between multi-spectral images and another space through linear transformation, replacing the main components of the multi-spectral image after some processing of the panchromatic image. The fusion image in the original space can be obtained through inverse transformation. The component replacement-based algorithms (e.g., IHS transform and PCA transformation) are the earliest algorithm and run fast, leading to wide applications.

The fusion algorithms based on multi-resolution analysis mainly include various wavelet transform algorithms. At present, common multi-resolution analysis tools include Laplace pyramid transform, wavelet transform, curvelet transform, second-generation curvelet transform and non-down sampling contourlet transform. Studies on multi-resolution analysis methods worldwide led to a sufficient theoretical basis, suggesting their great applicable potential. The detailed information of the image after multi-resolution analysis is different at different resolutions and changes layer by layer. Its principle simulates the visual characteristics of human eyes so that the analysis results are more consistent with the interpretation of human eyes.

For existing deep learning methods for remote sensing image fusion, most scholars directly use the classical network SRCNN in super-resolution reconstruction to perform remote sensing image fusion. These methods only use the three-layer convolution network structure and fail to extract deeper features. At the same time, these methods regard the panchromatic image as an additional band superimposed on the multi-spectral image to form the input of the network, ignoring the respective features of the two images. The process of spatial-spectral fusion of remote sensing images is consistent with the current classical methods that include two processes: feature extraction and feature fusion. Different from these methods, Shao and Cai (2018) designed two lines to extract their features for multi-spectral images and panchromatic images. The training process of the whole network is shown in Figure 4.12.

Downloaded from www.worldscientific.com
by fac sciences de la terre universite annaba on 07/30/24. Re-use and distribution is strictly not permitted, except for Open Access articles.

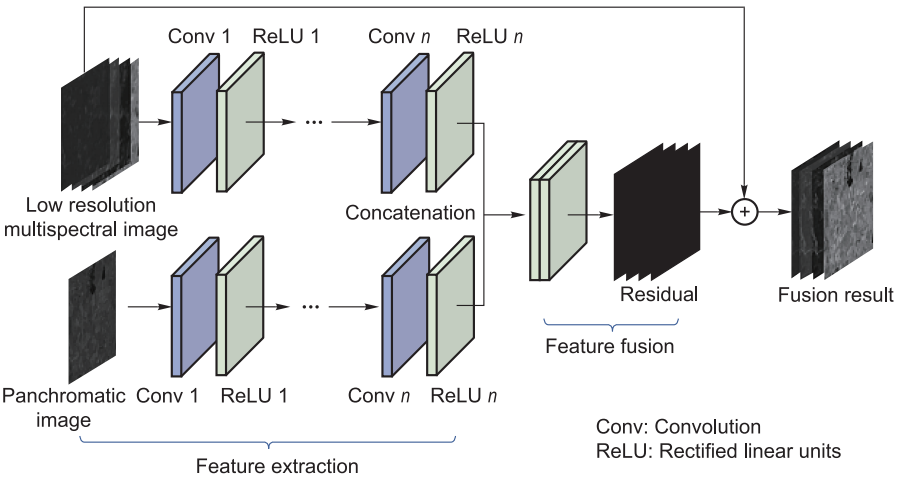

Figure 4.12 The workflow of fusion method proposed by Shao and Cai (2018).

The network depths of the two branches used to extract the features of the multi-spectral image and panchromatic image are m and p, respectively. In the branch line, except for the input and output of the branch line (m or p layers), the parameter settings of other layers remain the same: 64, with a size of $3 \times 3 \times 64$ filters, each filter will test each of the 64 bands (characteristic map), and the space size is 3×3 filtering. The first layer of each branch line also contains 64 filters, but with a size of the filter of $3 \times 3 \times k$, where k represents the number of bands of the input image. The output of each branch line consists of 32 filters, with a size of $3 \times 3 \times 64$, aiming to obtain the features extracted from the input image. After obtaining the results of the branch lines, enter the feature fusion stage where the feature maps of the two branch lines are split according to the dimensions and set for sizes 3 on the last layer of the whole network obtain the same result as the label dimension. The spatial-spectral fusion results of urban remote sensing images based on deep learning are shown in Figure 4.13.

Table 4.1 lists the values of the five indices for accuracy assessment for the entire training area. For the fused images of these two dates, the fusion network produced an RMSE less than 0.05, CC larger than 0.95, UIQI greater than 0.94, ERGAS less than 1.2 and SAM less than 0.8. These metrics clearly showed that the fused images were spectrally and spatially consistent with original images.

Downloaded from www.worldscientific.com
by fac sciences de la terre universite annaba on 07/30/24. Re-use and distribution is strictly not permitted, except for Open Access articles.

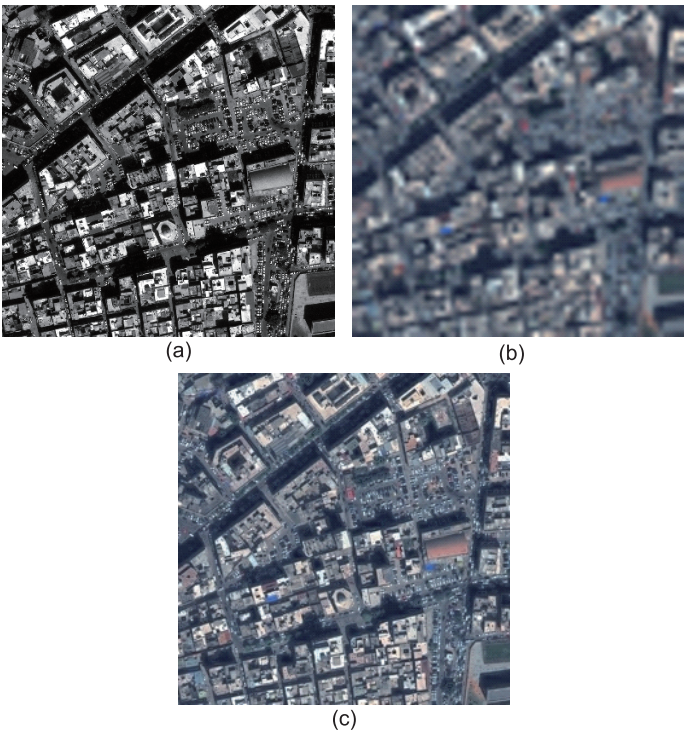

Figure 4.13 An example of spatial-spectral fusion result of an urban remote sensing image based on deep learning: (a) Panchromatic image; (b) Multi-spectral image; (c) Fusion image.

Table 4.1 Results of fusion method proposed by Shao and Cai (2018) based on Landsat data.

Date	Band	RMSE	CC	UIQI	ERGAS	SAM (degree)
June 15, 2017	Band 1	0.0243	0.9860	0.9710	1.1817	0.7042
	Band 2	0.0242	0.9869	0.9737		
	Band 3	0.0260	0.9861	0.9726		
	Band 4	0.0258	0.9875	0.9755		
	Band 5	0.0405	0.9569	0.9415		
	Band 6	0.0263	0.9848	0.9738		
	Band 7	0.0263	0.9864	0.9757		
July 01, 2017	Band 1	0.0193	0.9899	0.9683	1.0741	0.7904
	Band 2	0.0192	0.9904	0.9732		
	Band 3	0.0210	0.9894	0.9731		
	Band 4	0.0217	0.9897	0.9749		
	Band 5	0.0399	0.9599	0.9420		
	Band 6	0.0254	0.9830	0.9698		
	Band 7	0.0254	0.9854	0.9727		

Notes: CC: correlation coefficient; UIQI: universal image quality index; ERGAS: relative global-dimensional synthesis error; SAM: the spectral angle mapper.

Downloaded from www.worldscientific.com
by fac sciences de la terre universite annaba on 07/30/24. Re-use and distribution is strictly not permitted, except for Open Access articles.

4.5.2 Spatio-temporal fusion methods

The spatio-temporal fusion of remote sensing images aims to fuse multi-temporal images obtained by different satellites. Taking the fusion of MODIS and Landsat data as an example, the revisiting cycle of MODIS is 1–2 days, and its high time resolution is very conducive to the continuous observation of the surface on a global scale. However, the spatial resolution of MODIS image is relatively coarse, ranging from 250 m to 1 km. On the contrary, the temporal resolution of Landsat image is low, with a revisiting cycle of 15 days. However, the spatial resolution of Landsat can reach 30 m. Therefore, by fusing MODIS and Landsat images, one is able to obtain MODIS images with 30-m spatial resolution for almost daily surface monitoring.

The traditional methods of spatio-temporal fusion of remote sensing images can also be roughly classified into three categories: methods based on transform domain, methods based on weighting and methods based on dictionary learning.

The method based on the transform domain conducts image fusion in the transform domain. Notable algorithms include the wavelet transform and tasseled cap transformation. The fusion effect of the wavelet transform method is shown in Figure 4.14.

The weighting-based method is usually carried out in the form of weighted summation of high spatial resolution, low time resolution and low spatial resolution, and high time resolution images with similar spectral neighborhood information. STARFM (enhanced spatial and temporal adaptive reflection fusion model) is the earliest and most classical weighting-based fusion algorithm that combines the time-phased difference of pixels, fully considers the similarity of distance, time and spectrum, and obtains the fusion result through local weighting. The advantage of this method is its capability of eliminating the influence of singular points on the fusion results as well as performing well in a wide range of areas where the changes of ground features are unnoticeable. However, its performance tends to drop in areas where the surface composition is complex and the changes of ground features are significant.

Downloaded from www.worldscientific.com
by fac sciences de la terre universite annaba on 07/30/24. Re-use and distribution is strictly not permitted, except for Open Access articles.

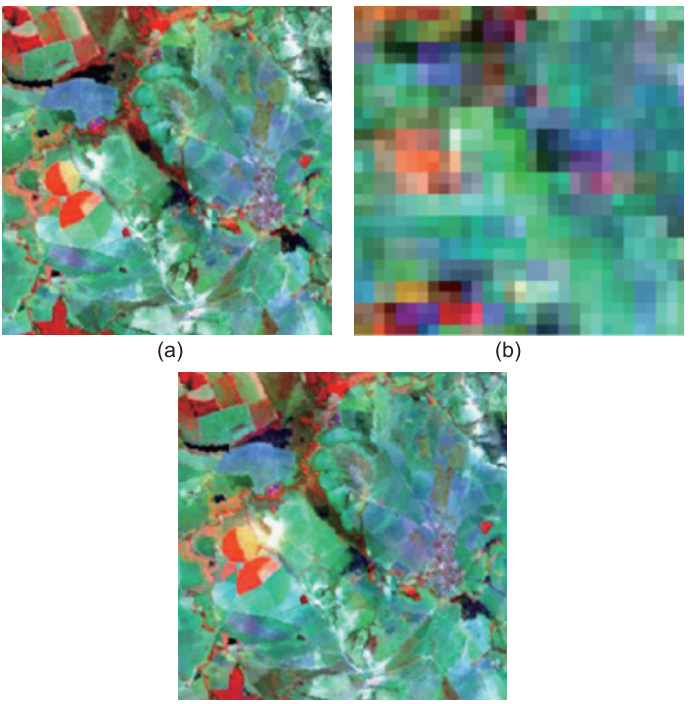

Figure 4.14 Spatio-temporal fusion results of urban remote sensing images based on wavelet transform: (a) Landsat image; (b) MODIS image; (c) Fusion image.

Questions

1. What are the main methods of cloud detection in urban remote sensing images? What are the characteristics of each method?
2. What are the difficulties in shadow detection of urban remote sensing images?
3. What are the main methods for image enhancement of urban remote sensing images?
4. What are the purposes of super-resolution reconstruction of urban remote sensing images?
5. What are the similarities and dissimilarities between spatial-spectral fusion and spatio-temporal fusion?
6. Review the literature related to image fusion. What are the fusion methods based on feature level and decision level?

Downloaded from www.worldscientific.com
by fac sciences de la terre universite annaba on 07/30/24. Re-use and distribution is strictly not permitted, except for Open Access articles.

Downloaded from www.worldscientific.com
by fac sciences de la terre universite annaba on 07/30/24. Re-use and distribution is strictly not permitted, except for Open Access articles.

References

Ackerman S A, Strabala K I, Menzel W P, Frey R A, Moeller C C. 1998. Discriminating clear sky from clouds with MODIS. *Journal of Geophysical Research: Atmospheres*, 103: 32141–32157.

Baum B, Tovinkere V, Titlow J. 1997. Automated cloud classification of global AVHRR data using a fuzzy logic approach. *Journal of Applied Meteorology*, 36: 1519–1540.

Chao D, Chen C L, He K. 2014. Learning a deep convolutional network for image super-resolution. *European Conference on Computer Vision*. Ch. Zurich, Switzerland Springer, Cham.

Ebert E. 1987. A pattern recognition technique for distinguishing surface and cloud types in the polar regions. *Journal of Climate and Applied Meteorology*, 26(10): 1412–1427.

Freeman W T, Jones T R, Pasztor E C. 2002. Example-based super-resolution. *IEEE Computer Graphics and Applications*, 22(2): 56–65.

Garand L. 2009. Automated recognition of oceanic cloud patterns. Part I: Methodology and application to cloud climatology. *Journal of Climate*, 1(1): 20–39.

Jiang C, Ward M O. 1992. Shadow identification. *IEEE Computer Society Conference on Computer Vision and Pattern Recognition*, USA. IEEE, Champaign, IL, pp. 606–612.

Key J R, Maslanik J A, Schweiger A J. 1989. Classification of merged AVHRR and SMMR Arctic data with neural networks. *Photogrammetric Engineering and Remote Sensing*, 55(9): 1331.

Kim J, Lee J K, Lee K M. 2016. Accurate image super-resolution using very deep convolutional networks. *Proceedings of the IEEE Conference on Computer Vision and Pattern Recognition*, Las Vegas, Nevada, USA, pp. 1646–1654.

Merchant C J, Harris A R, Maturi E. 2010. Probabilistic physically based cloud screening of satellite infrared imagery for operational sea surface temperature retrieval. *Quarterly Journal of the Royal Meteorological Society*, 131(611): 2735–2755.

Movia, A, Beinat A, Crosilla F. 2016. Shadow detection and removal in RGB VHR images for land use unsupervised classification. *ISPRS Journal of Photogrammetry and Remote Sensing*, 119(Sep.): 485–495.

Park S C, Park M K, Kang M G. 2003. Super-resolution image reconstruction: A technical overview. *IEEE Signal Processing Magazine*, 20(3): 21–36.

Saunders R W, Kriebel K T. 1988. An improved method for detecting clear sky and cloudy radiances from AVHRR data. *International Journal of Remote Sensing*, 9(1): 123–150.

Surya S R, Simon P. 2015. Automatic cloud removal from multitemporal satellite images. *Journal of the Indian Society of Remote Sensing*, 43(1): 57–68.

Salvador E, Cavallaro A, Ebrahimi T. 2001. Shadow identification and classification using invariant colormodels. Acoustics, Speech, and Signal Processing, Salt Lake City, UT, USA, 3, pp. 1545–1548.

Stevens I. 2011. Shadow catchers: Camera-less photography. *Aperture*, 204: 81–82.

Shi W, Caballero J, Huszár F. 2016. Real-time single image and video super-resolution using an efficient sub-pixel convolutional neural network. *IEEE Conference on Computer Vision and Pattern Recognition*. Las Vegas, USA, pp. 1874–1883.

Shao Z, Cai J. 2018. Remote sensing image fusion with deep convolutional neural network. *IEEE Journal of Selected Topics in Applied Earth Observations and Remote Sensing*, 99: 1656–1669.

Tian B, Azimi-Sadjadi M R, Haar T H, Reinke D. 2000. Temporal updating scheme for probabilistic neural network with application to satellite cloud classification. *IEEE Transactions on Neural Networks*, 11(4): 903–920.

Vivone G, Addesso P, Conte R. 2014. A class of cloud detection algorithms based on a MAP-MRF approach in space and time. *IEEE Transactions on Geoscience and Remote Sensing*, 52(8): 5100–5115.

Welch R M, Sengupta S K, Goroch A K, Palikonda R, Rangaraj N, Navar M S. 1992. Polar cloud and surface classification using AVHRR imagery: An inter comparison of methods. *Journal of Applied Meteorology*, 31: 405–420.

Downloaded from www.worldscientific.com
by fac sciences de la terre universite annaba on 07/30/24. Re-use and distribution is strictly not permitted, except for Open Access articles.

Downloaded from www.worldscientific.com
by fac sciences de la terre universite annaba on 07/30/24. Re-use and distribution is strictly not permitted, except for Open Access articles.

Chapter 5

Classification and Information Extraction Methods for Urban Remote Sensing Imagery

With geo-objects that include roads, green spaces, buildings and lakes, cities carry out most of the economic activities. Due to the continuation of urbanization, prominent environmental problems become notable and seriously affect the sustainable development of cities. Remote sensing-based methods have been widely applied to grasp the information of urban land and features in time, maintain the current status of geospatial information, and effectively monitor the urban ecological environment. An in-depth understanding of urban feature information is practically significant (Li *et al*., 2014).

In this chapter, we introduce the classification and information extraction methods for urban remote sensing imagery from seven perspectives, including the classification and information extraction demands, unsupervised classification methods, supervised classification methods, new classification methods, urban road extraction, urban building extraction and urban lake extraction.

5.1 Classification and Information Extraction Demands for Urban Remote Sensing Imagery

Urbanization has led to sharp changes in land use and land cover types. In addition, urban scenes become complex and diverse, requiring urban managers to grasp land changes in urban areas timely.

Downloaded from www.worldscientific.com
by fac sciences de la terre universite annaba on 07/30/24. Re-use and distribution is strictly not permitted, except for Open Access articles.

Land use types are mainly divided according to the functional attributes of urban land, so urban land use types can include roads, residential areas, commercial areas, industrial areas, water areas and green space. Some land use types can be further divided on the basis of these use types. For example, residential areas can be divided into high-density residential areas (shanty town, old-fashioned residential areas, etc.), medium-density residential areas (residential areas with more high-rise residences and green spaces) and low-density residential areas (mainly villa areas).

The land cover type is mainly based on the material attribute and the functional attribute of urban land. Urban land cover types can be divided into buildings, roads, water bodies, vegetation, etc. Due to the diversity of urban land use types, many scenarios consist of basic land use and land cover mixed units, such as urban residential areas, ports, airports, and schools, complex urban road networks, buildings of different colors and shapes and so on. These objects together form complex urban remote sensing image features.

In the scene classification of urban remote sensing image, there are also many difficulties.

First of all, the classification standards of urban scenes are not unified, and different application requirements have different requirements for scene classification. For example, in a scene area such as a school, there are both living and working areas. Therefore, the school scene can be divided into schools and further subdivided into working and living areas. The remote sensing image data of living area and off-campus living area are not very different in essence. Work area and the work area outside school also are very similar (e.g., tall teaching building, scientific research building and office building). Therefore, scenes such as schools and scenes such as living areas and working areas do not simply belong to each other.

Secondly, the internal situation of the image scene is complicated. Scenarios such as urban roads (including various levels of roads, such as urban highways, viaducts, urban general main roads, and general roads) can also be extremely complex, with varying levels, widths, traffic flows, and congestion. Urban roads are paved with different materials (such as asphalt and cement). Since scene classification involves more ground object categories and social attribute information, it faces some similar problems with map covered land use classification, which makes the scene classification task also challenging.

As the main habitat of human beings, cities carry out most of the economic activities, and their typical land features mainly include roads, green spaces,

Downloaded from www.worldscientific.com
by fac sciences de la terre universite annaba on 07/30/24. Re-use and distribution is strictly not permitted, except for Open Access articles.

buildings and lakes. Increasingly prominent with the expansion of the city, the urban environment problem is affecting the sustainable development of the city. In order to grasp the features of urban land information in time, keep the geospatial information, effectively monitor the urban ecological environment, using remote sensing method extract feature information has important practical significance.

In recent years, countries all over the world have paid more and more attention to the development of satellite remote sensing, and more and more countries have begun to establish independent and controllable earth observation systems. At the same time, the commercial satellite market has continued to grow, the observation forms of remote sensing satellites have become more and more diversified, and the observation objects have become increasingly abundant.

At present, many special projects related to urban remote sensing information extraction have been carried out, and several sets of global land use/cover data products have been produced and released. China has launched a global mapping project and every year carries out a national land survey or change survey, a general survey and monitoring of geographical conditions, a general survey of urban impervious surface and remote sensing monitoring of sponge cities, which mainly include the following:

1. *Global land cover data*: Land cover and its changes are indispensable basic information and key factors in environmental change, geographic national conditions monitoring, sustainable development planning and other researches. Global earth observation already has the powerful ability to acquire data with high precision, high temporal and high spatial resolution of the atmosphere, ocean, and land. Based on major requirements of applications, many countries started to share multiple sets of global surface coverage data products with different resolutions (He *et al.*, 2018).
2. *National land survey*: The national land survey documents major national situations and national strengths. The purpose is to fully investigate the state of land use, grasp the real basic land data, implement information and network management of the survey results. The land survey and the statistical systems need to be further established and improved.
3. *Geographic city survey and monitoring*: The ecosystems in some areas have been seriously affected by various factors that include continuously increasing population pressure, high-intensity land development,

construction activities, and large-scale development, and utilization of natural resources. In response to these ecologically degraded areas, local governments have successively organized and conducted a series of major ecological protection and construction projects, aiming to further improve the coverage of forest and grass.

4. *30-m resolution, global land cover information product*: The dynamics of global land cover are able to reflect the interaction between humans and nature, surface water, heat and material balance, biogeochemical cycles, etc. A better understanding of global land cover changing patterns provides the scientific basis for ecological environment monitoring, climate change research and sustainable development planning. In the past, Europe and the United States have developed multiple sets of global surface coverage information products, but with coarse resolution (from 300 m to 1 km), low accuracy, and poor timeliness. Such products fail to reflect the temporal and spatial patterns and transformation laws of large-scale surface coverage in an effective manner. Mapping global land cover at a spatial resolution of 30 meters involves many difficulties, e.g., refined extraction, product quality control and optimal coverage and effective processing of massive images (Chen *et al.*, 2017).

5.2 Unsupervised Classification Methods for Urban Remote Sensing Imagery

The design of the unsupervised classification method aims to form clusters through pre-classification processing of various image data according to the spectral characteristics of remote sensing image features and adjust the preset parameters by the statistical parameters of the clusters, followed by numerous steps that include re-clustering and re-adjustment until the changes of the relevant parameters are within the pre-selected threshold range. Selected representative methods include K-means classification and ISODATA classification, to list a few. In this section, we explain the classification procedure of K-means for example.

The K-means algorithm is able to minimize the sum of squared distances from all samples in the clustering domain to the cluster center. Its main steps are as follows:

Downloaded from www.worldscientific.com
by fac sciences de la terre universite annaba on 07/30/24. Re-use and distribution is strictly not permitted, except for Open Access articles.

Downloaded from www.worldscientific.com
by fac sciences de la terre universite annaba on 07/30/24. Re-use and distribution is strictly not permitted, except for Open Access articles.

Step 1: Select k initial cluster centers: Z_1^l, Z_2^l, Z_3^l, ..., Z_k^l (the upper corner mark contains the number of iterative operations in the search for clusters). Let the array *classp* [$6 * clsnumber$] store the value of the class center. In general, the first k samples of the sample set can be selected as the initial cluster centers. However, given the fact that it is not conducive to the convergence of the following algorithm, it is common to adopt the method of selecting the center of the maximum and minimum distance. The rule of thumb is to keep the initial categories as far as possible.

Choose 50 initial centers arbitrarily and store their values in *iGrayValue* [$6 * 50$]; use the first point X_1 as the center Z_1 of the first initial category.

Calculate the distance D between X_1 and other sampling points. Take the sampling point with the farthest distance (such as X_7) as the second initial category center Z_2, then the second initial category center $Z_1 = X_7$.

For each remaining sampling point, calculate the distance D_{ij} from the center of each initial category (the initial number of categories is m), and the smallest distance among them is taken as the representative distance D_j of the following point (Equation (5.1)):

$$D_j = \min(D_{1j}, D_{2j}, \ldots, D_{mj}) \tag{5.1}$$

The minimum distances of all remaining points are compared with each other, and the largest of them is selected. The sampling point corresponding to the largest minimum distance (such as X_{11}) is selected as the new initial class center point, i.e., $Z_3 = X_{11}$. At this step, $m = m + 1$.

Iterate in this way until $m \geqslant clsnumber$; that is, $m = 0, 1, 2, \ldots, clsnumber$.

Step 2: Assuming that a total of k iterations have been carried out, if there is $|X - Z_j^k| < |X - Z_i^k|$ for a certain sample X, $X \in S_j^k$. All samples are allocated to k classes, i.e., determine the category k_7 of each pixel, such as $k_7 = 3$, meaning that the pixel belongs to the third category, and assign it to the array accordingly.

Step 3: Calculate the new vector value $class[i]$ of each cluster center (Eqs. 5.2 and 5.3):

$$Z_j^{k+1} = \frac{1}{n_j} \sum_{x \in s_j^k} X \ (j = 1, 2, \ldots, k) \tag{5.2}$$

$$classo[i] = classo1[i]/NL[i] \tag{5.3}$$

where $classo1[i]$ represents the accumulation of the values of all pixels belonging to the ith category.

$NL[i]$ represents the total number of pixels belonging to the ith category. $classo[i]$ denotes the cluster center value after reclassification. As the sample mean of k cluster centers needs to be re-calculated in this step, it is called the K-means algorithm.

Step 4: If $Z_j^{k+1} \neq Z_j^k$, $j = 1, 2, \ldots, k$, repeat the second step, reclassify all samples n and repeat the iterative calculation. If $Z_j^{k+1} = Z_j^k$, $j = 1, 2, \ldots, k$, the iteration ends. When implementing this step, the threshold c is set, and the iterating processes are complete if the difference between the class centers before and after the change is within the threshold range:

$$((|classo[i] - classp[i]|)/classp[i]) < c$$

The result of the K-means algorithm is affected by the number k of the selected clustering centers and the selection of the initial clustering centers, as well as the geometric properties and arrangement order of the samples. Different k settings should be tested. If the geometrical properties of the samples indicate that they can form several small isolated areas that are far apart, the algorithm tends to converge. Figure 5.1 shows the K-means classification diagram when the number of cluster categories is set to 3, the maximum change threshold is set to 5 and the maximum number of iterations is set to 5.

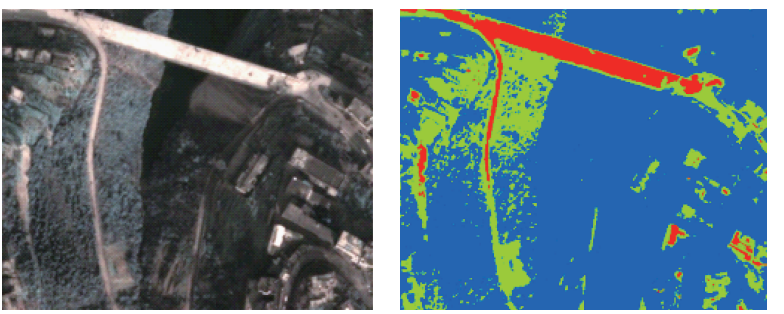

(a) (b)

Figure 5.1 Classification results based on the K-means algorithm: (a) Original image; (b) Classification result.

Downloaded from www.worldscientific.com
by fac sciences de la terre universite annaba on 07/30/24. Re-use and distribution is strictly not permitted, except for Open Access articles.

Downloaded from www.worldscientific.com
by fac sciences de la terre universite annaba on 07/30/24. Re-use and distribution is strictly not permitted, except for Open Access articles.

5.3 Supervised Classification Methods for Urban Remote Sensing Imagery

The urban remote sensing image supervised classification methods rely on samples provided by the category training area. Through the selection of feature parameters, classifiers are able to learn the importance of different features. In general, supervised classification methods belong to a series of methods that classify the sub-pixels according to the classification decision rules (Li *et al.*, 2010; He *et al.*, 2017). Commonly used supervised classification methods include minimum distance classification, maximum likelihood classification, Mahalanobis distance classification and support vector machine, to list a few (Huang *et al.*, 2002). In this section, we illustrate the process of the maximum likelihood classification method (Chen *et al.*, 2017).

The maximum likelihood method is a widely used supervised classification method. The discriminant function (f) used in the classification is the probability or possibility that each pixel value belongs to each category. For handling optical remote sensing images, we usually assume that the spectral characteristics conform to the normal distribution, i.e., the probability density function is shown in Eq. (5.4):

$$p(f|\omega_i) = \frac{1}{(|\boldsymbol{C}_i|^{\frac{1}{2}} 2\pi)^{\frac{k}{2}}} \mathrm{e}^{-(f-\boldsymbol{m}_i)^{\mathrm{T}} \boldsymbol{C}_i^{-1} (f-\boldsymbol{m}_i)/2} \tag{5.4}$$

where k refers to dimensions.

Therefore, the maximum likelihood decision function of the K-dimensional class follows Eq. (5.5):

$$\begin{aligned} D_i(f) &= \ln[p(\omega_i) \times p(f|\omega_i)] \\ &= \ln P(\omega_i) + \ln P(f|\omega_i) \\ &= \ln P(\omega_i) + \ln \frac{1}{(|\boldsymbol{C}_i|^{\frac{1}{2}} 2\pi)^{\frac{k}{2}}} \mathrm{e}^{-(f-\boldsymbol{m}_i)^{\mathrm{T}} \boldsymbol{C}_i^{-1} (f-\boldsymbol{m}_i)/2} \end{aligned} \tag{5.5}$$

where $\boldsymbol{m}_i$ refers to the mean vector of the class ω_i; $\boldsymbol{C}_i$ refers to the covariance matrix of the class.

$$D_i(f) = \ln p(\omega_i) - \frac{1}{2}\left\{K \ln 2\pi + \ln |\boldsymbol{C}_i| + (f - \boldsymbol{m}_i)^{\mathrm{T}} \boldsymbol{C}_i^{-1} (f - \boldsymbol{m}_i)\right\} \tag{5.6}$$

For any pixel value, it belongs to a category with the largest $D_i(f)$.

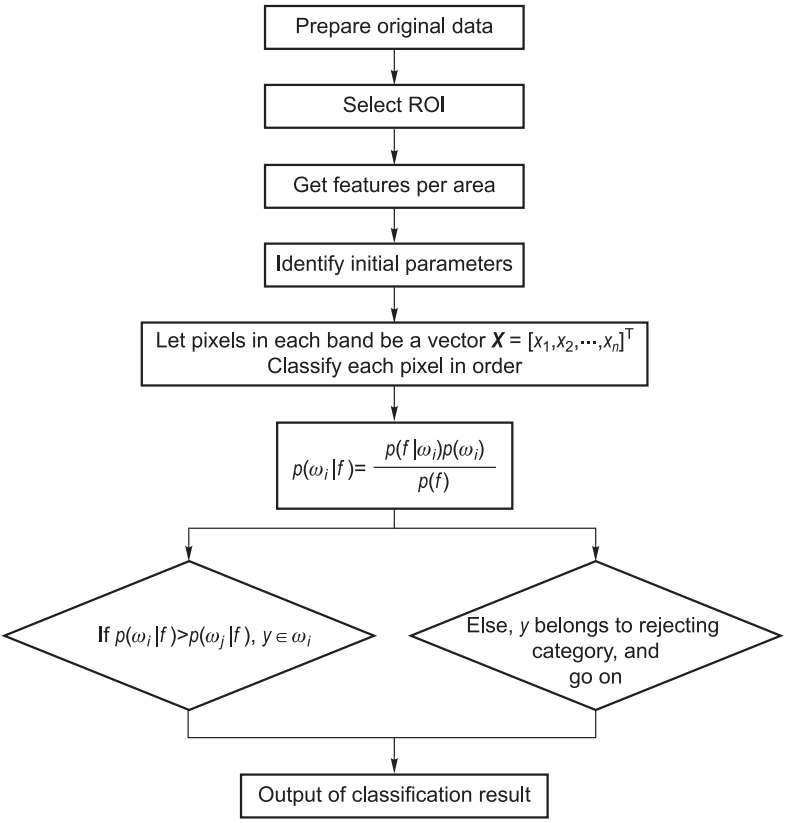

Figure 5.2 The workflow of maximum likelihood classification method.

The workflow of the maximum likelihood method is presented in Figure 5.2.

5.4 New Classification Methods for Urban Remote Sensing Imagery

CNN is an efficient classification method in the field of pattern recognition. It is the first successful learning algorithm for training multilayer network structures (Li *et al.*, 2016). Combining artificial neural network technology and deep learning method, CNN has the characteristics of sparse connection and weight sharing. A gradient-based improved backpropagation algorithm

Downloaded from www.worldscientific.com
by fac sciences de la terre universite annaba on 07/30/24. Re-use and distribution is strictly not permitted, except for Open Access articles.

Downloaded from www.worldscientific.com
by fac sciences de la terre universite annaba on 07/30/24. Re-use and distribution is strictly not permitted, except for Open Access articles.

can be used for weight training in an end-to-end manner, avoiding the complicated early stage of input data preparation. Deep learning approaches have therefore been widely applied in the field of image classification (Krizhevsky *et al.*, 2012). The basic structure of the current CNN includes convolutional layers, pooling layers, fully-connected layers and other improved modules.

Commonly used typical CNN networks include AlexNet (Krizhevsky *et al.*, 2012), VggNet series, InceptionNet series (Szegedy *et al.*, 2016) and ResNet series (He *et al.*, 2016), to list a few. Figure 5.3 shows the basic structure of selected standard networks.

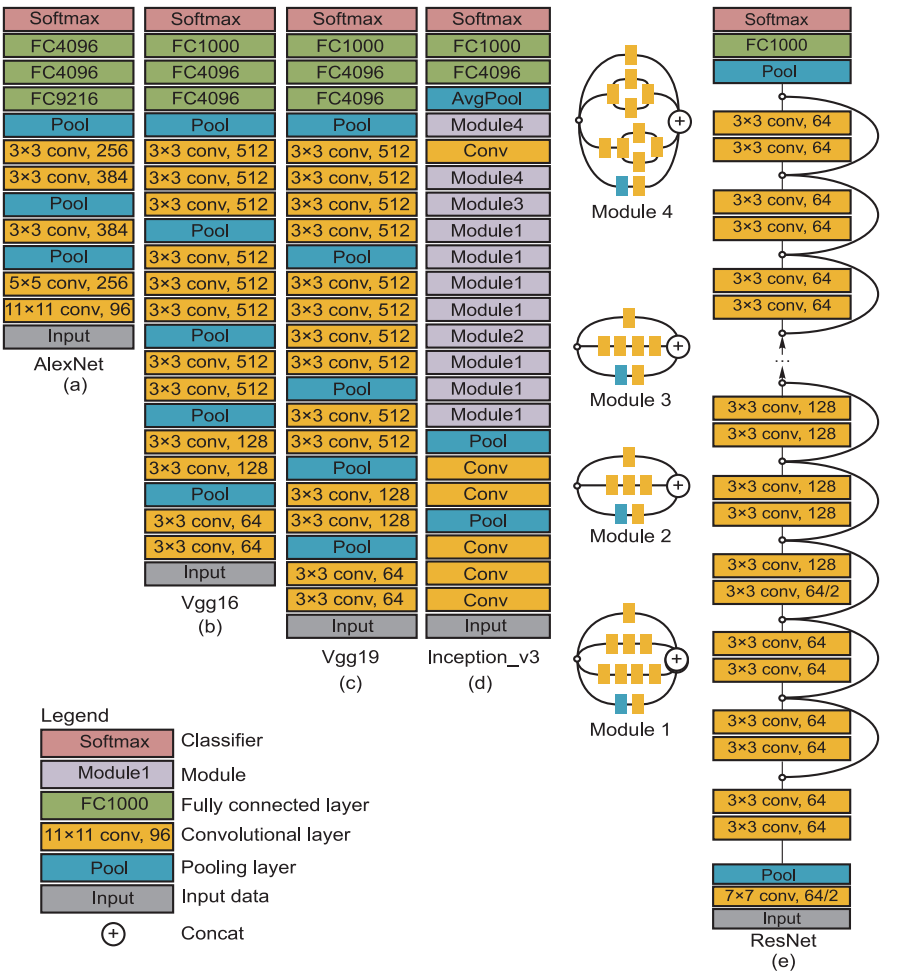

Figure 5.3 Typical CNNs in computer vision in past years.

Downloaded from www.worldscientific.com
by fac sciences de la terre universite annaba on 07/30/24. Re-use and distribution is strictly not permitted, except for Open Access articles.

AlexNet has five convolution layers, three pool layers, three local response normalization layers and three full connection layers. The input data are a set of images of size 227 × 227 × 3. The activation function is ReLU, which maps the input from the previous neuron layer to the next layer. The last fully connected layer is a one-dimensional vector with 4096 features. AlexNet's classifier is Softmax.

VggNets have five types of networks and are an in-depth study and improvement of AlexNet. VggNets' frameworks are much cleaner and simpler than AlexNet's. VggNet has a small filter of 3 × 3 size for the convolution layer and a filter of 2 × 2 for the merge layer. Some combinations of small filters have better training performance than large filters. In addition, VggNets demonstrate that performance can be improved by deepening the network structure. Vgg16 and Vgg19 are the most widely used VggNet networks. Vgg16 has 16 hidden layers, including 13 convolutional layers and 3 fully connected layers. Vgg19 has 19 hidden layers, including 16 convolutional layers and 3 fully connected layers. ReLU is the activation function of Vgg16 and Vgg19. In addition, VggNets removes the local response normalization layer.

GoogleNets overcome problems such as gradient disappearance, gradient explosion and the overfitting problem of AlexNet and VggNets by adding layer depths and start modules. The initial model can make more efficient use of computational resources and extract more features for the same amount of computation. The initial model involves two aspects: 1 × 1 convolution module and multi-scale convolution combination module. The convolution module with a size of 1 × 1 not only reduces the amount of data but also modifies the linear function ReLU. In addition, reducing the data size has no effect on the characteristics. Multi-scale convolution of different features is extracted by convolution or merging of input data with filters of different sizes. It can also speed up network convergence by convolving data over different filters. GoogleNets has many spin-off networks. The most popular GoogleNets network is Inception_v3, as shown in Figure 5.3(d).

As the depth of the network increases, the degradation problem starts to appear, leading to performance loss. Researchers have proposed ResNet, a residual learning method that uses skip connections to solve the problem. The basic idea of ResNet is to change the learning purpose of the network structure. The initial understanding is the image feature $H(X)$ obtained directly through convolution. In ResNet, it learns the residual $H(X) - X$ of the image and feature. The reason is that residual learning is more efficient

Downloaded from www.worldscientific.com
by fac sciences de la terre universite annaba on 07/30/24. Re-use and distribution is strictly not permitted, except for Open Access articles.

than learning directly from the original function. Figure 5.3(e) presents the structure of ResNet.

The classification process of CNN actually belongs to supervised classification, that is, the sample training network requiring manual labeling.

Table 5.1 presents some typical publicly available datasets of remote sensing scene classification.

Table 5.1 Commonly used remote sensing scene classification datasets.

Dataset	Number per category	Number of categories	Total images	Spatial resolution	Image size	Published date
UC Merced Land Use	100	21	2,100	0.3	256 × 256	2010
WHU-RS19	~50	19	1,005	~0.5	600 × 600	2010
RSSCN7	400	7	2,800	—	400 × 400	2015
RSC11	~100	11	1,232	0.2	512 × 512	2016
SIRI-WHU	200	12	2,400	2.0	200 × 200	2016
AID	200–400	30	10,000	0.5–0.8	600 × 600	2017
EuroSAT	2,000	10	27,000	—	64 × 64	2017
	3,000					
	5,000					
NWPU-RESISC45	700t	45	31,500	~30–0.2	256 × 256	2017
PatterNet	800	38	30,400	0.06–4.69	256 × 256	2017
RSI-CB	CB128:800	CB128:45	CB128:36,707	0.3–3.0	128 × 128	2017
	CB256:600	CB256:35	CB256:24,747		256 × 256	
RSD46-WHU	500–3,000	46	117,000	0.5–2.0		2017

Take the AlexNet, for example; due to the limited amount of data, a transfer learning method is often chosen to train AlexNet, i.e., using the trained network parameters and retraining the parameters of the fully connected layer. The training results show that CNN can extract the depth features in the image and has high adaptability to complex remote sensing scenes. The accuracy of the AlexNet test classification can reach 96%, which is significantly better than the existing methods. Figure 5.4 shows the testing results of AlexNet.

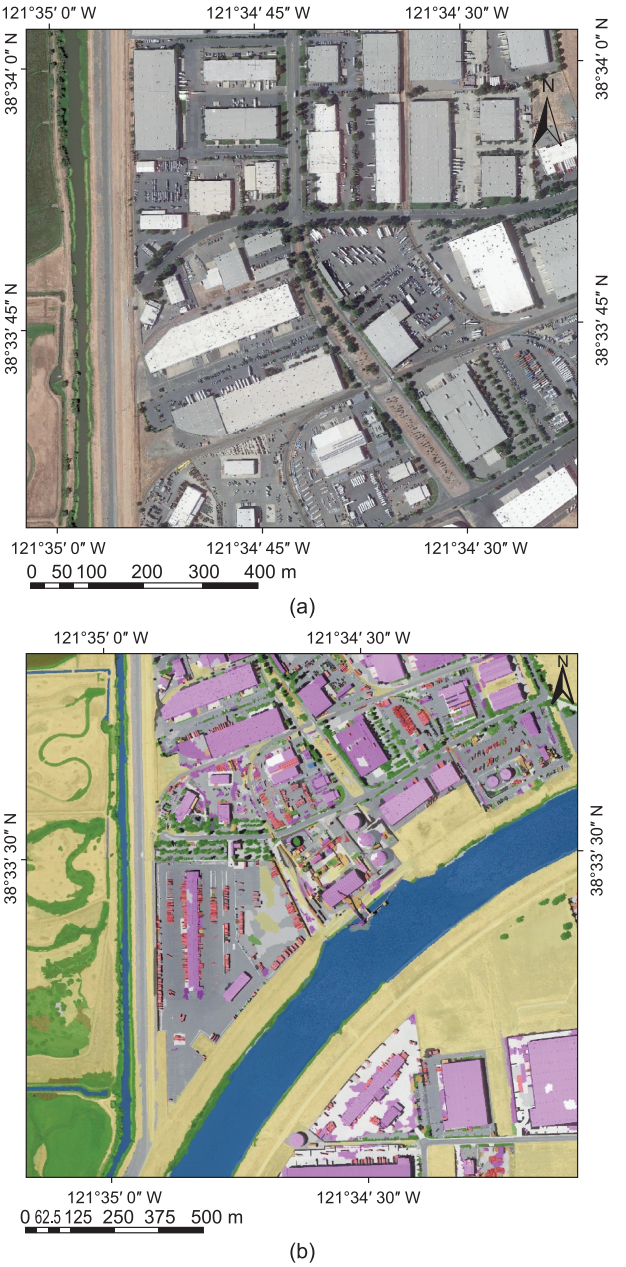

Figure 5.4 Classification results of the testing data using AlexNet: (a) Original image; (b) Classification results.

Downloaded from www.worldscientific.com
by fac sciences de la terre universite annaba on 07/30/24. Re-use and distribution is strictly not permitted, except for Open Access articles.

Downloaded from www.worldscientific.com
by fac sciences de la terre universite annaba on 07/30/24. Re-use and distribution is strictly not permitted, except for Open Access articles.

5.5 Urban Road Extraction Methods Based on Remote Sensing Imagery

Roads are typical artificial linear targets in cities. Thus, road extraction is of great significance for GIS database updates image matching, target detection and digital mapping automation. The extracted road features using remote sensing techniques have been widely used in traffic management and land use analysis, among others (Li *et al*., 2016). Compared with rural roads, the remote sensing extraction of urban roads has the following difficulties:

1. In a high-resolution remote sensing image, the urban roads are distributed in a plane shape, their edges and center lines have obvious linear geometric characteristics, the details of the ground objects are more abundant and the image information is more complicated.
2. In terms of spectral characteristics, there are a large number of same objects with different spectrum and different objects with same spectrum phenomena in high-resolution remote sensing images. Urban roads are close to buildings and their spectral and texture characteristics are very similar.
3. The materials of urban roads are diverse, including impervious cement, asphalt and permeable gravel, to list a few. The internal spectral difference of the road can be large, leading to a serious isomorphism problem.
4. In terms of geometric characteristics, there are a large number of adhesion phenomena around the road, e.g., telephone poles, buildings, sidewalk trees, overpasses, shadows of tall objects, cars on the road, isolation belts in the center of the road and traffic management lines, to list a few. In addition, roads might be covered by buildings, trees and other vertical objects.
5. In addition, the urban space layout is compact, often connected with buildings, parking lots and other residential areas or artificial facilities, and a function division is not clear. Figure 5.5 shows an example remote sensing image that contains multiple noises when extracting roads.

According to different degrees of automation, road extraction methods can be divided into manual tracking methods, semi-automatic extraction methods and automatic extraction methods. The manual tracking method is the most primitive method, but it is a practical method that has been used by production units for a long time. Current digital photogrammetric

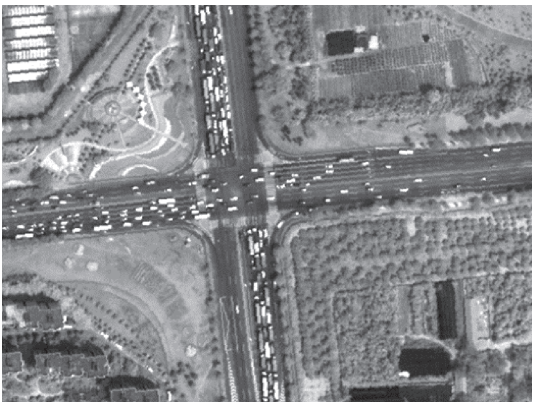

Figure 5.5 Remote sensing image with multiple noises when conducting road extraction.

workstations provide such a function, so its details are not introduced here; the automatic extraction method is the ultimate ground feature extraction. There have been many attempts and initial experimental results, but there exists no practical system available for actual production (a system that can perform a full automatic road extraction system without any manual intervention). The guided semi-automatic extraction organically combines human perceptions and computers and greatly improves efficiency and reduces labor intensity under current conditions.

The representative automatic road extraction method and deep-learning-based new road extraction method are introduced in the following.

5.5.1 Automatic extraction method of urban roads

The automatic extraction method of urban roads follows four main steps:

1. Enhance road features, e.g., image filtering and wavelet transform.
2. Determine the "seed point" of the road and determine the possible road points. Various road point detection operators have been proposed, including methods based on pixel classification, edge detection and template matching.
3. Extend the "seed point" into segments. Numerous approaches for rule-based automatic connection of edge points approaches have been proposed, including dynamic programming and Kalman filtering, among others.

Downloaded from www.worldscientific.com
by fac sciences de la terre universite annaba on 07/30/24. Re-use and distribution is strictly not permitted, except for Open Access articles.

4. Confirm the road section and automatically connect to form a road network. This step involves automatic grouping algorithms, high-level automatic image interpretation methods such as connection hypothesis generation and hypothesis validation, taking into account contextual knowledge, the expression of semantic relations of ground objects and the fusion of multi-source data.

Figure 5.6 shows the various guidance methods in the interactive extraction process of roads. For curved roads, the seed point guidance method shown in Figure 5.6(a) is commonly used, combined with a certain spline function to achieve road segment segmentation extraction (see Figure 5.7).

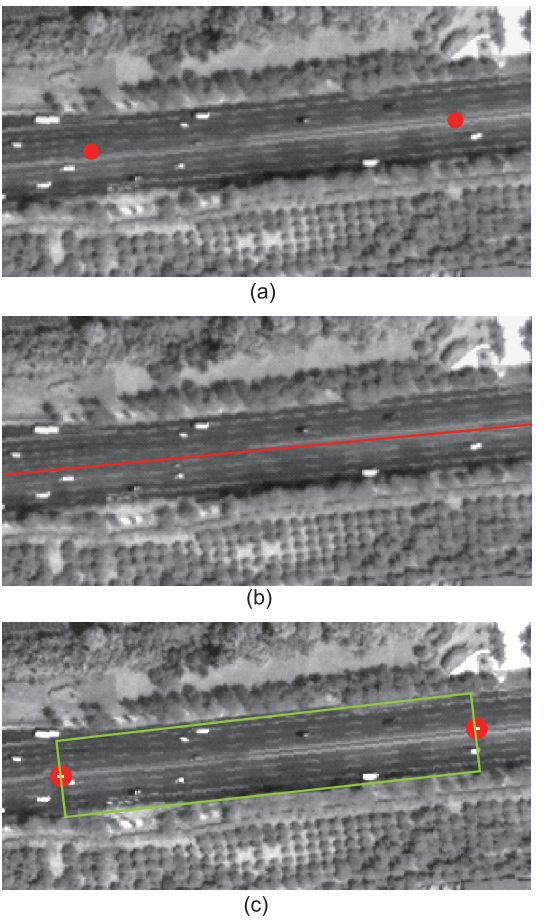

Figure 5.6 Three guidance methods in road extraction: (a) Seed point guide; (b) Centerline guide; (c) Rectangle guide.

Downloaded from www.worldscientific.com
by fac sciences de la terre universite annaba on 07/30/24. Re-use and distribution is strictly not permitted, except for Open Access articles.

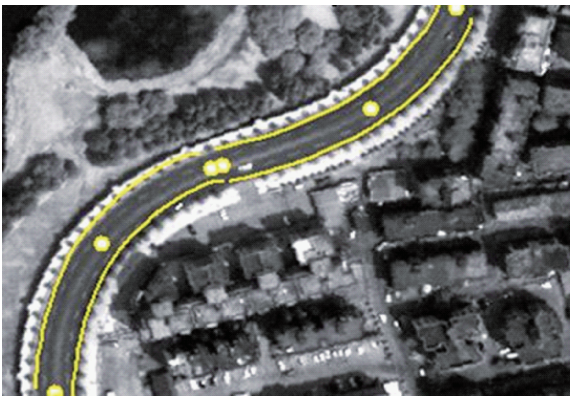

Figure 5.7 Winding roads can be detected by combining seed points and spline function.

5.5.2 Road extraction method based on deep learning models

Recent years have seen great advancement in deep learning technology. Deep learning algorithms are essentially multilayer neural networks. Massive training data, evolving computer skills and the development of network training methods have led to rapid advancement in deep learning technology. Based on object-oriented classification ideas, deep learning models can be applied to road information extraction, and convolutional neural networks can be used to achieve the mapping of remote sensing images from input to output (Figure 5.8).

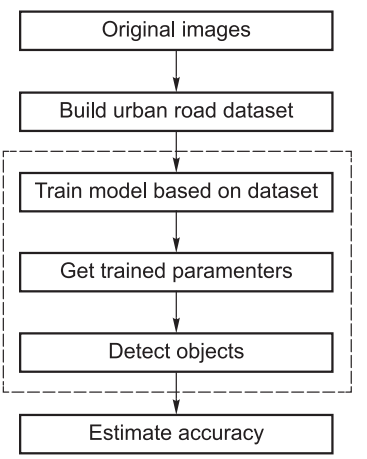

Figure 5.8 The technical route of urban roads extraction based on the deep learning models.

Downloaded from www.worldscientific.com
by fac sciences de la terre universite annaba on 07/30/24. Re-use and distribution is strictly not permitted, except for Open Access articles.

Downloaded from www.worldscientific.com
by fac sciences de la terre universite annaba on 07/30/24. Re-use and distribution is strictly not permitted, except for Open Access articles.

5.6 Urban Building Extraction Methods Based on Remote Sensing Imagery

Buildings are one of the important components of the types of features. Due to the rich feature information and notable noises in high spatial resolution remote sensing images, accurate building extraction is challenging. To automatically extract buildings from remote sensing images, commonly used approaches process remote sensing images according to the shape, spectral and spatial semantic features of different types of features:

Compared with rural buildings, the extraction of urban buildings from remote sensing images has the following difficulties:

1. In terms of spectral characteristics, there are a large number of same objects with different spectrum and different objects with same spectrum in high-resolution remote sensing images. Urban buildings and urban roads tend to have very similar spectral and textural characteristics.
2. The brightness value of the roof of a building in the remote sensing image can vary. Due to the diversity of roof materials, as well as the existence of solar heating panels and skylights, roofs tend to show different spectral characteristics.
3. In terms of shape characteristics, urban buildings are distributed in a concentrated manner, with complex shapes and changeable sizes. In most cases, buildings in the same neighborhood, city or village tend to have the same orientation and distribution rules.
4. The urban spatial layout is compact, and low-rise buildings are easily obscured by urban greenery and high-rise buildings, posing great challenges in building identification from remote sensing images.

Due to the complexity of a building structure and its surrounding environments, in order to improve the accuracy of building extraction, many scholars have developed new mathematical tools and theories to mine the features of shadows, textures and geometric structures in images.

Based on the images provided by the Massachusetts building public dataset and taking advantage of an improved fully convolutional network (FCN) structure (Long *et al.*, 2015), the automatic extraction of optical image buildings can be realized. Firstly, the features of the input image are extracted through convolution operation. Secondly, after each convolution layer, the ReLU activation function is used to further extract the deeper features of the

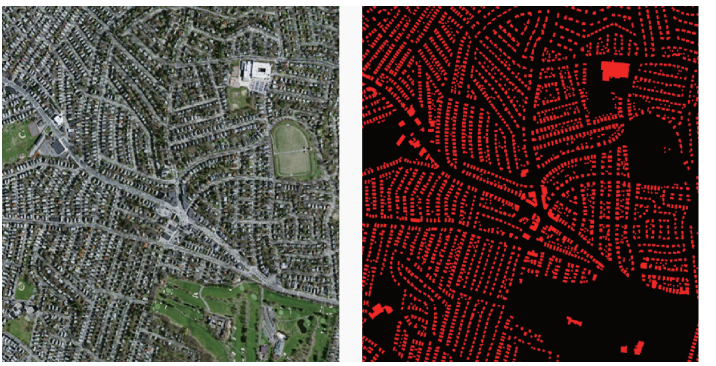

Figure 5.9 Using deep learning methods to extract urban buildings.

input image. Finally, the pixel-level buildings of the input image are extracted through the Softmax classifier. Figure 5.9 shows the extraction results of urban buildings in the Massachusetts region of the United States (Shao *et al.*, 2020).

5.7 Urban Lake Extraction Methods Based on Remote Sensing Imagery

The earth's surface is covered by approximately 70% of water bodies. Water bodies are one of the resources that have been widely exploited and utilized by mankind. With the continuous development of the economy and the increasing demand of human beings for a living environment, more and more attention has been paid to the monitoring, management and analysis of water resources. As an important factor in the urban ecosystem, urban lakes are a typical water body type in the city. Affected by the urban landscape design, trees are planted extensively around urban lakes and covered with related municipal garden facilities, affecting the development of the city and the living environment of residents. In recent years, remote sensing technology has been widely used in acquiring temporal and spatial information on water bodies, providing important information for maintaining the management and sustainable development of water ecosystems (Wu, 2009).

Theoretically speaking, the water radiation received by the sensor includes the reflected light from the water surface, from suspended objects, from the bottom of the water and the scattered light from the sky. The spectral

Downloaded from www.worldscientific.com
by fac sciences de la terre universite annaba on 07/30/24. Re-use and distribution is strictly not permitted, except for Open Access articles.

Downloaded from www.worldscientific.com
by fac sciences de la terre universite annaba on 07/30/24. Re-use and distribution is strictly not permitted, except for Open Access articles.

characteristics of the water body result from the interaction between the light transmitted into the water and the chlorophyll, sediment, yellow substance, water depth and thermal characteristics of the water body, thereby forming the difference in the characteristics of the reflection spectrum received on the sensor, providing the foundation of remote sensing-based water detection. Generally speaking, the yellow substance at 0.41 μm has a notable absorption peak, so 0.43–0.65 μm is the best band for measuring chlorophyll in water; 0.58–0.68 μm has peaks for different sediment concentrations, leading to the wide application of the near-infrared band in evaluating the concentration of suspended solids in water. After 0.75 μm, the water body becomes a total absorber, which is shown in the near-infrared remote sensing image, and the clear water body appears black.

As for lake water body information extraction technology, the commonly used method relies on water body index. Based on the water body spectral characteristic curve, the appropriate waveband is selected to construct a model, and the water body is classified and extracted. In 1996, McFeeters (1996) first proposed the usage of green light and near-infrared bands to calculate the NDWI to extract water body information. NDWI is able to distinguish between land vegetation and water bodies; Xu (2006) used an improved NDWI (MNDWI) to extract water body information, leading to improved identification of urban areas, which is more suitable for water body extraction in urban water networks. With the deepening of research and application, a variety of targeted water extraction models based on the characteristics of regional water systems have been proposed. Table 5.2

Table 5.2 Common indices for lake extraction.

Indices	Formula
NDWI	$\mathrm{NDWI} = \dfrac{\mathrm{Green} - \mathrm{NIR}}{\mathrm{Green} + \mathrm{NIR}}$
NDWI_3	$\mathrm{NDWI3} = \dfrac{\mathrm{NIR} - \mathrm{MIR}}{\mathrm{NIR} + \mathrm{MIR}}$
MNDWI	$\mathrm{MNDWI} = \dfrac{\mathrm{Green} - \mathrm{MIR}}{\mathrm{Green} + \mathrm{MIR}}$
EWI	$\mathrm{EWI} = \dfrac{\mathrm{Green} - \mathrm{NIR} - \mathrm{MIR}}{\mathrm{Green} + \mathrm{NIR} + \mathrm{MIR}}$
RNDWI	$\mathrm{RNDWI} = \dfrac{\mathrm{MIR} - \mathrm{Red}}{\mathrm{MIR} + \mathrm{Red}}$

shows the common indices for lake extraction. Figure 5.10 shows the comparison of the extraction effect between NDWI and MNDWI.

(a)

(b)

(c)

Figure 5.10 Comparison of extraction effect between NDWI and MNDWI: (a) Original image; (b) NDWI index; (c) MNDWI index.

Downloaded from www.worldscientific.com
by fac sciences de la terre universite annaba on 07/30/24. Re-use and distribution is strictly not permitted, except for Open Access articles.

Downloaded from www.worldscientific.com
by fac sciences de la terre universite annaba on 07/30/24. Re-use and distribution is strictly not permitted, except for Open Access articles.

After experimental comparison, NDWI may have certain errors for areas with more suspended solids, and MNDWI is more suitable for extracting the water boundary of eutrophic lakes.

Questions

1. What remote sensing software is currently available for remote sensing extraction of urban information? Please briefly introduce their feature extraction process.
2. As roads and buildings are typical types of urban features, what are the similarities and differences in their extraction methods?
3. Illustrate an index method for urban lake extraction.
4. How to apply deep learning technology to the extraction of urban remote sensing information?

References

Chen J, Liao A P, Chen J, Peng S, Chen L J, Zhang H W. 2017. 30-meter global land cover data product-global land30. *Geomatics World*, 24(1): 1–8.

He G J, Wang G Z, Long T F, Peng Y, Jiang W, Yin R Y, Jiao W L, Zhang Z M. 2018. Opening and sharing of big earth observation data: Challenges and countermeasures. *Bulletin of Chinese Academy of Sciences*, 33(8): 783–790.

He L, Li J, Liu C, Li S T. 2017. Recent advances on spectral-spatial hyperspectral image classification: An overview and new guidelines. *IEEE Transactions on Geoscience and Remote Sensing*, 56(3): 1579–1597.

He K, Zhang X, Ren S, Sun J. 2016. Deep residual learning for image recognition. *Proceedings of the IEEE Conference on Computer Vision and Pattern Recognition*, pp. 770–778.

Huang C, Davis L S, Townshend J R G. 2002. An assessment of support vector machines for land cover classification. *International Journal of Remote Sensing*, 23(4): 725–749.

Krizhevsky A, Sutskever I, Hinton G. 2012. ImageNet classification with deep convolutional neural networks. *Advances in Neural Information Processing Systems*, 25: 1097–1105.

Li J, Bioucas-Dias J M, Plaza A. 2010. Semisupervised hyperspectral image segmentation using multinomial logistic regression with active learning. *IEEE Transactions on Geoscience and Remote Sensing*, 48(11): 4085–4098.

Li S W, Wang Z B, Yang J. 2014. Method of fast extracting typical urban land cover information using remote sensing. *Computer Engineering and Design*, 35(03): 1088–1094.

Li M M, Stein A, Bijker W, Zhan Q M. 2016. Region-based urban road extraction from VHR satellite images using binary partition tree. *International Journal of Applied Earth Observation and Geoinformation*, 44: 217–225.

Long J, Shelhamer E, Darrell, T. 2015. Fully convolutional networks for semantic segmentation. In *Proceedings of the IEEE Conference on Computer Vision and Pattern Recognition*, pp. 3431–3440.

McFeeters, S. K. 1996. The use of the Normalized Difference Water Index (NDWI) in the delineation of open water features. *International Journal of Remote Sensing*, 17(7): 1425–1432.

Szegedy C, Vanhoucke V, Ioffe S, Shlens J, Wojna Z. 2016. Rethinking the inception architecture for computer vision. *Proceedings of the IEEE Conference on Computer Vision and Pattern Recognition*, pp. 2818–2826.

Shao Z F, Tang, P H, Wang Z Y, Saleem N, Yam S, Sommai, C. 2020. BRRNet: A fully convolutional neural network for automatic building extraction from high-resolution remote sensing images. *Remote Sensing*, 12(6): 1050.

Wu G. 2009. A review of remote-sensing-based spatial/temporal information capturing for water resource studies in Poyang Lake. *Proceedings of SPIE — The International Society for Optical Engineering*, p. 7492.

Xu H Q. 2006. Modification of normalised difference water index (NDWI) to enhance open water features in remotely sensed imagery. *International Journal of Remote Sensing*, 27(14), 3025–3033.

Downloaded from www.worldscientific.com
by fac sciences de la terre universite annaba on 07/30/24. Re-use and distribution is strictly not permitted, except for Open Access articles.

Downloaded from www.worldscientific.com
by fac sciences de la terre universite annaba on 07/30/24. Re-use and distribution is strictly not permitted, except for Open Access articles.

Chapter 6

Urban 3D Reconstruction Methods Based on Multi-source High-Resolution Remote Sensing Imagery

Cities are characterized by complex 3D scenes. When can we start using real 3D map navigation? We often encounter no communication signal in the corner of the city, caused mainly by inaccurate attenuation calculation when the signal penetrates and diffracts urban buildings. When will there be a fine 3D model of the city to support signal coverage optimization? When a public epidemic occurs, it is necessary to accurately locate people's social distance. When can we build a high-precision indoor and outdoor fine 3D model with extensive coverage? The Urban 3D model has become an important part of the urban spatial infrastructure and deserves detailed investigation.

The 3D reconstruction in this chapter refers to the reconstruction of the 3D model of the target from remote sensing data. According to the different technical routes adopted, 3D models can be reconstructed based on stereo-pair image, street views, laser scanning technology, mobile measurement technology and texture-based reconstruction methods. In this chapter, we aim to introduce these techniques. Then the quality control strategy of 3D reconstruction is discussed. Finally, we introduce the 3D reconstruction management platform under the urban scene and the real 3D planning of China.

6.1 Urban 3D Reconstruction Demands

As an important part of the geospatial framework of a digital city, 3D modeling can better reflect the 3D landscape of the city from multiple angles, intuitively and truly restore the urban style, and bring convenience to urban planning, construction and people's life (Figure 6.1). With the deepening of digital city construction, 3D geographic information systems have become an important content of digital city construction. The traditional manual 3D modeling method has numerous limitations, such as high investment cost, long construction cycle, insufficient data coverage and large model error, resulting in inaccurate spatial analysis results, slow data loading leading to slow response and weak ability of multi-source data integration. Despite the existence of many application cases and mature methods, 3D data publishing platforms are rare.

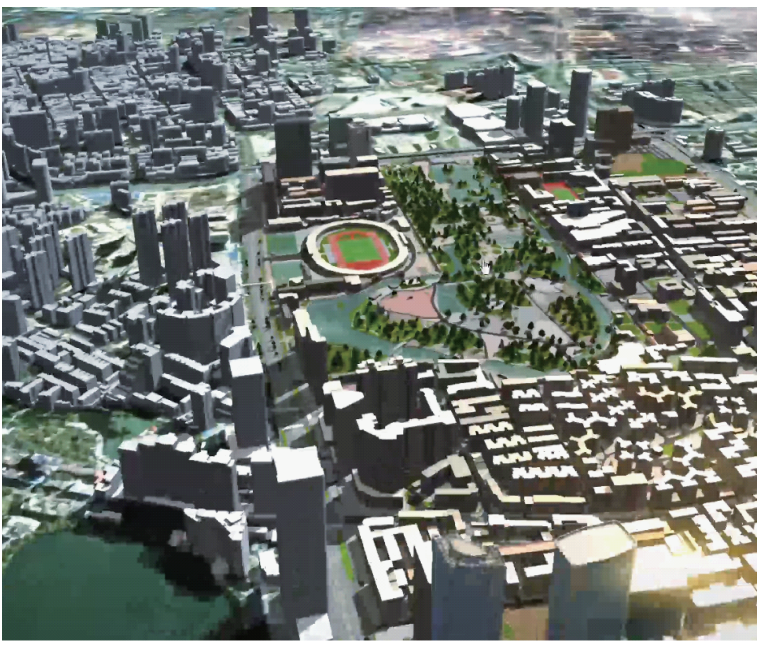

Figure 6.1 3D model of digital city.

The 3D remote sensing technology based on tilt photography has the advantages of a shorter modeling cycle, lower cost, higher accuracy and more realistic scene. Now, the tasks of 3D reconstruction include the following:

Downloaded from www.worldscientific.com
by fac sciences de la terre universite annaba on 07/30/24. Re-use and distribution is strictly not permitted, except for Open Access articles.

1. It is necessary to explore a set of the technical routes of "tilt data acquisition + real scene 3D modeling + scene data release and display", aiming to address the problems of high cost, long cycle and poor effect of traditional manual modeling.
2. Realize the integration of real 3D scenes, urban street view data and 360° panoramic data, making up for the disadvantage of poor 3D effect under head up.
3. Realize 3D spatial analysis functions, e.g., sunshine analysis, viewable analysis and slope analysis.
4. Realize monomer information query and solve the problem of attribute linkage between 3D modeling data and vector electronic data.

We are facing increasingly urgent demands for urban planning departments relying on intuitive, real and high-precision 3D spatial data as the urban spatial carrier. Thus, it is necessary to integrate tilt photography technology and real-scene 3D modeling technology to realize the functions of rapid browsing, query, analysis and management of massive and two-dimensional data.

Given the diversity of 3D representation, 3D models have different representation accuracy under different source data and different needs. The different performance accuracy positioning has obvious differences in the requirements of modeling source data, modeling workload and modeling cost. Given the accuracy of 3D model construction, 3D models can be divided into three categories: (i) measurable fine 3D model; (ii) analysis application display 3D model; and (iii) general display 3D model. The accuracy requirements of each type can be divided into four aspects, i.e., plane accuracy, elevation accuracy, texture accuracy and performance accuracy.

Measurable fine 3D model: In general, the plane and height spatial coordinates of each point, line and surface of the ground object are obtained through the topographic survey, aerial photogrammetry and airborne LiDAR, respectively. Further, the stereo-pair image of the aerial survey is used to collect the height and top structure of the ground object, combined with the texture collected on the spot, and the modeling platform is used to produce the model. The accuracy of the measurable real scene 3D model can be at the decimeter level, which has the characteristics of mature technology, high accuracy, high cost, and the instrument and equipment can be shared with conventional measurement projects.

Downloaded from www.worldscientific.com
by fac sciences de la terre universite annaba on 07/30/24. Re-use and distribution is strictly not permitted, except for Open Access articles.

Downloaded from www.worldscientific.com
by fac sciences de la terre universite annaba on 07/30/24. Re-use and distribution is strictly not permitted, except for Open Access articles.

Analysis application display 3D model: In general, the spatial plane position of the ground object is obtained through satellite remote sensing images (ground resolution less than 0.5 m). The height of buildings and other ground objects is estimated through the number of floors combined with the inferred floor height. The detailed structure and height of the ground object are modified according to the photos collected on the spot to form a model with relatively correct position, size and height. The accuracy of 3D analysis, application and the display is generally meter level, characterized by low technical requirements, high modeling efficiency and moderate cost. Such a technique has been mostly used in the construction of "digital cities" with a lack of source data and limited investment. It is mainly used for government services such as display, general analysis, search and positioning, aiming to provide more comprehensive real data reference.
General display 3D model: Simple modeling is often used to schematically represent the 3D distribution of the region. The building model structure generally adopts the outer contour of measured terrain data multiplied by the unified inferred floor heights. The texture generally adopts the schematic general texture library, while the ground part is produced by an orthophoto image and digital elevation model (DEM). Such a model is featured by low requirements for source data, high modeling efficiency and low cost, aiming to schematically represent the 3D geomorphic characteristics of the region. Such a model has been widely used in areas that lack source data, urban-rural fringes rural areas, as well as some plant areas and areas to be demolished with low accuracy requirements.

Urban 3D reconstruction is the technical basis for building a digital city, as well as for developing smart cities and their related applications. In recent years, with the rapid development of emerging technologies and industries, the construction of smart cities has gradually evolved from the original static 3D modelling level to the digital twin level where dynamic digital technologies are combined with static 3D models, thus giving rise to the new concept of digital twin cities to assist in the construction of smart cities. Obviously, the digital twin city is an extensive application of the digital twin concept at the city level, which aims to build a complex giant system in the physical world and the virtual space, where the two can be mapped and interact in both directions, and aims to recreate a twin city in the virtual space that matches and corresponds to the real city, forming a physical city in the physical dimension and a digital city in the information

dimension. The twin city will be a physical city in the physical dimension and a digital city in the information dimension, coexisting and blending the real and the virtual. The construction of a digital twin city requires both a database and a technology base. The database refers to the various sensors and cameras in the city, as well as the massive amount of urban big data generated by the digital subsystems built by various municipal administrations one after another on a daily basis. Technologies such as the Internet of Things, cloud computing, big data and artificial intelligence, including 5G, form the technical basis. In a digital twin city, the operational status of infrastructure, the deployment of municipal resources, and the safe transport and control of human, logistic and vehicular flows are all collected by sensors, cameras and digital subsystems and transmitted to the cloud and city managers via IoT technologies, including 5G. Based on this data and the city model, a digital twin of the city can be built to manage the city more efficiently.

6.2 Urban 3D Reconstruction Based on Stereo-Pair Image

At present, stereo-pair image technology is widely used to produce 3D model data. Data collected from stereo images are used to reconstruct the 3D model of buildings, as shown in Figure 6.2. However, due to the huge amount of data, monomer and other difficulties, the tilt photography model failed to be applied in a wide range, posing challenges to the application of 3D GIS. Tilt photography 3D model real-scene 3D data are continuous irregular triangulation data with mapping. It is not monomer, i.e., it is impossible to select buildings alone, let alone perform GIS functions such as query and production. As it can not be divided into objects that can be selected and queried separately according to buildings, roads and other features, it often serves as the base map. To better apply the data to the current 3D data application platform and realize the local update of the data, it is necessary to develop the real 3D data model monomer technology.

The original monomer technology aims to directly cut the tilt photography 3D model by inputting the vector base map of the corresponding ground object. However, given the fact that tilt photography 3D model data are of a triangular patch and texture, the triangular patch at the edge of the monomer object left by direct cutting presents sawtooth and cavity phenomenon and the aesthetics and accuracy cannot meet the needs of practical application.

Downloaded from www.worldscientific.com
by fac sciences de la terre universite annaba on 07/30/24. Re-use and distribution is strictly not permitted, except for Open Access articles.

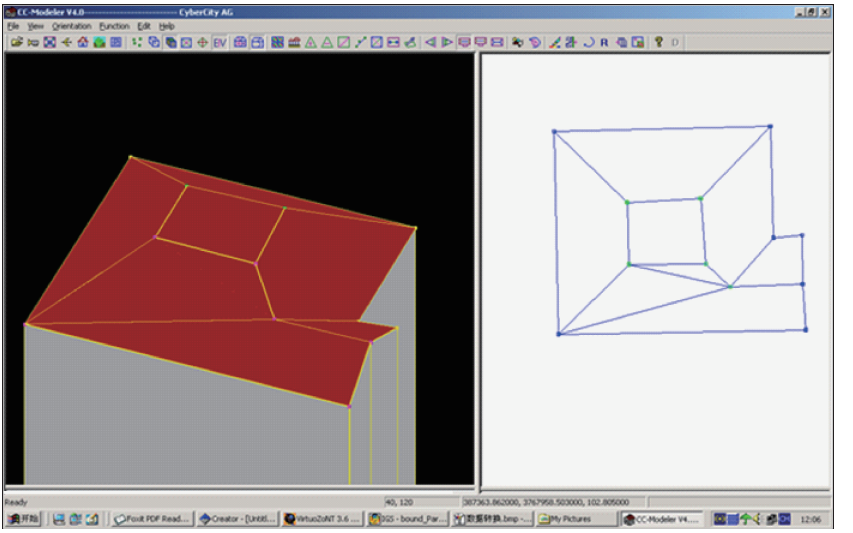

Figure 6.2 Building 3D model reconstruction based on 3D feature data.

In addition, information loss tends to occur for the model data after cutting. Thus, the GIS platform can only build level of detail (LOD) according to the method of the ordinary model, and the amount of data is huge. If the input corresponding to the figure vector base map changes slightly, a re-cutting needs to be performed.

Another approach is to store the two-dimensional feature vector base map and inclined 3D model data, respectively, and only use the vector layer for selection and query. However, if changes occur for ground features, it is necessary to re-measure and update the vector data layer, leading to a heavy workload. This method makes full use of the tilt photography 3D model data, generates a high-precision DSM then makes a high-precision real projective image, extracts the outer contour of the model through the object-oriented image segmentation technology and finally generates the single-object vector layer through topology construction "tilt photography 3D model data + figure monomer object vector layer" to select buildings, roads and other ground objects from the real scene 3D. The tilt photography 3D model data are used as the data basis of real-scene expression and 3D geospatial analysis, and the vector layer data of a single object of ground objects are used in the selection and query of 3D objects. The selection of 3D objects and the thematic display of analysis results are dependent on the vector map of a single object.

Downloaded from www.worldscientific.com
by fac sciences de la terre universite annaba on 07/30/24. Re-use and distribution is strictly not permitted, except for Open Access articles.

At present, the monomer technology usually adopts the method of superimposing the two-dimensional vector plane matched with the tilt photography model, aiming to realize the monomer at the rendering level and achieving the expression and operation of the monomer. For example, the model building can be highlighted, and the map attribute can be checked to ensure original data and LOD are not destroyed. The two-dimensional and 3D integrated channel between measurement planes is the key technology to achieve the object-oriented management of tilt photography data and multi-industry applications.

6.3 3D Reconstruction Based on Onboard LiDAR

Airborne LiDAR (light detection and ranging) is an emerging detection technology that has seen rapid development in recent years (Wehr and Lohr, 1999). LiDAR is the concentrated embodiment of the rapid development of laser ranging technology, computer technology, high-precision dynamic carrier attitude measurement technology (INS) and high-precision dynamic GNSS differential positioning technology, providing strong technical support for fast and efficient acquisition of 3D information in the measured area. LiDAR is able to quickly, actively and directly obtain the 3D information of a large range of surface and surface feature intensive sampling points in a real-time manner. An example of LiDAR data is shown in Figure 6.3. The general process of reconstructing a 3D model from airborne LiDAR data is presented in Figure 6.4.

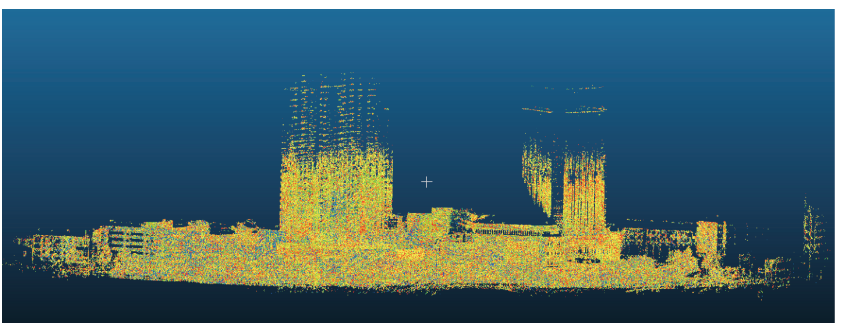

Figure 6.3 Point cloud data.

Downloaded from www.worldscientific.com
by fac sciences de la terre universite annaba on 07/30/24. Re-use and distribution is strictly not permitted, except for Open Access articles.

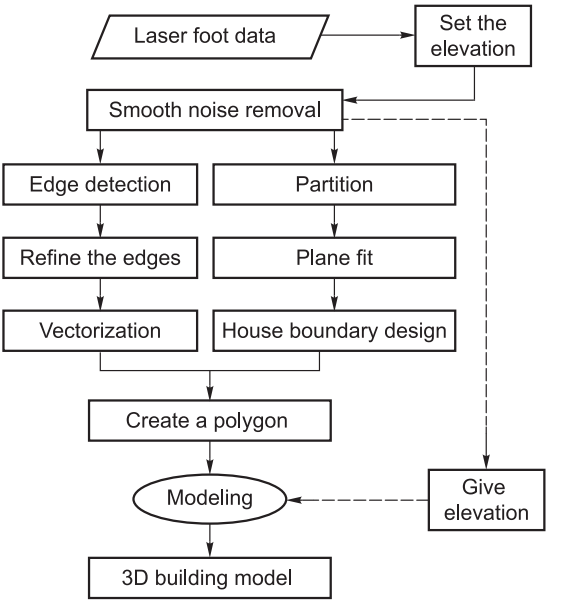

Figure 6.4 The general workflow of 3D model reconstruction from airborne LiDAR. Dash lines show the process of accuracy evaluation.

6.4 3D Reconstruction Based on Mobile Mapping Systems

The mobile mapping system is able to quickly collect spatial position data and attribute data, high-density laser point cloud data and high-definition continuous panoramic image data during the high-speed travel of the carrier, providing a fast, flexible and integrated 3D mobile measurement through the data processing, massive data management and application service software equipped with the system. Mobile mapping systems can achieve vector map data database building, 3D geographic data production, street view data production, which meet the application needs of the construction of 3D digital cities, street view map service, urban management component survey, public security emergency, security deployment and transportation infrastructure measurement, to list a few.

As shown in Figure 6.5, a commonly used mobile measuring vehicle is composed of a inertial measuring unit (IMU), digital and thermal camera, GNSS antenna and a laser scanner (LiDAR) (Christian, 2010; Hossain *et al.*, 2015).

Downloaded from www.worldscientific.com
by fac sciences de la terre universite annaba on 07/30/24. Re-use and distribution is strictly not permitted, except for Open Access articles.

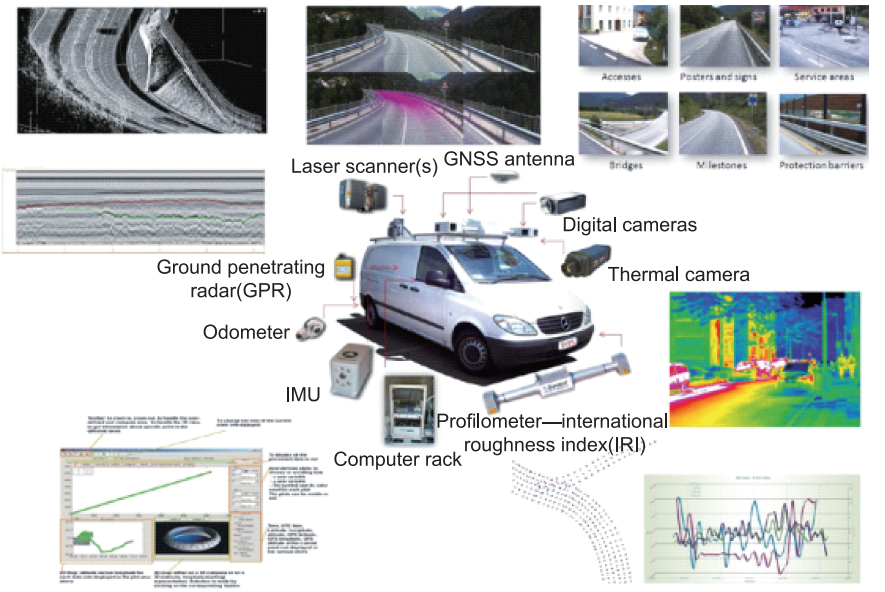

Figure 6.5 A mobile measuring vehicle.

6.5 3D Reconstruction of Urban Ancient Buildings Based on Ground LiDAR

As a new technology, ground LiDAR can directly obtain high-quality spatial information 3D data. Characterized by its strong real time high precision, fast scanning speed, strong initiative, strong universality, full digitization and less manual intervention, ground LiDAR has set off a new revolution in 3D information acquisition technology and application. In recent years, with the advance of 3D laser scanning technology in measurement accuracy, data processing and 3D visualization, the application fields of ground LiDAR are becoming increasingly extensive. At present, it has been widely used in 3D ground landscape measurement, the establishment of high-precision digital ground models, topographic measurement, ancient building structure measurement, 3D reconstruction of buildings, deformation detection, manufacturing design, game scene production and film stunts, among other fields.

Data obtained by the ground laser scanner are point cloud data of the target object, including the 3D position information and intensity information

Downloaded from www.worldscientific.com
by fac sciences de la terre universite annaba on 07/30/24. Re-use and distribution is strictly not permitted, except for Open Access articles.

of the point. Some ground LiDAR scanners are also equipped with CCD cameras, enabling the collection of texture and spectral information of the target objects, providing corresponding texture data for the 3D reconstruction of the target.

The processes and methods of ground laser scanning data processing are different given different application objects and different characteristics of point cloud data. Data preprocessing can be subdivided into point cloud data denoising, point cloud data resampling, point cloud data registration, point cloud data simplification, point cloud data blocking, etc. The 3D reconstruction stage mainly includes model reconstruction, smoothing and hole repair after model reconstruction, incomplete data processing and texture mapping.

The field ground LiDAR data acquisition system is mainly composed of a 3D laser scanner, digital camera, software control platform and auxiliary equipment. The 3D laser scanner adopts the non-contact high-speed laser measurement method and can obtain the high-density and high-precision array geometry data of space objects and ground 3D surfaces in a relatively short time, with data stored in the form of the point cloud. The instrument is mainly composed of a high-speed and accurate laser rangefinder and a group of reflection prisms guiding the laser and scanning at a uniform angular velocity. When acquiring the single-station scanning point cloud data, the laser scanner customizes the coordinates for the rangefinder. The laser rangefinder actively sends a laser pulse signal, transmitted back to the receiver after diffuse reflection on the object surface. Thus, the distance between the target point and the scanner can be calculated. The encoder can be controlled to measure the longitudinal scanning angle and transverse scanning angle of each laser pulse in a synchronous manner to obtain the coordinates of the target point relative to the center of the laser scanner.

Scanning control points can be arranged in the survey area before scanning. Generally, the geodetic coordinates of scanning control points can be obtained via traditional measurement methods, e.g., total station or GPS. The 3D geographical coordinates of scanning points can also be obtained. A ground 3D laser scanner is used to obtain the point cloud data and scanning point coordinates, and digital cameras are used to obtain the texture pictures of terrain and features. Further, the collected point cloud data are processed, and image data by the post-processing software are used to convert them into absolute coordinates or model data.

Downloaded from www.worldscientific.com
by fac sciences de la terre universite annaba on 07/30/24. Re-use and distribution is strictly not permitted, except for Open Access articles.

Downloaded from www.worldscientific.com
by fac sciences de la terre universite annaba on 07/30/24. Re-use and distribution is strictly not permitted, except for Open Access articles.

Different processes and methods of 3D laser scanning data processing are being used given the different application objects and different characteristics of point cloud data, when point cloud data obtained by a 3D laser scanner are applied to build the solid 3D geometric model (Ekin *et al.*, 2015). In general, data processing mainly includes data acquisition, data registration and fusion of different stations, geometric model reconstruction and post-processing, and texture mapping. Figure 6.6 shows the general process from collecting point cloud data to 3D reconstruction based on a station laser scanner.

Figure 6.7 shows the point cloud data of an ancient building obtained by the 3D laser scanner, and the corresponding 3D reconstruction effect is shown in Figure 6.8.

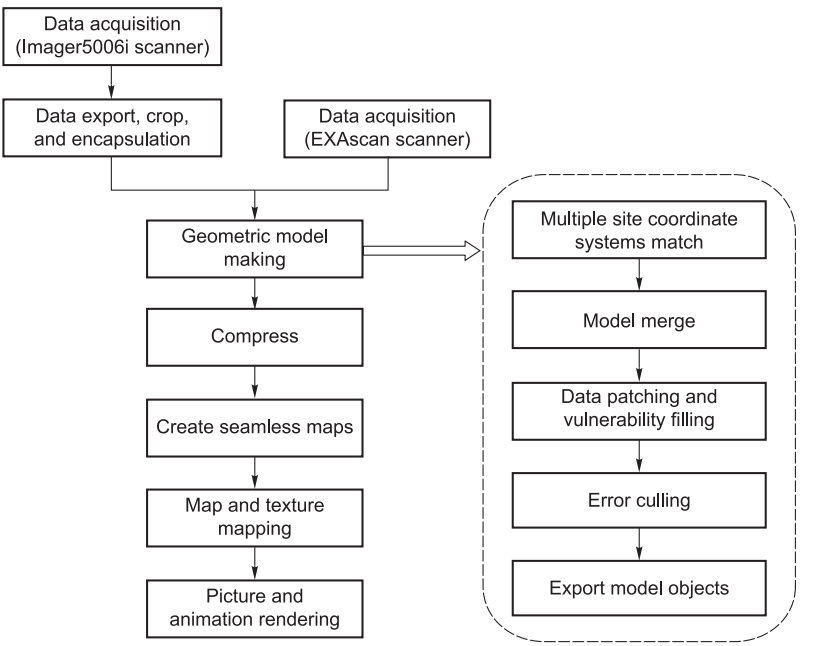

Figure 6.6 The general workflow of point cloud data acquisition to 3D reconstruction based on station laser scanner.

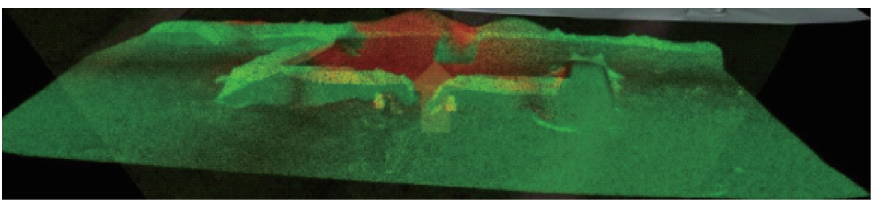

Figure 6.7 Point cloud data of an ancient building obtained by 3D laser scanner.

Figure 6.8 3D model of an ancient building reconstructed from laser scanning point cloud data.

6.6 Texture Reconstruction of Urban 3D Model

3D reconstruction includes two aspects: (i) geometric reconstruction and (ii) texture reconstruction. Texture reconstruction aims to address two problems: one is to register the texture image with the geometric model, and the other is to paste the texture image seamlessly onto the surface of the 3D model (Kang *et al.*, 2016). With the development of image computing power and computer vision technology, massive 2D images and video data based on aerial photography can be used to restore the texture data close to the real world and urban 3D panoramic model with rich details in the virtual world, allowing users to interactively view the appearance and changes of small and medium-sized urban elements, from green space and vegetation to building terrain online.

As shown in Figure 6.9, several process are performed as follows: (i) mesh segmentation; (ii) mesh unfolding; (iii) texture atlas generation; and

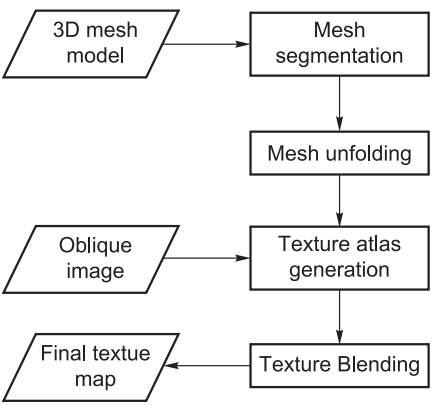

Figure 6.9 The flow of texture reconstruction from images.

Downloaded from www.worldscientific.com by fac sciences de la terre universite annaba on 07/30/24. Re-use and distribution is strictly not permitted, except for Open Access articles.

Figure 6.10 Texture reconstruction of the 3D model.

(iv) texture blending. Figure 6.10 shows an example of texture reconstruction of the 3D model.

6.7 Urban 3D Reconstruction Based on Street View Data

The vehicle mobile measurement system is adopted to collect street view data along the street. With the development of massive multi-source data, urban street view images can provide low-cost high-definition panoramic pictures of a large number of places. Using the panoramic street view pictures and the extracted depth information, a low-cost and automatic urban 3D modeling solution can be achieved.

Urban street view can be regarded as a browsable online database that contains billions of street panoramic images. For example, Google Street view is captured at 5–10 m in urban areas. According to a GNSS coordinate or a single recognition point, a virtual camera image of a panoramic picture can be obtained. These images are right-angle projections of panoramic images, allowing users to change field of view (FOV), directions and angles. These images can be regarded as undistorted images taken by small-hole imaging, with the availability for some 360° panoramic images.

In addition, according to the reflection speed of Google laser scanning on the object surface, the distance between the camera and the reflected object or

Downloaded from www.worldscientific.com
by fac sciences de la terre universite annaba on 07/30/24. Re-use and distribution is strictly not permitted, except for Open Access articles.

Figure 6.11 3D reconstruction based on street view image.

building can be calculated, leading to the capacity of establishing 3D models from Google maps and other applications. Google's API provides a method to obtain depth information corresponding to panoramic images, which can be used to reconstruct 3D scenes. After decoding and reconstructing, these models based on depth information can be used in multiple directions, e.g., navigation, AR and VR. In general, major steps of 3D modeling using street view data include synthesizing panoramic images, calculating depth maps, creating point clouds and synthesizing point clouds. An example of 3D modeling using street view images is shown in Figure 6.11.

6.8 3D Modeling Technology Based on Integrated Aerial-Ground Panoramic Imagery from Indoor and Outdoor

Compared with outdoor 3D modeling, the difficulty of indoor modeling lies in the 3D data acquisition. Recent years have seen wide usage of ground laser scanning and handheld laser scanning point cloud. For different scanning objects, scanners with different resolutions and different ranges are used for data acquisition, which reduces the redundancy of data with the capability of showing full details. For small scanning objects, handheld laser scanners are generally used to scan the details, and ground laser scanners are used to obtain the flat and rough parts of objects. The data of the two parts need to

Downloaded from www.worldscientific.com
by fac sciences de la terre universite annaba on 07/30/24. Re-use and distribution is strictly not permitted, except for Open Access articles.

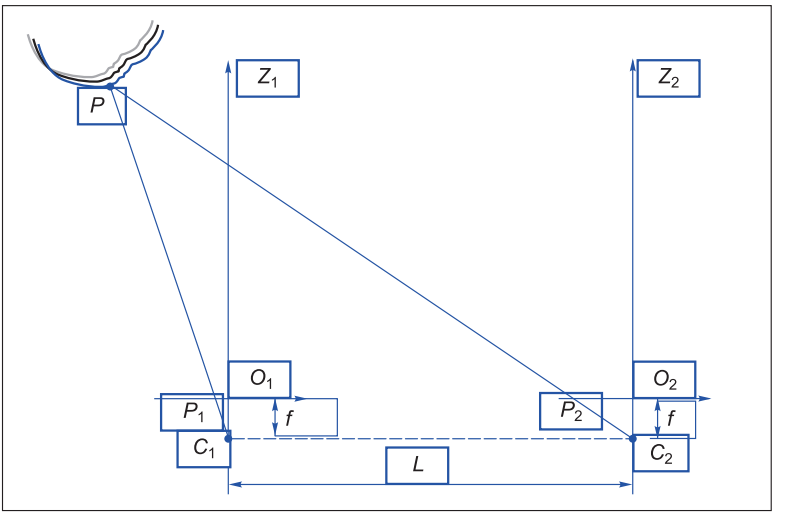

Figure 6.12 Principle of stereo vision measurement system.

be incorporated into a unified reference framework. Figure 6.12 shows the principle of a stereo vision measurement system.

In point cloud data fusion, the combination of coarse registration and fine registration is needed to achieve the fusion of ground laser scanning and handheld laser scanning point cloud data. Coarse registration (also called global registration) aims to find common feature points in two-point cloud data through the manual selection method and then realizes coarse registration of point cloud through the coordinate transformation model. At the same time, the registration parameters are used as the initial value of fine registration. Fine registration aims to complete iterative registrations through the improved iterative closest point (ICP) algorithm to improve the registration accuracy and realize the effect of seamless splicing.

In addition, the portable 3D digital system based on computer stereo vision and close-range photogrammetry is also an efficient information acquisition tool. The portable 3D digital system obtains images of target objects using photography and determines the spatial position, shape, direction and motion state. It is widely used in many fields. Portable 3D digital systems have many advantages: a large amount of physical and geometric information of the measured object can be obtained instantly; the utility model relates to a non-contact measurement method, which does not interfere with the natural state of the measured object. It is suitable for measuring the shape and motion state of dynamic objects and is also a means for measuring micro and

Downloaded from www.worldscientific.com by fac sciences de la terre universite annaba on 07/30/24. Re-use and distribution is strictly not permitted, except for Open Access articles.

distant targets. Based on rigorous theory and modern software, Portable 3D digital systems can provide accuracy of one-thousandth to ten-thousandth according to different processing methods, technical means and hardware investment, convenient for storage, management and reproduction.

Figure 6.13 shows the re-planning and protection application of ancient buildings.

The indoor 3D modeling of famous historical and cultural cities realizes the real-scene 3D modeling from outdoor to indoor (Figure 6.14). This achievement realizes the protection and maintenance of famous historical and

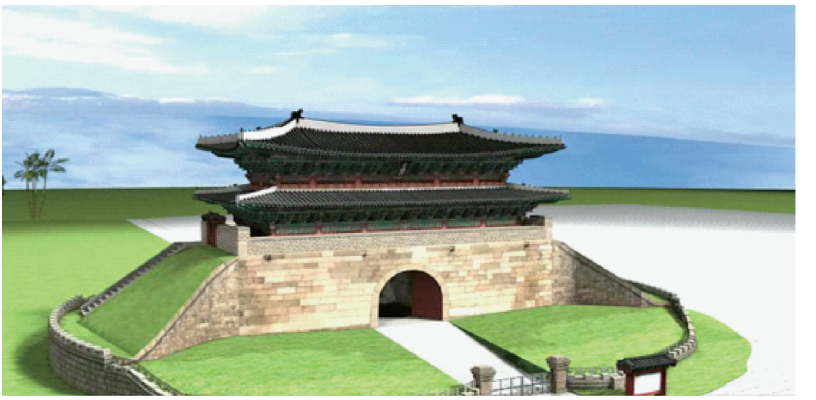

Figure 6.13 3D reconstruction of indoor and outdoor integration of Chonglimen, South Korea.

Figure 6.14 Indoor and outdoor integrated 3D modeling of Taizhou Wanghai Building, Taizhou, China.

Downloaded from www.worldscientific.com
by fac sciences de la terre universite annaba on 07/30/24. Re-use and distribution is strictly not permitted, except for Open Access articles.

cultural cities, leading to information sharing with cultural relics, tourism and other industries.

Downloaded from www.worldscientific.com
by fac sciences de la terre universite annaba on 07/30/24. Re-use and distribution is strictly not permitted, except for Open Access articles.

6.9 Quality Control Strategy for 3D Reconstruction of the Urban Scene

The quality control strategy of 3D reconstruction refers to the data quality inspection in the process of model reconstruction, which involves three major aspects: (i) the integrity of the 3D reconstruction model; (ii) the geometric accuracy of feature points of 3D reconstruction model; and (iii) the topological correctness of 3D reconstruction model.

The integrity check of the 3D reconstruction model refers to whether the production of 3D data covers the ground object types and entities defined in the production regulations and visible in the stereo image.

Combined with the characteristics of 3D reconstruction of urban artificial targets, the above quality control strategy can be achieved based on the stereo model of the stereo-pair image by checking the extracted vector feature points (or feature lines) onto the stereo image.

From the perspective of 3D reconstruction, 3D model checking mainly includes geometric model checking and topology checking.

The inspection of the geometric model aims to compare the established 3D model with the 3D model in the stereo-pair image after a model is established, check the correctness of the geometric structure of the three-dimensional model and determine the ground objects whose accuracy exceeds the limit and needs to be re-measured. In practice, the correctness of the model structure can be determined according to the different levels of points, lines, surfaces and bodies. The inspection methods and contents are different given different levels:

1. *Point inspection*: The geometric accuracy inspection of feature points of 3D reconstruction model refers to whether the geometric accuracy of feature points of image reconstruction indoor production meets the accuracy requirements defined in relevant data production specifications. It includes the accuracy of feature points for edge extraction and the accuracy of spline interpolation, specifically related to the plane accuracy and elevation accuracy of feature points.

2. *Line inspection*: Line inspection aims to check if the vertical and parallel conditions of the house edge are met. On most occasions, the edges of houses are vertical and parallel structures. However, it is generally difficult to meet in the actual measurement process. At present, the commonly used method is to use the grid function to edit and correct the parts that fail to meet the vertical and parallel structures.
3. *Plane inspection*: Plane inspection aims to check whether the plane structure is reasonable and whether the coplanar error meets the given limit.
4. *Physical examination*: Physical examination checks whether the height of the model is correct, whether the combination is complete and whether the geometric structure is reasonable.

Topological structure inspection: The topological correctness inspection of the 3D reconstruction model refers to the quality inspection of the topological structure of the 3D model based on the geometric constraint relationship among 3D model points, lines, faces and bodies. To complete topological structure inspection, 3D models need to be traversed and compared against the 3D images in the image pair to check whether the topology of the 3D model is correct. The main contents include the following:

1. *Visual inspection*: Visual inspection checks whether the established 3D model is visually consistent with the 3D image in terms of main structural features according to the 3D model.
2. *Redundant face check*: Redundance face check aims to determine whether there are redundant faces that destroy integrity.
3. External topology inspection between complex houses and their ancillary facilities.

6.10 3D Reconstruction Management Platform of the Urban Scene

At present, the popular 3D management platforms include TrueMap Globe, GeoGlobe, SuperMap, Skyline and MAPGIS platform.

Among them, GeoGlobe (shown as Figure 6.15) is a global massive seamless spatial data organization, management and visualization software under the network environment developed by the State Key Laboratory

Downloaded from www.worldscientific.com
by fac sciences de la terre universite annaba on 07/30/24. Re-use and distribution is strictly not permitted, except for Open Access articles.

of surveying, mapping and remote sensing information engineering of Wuhan University. Through the efficient organization, management and visualization of global massive image data, terrain data and 3D city model data, GeoGlobe achieves dynamic observations from any corner of the earth at any height and angle anywhere, by anyone and at any time. With its extensive satellite map library and topographic data, GeoGlobe gives users an immersive feeling via the application of 3D technology. GeoGlobe contains three major parts: GeoGlobe server, GeoGlobe builder and GeoGlobe viewer. The GeoGlobe server organizes registered spatial data through a distributed spatial data engine and provides real-time multi-source spatial data services. GeoGlobe builder realizes the efficient multi-level and multi-layer organization of massive image data, terrain data and 3D urban model data, and provides the data basis for realizing continuous global

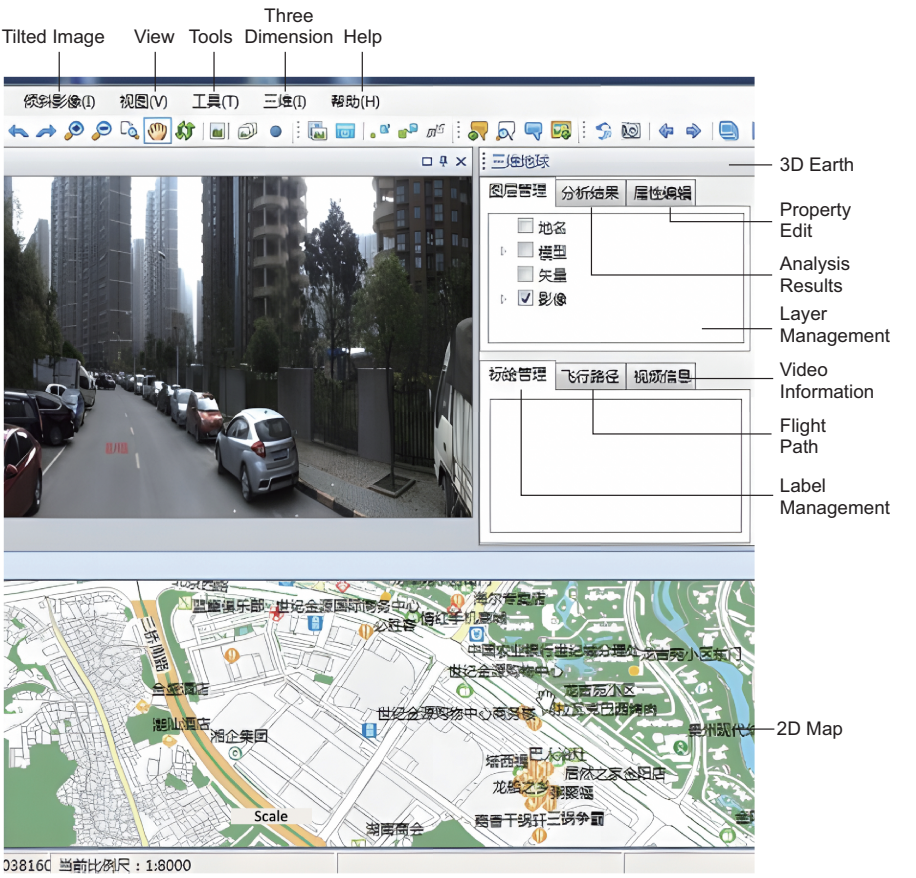

Figure 6.15 Integrated 2D–3D platform.

Downloaded from www.worldscientific.com
by fac sciences de la terre universite annaba on 07/30/24. Re-use and distribution is strictly not permitted, except for Open Access articles.

visualization. The GeoGlobe viewer is installed on the client to obtain server-side data through the network for 3D real-time display, query and analysis.

The great performance of the GeoGlobe software platform relies on three aspects: data management ability, application serviceability and visualization ability. Its main features include the following:

1. 2D and 3D integrated design, a software platform with independent knowledge copyright;
2. Support seamless integration with GIS platform;
3. Seamless organization and visualization of multi-source and multi-scale spatial data;
4. The open interface facilitates the seamless integration and application of secondary development and business system;
5. The realization of spatial information sharing and service by supporting WMS (Web map service), WCS (Web coverage service) and WFS (Web feature service) service specifications;
6. Supporting application integration of remote sensing image processing;
7. Supporting applications embedded in IE browser;
8. Supporting KML importing of Google Earth.

The 2D and 3D integrated technology system of the data management platform systematically integrates the powerful GIS function and gorgeous 3D visualization effect breaks through the application bottleneck that is not useful in simple 3D software and provides practical GIS functions, e.g., 3D spatial data management and query, 3D symbol system, and 2D and 3D spatial analysis. By applying the 2D and 3D integration technology to products that include servers, components, desktops, clients and mobile terminals, we are able to build practical 3D GIS applications that meet the needs of the in-depth analysis.

6.11 The Planning and Construction Practice of Real-Scene 3D in China

Real 3D data are featured by materialization, monomer, semantics and structure. It is a dataset of non-scale and all elements to express spatial

Downloaded from www.worldscientific.com
by fac sciences de la terre universite annaba on 07/30/24. Re-use and distribution is strictly not permitted, except for Open Access articles.

relationship and attribute information. The construction of real 3D China includes three-level construction: (i) terrain level; (ii) city level; and (iii) component level. Among them, the terrain-level real 3D scene reflects characteristics of terrain fluctuation and ground texture and can be used for large-scene and 3D visual expression of the current situation of natural resources and the geographical pattern of natural resources. The three-dimensional urban scene reflects the situation of the urban surface and can be used for fine expression of natural resources. The component-level real 3D scene reflects the locations, geometric forms, spatial relationships and attributes of solid elements in 3D space, mainly based on building information model (BIM) data, which can be used for personalized applications. Real 3D data are expected to replace traditional 4D products and gradually become the standardized achievement of new basic surveying and mapping in the future.

In terms of using science and technology to support intelligent urban management, urban managers hope to build a digital twin smart city. A digital twin city represents the concept of rebuilding a corresponding virtual city in cyberspace by digitizing all the elements of the physical city, e.g., people, things and events, to form a pattern of coexistence and blending of virtual and real cities in the physical dimension and digital cities in information dimension. Urban 3D spatial visualization, as key content of the digital twin city, has become an important issue in urban construction management. Upgrading from a 2D plane to a 3D plane has become an urgent demand for digital twin city construction. The construction of an urban real-scene 3D model is able to describe the urban spatial characteristics and realize the fine expression of urban 3D in an effective manner. The urban real-scene 3D realizes the real-scene visual query of the target and carries out intelligent planning and management of the digital twin city. Figure 6.16 shows the application of a real 3D map.

With the development of remote sensing technology, orthophoto and measurable real images, real 3D has become an important content of digital twin cities. Urban municipal fine management based on the electronic map is expected to develop towards the direction of image urban 3D real-scene management and service.

Downloaded from www.worldscientific.com
by fac sciences de la terre universite annaba on 07/30/24. Re-use and distribution is strictly not permitted, except for Open Access articles.

Figure 6.16 A real 3D map.

Questions

1. What are the main available remote sensing data sources for urban 3D reconstruction?
2. Compare the three-dimensional reconstruction differences between ground laser scanning technology and airborne laser scanning technology and tilt photography aerial image pair.
3. How can one realize 3D reconstruction based on urban street view data?
4. Describe the technical solution and application prospect of indoor and outdoor integrated 3D reconstruction.
5. What are the quality control strategies for urban 3D modeling?
6. What are the current software platforms for urban 3D reconstruction? Give an example to illustrate the purpose of the urban 3D model.

References

Christian H. 2010. Crowdsourcing geospatial data. *ISPRS Journal of Photogrammetry and Remote Sensing*, 65(6): 550–557.

Downloaded from www.worldscientific.com
by fac sciences de la terre universite annaba on 07/30/24. Re-use and distribution is strictly not permitted, except for Open Access articles.

Ekin O, Maria Q F, Feng D M. 2015. Citizen sensors for SHM: Towards a crowdsourcing platform. *Sensors*, 15(6): 14591–14614.

Hossain M, Kauranen I. 2015. Crowdsourcing: A comprehensive literature review. *Strategic Outsourcing: An International Journal*, 8(1): 2–22.

Kang J H, Deng F, Li X W, Wan F. 2016. Automatic texture reconstruction of 3D city model from oblique images. *International Archives of the Photogrammetry, Remote Sensing and Spatial Information Sciences*, XLI-B1: 341–347.

Wehr A, Lohr U. 1999. Airborne laser scanning — An introduction and overview. *ISPRS Journal of Photogrammetry and Remote Sensing*, 54(2–3): 68–82.

Downloaded from www.worldscientific.com
by fac sciences de la terre universite annaba on 07/30/24. Re-use and distribution is strictly not permitted, except for Open Access articles.

This page intentionally left blank

Downloaded from www.worldscientific.com
by fac sciences de la terre universite annaba on 07/30/24. Re-use and distribution is strictly not permitted, except for Open Access articles.

Downloaded from www.worldscientific.com
by fac sciences de la terre universite annaba on 07/30/24. Re-use and distribution is strictly not permitted, except for Open Access articles.

Chapter 7

Change Detection Methods and Applications of Urban Remote Sensing

Change detection, as a frontier branch in the field of digital image processing and understanding, is an important means to recognize and analyze the changes of targets in different time periods. At the end of the 1970s, as satellite earth observation became a reality, people began to study the characteristics of satellite periodic and repeated earth observations and use remote sensing data to extract surface information for change detection. By comparing remote sensing images from two different phases, the change detection methods present notable advantages in urban land cover change monitoring, urbanization dynamic monitoring, environmental change dynamic monitoring, natural disaster monitoring and crop yield estimation, to list a few.

7.1 Change Detection Demands of Urban Remote Sensing

Cities, often with dense population, industry, economy, technology, culture and architecture, are formed by the agglomeration of non-agricultural industries and strong human activities. With the development of national or regional social productive forces, the progress of science and technology and the adjustment of industrial structure, urbanization has become an inevitable trend of regional development. Besides, with the progress of human science and technology, the speed of urban development has been increasingly intensified. However, rapid urbanization is usually accompanied by issues that include environmental pollution, ecological destruction, low efficiency

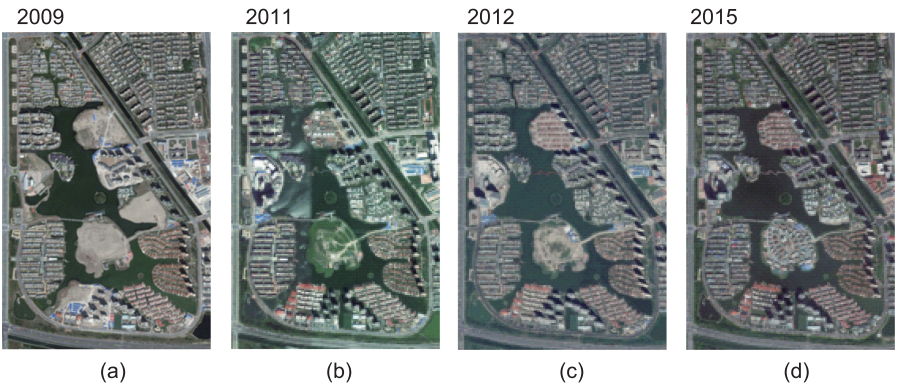

Figure 7.1 Multi-temporal remote sensing image used for urban change detection.

of land use, traffic congestion and other problems that pose challenges to urban security and urban management and development.

The development of remote sensing technology and the increasing popularity of remote sensing data establish a new venue where efficient urban planning, construction and management can happen due to its advantages of fast data acquisition, short revisiting cycle and synchronous observation in large areas. The use of multi-temporal remote sensing images to detect urban change has attracted more and more attention in recent years. Change detection technology can track urban development, monitor ecological environment change and assist urban management. The implementation of change detection approaches largely benefits our understanding of the human and natural environment, urban development and urban management.

Figure 7.1 shows the construction and development process of the same city from 2009 to 2015 using high-resolution remote sensing images.

7.1.1 Urban construction monitoring demands

The change detection technology can be used to identify and extract the changes of artificial ground objects that include roads, buildings and structures within the urban scope, facilitating our understanding of the progress of urban construction, urban expansion trend and engineering construction progress.

Downloaded from www.worldscientific.com
by fac sciences de la terre universite annaba on 07/30/24. Re-use and distribution is strictly not permitted, except for Open Access articles.

Figure 7.2 presents a scene of Nanhu Street, Wuhan City, in China. Figures 7.2(a) and (b) are satellite images obtained in July 2011 and April 2012, respectively. Many buildings in this area were demolished from 2011 to 2012.

Figure 7.3 shows the new and demolished buildings extracted by the object-level change detection method in two time-phase images. The change detection technology is able to quickly discover, accurately locate and extract

Figure 7.2 Satellite images of Nanhu Street, Wuhan City, China, in 2011 (a) and 2012 (b).

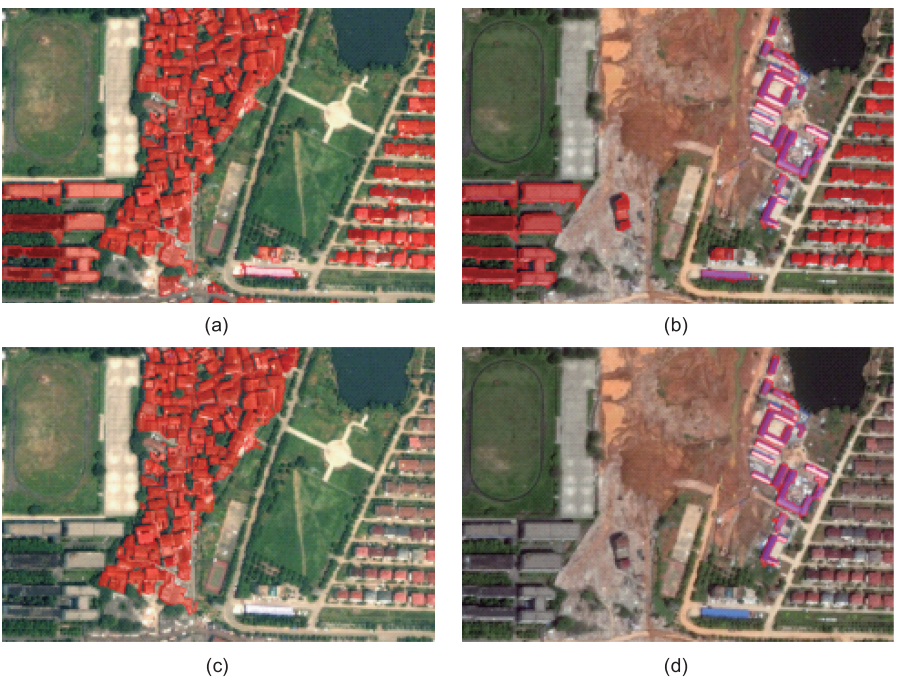

Figure 7.3 The results of building extraction and change detection in Nanhu Street, Wuhan City, China, in 2011 and 2012: (a) Building extraction results in 2011; (b) Building extraction results in 2012; (c) Demolished buildings; (d) New buildings.

Downloaded from www.worldscientific.com
by fac sciences de la terre universite annaba on 07/30/24. Re-use and distribution is strictly not permitted, except for Open Access articles.

changed urban features, greatly benefiting the monitoring of engineering construction and urbanization.

7.1.2 Urban management monitoring needs

High-resolution remote sensing data feature the characteristics of high spatial, high spectral and high temporal resolution, which can better observe various urban construction factors and master urban change factors. Change detection techniques greatly benefit the improvement of urban planning, construction and management. At present, change detection has been widely used in urban land use monitoring and illegal construction monitoring. In addition, it has also been applied in inspection, illegal dumping investigation and punishment.

7.2 Change Detection Process of Urban Remote Sensing

The change detection process of remote sensing images can be mainly divided into five stages (Figure 7.4):

1. *Image selection and acquisition*: The type, source, resolution, band and time of remote sensing images are determined to carry out data acquisition by considering change detection requirements, target characteristics, data acquisition cost and feasibility.

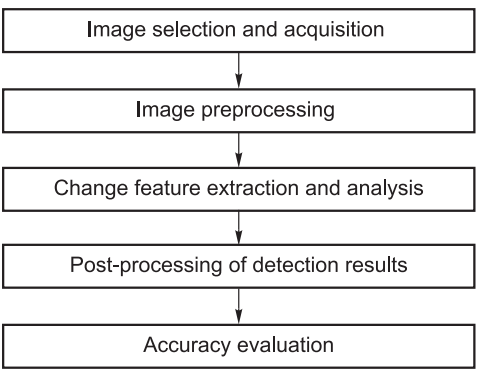

Figure 7.4 The basic 5-step process of remote sensing image change detection.

Downloaded from www.worldscientific.com
by fac sciences de la terre universite annaba on 07/30/24. Re-use and distribution is strictly not permitted, except for Open Access articles.

2. *Image preprocessing*: In order to minimize the influence of image differences on the change detection results, a series of pretreatments are demanded. Generally, radiation correction is used to reduce the radiation difference caused by atmospheric conditions, illumination conditions and other environmental factors during the image acquisition phase. Geometric correction denotes the process used to reduce the positional difference of images, and image enhancement is used to improve image quality and highlight the change detection characteristics.
3. *Change feature extraction and analysis*: The extraction of features is essential to detect changes in remote sensing images. It is usually necessary to determine the basics of change analysis, whether a classification system is needed, what comparison methods of multi-temporal images should be used and what quantitative methods of change extraction need to be implemented.
4. *Post-processing of detection results*: In most cases, pseudo changes tend to occur in the detected results. In order to improve the detection accuracy, filtering or morphology algorithms are commonly used approaches for post-processing, aiming to optimize the extraction results.
5. *Accuracy evaluation*: By establishing evaluation metrics and methods, the reliability and accuracy of the change detection results can be analyzed qualitatively and quantitatively by comparing the change detection results with the ground truth.

Change detections are generally regarded as a binary classification process, and the confusion matrix is used to calculate producer accuracy (PA), user accuracy (UA) and overall accuracy (OA) to evaluate the change detection results. Table 7.1 shows the evaluation metrics of pixel-level change detection results.

Table 7.1 Evaluation metrics of pixel-level change detection results.

Number of pixels		Reference results	
		Actual changes	**Actually unchanged**
Detection results	Changed	True positives (TP)	False positives (FP)
	Unchanged	False negatives (FN)	True negatives (TN)

Producer accuracy: The producer accuracy of the change category refers to the proportion of the correct detected changes in the actual changes. Its calculation is as follows:

Downloaded from www.worldscientific.com
by fac sciences de la terre universite annaba on 07/30/24. Re-use and distribution is strictly not permitted, except for Open Access articles.

$$PA = TP/(TP + FN)$$

User accuracy: The user accuracy of the change category refers to the ratio of correctly detected changes in all detected changes. Its calculation is as follows:

$$UA = TP/(TP + FP)$$

Overall accuracy: Overall accuracy refers to the ratio of the correctly detected changes to the correctly detected non-changes in the total. Its calculation is as follows:

$$OA = (TP + TN)/(TP + FP + FN + TN)$$

7.3 Change Detection Methods of Urban Remote Sensing

Change detection methods are application dependent. Traditional image interpretation mainly relies on interpreters' expertise, with low repeatability and accuracy and a long processing cycle. The interpretation over extensive regions can be labor intensive. Therefore, rapid and automatic detection methods are increasingly valued, especially with the continuous increase of remote sensing data. It is necessary to explore technical and practical methods. The core of change detection lies in the extraction and analysis of image changes. According to different analysis elements and data, change detection methods can be divided into 2D and 3D methods.

7.3.1 2D change detection methods

7.3.1.1 Pixel-level change detection method

The pixel-level change detection method takes the pixels in the image as the analytical unit and extracts the change information of the gray value through specific methods such as image difference, image regression and pixel ratio, while generally ignoring the relationship between pixels.

Difference method: The image difference method subtracts the gray values of corresponding pixels in multi-temporal images. The resulting images represent the changes of two temporal images. The image difference method

Downloaded from www.worldscientific.com
by fac sciences de la terre universite annaba on 07/30/24. Re-use and distribution is strictly not permitted, except for Open Access articles.

Downloaded from www.worldscientific.com
by fac sciences de la terre universite annaba on 07/30/24. Re-use and distribution is strictly not permitted, except for Open Access articles.

can be applied to a single band (i.e., univariate image difference) and multiple bands (i.e., multivariable image difference). The expression is as follows:

$$Dx_{ij}^{k} = x_{ij}^{k}(t_2) - x_{ij}^{k}(t_1) + C \tag{7.1}$$

where i and j are pixel coordinate values, k is for the band, t_1 and t_2 are the time of the first image and the second image and C is a constant to get a positive value.

To identify the region of change, the image difference formula (7.1) can be converted to formula (7.2):

$$Dx_{ij}^{k} = \left| x_{ij}^{k}(t_2) - x_{ij}^{k}(t_1) \right| \tag{7.2}$$

The mean and standard deviation of difference images were calculated by statistical processing. If the gray value of the pixel in the difference image satisfies formula (7.3), the change occurs:

$$Dx_{ij}^{k} - m \geqslant T_d * \mathrm{STD} \tag{7.3}$$

where m is the mean value of difference image, STD stands for the standard deviation of difference image and T_d is the thresholding value.

In most cases, directly subtracting the gray value of the corresponding pixel leads to poor performance in change detection. Thus, the gray value of the center pixel is often replaced by the window mean for calculation.

Correlation coefficient method: The correlation coefficient method calculates the correlation of corresponding pixels in two temporal images. In general, windows are constructed, and the correlation coefficient of the corresponding window in the two images is calculated to represent the correlation of the window center pixel. A correlation value close to 1 denotes high correlation, i.e., no change occurs. The correlation coefficient is obtained by formula (7.4). If the correlation coefficient r satisfies formula (7.5), it is considered that the pixel has changed, and T_r is the threshold value:

$$r_{ij} = \frac{\sum_{m=1}^{n} (x_m - \bar{x})(y_m - \bar{y})}{\sqrt{\sum_{m=1}^{n} (x_m - \bar{x})^2} \sqrt{\sum_{m=1}^{n} (y_m - \bar{y})^2}} \tag{7.4}$$

where n is the number of all pixels in a window; $\bar{x}$, $\bar{y}$ are the average values of the pixel gray in the corresponding windows.

$$r \leqslant T_r \tag{7.5}$$

Downloaded from www.worldscientific.com
by fac sciences de la terre universite annaba on 07/30/24. Re-use and distribution is strictly not permitted, except for Open Access articles.

Ratio method: The ratio method achieves change detection tasks by calculating the ratio of gray values of corresponding pixels in multi-temporal images. An unchanged pixel is with a ratio close to 1. In contrast, a changed pixel is with a ratio much greater than or much less than 1 (depending on the direction of the change). The mathematical expression is shown in Eq. (7.6):

$$Rx_{ij}^{k} = \frac{x_{ij}^{k}(t_2)}{x_{ij}^{k}(t_1)} \tag{7.6}$$

The process of the ratio method is similar to that of the image difference method, except that the ratio of the window mean is calculated at the end instead of the difference. When Rx_{ij}^{k} satisfies Eq. (7.7), it is considered that the pixel has changed:

$$Rx_{ij}^{k} \leqslant T_l \quad \text{or} \quad Rx_{ij}^{k} \geqslant T_h \tag{7.7}$$

where T_l and T_h represent two lower-bounded and higher-bounded thresholds, respectively.

Image regression method: In the image regression method, the pixel in the image obtained at time t_1 should be represented as a linear function of the corresponding pixel in the image obtained at time t_2. Thus, the least mean square error estimate can be used to estimate this linear function. Given the gray values of the pixel at points (i, j) in the two images are $x_{ij}^{k}(t_1)$ and $x_{ij}^{k}(t_2)$, respectively, where k represents the number of bands, the estimated pixel value of the second image can be calculated by the estimated linear function of $x_{ij}^{k}(t_1)$ is $\hat{x}_{ij}^{k}(t_2)$. The difference image can be expressed as follows:

$$Dx_{ij}^{k} = \hat{x}_{ij}^{k}(t_2) - x_{ij}^{k}(t_2) \tag{7.8}$$

By selecting an appropriate threshold, the changed areas can be determined. The image regression method can be used to deal with the difference between the mean and variance of images in different periods.

Change vector analysis: Multi-spectral remote sensing image data can be represented in the vector space with the same dimension as the spectral component of the image. A particular pixel in the image can be represented by a point in this vector space, whose coordinates are related to the brightness values of the corresponding spectral components. Thus, those data values associated with each pixel define a vector in the multidimensional space.

Given a pixel that changes from time t_1 to t_2, its change can be quantified by the difference in vectors at t_2 and t_1, i.e., the spectral change vector. If the

Downloaded from www.worldscientific.com
by fac sciences de la terre universite annaba on 07/30/24. Re-use and distribution is strictly not permitted, except for Open Access articles.

magnitude of the spectral change vector exceeds a specific threshold, a change is considered to occur. The direction of this vector contains the change type information.

Principal component analysis: Principal component analysis (PCA) uses principal component transformation. In the covariance or correlation matrix of the original data, a linear transformation defines a new Cartesian coordinate system, and the data can be expressed in an uncorrelated form. Each axis of the new coordinate system is defined by the corresponding eigenvectors of the matrix. Each pixel can be transformed by the vector product of its original vector (e.g., the pixel brightness value) and the feature vector. Further, the coordinates of the new space (e.g., a new pixel vector) can be obtained. Each feature vector can be regarded as a defined new band, and the coordinates of each pixel can be regarded as its brightness in that "band".

The total scene variation represented by each new "band" is given by the eigenvalue of the corresponding eigenvector. For regions that do not change in a significant manner, the correlation between images is high. In contrast, for regions that change in a significant manner, the correlation is low. It is assumed that the main part of the variation in the multi-temporal images is associated with a constant type, then the region with local variation is enhanced in the higher principal component. Note that the principal components determined by the covariance matrix are different from those determined by the correlation matrix.

Normalized image difference method: The normalized image difference method slightly differs from the original image difference method. In the normalized image difference method, two images are normalized before comparison to generate an image with a comparable mean and variance, and the normalized image is subtracted to derive the difference image. The normalization approaches can vary, but the commonly used approach is as follows:

$$\mu_k = a_k + b_k(x_k - \bar{x}_k) \tag{7.9}$$

where x_k is the pixel value of the kth band, $\bar{x}_k$ is the mean value of the kth band of a given image, μ_k is the output value of the kth band, a_k and b_k are parameters whose calculation is as follows:

$$a_k = \bar{\mu}_k; \quad b_k = \frac{s_{\mu_k}}{s_{x_k}} \tag{7.10}$$

where $\bar{\mu}_k$ represents the mean of μ_k; s_{x_k} and s_{μ_k} are standard deviations of x_k and μ_k, respectively.

Downloaded from www.worldscientific.com
by fac sciences de la terre universite annaba on 07/30/24. Re-use and distribution is strictly not permitted, except for Open Access articles.

The implementation of the normalized image difference method can improve the detection performance. However, its performance is highly dependent on the selection of the transformation coefficient. In the normalization process, the mean and variance need to be calculated before transformation, leading to increased running time.

Inner product analysis: The inner product analysis method regards the gray values of pixels as multi-spectral vectors. Thus, the difference between two vectors can be expressed by the cosine of the angle between them. If two vectors are consistent with each other, the inner product is equal to 1; if the corresponding pixels of two different periods change, the inner product fluctuates between -1 and 1. The changes can be reflected by generating a single band image to record the inner product.

Let x and y be the spectral vectors taken from the corresponding pixels of two images at different times, and the inner product of the two vectors can be expressed as follows:

$$\langle x(t_1), x(t_2)\rangle = \sum_{k=1}^{b} x(t_1)_k x(t_2)_k \tag{7.11}$$

The difference in surface reflection values can be expressed as follows:

$$d = \frac{\langle x(t_1), x(t_2)\rangle}{\sqrt{\langle x(t_1), x(t_1)\rangle\langle x(t_2), x(t_2)\rangle}} \tag{7.12}$$

Given $-1 < d < 1$, the inner product can be expressed as follows:

$$C = a_1 d + a_0 \tag{7.13}$$

where a_1 and a_0 are two constants, leading to the inner product C as non-negative interval.

Texture feature difference method: The gray co-occurrence matrix emphasizes the spatial dependence of the gray scale, which is characterized by reflecting the spatial relationship of pixel gray scale in a texture mode. Here, the texture characteristic value is used as the change detection object of the center pixel of the region, and the contrast is chosen as the texture feature.

The value of each element in the gray level co-occurrence matrix is determined by Eq. (7.14):

$$p_{ij} = \frac{p(i, j, d, \alpha)}{\sum_i \sum_j p(i, j, d, \alpha)} \tag{7.14}$$

where $p(i, j, d, \alpha)$ is the occurrence times of pixel point pairs with gray scales of i and j, distance of d and direction of α.

$$f = \sum_{i,j} (i - j)^2 p_{ij} \tag{7.15}$$

The expression is as follows:

$$Dx_{ij} = f_{ij}(t_2) - f_{ij}(t_1) + C \tag{7.16}$$

where f_{ij} is texture feature value, i and j are pixel coordinate values, t_1 and t_2 are acquisition time of two images, and C is a constant.

Wavelet transform coefficient difference method: Remote sensing images can be decomposed by wavelet transform. For unchanged pixels, the wavelet coefficients of the corresponding regions are close to each other. Otherwise, the wavelet coefficients of the corresponding region differ greatly. The difference of wavelet coefficients corresponding to each band of images can be calculated, and for unchanged regions, the obtained wavelet coefficients are close to 0.

Therefore, when the inverse wavelet transform is carried out, the brightness value of image spots in the obtained image where the target changes is large. However, the brightness value of the unchanged area is small, and the changing target can be distinguished according to the brightness difference of image spots. Figure 7.5 presents a QuickBird image scene in Wuhan in 2002 and 2004. Figure 7.6 shows the detection results of using the ratio method.

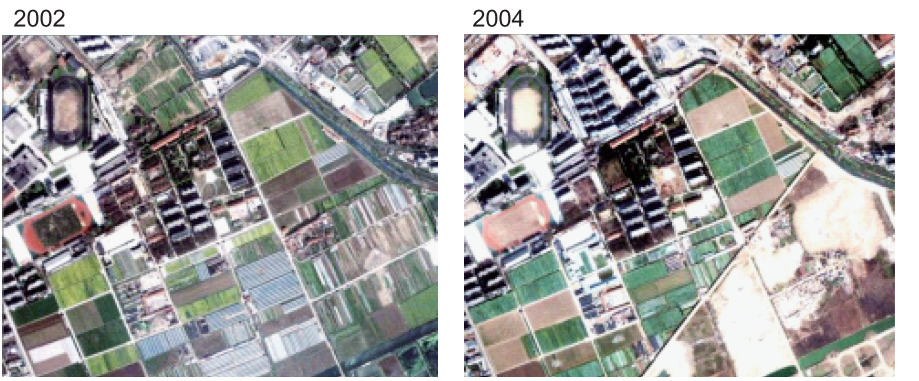

Figure 7.5 QuickBird image scene in Wuhan in 2002 (a) and 2004 (b).

Downloaded from www.worldscientific.com by fac sciences de la terre universite annaba on 07/30/24. Re-use and distribution is strictly not permitted, except for Open Access articles.

Figure 7.6 The change detection results using the ratio method from Figure 7.5.

In general, pixel-level change detection methods are simple and easy to operate. With the popularity of high-resolution remote sensing images, however, the limitations are becoming notable. These limitations include the following: (i) heavy workload and low efficiency; (ii) detection results sensitive to external influences, e.g., radiation differences; (iii) difficulty in threshold setting; and (iv) notable pepper-and-salt noises in the detected results.

7.3.1.2 Object-level change detection method

The object-level change detection method, unlike the pixel-level change detection method, is able to handle high-resolution images. This kind of method takes multi-temporal image objects as the primitive of change feature extraction and analysis and requires image segmentation of multi-temporal remote sensing images. In the process of image segmentation, the changes can be determined by comparing the characteristics or categories of image objects in different periods while considering the problems of multi-temporal objects.

The multi-temporal object construction method of homonymous objects refers to image segmentation of remote sensing images of different time phases. In the process of change detection, in order to achieve the change analysis of image objects at different times, it is necessary to establish the relationship between the homonymous objects from multi-temporal images

Downloaded from www.worldscientific.com
by fac sciences de la terre universite annaba on 07/30/24. Re-use and distribution is strictly not permitted, except for Open Access articles.

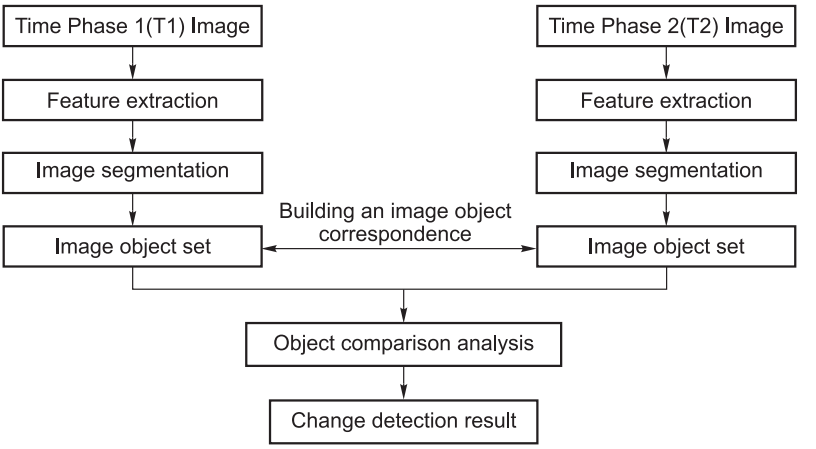

Figure 7.7 The flowchart for detecting structure changes of homonymous objects.

(Figure 7.7). In the process of image object change analysis, geometric features such as spectral features, size and shape of the object, and contextual features such as spatial relations of the object can be fully utilized. However, such a homonymous object approach is more difficult to implement.

In addition, due to the sensor problems (e.g., imaging position, camera attitude and system error), unsatisfactory external environments (e.g., solar height, atmospheric conditions, weather conditions, lighting conditions, shadow occlusion and seasonal phenology change) and other factors, there exist significant spectral and geometric disparities in remote sensing images obtained at different times, potentially leading to the detection of false changes. Therefore, establishing the relation of the image objects in different images and determining the homonymous object are of great importance.

Figure 7.8 shows the remote sensing images of the Meijiang Eco-residential Area in Tianjin, China, acquired in May 2009 and March 2016. Meijiang

Figure 7.8 Remote sensing images of the Meijiang Eco-residential Area in Tianjin, China, in 2009 (a) and 2016 (b), respectively.

Downloaded from www.worldscientific.com
by fac sciences de la terre universite annaba on 07/30/24. Re-use and distribution is strictly not permitted, except for Open Access articles.

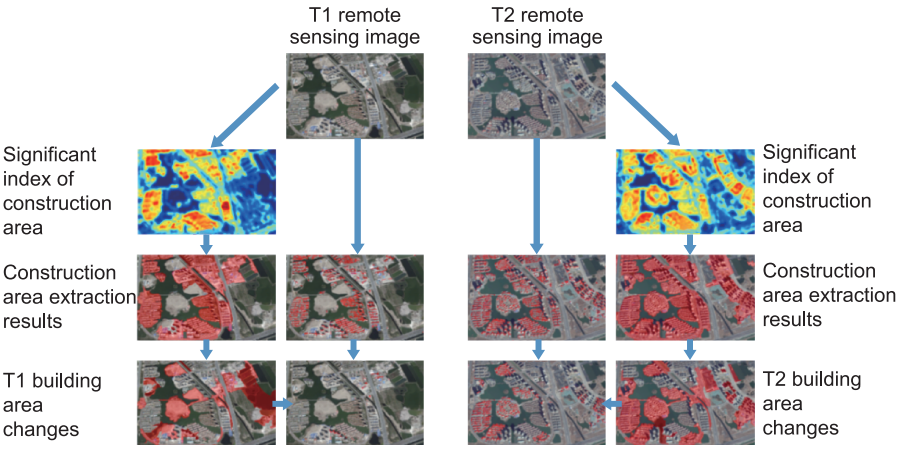

Figure 7.9 Urban building change detection process based on building district-building double scale object of the same name.

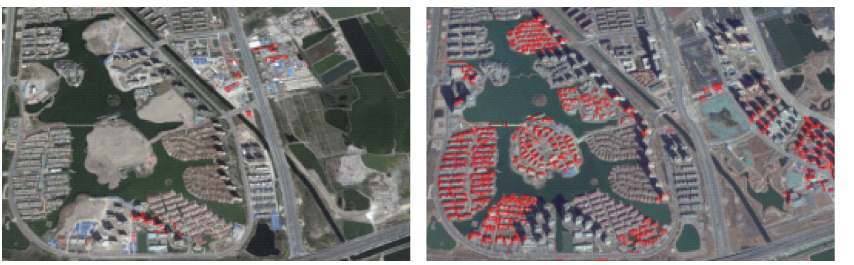

Figure 7.10 Building detection results at different times.

Eco-residential Area is one of the four major residential areas in Tianjin. Since 1999, it has undergone frequent changes.

Urban building change detection based on dual-scale homonymous objects first uses multi-scale segmentation and object matching algorithm for phase images (by setting different thresholds to detect the changes of construction in large-scale object area) and then detects the changes in construction areas. Figures 7.9 and 7.10 show the change detection process of dual-scale urban homonymous buildings and the detection results of the changed buildings at different times, respectively.

7.3.1.3 Post-classification change detection method

The post-classification change detection method is the simplest change detection and analysis method based on classification. It can be used for two

Downloaded from www.worldscientific.com
by fac sciences de la terre universite annaba on 07/30/24. Re-use and distribution is strictly not permitted, except for Open Access articles.

Downloaded from www.worldscientific.com
by fac sciences de la terre universite annaba on 07/30/24. Re-use and distribution is strictly not permitted, except for Open Access articles.

or more registered images, including a classification step and a comparison step. The post-classification change detection method requires each image of multi-temporal images to be separately classified, followed by the comparison between the results of classification.

If the category of the corresponding pixel is the same, the pixel is considered as an unchanged pixel; otherwise, the pixel is considered as a changed pixel. The classification method can be either supervised or unsupervised. An important advance in post-classification change detection is that it can overcome the inconvenience caused by the difference of sensor properties and resolution of multi-temporal images and does not require data normalization, given the fact that two images are separately classified. The post-classification comparison method is able to detect changes of non-urban areas to urban areas, the change of forest to farmland, the change of general land use and marshland.

However, the post-classification comparison method owns its own limitations from these three aspects:

1. The post-classification comparison method demands reasonable classification. Too fine a classification can produce a large number of edge points, resulting in the increase of detection error. Too rough a classification ignores the differences between some categories, failing to reflect the actual situation well.
2. Classification and change detection steps are separated. When classification and change detection are relatively independent processes, a comparative analysis is based on the processed information obtained from the two images rather than the original information, leading to a decrease in information and accuracy.
3. The post-classification comparison method is more sensitive to classification errors, as it needs to classify multiple images used for change detection separately. Any classification error can be translated to errors in detected changes.

Figure 7.11 shows the change detection results of the Spring Nature Reserve in Jinan City, China. Figures 7.11(a) and (b) are high-resolution remote sensing images in this region in 2019 and 2020, respectively. Figures 7.11(c) and (d) are image classification results in these two periods.

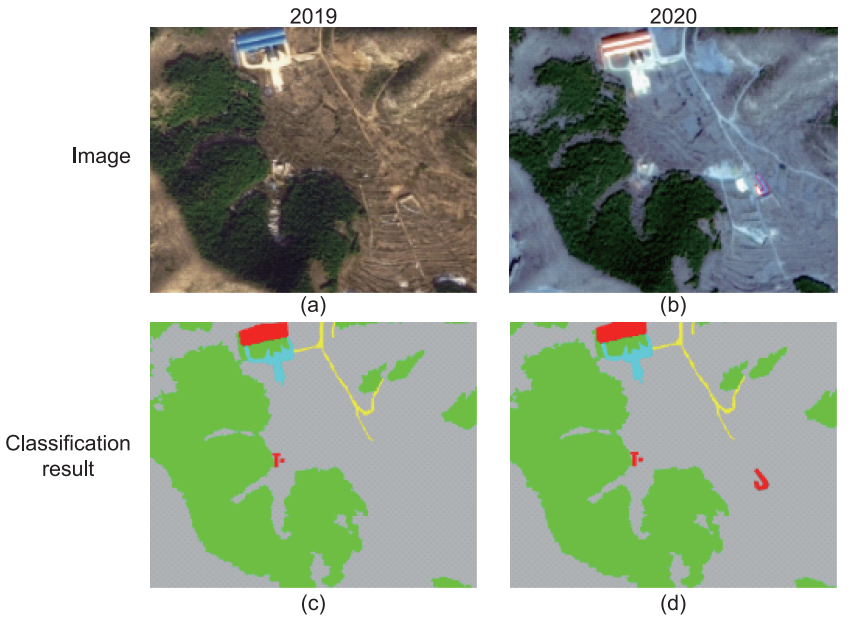

Figure 7.11 Change detection by post-classification change detection method.

7.3.1.4 Urban change detection method based on deep learning model

Deep learning models have strong learning capability and advanced performance and have been widely used in many fields such as computer vision, speech recognition and information retrieval. With the explosive growth of remote sensing data, the deep learning model, as an effective means of mining remote sensing big data, is being gradually applied to various remote sensing tasks.

Compared with traditional machine learning methods, deep learning models can efficiently and automatically extract the abstract features of complex objects, greatly improving the accuracy of pattern recognition. In the change detection field, deep learning models can handle the same or different sources of remote sensing images and can effectively extract the spatial and spectral integral features in a noise-tolerant manner. It can also be used to establish a long nonlinear correlation of ground objects in remote sensing images to achieve accurate change detection results.

In the early stage, a series of methods that include stacked auto-encoders (SAE), convolutional auto-encoder (CAE) and deep confidence network (DBN) have been widely used in change detection. With the continuous optimization and development of deep learning, convolutional neural

Downloaded from www.worldscientific.com
by fac sciences de la terre universite annaba on 07/30/24. Re-use and distribution is strictly not permitted, except for Open Access articles.

network (CNN), recurrent neural network (RNN) and VGG-16, PCANet, FCN, SegNet, UNet, UNet++, as well as other deep learning models have been proposed to tackle change detection tasks.

At present, most of the deep learning models used in image change detection are supervised training based on a backpropagation algorithm. In the absence of a sufficient number of labeled samples, the description ability of features extracted by the deep learning model may be limited, thus affecting the accuracy of change detection results. Therefore, how to efficiently acquire training samples and extract effective features remains a challenge. However, when the number of labeled samples is too small, or there is no labeled sample data at all, weakly supervised or unsupervised deep learning models, another major direction of deep learning model, can be used to carry out change detection tasks.

7.3.2 3D change detection methods

3D change detection mainly uses LiDAR point cloud and aerial image sets (Figure 7.12) as data sources. The change detection framework consists

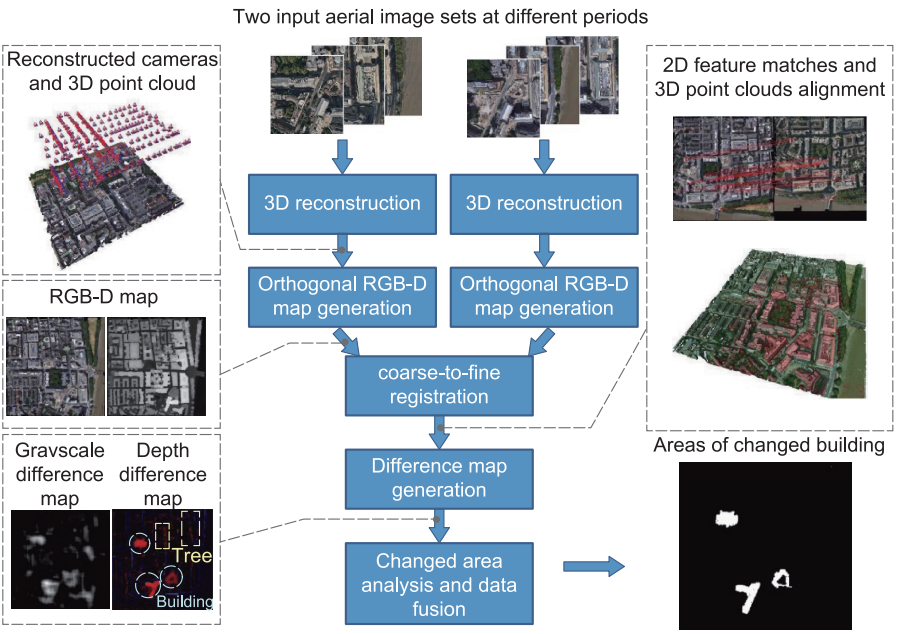

Figure 7.12 Change detection method based on MVS dense matching point cloud.

Downloaded from www.worldscientific.com by fac sciences de la terre universite annaba on 07/30/24. Re-use and distribution is strictly not permitted, except for Open Access articles.

Downloaded from www.worldscientific.com
by fac sciences de la terre universite annaba on 07/30/24. Re-use and distribution is strictly not permitted, except for Open Access articles.

of 3D reconstruction from two aerial image sets captured by a UAV at a different time, orthogonal RGB-D map generation and registration, difference map generation, changed area analysis and data fusion. According to the differentiation of change detection units, 3D change detection can be divided into point-by-point detection and object-based change detection.

Point-by-point change detection mostly derives the changed areas by calculating the height difference and by identifying the building targets by combining geometric structure and spectral features. Du *et al.* (2016) fused aerial image and LiDAR point cloud data, used height difference and gray level similarity as change indicators, obtained change areas through graph cutting combined with context information, and identified building targets by integrating spectral and geometric features. Similarly, Chen *et al.* (2016) proposed a change detection framework based on 3D reconstruction to generate an RGB-D graph, using MVS dense matching point cloud as the data source for building change detection (Figure 7.12). Pang *et al.* (2018) transformed the change detection problem into a dichotomic problem by extracting the changing areas point by point with a graph cutting algorithm and identifying the building targets through the structural features.

The above models are sensitive to point cloud quality and multi-temporal data registration errors are susceptible to seasonal changes of trees. In addition, the integrated multi-source information posed challenges to these methods, as it is difficult to determine the optimal weight allocation.

Object-based change detection usually divides or classifies the point cloud first, and then analyzes the changes within each segmented/classified object block. Pang *et al.* (2014) first extracted the building targets using the smooth feature of the building surfaces and then detected the changes and determined the change types based on the results of the target extraction. Qin (2014) combined textures and geometric features contained in point clouds of UAV-MVS images in different ways to generate a complementary multi-element segmentation, followed by a multi-criteria decision analysis based on segmented surfaces to achieve building extraction and change detection. Vosselman *et al.* (2004) detected changes through machine learning methods by making full use of geometric shape and spectral information to extract buildings and detected changes. Rastiveis *et al.* (2015) extracted buildings by mapping building layers to LiDAR data from vector data and detected changes with machine learning methods. The aforementioned models separate the segmentation/ classification process from the change detection process so that the final change detection result

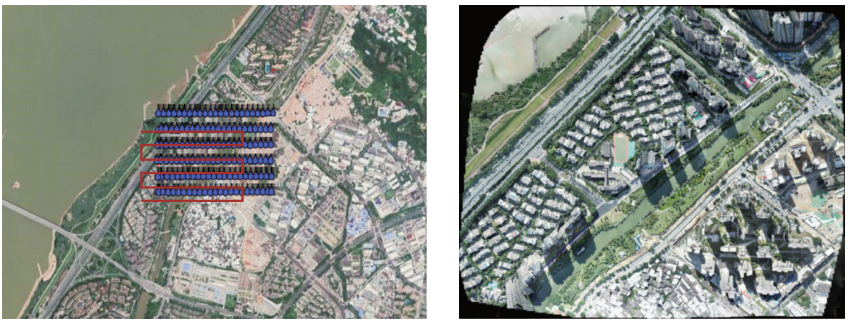

(a) (b)

Figure 7.13 The flight route of UAV (a) and the 3D surface model based on UAV images (b).

(a) (b)

Figure 7.14 3D change detection results based on surface models.

is affected by the pre-order error, forming error accumulation, and the detection accuracy depends on the quality of point cloud segmentation/classification.

In addition, UAV can be used to collect multi-period high-resolution images, and then the images can be used to establish real surface models for 3D change detection. Figure 7.13 shows the flight route of UAV and the 3D surface model based on UAV images. Figure 7.14 shows the 3D change detection results based on surface models.

7.4 Change Detection Practice of Urban Remote Sensing

With the development of technology and economy, the urban population is increasing, and the surface of urban areas is also undergoing notable changes.

Downloaded from www.worldscientific.com
by fac sciences de la terre universite annaba on 07/30/24. Re-use and distribution is strictly not permitted, except for Open Access articles.

In this section, we introduced the change detection methods and practices of urban land cover/use, impervious surface and cultivated land.

Downloaded from www.worldscientific.com
by fac sciences de la terre universite annaba on 07/30/24. Re-use and distribution is strictly not permitted, except for Open Access articles.

7.4.1 Urban land cover/use change detection methods

Urban land cover/use change has a significant impact on urban ecosystems. Therefore, determining urban land cover/use change is an important task to understand the trends and conditions of urban ecosystems, support urban planning and assist urban project decision-making. Satellite images can be used to accurately, regularly and rapidly map urban land cover/use and its changing dynamics.

Wang *et al.* (2018) analyzed the land cover/use changes and changes in ecosystem service functions in Dongying, the core city of the Yellow River Delta High-Efficiency Ecological Economic Zone in China. In the process of urbanization, local governments need to take care of both ecological protection and economic development pressure. The study investigated the land use/cover changes from 1995 to 2015 and found that the area of grassland, farmland, water area and bare land decreased by 21.43%, 38.72%, 7.36% and 22.54%, respectively, and the area of construction land increased by 347.34%. In addition, the simulated results indicate that by 2025, the area of urban construction land will continue to increase (Figure 7.15).

7.4.2 Urban impervious surface change detection methods

On global, national and regional scales, urban expansion always leads to an increased proportion of impervious surface, which plays an important role in global climate change research and ecological environment monitoring. The possibility of Landsat data for continuous monitoring of surface dynamics is still limited by the availability of cloud-free surface observation data. Many existing studies mostly use Landsat images of discontinuous times to gauge impervious surface changes. Dynamic information of impervious surface can be extracted from multi-temporal Landsat images, and impervious surface can be extracted from single temporal images. First, a spatial distribution map of impervious surfaces of each phase is obtained, and

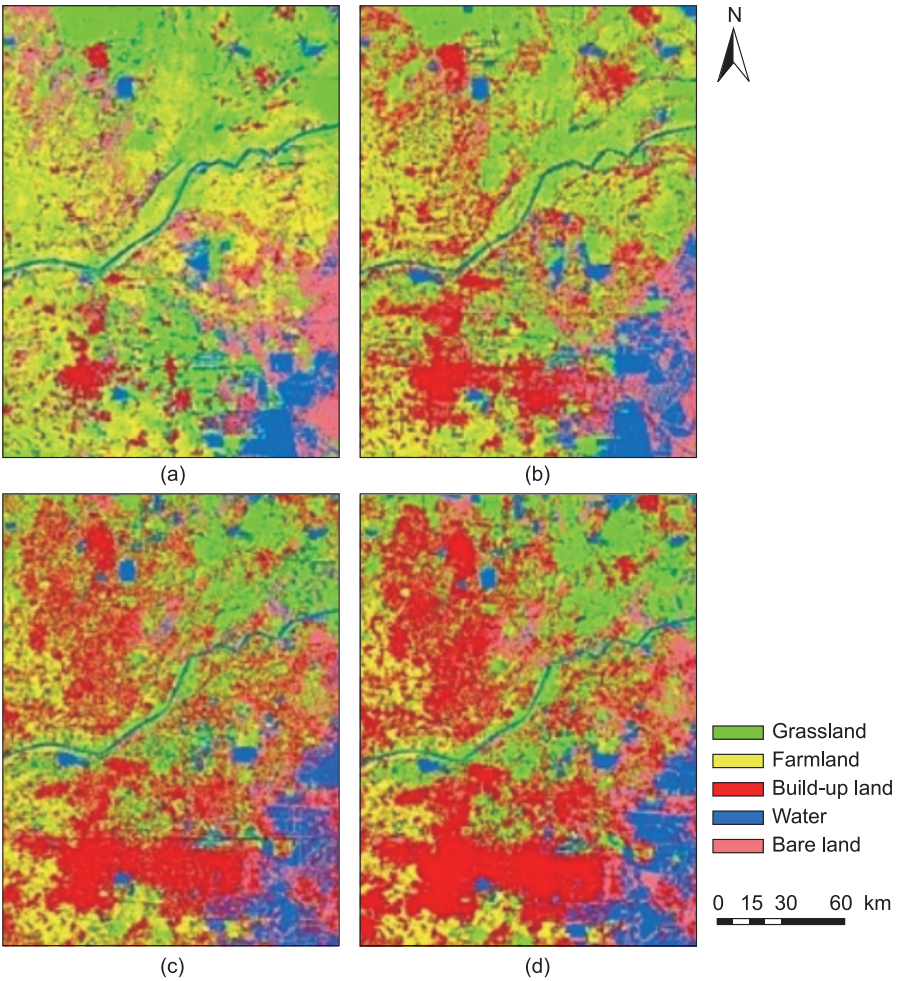

Figure 7.15 Land cover/use results in Dongying City, China, obtained in 1995 (a), 2004 (b), 2015 (c), and simulated in 2025 (d).

spatio-temporal dynamics of impervious surface distribution are obtained through comparative analysis of each phase (Shao and Liu, 2014; Shao *et al.*, 2016).

Here we take Wuzhou city of Guangxi Zhuang Autonomous Region as an example and monitor impervious surfaces using Landsat data from 2007 to 2018 (Figure 7.16). As can be seen from Figure 7.17, the distribution of impervious surfaces shows an increasing trend year by year.

Downloaded from www.worldscientific.com
by fac sciences de la terre universite annaba on 07/30/24. Re-use and distribution is strictly not permitted, except for Open Access articles.

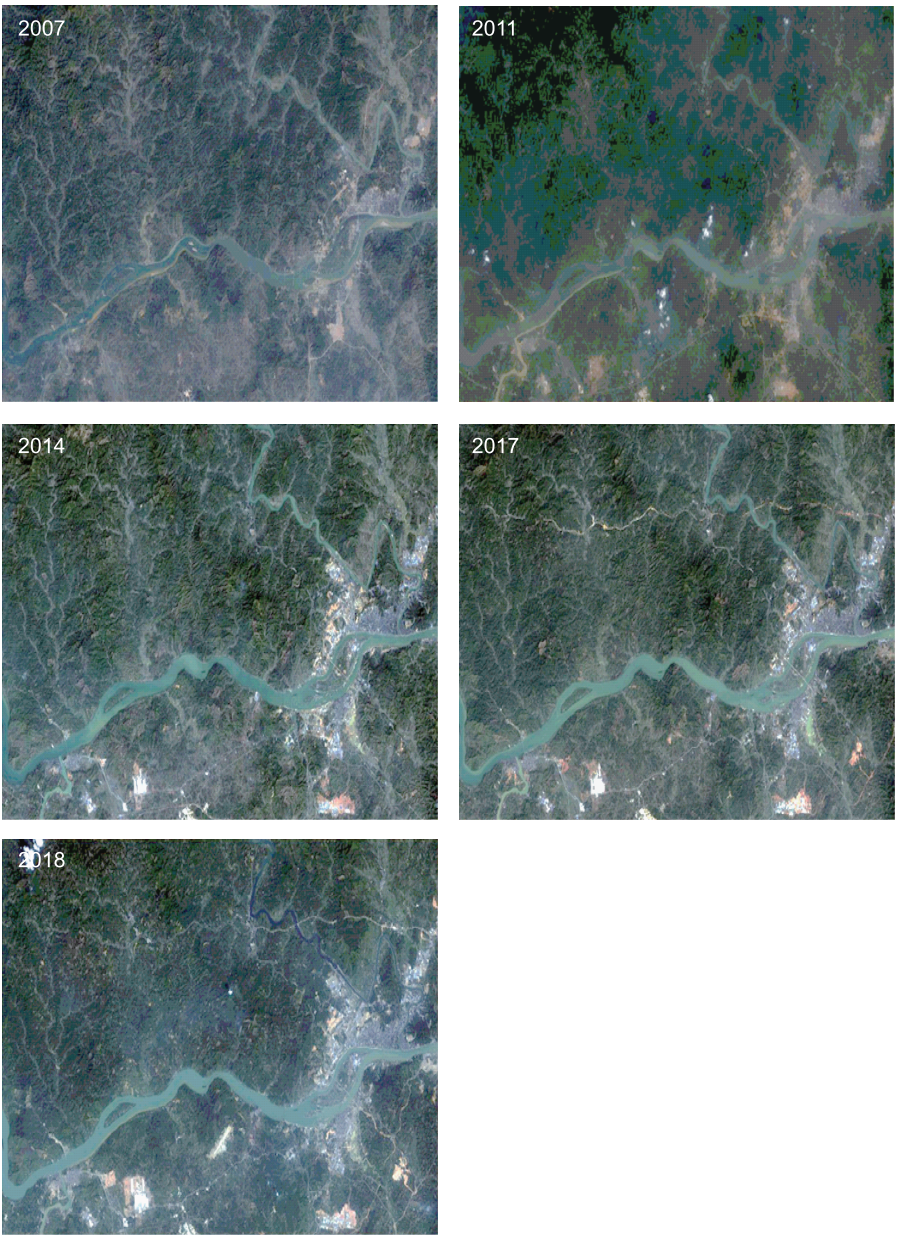

Figure 7.16 Multi-temporal Landsat image of Wuzhou City.

Downloaded from www.worldscientific.com
by fac sciences de la terre universite annaba on 07/30/24. Re-use and distribution is strictly not permitted, except for Open Access articles.

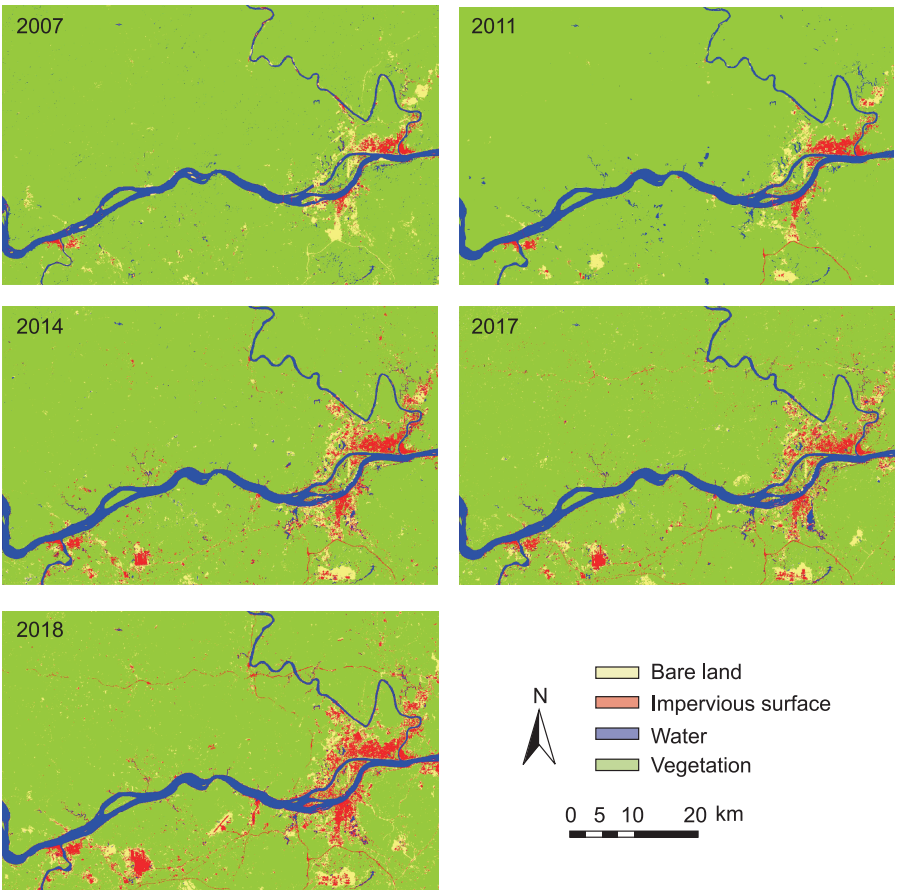

Figure 7.17 Change detection results of impervious surface extracted from multi-temporal Landsat images in Wuzhou City.

7.4.3 Urban cultivated land change detection methods

During urban expansion, a large amount of cultivated land is occupied and converted to other uses, e.g., residential, industrial, commercial, infrastructure and institutional uses. At the same time, due to urbanization or unclear ownership, idle cultivated land becomes common in rural areas. China is a developing country with a large population and scarce land resources. The loss of cultivated land greatly threatens food security and social stability. In this respect, the accurate monitoring of cultivated land plays a vital role in the protection of cultivated land.

Downloaded from www.worldscientific.com
by fac sciences de la terre universite annaba on 07/30/24. Re-use and distribution is strictly not permitted, except for Open Access articles.

Downloaded from www.worldscientific.com
by fac sciences de la terre universite annaba on 07/30/24. Re-use and distribution is strictly not permitted, except for Open Access articles.

Relying on matching the 2D image coordinates from video frames with orthophoto maps and vector surveying and mapping data, Shao *et al.* (2020) proposed an accurate matching method for projecting vector data into surveillance video to monitor and protect the cultivated land. The flowchart of the integration of 2D GIS data and pan-tilt-zoom surveillance video is shown in Figure 7.18. On the basis of the proposed method, a prototype of the cultivated land monitoring system is designed and implemented. The implemented prototype is further applied to monitor cultivated land in Dongyang City, Zhejiang Province, China. The cross-mapping between 2D basic farmland protection zones and the preset video frame of the upper row and lower row dataset are shown in Figure 7.19.

Based on the alignment results, it is possible to easily identify the occurrence of farmland damage through visual inspection of the image content covered in the two-dimensional vector area. China forbids the permanent conversion of agricultural land to other uses. The nature of the use of non-permanent agricultural land can be changed to construction land with the approval of relevant departments. Given that these two types of cultivated land are very similar in the video image, it is difficult to distinguish

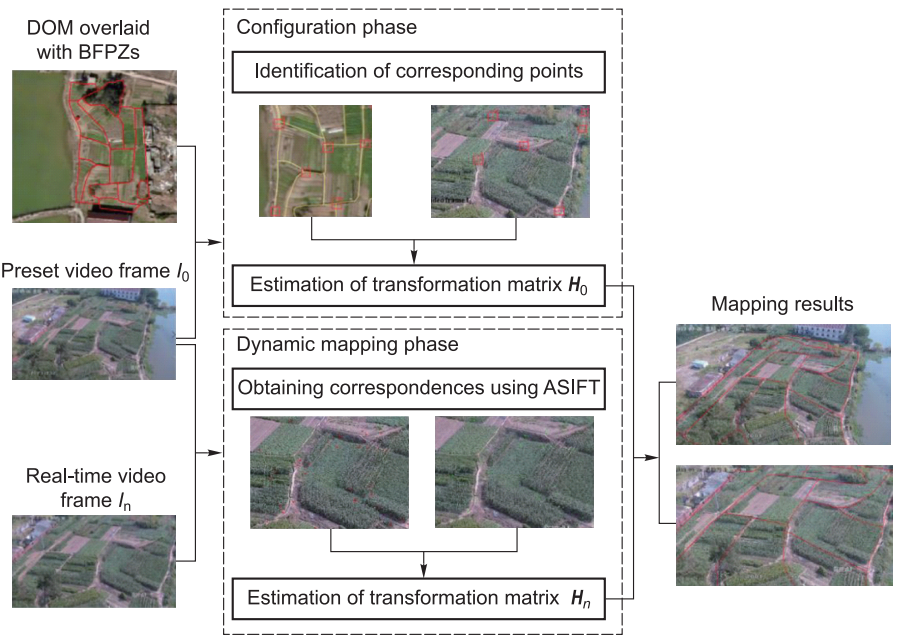

Figure 7.18 The flowchart of the integration of 2D GIS data and pan-tilt-zoom surveillance video.

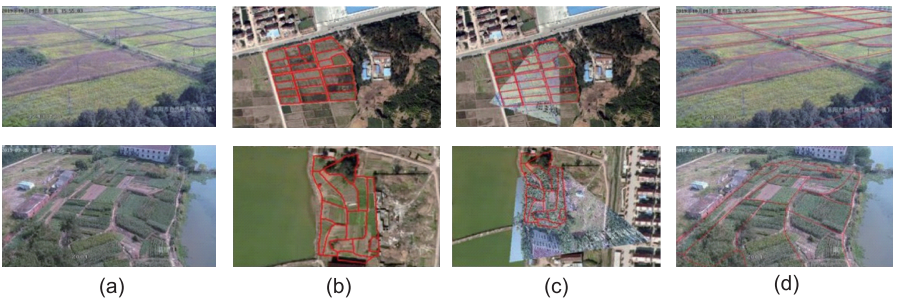

Figure 7.19 (a) The preset video; (b) the corresponding ortho-image overlaid with 2D vector basic farmland protection zones; (c) the preset video frame projected into the geospatial space; (d) the 2D vector basic farmland protection zones projected into the image space.

them. Thus, it is necessary to mark the protected area in the video image. This method establishes a new venue to solve the problem of identifying basic farmland from videos. The polygons in the two-dimensional GIS data define the boundaries of protected farmland. If the image content divided by polygons is recognized as construction land, it can be recognized as an illegal change.

Questions

1. What are the applications of image change detection in urban planning, construction, management and services?
2. What are the factors that affect the accuracy of urban remote sensing image change detection algorithms?
3. What are the advantages and disadvantages of the object-oriented urban change detection method and deep learning model-based urban change detection method?

References

Chen B, Chen Z, Deng L, Duan Y, Jie Z. 2016. Building change detection with RGB-D map generated from UAV images. *Neurocomputing*, 208(C): 350–364.

Du S, Zhang Y, Qin R, Yang Z, Zou Z, Tang Y, Fan C. 2016. Building change detection using old aerial images and new LiDAR data. *Remote Sensing*, 8(12): 1030.

Downloaded from www.worldscientific.com
by fac sciences de la terre universite annaba on 07/30/24. Re-use and distribution is strictly not permitted, except for Open Access articles.

Pang S, Hu X, Wang Z, Lu Y. 2014. Object-based analysis of airborne LiDAR data for building change detection. *Remote Sensing*, 6(11): 10733–10749.

Pang S, Hu X, Cai Z, Gong J, Zhang M. 2018. Building change detection from bi-temporal dense-matching point clouds and aerial images. *Sensors*, 18(4): 966.

Qin R. 2014. An object-based hierarchical method for change detection using unmanned aerial vehicle images. *Remote Sensing*, 6(9): 7911–7932.

Rastiveis H, Eslamizade F, Hosseini-Zirdoo E. 2015. Building damage assessment after earthquake using post-event LiDAR data. *International Archives of the Photogrammetry, Remote Sensing and Spatial Information Sciences*, 40: doi: 10.5194/isprsarchives-XL-1-W5-595-2015.

Shao Z F, Liu C. 2014. The integrated use of DMSP-OLS nighttime light and MODIS data for monitoring large-scale impervious surface dynamics: A case study in the Yangtze River Delta. *Remote Sensing*, 6(10): 9359–9378.

Shao Z, Fu H, Fu P, Yin L. 2016. Mapping urban impervious surface by fusing optical and SAR data at the decision level. *Remote Sensing*, 8(11): 945–966.

Shao Z, Li C, Li D, Altan O, Zhang L, Ding L. 2020. An accurate matching method for projecting vector data into surveillance video to monitor and protect cultivated land. *ISPRS International Journal of Geo-Information*, 9(7): 448.

Teo T, Shih T. 2013. Lidar-based change detection and change-type determination in urban areas. *International Journal of Remote Sensing*, 34(3): 968–981.

Vosselman G, Gorte B, Sithole G. 2004. Change detection for updating medium scale maps using laser altimetry. *International Archives of Photogrammetry, Remote Sensing and Spatial Information Sciences*, 34(B3): 207–212.

Wang C, Wang Y, Wang R, Zheng P. 2018. Modeling and evaluating land-use/land-cover change for urban planning and sustainability: A case study of Dongying city, China. *Journal of Cleaner Production*, 172: 1529–1534.

Downloaded from www.worldscientific.com
by fac sciences de la terre universite annaba on 07/30/24. Re-use and distribution is strictly not permitted, except for Open Access articles.

Downloaded from www.worldscientific.com
by fac sciences de la terre universite annaba on 07/30/24. Re-use and distribution is strictly not permitted, except for Open Access articles.

Chapter 8

Dynamic Monitoring Methods and Applications through Urban Remote Sensing

The advantages of remote sensing technology include wide observation range, fast update speed and strong data integration, using technology such as remote sensing image comparative analysis, automatic extraction of map spots, planning management rules and other digital technologies to realize the supervision of urban planning, the supervision of urban master planning, and the supervision of major projects and monitoring of construction land. Remote sensing technology can perceive objects or natural phenomena from a long distance without direct contact and quickly obtain relevant information about urban development, including not only the macroscopic data of the city but also the microscopic image data of the first building and the bridge in the city. Remote sensing images are an important source of information for urbanization monitoring, management and analysis research.

8.1 Demands of Dynamic Urban Monitoring

In recent decades, the world has experienced rapid urbanization. According to the statistics from the United Nations, the global urban population accounted for about 30% of the total population in 1950, and this proportion has reached 55% in 2018 (Peng *et al.*, 2019). It is expected that around 68% of the population will live in cities in 2050. Urbanization has brought about the development of society and improved the material and spiritual living standards of humans. At the same time, it has brought about a

Downloaded from www.worldscientific.com
by fac sciences de la terre universite annaba on 07/30/24. Re-use and distribution is strictly not permitted, except for Open Access articles.

series of negative effects, e.g., the encroachment and destruction of the green space system, environmental pollution and resource shortage. How to take advantage of remote sensing technology to better monitor urban development and the ecological environment has become a hot issue.

The healthy development of cities is the focus of the United Nations 2030 Agenda for Sustainable Development, which includes a total of 17 sustainable development goals. These goals cover topics such as climate change, economic inequality and sustainable consumption, committing to eradicating poverty through coordinated actions, protecting the planet and ensuring that mankind enjoys peace and prosperity. It also includes 232 specific indicators such as the incidence of undernourishment, the proportion of the population using safely managed drinking water services, the proportion of the population with access to electricity and the proportion of the urban population living in slums and informal settlements or under-housing. Among them, 15 indicators are related to cities, including the proportion of the urban population living in slums and informal settlements or under-housing, the ratio between land use rate and population growth rate and the openness of urban construction areas for all people. Remote sensing technology can be used to monitor objects or natural phenomena from a long distance without direct contact and quickly obtain relevant information about urban development, including both macroscopic and microscopic urban information. Urban remote sensing monitoring is an important application branch of remote sensing application and is an interdisciplinary field that integrates remote sensing and urban science.

Urban remote sensing monitoring can provide basic data and supporting technology for urbanization planning and ecological construction. During the rapid development of China's urbanization, certain problems must be addressed. For example, the spatial distribution and scale of cities are unreasonable, as they do not often match the carrying capacity of resources and the environment. The level of urban management services is not high enough, and the protection of natural, historical and cultural heritage is not effective. Urban monitoring based on remote sensing techniques is able to provide urban managers with basic geographic information and other data related to urban development. It can become the basis for optimizing the urbanization pattern, scientifically planning urban development and improving the urbanization system and mechanism. In the past 30 years, the advantages of remote sensing technology have been recognized by scholars, and it has been widely applied in various aspects of urban monitoring.

8.2 Urban Dynamic Monitoring Process

Remote sensing technology is an important technical support for urban development and planning and has been widely used in various fields in cities. The development of urban remote sensing provides a great impetus for the optimization of urban construction, which is necessary for the research of urban remote sensing. As shown in Figure 8.1, the urban remote sensing dynamic monitoring process can be mainly divided into six stages. The details are as follows:

1. *Determination of monitoring objects*: Cities are complex systems with constantly changing mechanisms responsible for the main production activities of mankind. In recent years, remote sensing technology has been increasingly used in urban monitoring. The first step of remote sensing monitoring is to determine the monitoring objects (i.e., lakes, impervious surfaces, arable land, urban planning and city conditions) according to the monitoring needs.
2. *Selection and acquisition of remote sensing images*: Researchers should consider monitoring requirements, target characteristics, data acquisition costs and feasibility factors, determine the type, source, resolution, band and time of remote sensing images in a comprehensive manner.
3. *Preprocessing of remote sensing images*: In order to minimize the impact of image differences on the monitoring results, a series of image

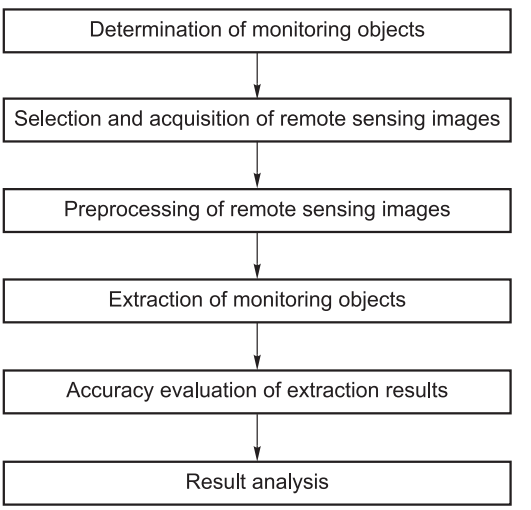

Figure 8.1 The basic process of urban dynamic remote sensing monitoring.

Downloaded from www.worldscientific.com
by fac sciences de la terre universite annaba on 07/30/24. Re-use and distribution is strictly not permitted, except for Open Access articles.

Downloaded from www.worldscientific.com
by fac sciences de la terre universite annaba on 07/30/24. Re-use and distribution is strictly not permitted, except for Open Access articles.

preprocessing steps is required. In general, radiation correction is used to reduce the difference in radiation caused by environmental factors. Geometric correction methods (e.g., image matching) are used to reduce the position difference of the image. Image quality can also be improved by means of image enhancement and feature highlights.

4. *Extraction of monitoring objects*: Extraction of monitoring objects is the key to urban remote sensing monitoring. It is necessary to determine the primitives of change analysis and whether classification and classification systems are needed, e.g., the comparison method of multi-temporal images, the quantitative description of changes and the method of change extraction.
5. *Accuracy evaluation of extraction results*: Through the establishment of evaluation indicators and methods, the extraction results are compared with the ground-truthing changes, aiming to qualitatively and quantitatively analyze the reliability and accuracy of the results. Gauging model performances benefit their future development. In most cases, monitoring results can be regarded as binary classification results. Thus, a confusion matrix can be used to calculate the producer accuracy (PA), user accuracy (UA) and overall accuracy (OA) to evaluate the accuracy monitoring results.
6. *Result analysis*: Urban remote sensing monitoring is mostly carried out based on time series remote sensing images. It is usually necessary to use spatial analysis, time-sequence analysis and correlation analysis, to list a few, to analyze the monitoring results, which are more easily accepted by stakeholders.

8.3 Urban Dynamic Monitoring Methods

Remote sensing monitoring methods are generally proposed for specific objects. Different objects need different detection methods, which can be divided into two categories according to the data source and monitoring platform: (i) dynamic monitoring based on time series remote sensing images and (ii) monitoring based on Earth observation sensor network. The core of urban remote sensing dynamic monitoring is to perform long-term or real-time monitoring through remote sensing objects to provide technical support for urban planning, urban construction and urban management.

Downloaded from www.worldscientific.com
by fac sciences de la terre universite annaba on 07/30/24. Re-use and distribution is strictly not permitted, except for Open Access articles.

8.3.1 Urban dynamic monitoring based on time series remote sensing imagery

Many pieces of evidence have shown that it is very important to monitor urban changes based on time series remote sensing images. The long-term remote sensing images can be used to recognize the inter-annual evolution characteristics of monitoring objects (Jiang *et al.*, 2018). In turn, they can also help decision-makers design and implement reasonable urban management policies. However, due to the incompatibility of the temporal resolution and spatial resolution of remote sensing data, it is challenging to obtain urban remote sensing data with long time series and high spatial resolution. Existing medium- and low-resolution remote sensing data (e.g., MODIS and Landsat) and long-term public data can be obtained. They often fail to reflect the internal structure and phenomenon of the city due to their coarse resolution. The high-resolution remote sensing data are often not easy to obtain. Many urban monitoring tasks demand high requirements for time resolution and spatial resolution, which further increases the difficulty of data selection and acquisition. Thus, it is of great importance to solve the problem of the supply and demand of remote sensing data. Figure 8.2 shows the light distribution at night after threshold classification in Shandong Province, China, from 1993 to 2013 based on time series remote sensing images.

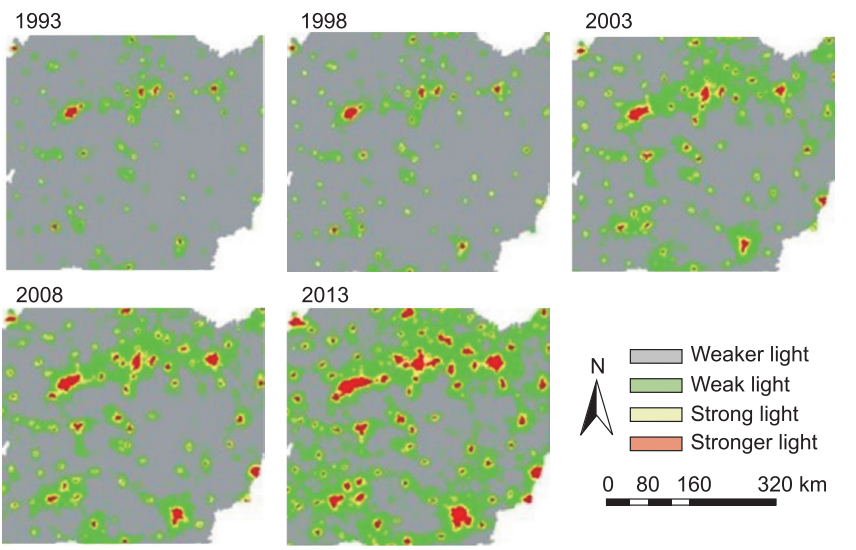

Figure 8.2 Luminous monitoring in Shandong Province, China, based on time series remote sensing images.

8.3.2 Urban dynamic monitoring based on the integration of earth observation sensor network

Earth observation sensor network, the Internet of things for earth observation, is the key to the global earth observation system. It embodies the concept of the smart planet, with comprehensive event perception capabilities, powerful collaborative observation capabilities, efficient data processing capabilities and intelligent decision support capabilities. It is especially suitable for fine-grained urban monitoring. Figure 8.3 shows a typical earth observation sensor network conceptual framework of NASA Sensor Web 2.0.

From the perspective of system science, the Earth observation web is an integrated collaborative sensing web that combines various sensor resources, which can form a self-organizing dynamic, collaborative observation system. Each sensor node has independent event perception and observation capabilities. For a certain observation target, all nodes can be dynamically integrated to form a global observation system, thus effectively solving

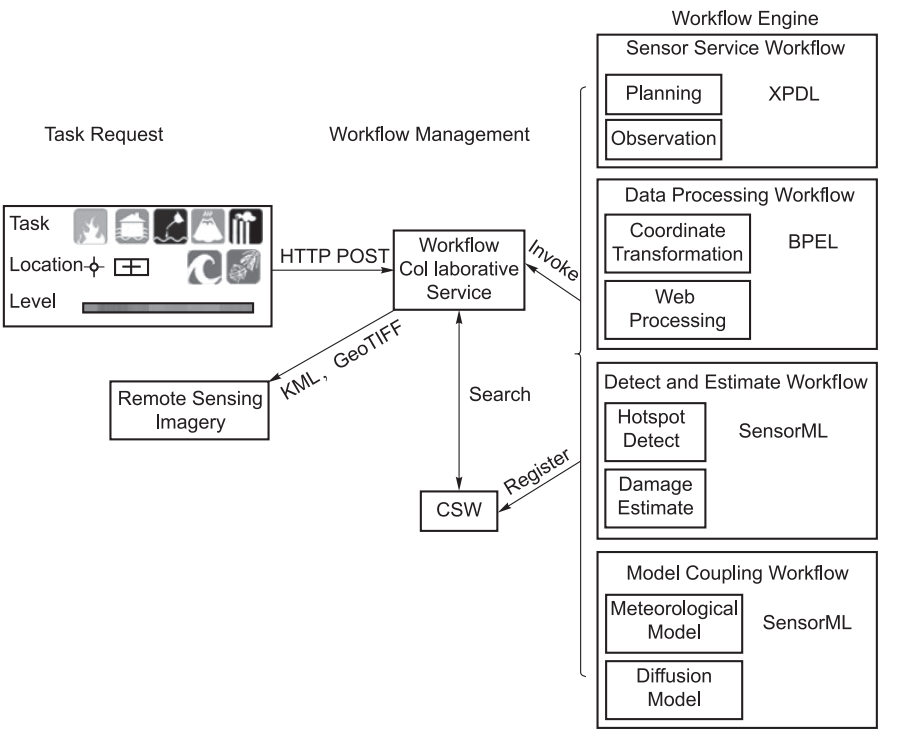

Figure 8.3 Function flow diagram of NASA Sensor Web 2.0.

Downloaded from www.worldscientific.com
by fac sciences de la terre universite annaba on 07/30/24. Re-use and distribution is strictly not permitted, except for Open Access articles.

Downloaded from www.worldscientific.com
by fac sciences de la terre universite annaba on 07/30/24. Re-use and distribution is strictly not permitted, except for Open Access articles.

the current bottleneck problem that sensors, data and information cannot complement each other between observation platforms, leading to an autonomous, task-customizable, dynamically adaptable and reconfigurable observation system.

From the perspective of computing, the Earth observation sensor network is a networked service web. Although the current definition of sensor network emphasizes network centricity and includes sensor data and information more than before, it does not include virtual sensors. There is no difference between a virtual sensor and a real physical sensor. Therefore, based on the service-oriented architecture and web service environment, the sensor network can be defined as a set of interoperable web services. In this sense, any Web service that contains an algorithm or simulation model can be regarded as a sensor in the sensor network, as long as the web service follows the standard specification interface and operation. Different sensor networks can be divided according to the norms followed. According to this definition, all the characteristics of Web services are applicable to Internet-enabled sensors that are characterized by the feature of dynamics, flexibility, plug-and-play, self-describing and scalability. At the same time, data and information generated by Internet-enabled sensors can be shared, forming an organized observation system with strongly linked sensors.

The Earth observation sensor network can be considered as a bridge between heterogeneous sensor systems, models and simulation, and decision support systems. It can provide a standardized description of sensors, observations and models, and a consistent understanding of multi-user tasks and variable sensor resources in a multi-granularity, asymmetric, highly dynamic and complex network environment.

8.4 Remote Sensing Monitoring Applications of Urban Natural Resources

Natural resources, referring to the natural environmental factors, can improve the current and future welfare of mankind. This section analyzes the application requirements of remote sensing technology in urban natural resource monitoring and expounds on the application practice of using high-resolution remote sensing images to monitor urban lake

changes, impervious surfaces and cultivated land resources. Routine monitoring is full-coverage dynamic remote sensing monitoring of natural resources within the scope of country around the goal of natural resource management. Thematic monitoring is dynamic tracking of surface coverage and characteristic indicators of a certain area and type of natural resources to master the surface coverage and changes in the quantity and quality of natural resources. Thematic monitoring mainly includes geographic and city situations, key areas and ecological status. Emergency monitoring aims to provide first-hand information for the decision-making and management of social focus and difficult issues. The urban remote sensing platform is equipped with visible light, infrared, hyperspectral, microwave, radar and other detectors to achieve regular image coverage and data acquisition (Shao *et al*., 2020).

Downloaded from www.worldscientific.com
by fac sciences de la terre universite annaba on 07/30/24. Re-use and distribution is strictly not permitted, except for Open Access articles.

8.4.1 Remote sensing monitoring of urban lake changes

In recent years, lakes have been gradually shrinking due to various reasons that include climate changes and human activities. The shrinking of lakes, as one of the important environmental crises facing contemporary humans, severely impacts the surrounding ecosystems, posing great threats to the safety of the ecological environment (Shao *et al*., 2019). Therefore, the timely and accurate dynamic monitoring of lakes is particularly important for the scientific and reasonable development, utilization, supervision and protection of lake resources.

As the capital of Hubei Province, Wuhan City is located in the center of China's hinterland (Figure 8.4). It is a typical representative of the country's megacities. Wuhan enjoys the name "the city of hundreds of lakes" due to the existence of many lakes and rivers. However, since the reform and opening up, China's economy has entered a period of rapid development, and the process of urbanization has become faster and faster. Wuhan is facing problems such as the shrinking and disappearing of lakes and the serious pollution of water resources, severely affecting the pace of sustainable development. We take Wuhan City as an example to use remote sensing to detect the dynamic changes of lake area from 1980 to 2015, aiming to demonstrate the feasibility and effectiveness of remote sensing in lake monitoring.

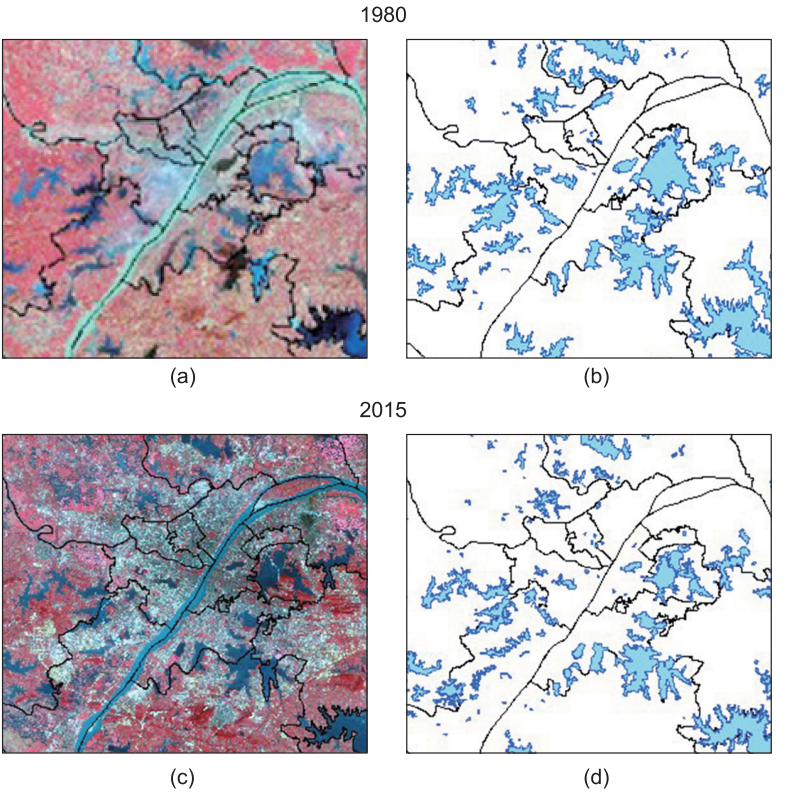

Figure 8.4 Regional (a), (c) and lake spatial distribution maps (b), (d) of Wuhan in 1980 and 2015.

In light of the great capability of improved normalized difference water index (NDWI) in identifying water bodies, Landsat images were used to construct an improved NDWI and set an appropriate threshold to extract the water body area in Wuhan. The regional and lake spatial distribution maps of Wuhan in 1980 and 2015 were obtained. The shrinking of lakes is notable in Wuhan.

According to the above-mentioned monitoring example, remote sensing technology can facilitate global observation of lakes. It can be used to conduct an in-depth study of the evolution mechanism of urban lakes under the influence of natural and human activities, providing reliable data support for urban environment and ecosystem protection and benefiting effective management of water resources.

Downloaded from www.worldscientific.com
by fac sciences de la terre universite annaba on 07/30/24. Re-use and distribution is strictly not permitted, except for Open Access articles.

8.4.2 Remote sensing monitoring of urban impervious surface

Urban waterlogging and urban heat island effects are typical urban issues, resulting from the rapid urbanization processes, e.g., the transformation of land types with better water permeability in the suburbs to urban land with poor water permeability, resulting in the construction of natural landscapes with vegetation coverage as the main component. Instead of roads, industrial land and low-density residential land in the old city have been developed into high-density residential land and commercial land (Shao *et al.*, 2018). These artificially constructed surfaces do not allow water to penetrate, thereby the name "impervious surface". Impervious surface is considered a key indicator parameter to measure the level of urbanization and environmental quality.

Since the 1950s, attention has been paid by the scientific community to impervious surfaces. The impervious surface is the matrix landscape of the city and dominates the urban landscape pattern and development process (Figure 8.5). In areas covered by an impervious surface, it is difficult for precipitation to return to the atmosphere through the canopy of trees to intercept evaporation or enter the soil in the form of infiltration

Regional impervious surface dynamics can affect the spread of pathogens and other non-point source pollutants, posing a potential threat to the health of urban residents (Figure 8.6). Compared with natural underlay surfaces such as vegetation, an impervious surface tends to have a stronger solar radiation absorption capacity. Part of the absorbed energy can be radiated outward in the form of long waves, largely changing the thermal environment within a city. Information regarding impervious surface distribution has been widely used in urban land use classification, urban population density assessment, urban planning, urban environmental assessment, heat island effect analysis, hydrological process simulation, etc.

According to the monitoring scales, we can select different remote sensing data sources. Aiming at the global or regional scale, Landsat data and MODIS data with the medium resolution are often used to carry out remote sensing monitoring of the impervious surface. At a local scale, city scale or block scale, high-resolution remote sensing images are widely used to carry out remote sensing monitoring of the impervious surface. In recent years, drones, often coupled with ground sensor networks, have become more and more popular in the application of impervious surface.

Downloaded from www.worldscientific.com
by fac sciences de la terre universite annaba on 07/30/24. Re-use and distribution is strictly not permitted, except for Open Access articles.

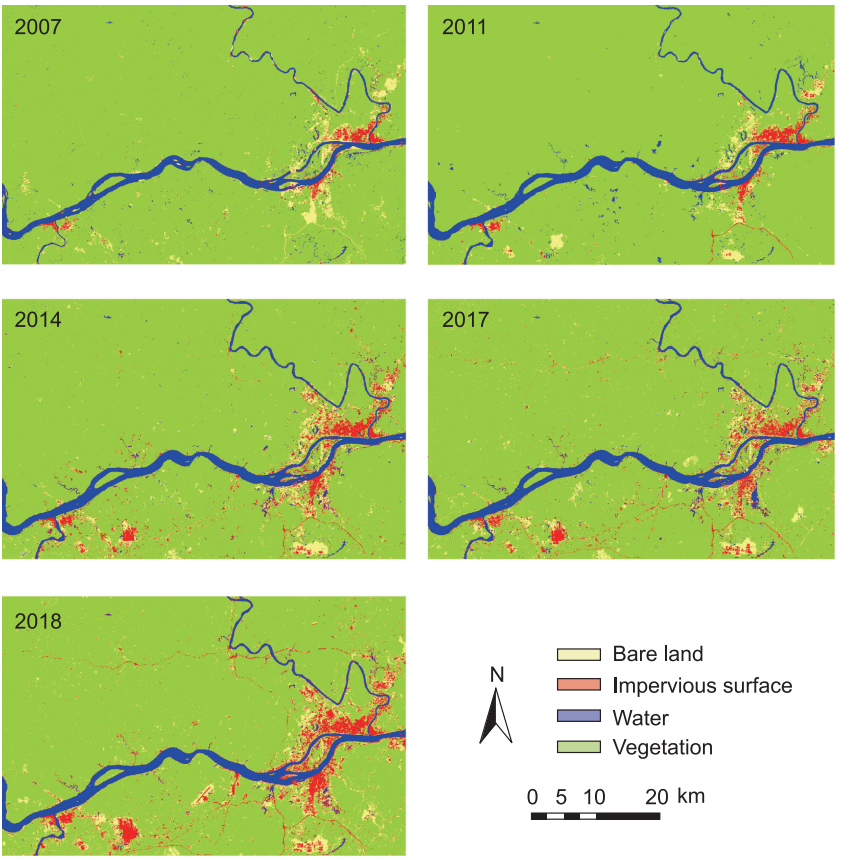

Figure 8.5 Dynamic monitoring of impervious surface coverage in Wuzhou City from 2007 to 2018.

Figure 8.6 Wuhan City waterlogging scenario map.

Downloaded from www.worldscientific.com
by fac sciences de la terre universite annaba on 07/30/24. Re-use and distribution is strictly not permitted, except for Open Access articles.

8.4.3 Remote sensing monitoring of urban cultivated land

Downloaded from www.worldscientific.com
by fac sciences de la terre universite annaba on 07/30/24. Re-use and distribution is strictly not permitted, except for Open Access articles.

Cultivated land is the most basic material resource for human survival and development. The quantity and quality of cultivated land have a significant impact on the food security and economic development of the country and region (Shao *et al.*, 2020). China is the largest developing country in the world, and it is now facing the problem of insufficient arable land resources that can be used to accommodate its growing population. Since 1978, China has experienced unprecedented economic growth and profound social transformation. Economic prosperity has greatly increased the area of residential, commercial and industrial buildings, leading to the loss of a large amount of high-quality cultivated land. A study shows that from 1978 to 1996, 4.73 million hectares of cultivated land was lost, mainly in the eastern coastal and central provinces of China (Kuang *et al.*, 2021). Due to the convenient transportation and complete facilities of the cultivated land close to the urban area, this part of the cultivated land has become a priority for occupation.

The traditional farmland monitoring method is field survey and measurement, suitable for local and refined farmland measurement management. The overall farmland monitoring consumes huge financial resources, material resources and manpower and fails to reflect the current changes in cultivated land. Since modern times, the most important means of cultivated land monitoring are UAV photogrammetry, remote sensing and geographic information technology. Through these methods, the cultivated land information can be obtained and then processed by manual and computer interaction to achieve rapid and real-time monitoring of cultivated land degradation. The two most important steps of modern farmland monitoring are manual visual interpretation and automatic computer recognition.

The distribution of the cultivated land was derived via an object-oriented method based on the CART algorithm from Landsat images (30 m × 30 m) in 1990, 2000, 2010 and 2018. We obtained the spatial distribution of cultivated land in the past 30 years by overlaying the cultivated land information (Figure 8.7).

As can be seen from Figure 8.7, cultivated land expanded from the middle to both east and west in the Sangong river basin. The area of cultivated land increased by 192.00 km^2 (316.42 km^2 in 1990 and 508.42 km^2 in 2018). The growth rate of the cultivated land area was unequal in different periods,

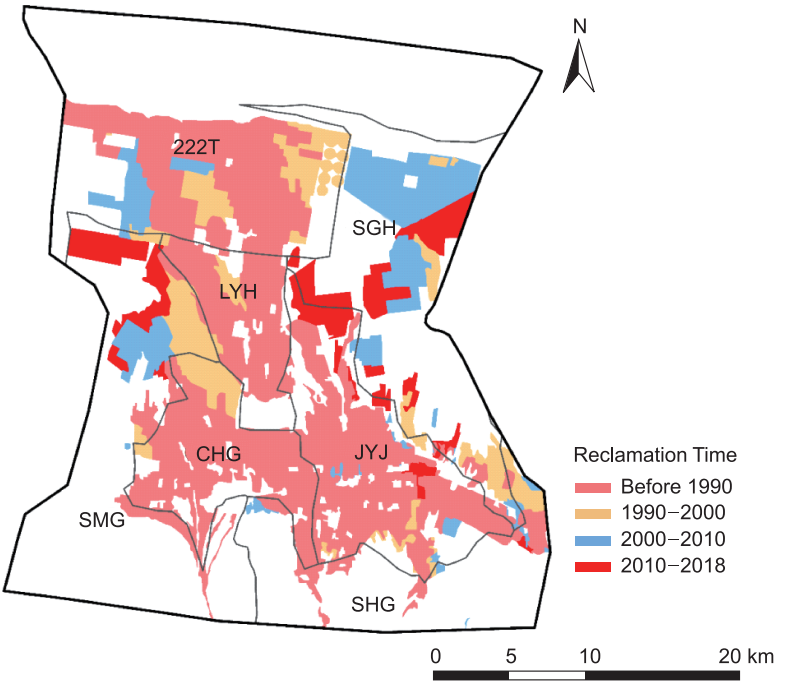

Figure 8.7 Spatio-temporal dynamic monitoring of cultivated land in the Sangong river basin during 1990–2018.

presumably due to the implementation of policies, dynamics of population and urbanization.

8.5 Remote Sensing Monitoring of Urban Planning

High-resolution satellite images and aerial remote sensing technology can provide the scientific decision-making basis for urban planning (Zhang *et al.*, 2018). In addition, timely measures can be achieved against various illegal constructions and undesirable development trends in urban construction to ensure the effective implementation of urban planning and the healthy development of the city. The specific content includes the following:

Establishing multi-temporal and multi-scale urban remote sensing image databases for urban planning: When using satellite remote sensing images for urban planning and supervision, remote sensing images with a spatial

Downloaded from www.worldscientific.com
by fac sciences de la terre universite annaba on 07/30/24. Re-use and distribution is strictly not permitted, except for Open Access articles.

Downloaded from www.worldscientific.com
by fac sciences de la terre universite annaba on 07/30/24. Re-use and distribution is strictly not permitted, except for Open Access articles.

resolution of 2–5 m are usually selected. Dynamic supervision of urban planning with an image resolution of 0.61–2 m can be conducted when the construction project database is superimposed with change information to discover and extract change information. Remote sensing images of different temporal phases and different resolutions are registered, corrected, fused and enhanced, and then collected into the database to establish a multi-temporal and multi-scale remote sensing image database.

Urban planning based on the latest current remote sensing images: The remote sensing images with various planning data can greatly benefit the construction of planning information database, urban layout planning, cultural preservation area planning, old city reconstruction planning, land change investigation and urban transportation planning.

Dynamic monitoring and establishment of the planning information database: We need to centralize the basic planning data such as the urban spatial planning database, the key construction project "one book with two certificates" database, the approval database and the "four lines" to establish a planning information database. On this basis, one of the applications is lake monitoring based on remote sensing images. Specific functions are detailed as follows:

1. Realize dynamic monitoring of the implementation of urban land use planning, including the scope and scale of urban land use, and monitoring the changes in layout, scope and nature of various urban land use changes.
2. Realize the dynamic monitoring of the implementation of urban construction project planning, including the monitoring of the construction of various buildings, structures, water plants, sewage plants and other infrastructure projects.
3. Realize dynamic monitoring of the implementation of the city's "four-line" plan, referring to the red lines (roads), green lines (landscaping, mountains and scenic spots), purple lines (historical and cultural blocks, historical buildings) and blue lines (river, lake and wetland). In addition, yellow lines (major infrastructure, public facilities and land use control) can also be included.

Establish a remote sensing monitoring system for urban planning: The urban planning remote sensing monitoring system mainly uses the change map obtained from remote sensing images to superimpose the urban spatial planning. Therefore, a complete urban planning dynamic monitoring system can be established based on remote sensing images to realize data integration

Downloaded from www.worldscientific.com
by fac sciences de la terre universite annaba on 07/30/24. Re-use and distribution is strictly not permitted, except for Open Access articles.

and information sharing and display various illegal construction cases in a dynamic and multi-faceted manner. Such a dynamic monitoring system can greatly improve work efficiency, reduce illegal construction activities in urban planning and construction, and provide strong technical support for urban planning administrative departments.

According to the existing data and the archive of aerial and satellite images, relevant remote sensing applications in the planning field can be carried out according to the framework detailed below:

1. On the basis of the existing digital achievements of the city, further digitization of the current status data can be conducted to form a current status digital library.
2. On the basis of previous digitization achievements, further digitization of the overall planning, zoning planning and detailed control planning can be conducted to form a planning digital library.
3. Grasp the implementation of the plan through methods, such as overlay analysis.
4. Based on the remote sensing image change detection technology, the changing dynamics in urban planning land can be obtained.
5. Establish a dynamic monitoring system for urban planning to grasp a more comprehensive construction situation and strengthen the supervision of urban planning.

Figure 8.8 shows an example of using remote sensing methods to monitor the land use structure adjustment. The left side of the figure shows a remote

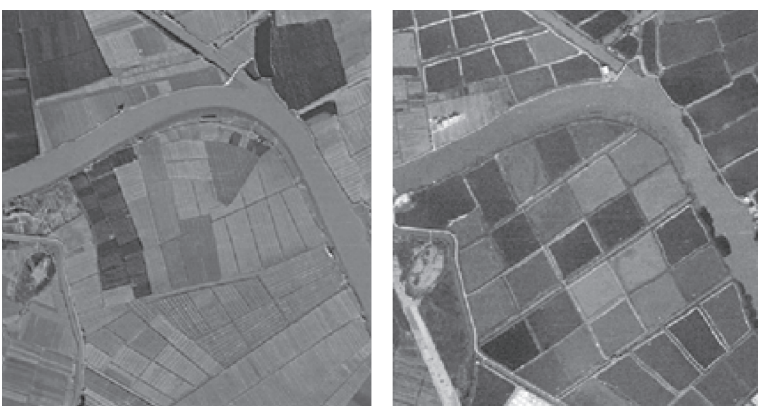

Figure 8.8 Using remote sensing images to monitor the land use structure adjustment.

sensing image in 1995, while the right figure presents the land use patterns in 1999. With the help of remote sensing images, we are able to grasp the land use changing patterns.

Downloaded from www.worldscientific.com
by fac sciences de la terre universite annaba on 07/30/24. Re-use and distribution is strictly not permitted, except for Open Access articles.

8.6 Remote Sensing Monitoring of Urban Conditions

Cities are a socio-economic complex composed of elements that belong to the economic, social and ecological systems. Urbanization is a necessary stage in the process of economic development of a country. The rapid progress of urbanization, while promoting economic development and improving the lives of residents, has also led to increased complexity in urban spatial structure and exposed many urban problems. For sustainable urban development, we must prevent blind expansion, grasp the status quo of urban development, delineate reasonable urban boundaries, optimize the urban spatial pattern and realize intensive use of land in order to achieve sustainable urban development. The urban boundary is the extension and framework of urban development, and the dynamic changes of urban areas can reflect the urban expansion process and spatial development mode. The monitoring of urban expansion and the analysis of spatial-temporal evolution facilitate in-depth exploration of urban development laws, providing strong support for scientifically guiding urban development and layout while improving urban environmental conditions and realizing sustainable urban development.

8.6.1 Difficulties of remote sensing monitoring of urban situations

The usage of remote sensing images for high-precision automatic interpretation of urban areas is the mainstream method of urban situation monitoring. However, many difficulties can occur. Firstly, the improvement of spatial resolution leads to the transition in feature extraction from "one pixel containing multiple feature information" to "multiple pixels forming a feature object". The spectral information of a single pixel fails to represent the spectral characteristics of the ground object, and it needs to be comprehensively processed to form the object. Secondly, the abundance of

details in features leads to the popularity of "the same objects with different spectra and foreign objects with the same spectra". The natural disadvantages of high-resolution remote sensing images in extracting spectral information result in difficulties in using spectral information to extract ground features. Thirdly, complex textures, shapes and urban scenes of the ground features, as well as the severe shadows of buildings, also pose challenges for urban monitoring. In addition, the monitoring of cities, as organic combinations of various features, is different from simple feature recognition, and the spatial semantic relationship of various features needs to be considered in a comprehensive manner. Existing urban expansion monitoring methods are still largely based on the idea of ground feature classification, mainly referring to land use types and using construction land or impervious surface as urban areas, resulting in rather fragmented extraction results.

Downloaded from www.worldscientific.com
by fac sciences de la terre universite annaba on 07/30/24. Re-use and distribution is strictly not permitted, except for Open Access articles.

8.6.2 Urban area extraction method based on progressive learning models

The urban area extraction method based on the progressive learning models makes full use of the data information in the unlabeled samples. Through the constraints of prior knowledge and rules, the workload of sample labeling is greatly reduced, and the resistance to sample noise is improved. The road network segmentation and scene classification methods are used to extract the urban area based on the block. The artificial features are designed according to the urban extraction principle, which solves the problem of high-level information expression in the identification and recognition of the urban area.

Progressive learning modes belong to a type of machine learning model that combines artificial features, prior knowledge and machine features using unlabeled samples. In progressive learning models, human cognition and machine learning are based on data under different systems and perspectives. For the understanding and expression of the set, samples that can be easily recognized by humans may be difficult for the machine. Similarly, samples that can be easily recognized by the machine may be difficult for humans to recognize. Thus, it is possible to form a win-win situation of reducing the workload of manual marking while improving the accuracy of machine recognition. Using high-resolution remote sensing images and the results of

the census of geography and national conditions and other thematic data in Beijing, the urban vector is extracted as the true value by a manual drawing (Figure 8.9). The results are the comparison and superposition effect of the extraction and the vector boundary of the artificially extracted urban true value.

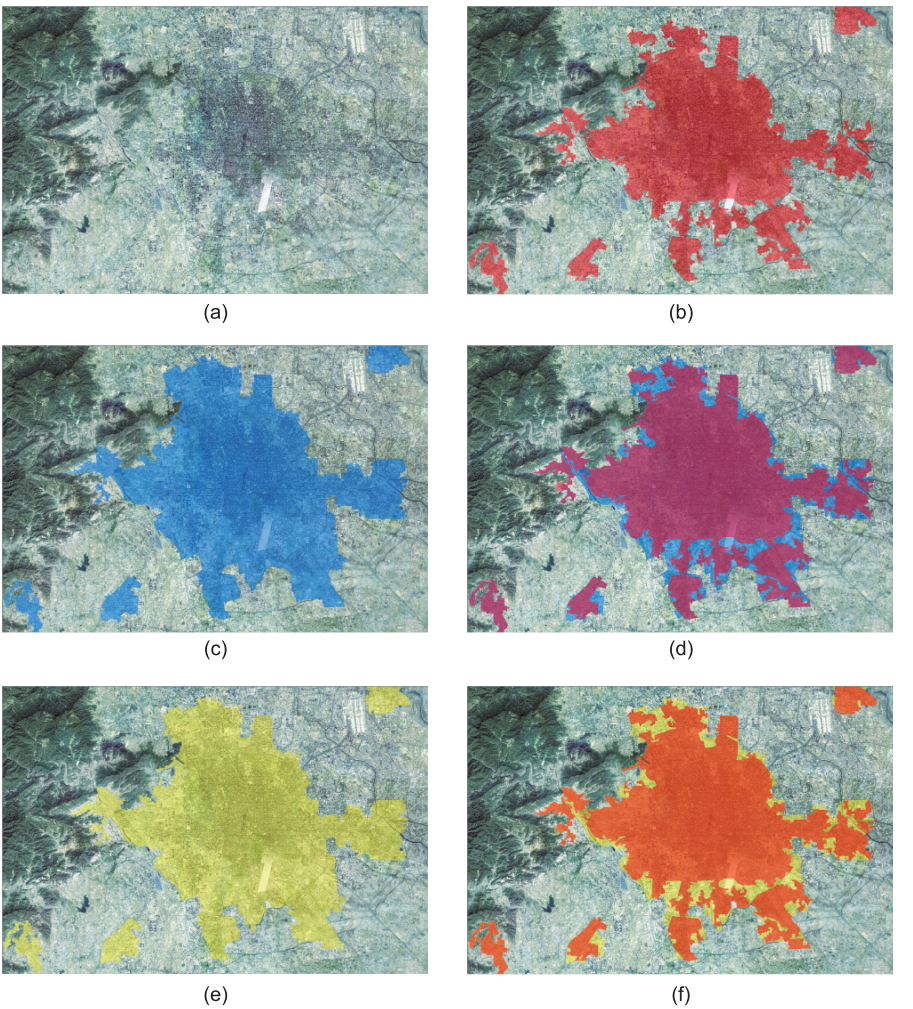

Figure 8.9 Comparison of extraction results in Beijing urban area: (a) Urban image map; (b) city true value and image overlay map; (c) rough extraction result graph; (d) overlay of rough extraction results and true value; (e) refined result graph; (f) refined result and true value overlay graph.

Downloaded from www.worldscientific.com
by fac sciences de la terre universite annaba on 07/30/24. Re-use and distribution is strictly not permitted, except for Open Access articles.

It can be seen that the extraction results from the progressive learning models are consistent with the spatial shape, direction and overall size of the manual extraction results. Thus urban boundaries can be automatically extracted using progressive leaning models.

8.7 Remote Sensing Monitoring of Urban Geological Hazards

China's mountainous and hilly regions, with complex geological conditions, frequent tectonic activities, many hidden dangers, wide distribution and difficult prevention of geological disasters (Liao *et al.*, 2018), account for about 65% of the country's total land area. Thus, China is one of the countries that faces the most severe geological disasters with the most threatened population in the world. A large number of Chinese cities are located in mountains, plateaus and hilly areas and are facing threats from numerous geological disasters (i.e., landslides, mudslides, rock slides), posing great challenges to the sustainable development of these cities (Li *et al.*, 2020). In addition, disasters such as road collapses and ground subsidence also seriously threaten coastal and plain cities. Global climate change has further exacerbated the scale and frequency of urban geological disasters. This section describes the feasibility and applicable methods of using remote sensing technology to investigate and monitor urban geological disasters and proposes the specific content of establishing a remote sensing monitoring and early warning system.

Remote sensing technology can play an essential role in early warning, dynamic monitoring, disaster assessment and decision-making assistance in urban disaster prevention and disaster relief. Taking advantage of urban remote sensing data, it is possible to conduct extensive surveys of the pregnancies and predisposing factors of geological disasters, disaster interpretation and cataloging, and provide technical support for the entire life cycle, i.e., early identification, long-term monitoring and post-disaster assessment of hidden geological hazards, of urban geological disaster prevention. In addition, remote sensing technology can also be used to assess the susceptibility, hazard and risk of geological disasters, and provide an important basis for disaster relief and mitigation decisions.

Downloaded from www.worldscientific.com
by fac sciences de la terre universite annaba on 07/30/24. Re-use and distribution is strictly not permitted, except for Open Access articles.

Downloaded from www.worldscientific.com
by fac sciences de la terre universite annaba on 07/30/24. Re-use and distribution is strictly not permitted, except for Open Access articles.

At present, in addition to visual interpretation, numerous efforts have been made to develop automatic landslide identification methods based on high-resolution remote sensing images, LiDAR and SAR images. A variety of statistical, machine identification and deep learning methods have been applied in landslide identification research. However, the accuracy and automation level of remote sensing recognition of landslides still fail to meet the requirements of large-scale engineering applications, and there exists a giant gap with conventional remote sensing classification. The main reason is that landslides tend to have many influencing factors, complicated formation mechanisms and changeable topographic and spectral characteristics.

Early identification of hazards and the use of multi-temporal remote sensing images to carry out change detection are able to discover the trend of changes in surface geological hazards, as shown in Figure 8.10.

After a disaster, remote sensing technology can be used to conduct disaster investigation and monitoring, analyze the loss of buildings, traffic and people's lives and property, and monitor the occurrence and development of

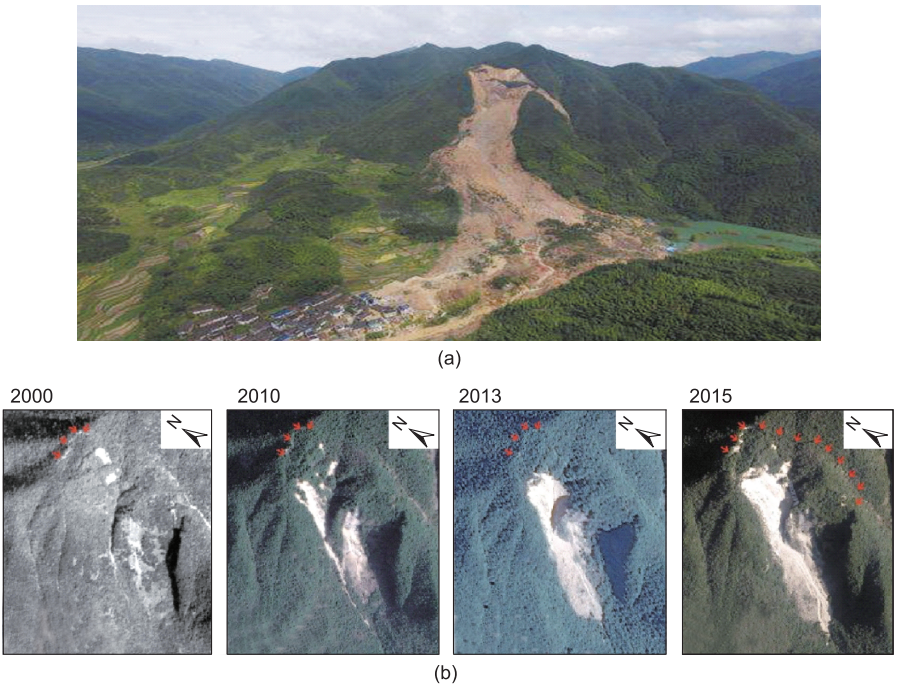

Figure 8.10 The photo (a) and remote sensing image (b) of the Sucun landslide in Lishui, Zhejiang, China, and its pre-sliding. The red arrows mark the direction of the landslide and the position of the trailing edge.

secondary disasters such as dammed lakes, landslides and mudslides. Remote sensing images can assist in the better implementation of post-disaster reconstruction planning, such as using remote sensing images to quickly generate 1:2000 DEM in cities and towns to support post-disaster planning and reconstruction.

Questions

1. How can one use remote sensing technology to monitor urban environmental changes?
2. How can one choose the most suitable remote sensing image according to the objects to be monitored?
3. Give examples of the processing steps and methods of urban remote sensing monitoring.

References

Jiang L, Zhan W F, Voogt J, Zhao L M, Gao L, Huang F, Cai Z, Ju W M. 2018. Remote estimation of complete urban surface temperature using only directional radiometric temperatures. *Building and Environment*, 135: 224–236.

Kuang W H, Liu J Y, Tian H Q, Shi H, Dong J W, Song C Q, Li X Y, Du G M, Hou Y L, Lu D S, Chi W F, Pan T, Zhang S W, Hamdi R, Yin Z R, Yan H M, Yan C Z, Wu S X, Li R D, Yang J C, Dou Y Y, Wu W B, Liang L Q, Xiang B, Yang S Q. 2021. Cropland redistribution to marginal lands undermines environmental sustainability. *National Science Review*, 9(1): nwab091.

Li M H, Zhang L, Ding C, Luo H, Liao M S, Xu Q. 2020. Retrieval of historical surface displacements of the Baige landslide from time-series SAR observations for retrospective analysis of the collapse event. *Remote Sensing of Environment*, 240: 111695.

Liao M S, Pei Y Y, Wang H M, Fang Z L, Wei L H. 2018. Subsidence monitoring in Shanghai using the PSInSAR technique. *Shanghai Land and Resources*, (33)3: 5–10.

Peng D, Yang W, Li H C, Yang X L. 2019. Superpixel-based urban change detection in SAR images using optimal transport distance. *Joint Urban Remote Sensing Event*, pp. 1–4.

Shao Z F, Zhang Y, Huang X, Zhu X L, Wu L, Wan B. 2018. Mapping impervious surface with 2 m using multi-source high resolution remote sensing images. *Geomatics and Information Science of Wuhan University*, 43(12): 156–162.

Shao Z F, Fu H Y, Li D R, Altan O, Cheng T. 2019. Remote sensing monitoring of multi-scale watersheds impermeability for urban hydrological evaluation. *Remote Sensing of Environment*, 232: 111338.

Downloaded from www.worldscientific.com
by fac sciences de la terre universite annaba on 07/30/24. Re-use and distribution is strictly not permitted, except for Open Access articles.

Shao Z F, Li C M, Li D R, Altan O, Zhang L, Ding L. 2020. An accurate matching method for projecting vector data into surveillance video to monitor and protect cultivated land. *ISPRS International Journal of Geo-Information*, 9: 448.

Zhang H C, Ning X G, Wang H, Shao Z F. 2018. High accuracy urban expansion monitoring and analysis of China's provincial capitals from 2000 to 2015 based on high-resolution remote sensing imagery. *Acta Geographica Sinica*, 73(12): 2345–2363.

Downloaded from www.worldscientific.com
by fac sciences de la terre universite annaba on 07/30/24. Re-use and distribution is strictly not permitted, except for Open Access articles.

Downloaded from www.worldscientific.com
by fac sciences de la terre universite annaba on 07/30/24. Re-use and distribution is strictly not permitted, except for Open Access articles.

Chapter 9

Remote Sensing Monitoring Technology and Practice of Urban Ecological Environment

The acceleration of urbanization has an incalculable ecological impact on the original natural environment in the region. The urban heat island effect is one of the most notable urban ecological environment problems in the process of urbanization. It not only affects people's daily life but also becomes a restrictive factor for the further improvement of people's quality of life and the further development of the city. For cities with a highly concentrated residential population, ecological protection is becoming the primary task to achieve sustainable urban development. Planting green vegetation in cities can promote the balance of urban ecosystems and is an important measure to beautify and purify the environment and improve environmental quality. The urban water environment is the core element of the urban environment. At present, the eutrophication of urban lakes has become a global problem. The quantitative monitoring capability provided by remote sensing techniques can largely benefit the planning and construction of ecologically friendly cities.

This chapter mainly introduces the remote sensing monitoring technology and practice of urban ecological environment. This chapter contains three topics: (i) remote sensing monitoring of the urban thermal environment; (ii) remote sensing inversion of urban aboveground biomass; and (iii) remote sensing quantitative monitoring of cyanobacteria in urban lakes.

9.1 Remote Sensing Monitoring Demands of Urban Ecological Environment

This section mainly introduces the remote sensing monitoring demands of urban thermal environments and the remote sensing inversion application demands of urban aboveground biomass.

9.1.1 The concept of urban heat island and the remote sensing monitoring demands of the urban thermal environment

In 1833, after comparing the observed temperatures in the urban and suburban areas of London simultaneously, the Englishman Lake Howard, for the first time, documented the phenomenon that the temperature in the urban center of London was higher than that in the suburbs. Manley first proposed the concept of urban heat island (UHI) in 1958, followed by many investigations on the UHI issues. It is now widely acknowledged that the UHI effect refers to the phenomenon that when the cities are developed to a certain scale, the urban temperature is significantly higher than that in the suburbs due to the change of urban underlying surface type, air pollution and artificial waste heat emission. As shown in Figure 9.1, urban surface materials (cement, asphalt, etc.) absorb and release a lot of heat, thus forming a phenomenon similar to the high-temperature island in the city. Many studies have shown that the formation of UHI is closely related to the degree of urbanization, population density, underlying surface properties, air pollutant

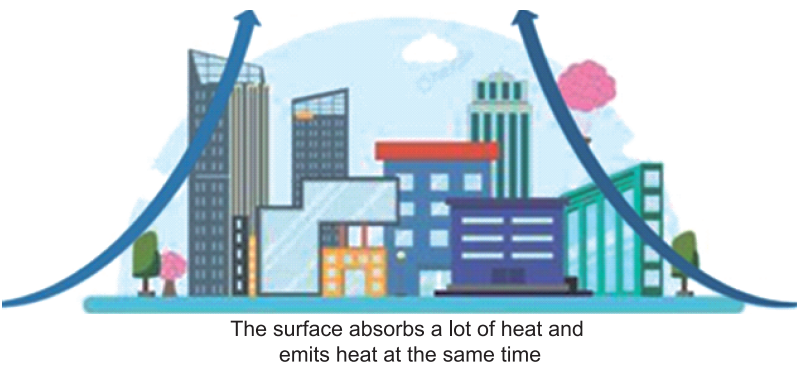

Figure 9.1 Urban heat island effect.

Downloaded from www.worldscientific.com
by fac sciences de la terre universite annaba on 07/30/24. Re-use and distribution is strictly not permitted, except for Open Access articles.

Downloaded from www.worldscientific.com
by fac sciences de la terre universite annaba on 07/30/24. Re-use and distribution is strictly not permitted, except for Open Access articles.

concentration and regional climate conditions. These influencing factors interact with urban microclimate in a complicated and intertwined manner. Recently, more attention has been paid to the extremely high-temperature events caused by climate change, as they pose great threats to personal life and property.

In the past few decades, studies on UHI have adopted three major methods: ground meteorological data observation method, remote sensing monitoring method and boundary layer numerical model simulation method. The ground observation method is mainly based on the data of fixed meteorological stations in the suburbs and can cooperate with the mobile observation data, aiming to conduct a comparative study on the temperature in the suburbs. Developed in an early stage, such methods apply statistical models to analyze the meteorological data of urban and suburban areas to obtain the regional heat island intensity. In comparison, the boundary layer model simulation uses one-dimensional to three-dimensional mesoscale models to simulate the temperature, humidity and wind field in the spatial region at a specific height.

The ground meteorological data observation method can most directly and objectively reveal the characteristics of urban heat island effect. Using ground observation stations and wind profilers, these tools can obtain the daily change, distribution and intensity of urban heat island through long-term time series observation of a station in the city, or comparative observation and statistical analysis of multiple urban and rural stations. This observation method has played an extremely important role in the initial discovery and understanding of urban heat island. However, due to the sparse distribution of meteorological stations, it is difficult to truly and effectively expand the research on point scale to the research on plane layout and internal structure of urban heat island, and it is difficult to meet the research needs of various heat island problems on an urban scale. At present, there are fewer and fewer urban heat island studies that only rely on traditional ground observation methods.

The boundary layer numerical simulation model is based on the theories of thermodynamics and dynamics to study the thermal exchange process between the earth and the atmosphere, and quantitatively analyze the basic characteristics of energy balance, energy exchange and temperature field of the urban underlying surface. This simulation method mainly focuses on the study of simple urban atmospheric environment problems, the content is limited to the comparative analysis of near-stratum meteorological elements

Downloaded from www.worldscientific.com
by fac sciences de la terre universite annaba on 07/30/24. Re-use and distribution is strictly not permitted, except for Open Access articles.

inside and outside the city, and the scale range of simulation is limited to hundreds of meters to several kilometers. In addition, the complexity of the underlying surface and the incompleteness of data also limit the development of the simulation model method.

Remote sensing is another widely used approach for monitoring UHI effects, thanks to its extensive spatial coverage and great time synchronization. Remote sensing sensors form different band radiation values according to the characteristics of solar longwave radiation absorbed by different ground objects. The surface temperature of the underlying surface is observed by the thermal infrared sensor, and then the surface temperature image is processed by a computer. In recent years, with the rapid development of remote sensing technology, a large number of advanced remote sensing sensors have been developed. With the improvement of high-resolution satellite thermal infrared remote sensing technology, remote sensing observation methods have a major research direction in the investigation of UHI issues. Commonly used satellite remote sensing thermal infrared data sources are shown in Table 9.1. The remote sensing monitoring method also has its limitations. Because the remote sensing sensor obtains the surface temperature of the underlying surface rather than the near-surface air temperature, it cannot reflect the real suburban air temperature difference. Some researchers have converted surface temperature into air temperature, but this method has a large error. The acquisition of remote sensing data is limited by many conditions, such as atmospheric conditions and cloud cover. The low resolution of remote sensing data also has an impact on the study of urban heat island effect.

9.1.2 Application demands for remote sensing inversion of urban aboveground biomass

As a primary producer of urban ecosystems, urban vegetation plays an irreplaceable role in ecological infrastructure. Urban vegetation generally refers to the living plants in the city, including vegetation types of forests, flower beds, lawns and trees in parks, campuses, squares, golf courses, farmland and roads (Figure 9.2). Urban vegetation is an important component of urban ecosystems and plays an essential role in improving the quality of urban construction and development. Therefore, planting

Downloaded from www.worldscientific.com
by fac sciences de la terre universite annaba on 07/30/24. Re-use and distribution is strictly not permitted, except for Open Access articles.

Table 9.1 Representative data sources and characteristics of urban heat island remote sensing platform/sensors.

Platform/ sensor	Band	Spectral range (μm)	Repetition period (day)	Spatial resolution (m)	Advantage	Disadvantage
NOAA/ AVHRR	4 5	10.5–11.3 11.5–12.5	0.5	1100	Wide observation range, short observation period and low price	Low data resolution
Terra/ MODIS	31 32 10 11	10.78–11.28 11.77–12.27 8.117–8.475 8.475–8.817	1 16 	1000 90 	Successor sensor equivalent to NOAA	Low data resolution
Terra/ ASTER	12 13 14	8.935–9.275 10.17–10.95 10.95–11.65			Visible light and thermal infrared channel data are homologous, with high data resolution and multiple thermal infrared channels	Few archived data and long revisit cycle
Landsat/TM, ETM+	6 10	10.4–12.5 10.6–11.2	16	120/60	Visible light and thermal infrared channel data are homologous, with high data resolution and many archived data	Single channel which is difficult to eliminate atmospheric impact, long revisit cycle
Landsat/ TIRS	11	11.5–12.5	16	100	Visible light and thermal infrared channel data are homologous, with high data resolution and many archived data	Single channel which is difficult to eliminate atmospheric impact, long revisit cycle

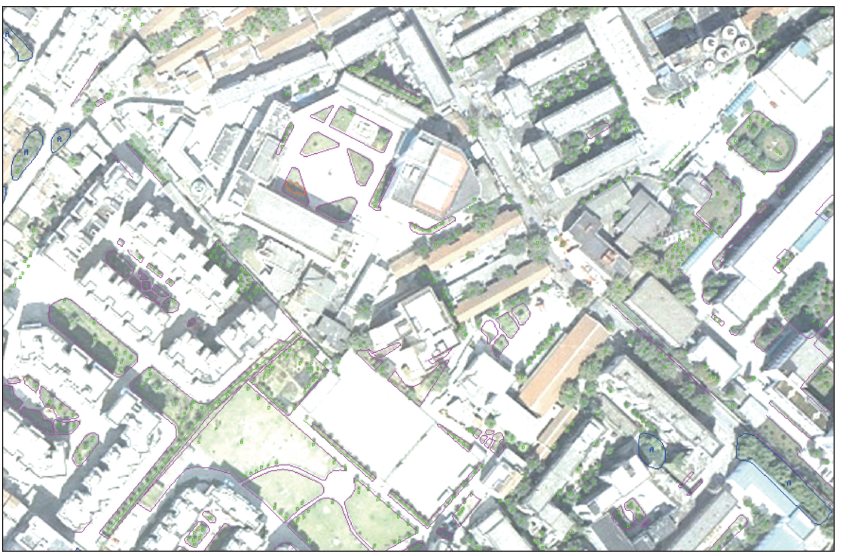

Figure 9.2 Urban vegetation.

green vegetation in cities is an important measure to beautify and purify the environment and improve environmental quality, thus promoting the balance of urban ecosystems.

Besides recreational purposes, urban vegetation also has the function of protecting and improving the environment. Plants can absorb carbon dioxide and release oxygen, serving the purpose of purifying the air; they can absorb harmful gas and dust to a certain extent and reduce pollution. In addition, urban plants are able to adjust the temperature and humidity of the air and improve the microclimate and play a protective role in reducing noise and preventing wind and fire. If urban vegetation cooperates well with other natural conditions, urban streets and architectural groups, it can add scenery, beautify streets and city appearance, and bring vitality to the city.

Quantitative research on urban vegetation, i.e., estimating urban aboveground biomass, is of great significance for the planning and construction of ecologically friendly cities. Urban aboveground biomass refers to the total amount of organic matter of vegetation per unit area in an urban environment (in units kg/m^2 or mg/ha). Urban aboveground biomass is an important index to measure the carbon sequestration level of urban vegetation. Fine knowledge of its distribution patterns provides not only theoretical support for investigating the carbon cycle of urban ecosystems but also quantitative references for mitigating the greenhouse

Downloaded from www.worldscientific.com
by fac sciences de la terre universite annaba on 07/30/24. Re-use and distribution is strictly not permitted, except for Open Access articles.

Downloaded from www.worldscientific.com
by fac sciences de la terre universite annaba on 07/30/24. Re-use and distribution is strictly not permitted, except for Open Access articles.

effect by accounting for energy conservation and emission reduction of afforestation and reforestation. Because of its macro dynamic, real-time and multi-source characteristics, remote sensing technology has been vigorously developed in the estimation of forest aboveground Biomass and other vegetation parameters. With the development of multi-scale, multi-sensor and multi/hyperspectral remote sensing technology, it provides a powerful tool for urban aboveground biomass monitoring. From the application and development of remote sensing technology, aboveground biomass monitoring is also one of the most widely used fields of remote sensing, which provides a convenient method to determine the correlation between some vegetation and biophysical and ecological parameters. Remote sensing has become an important measurement in recent years, as it can quickly and accurately obtain the distribution and green coverage information of urban green space, providing important knowledge on the composition, types and layout of urban green space landscapes. Taking advantage of high-resolution remote sensing images at different time phases, combined with field investigation, the dynamics of urban ecological green spaces can be extracted and retrieved, and the vegetation system database can be established.

9.2 Remote Sensing Monitoring Methods and Practice of Urban Heat Island Effect

The urban heat island is a typical manifestation of the impact of urbanization on the climate. At present, the remote sensing monitoring methods to study the urban heat island effect can be divided into the following categories: (i) heat island monitoring method based on temperature; (ii) heat island monitoring method based on vegetation index (VI); (iii) heat island monitoring method based on thermal landscape; and (iv) high-resolution heat island inversion method based on downscaling.

Remote sensing techniques use sensors to receive the energy of reflected radiation or emitted radiation from ground objects. Thermal infrared scanning images that record the sum of emitted radiation from surface objects, environment and atmosphere are generally used to study the urban heat island effect. Bands that cover 10.4–12.5 μm are used in Landsat sensors.

Downloaded from www.worldscientific.com
by fac sciences de la terre universite annaba on 07/30/24. Re-use and distribution is strictly not permitted, except for Open Access articles.

In the thermal infrared band, the solar radiation energy is very small, and most of the energy comes from the earth's radiation. Especially in the daytime, recorded thermal infrared energy only corresponds to large geothermal radiation, and the reflection of solar radiation can be ignored. It mainly reflects the radiation energy value of ground objects in the thermal infrared region. The relationship between the radiation energy of ground objects and temperature can be expressed by the Stephen Boltzmann law as follows:

$$W = \varepsilon \sigma T^4 \tag{9.1}$$

where ε is the emissivity of the radiator ($\leqslant 1$), σ is the Stephen Boltzmann constant and T is the thermodynamic temperature of the ground object.

Brightness temperature is closely related to ground temperature, and air temperature mainly comes from longwave radiation on the ground. Thus, the brightness temperature, ground temperature and air temperature are closely related. It is generally believed that these three temperatures can be converted, forming the theoretical basis for monitoring the heat island effect using remote sensing images. In practical application, given the small urban areas, the bright temperature can sometimes be directly used to characterize the UHI effects, which is called urban bright temperature heat island. Investigating UHI effects using bright temperature has the advantages of simplicity, great computationally efficiency and high data synchronization.

Vegetation index, widely used to qualitatively and quantitatively evaluate vegetation cover and its vitality, is an important information source reflecting surface vegetation information. In the process of urbanization, vegetation, water surface and other land cover types are replaced by impervious surfaces composed of cement and asphalt, unavoidably leading to a series of eco-environmental effects, e.g., reduced surface water transpiration, accelerated runoff, increased sensible heat storage and transmission, of which the two most significant consequences are the reduction of vegetation cover and exacerbated urban heat island effects.

In 1993, Gallo first used the vegetation index obtained from AVHRR data to estimate the intensity of urban heat island effects. The results show that, like the surface radiation temperature, there is a notable linear relationship between vegetation index and urban and rural temperature, and such a relationship can be used to explain the spatial variation of average minimum temperature. The seasonal relationship between NDVI and other driving factors and surface temperature is studied. Three Landsat-8 images

in different seasons in Shanghai in 2017 are selected to study the surface temperature in winter, transition season and summer (Figures 9.3–9.5). The correlation between driving factors and surface temperature is analyzed, and the results show that the effect of NDVI on surface temperature varies with seasons.

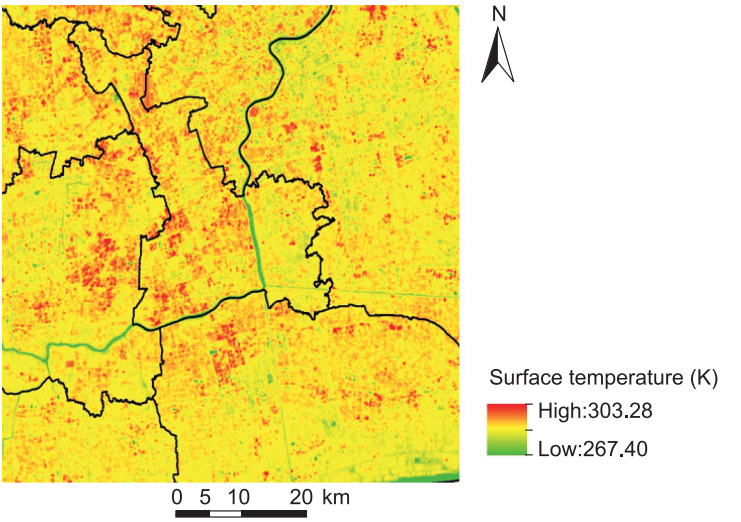

Figure 9.3 The distribution map of surface temperature in winter in Shanghai.

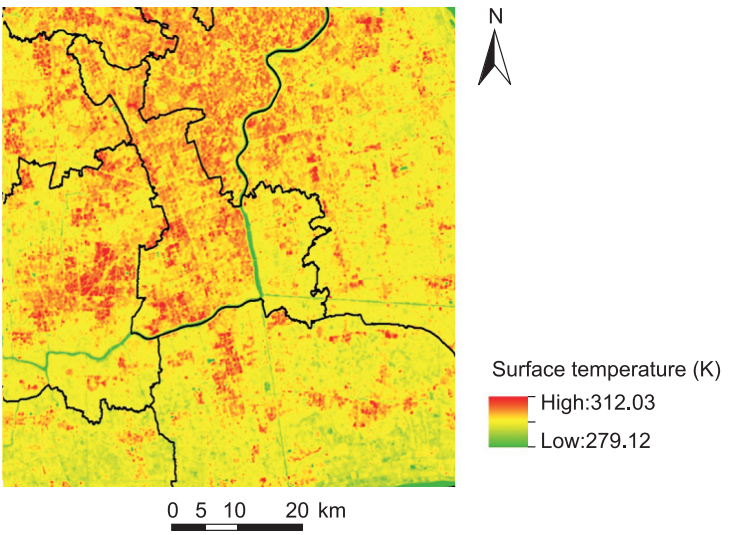

Figure 9.4 The distribution map of surface temperature in transition season in Shanghai.

Downloaded from www.worldscientific.com
by fac sciences de la terre universite annaba on 07/30/24. Re-use and distribution is strictly not permitted, except for Open Access articles.

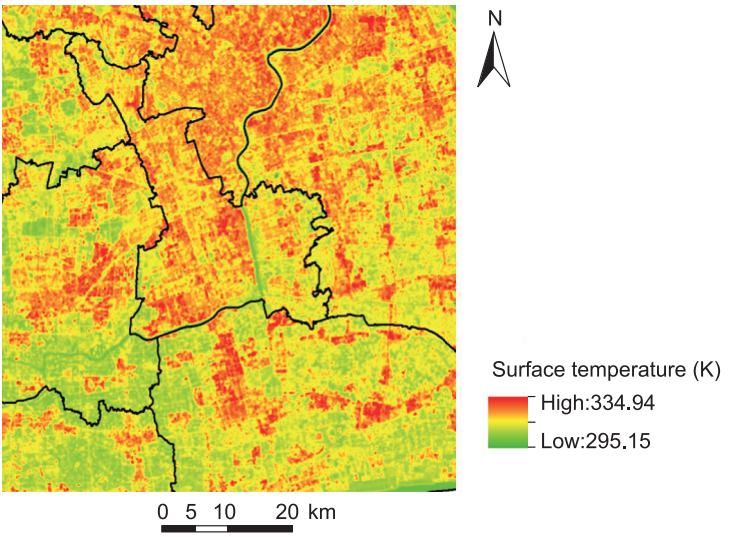

Figure 9.5 The distribution map of surface temperature in summer in Shanghai.

Borrowing the concept of landscape ecology, Chen *et al.* (2002) introduced the concept of "thermal landscape" and established the heat island monitoring method based on such a concept. They used the landscape index and GIS spatial analysis theory and technology to study the urban thermal environment from the perspective of the landscape and established a set of research methods and evaluation indices to understand the spatial patterns and evolving processes of thermal environments. Their study marks the entrance of the quantitative stage in urban thermal environment investigation.

The thermal landscape, composed of interactive thermal patches with certain laws, denotes a thermal area with high spatial heterogeneity formed by the interaction between the city and the surrounding environment. According to the difference of shape and function, elements in the thermal landscape can be divided into the thermal patch, thermal corridor and thermal matrix. A thermal matrix refers to the component of a relatively homogeneous background that accounts for the main body in the thermal landscape. The thermal patch with relative homogeneity is a mosaic different from the patch surrounding it. The thermal corridor refers to the strip-shaped thermal landscape reflected in the thermal landscape, e.g., green corridors, streets, canals and roads, to list a few. Based on the research methods of landscape ecology, the evaluation system of the thermal landscape

Downloaded from www.worldscientific.com
by fac sciences de la terre universite annaba on 07/30/24. Re-use and distribution is strictly not permitted, except for Open Access articles.

Downloaded from www.worldscientific.com
by fac sciences de la terre universite annaba on 07/30/24. Re-use and distribution is strictly not permitted, except for Open Access articles.

spatial pattern is further established and the evaluation indexes (such as fractal dimension, shape index, diversity, dominance and fragmentation) are defined. The characteristics of landscape patch complexity, patch shape characteristics, thermal landscape diversity and landscape patch fragmentation can be analyzed.

Due to the trade-off between spatial resolution and scanning bandwidth in satellite sensors, no global thermal infrared satellite remote sensing platform with the high spatial and temporal resolution is available. The lack of such a platform limits the expansion of quantitative research in the field of global temperature change. How to obtain surface temperature data with a high spatial and temporal resolution is a key issue that needs to be addressed in an urgent manner. The downscaling methods are promising techniques to obtain high spatio-temporal resolution surface temperature.

Yang *et al*. (2017) proposed a downscaling model called NDSI-RF for urban and complex regional surface temperature. In NDSI-RF the normalized difference sand index (NDSI), soil-adjusted vegetation index (SAVI), normalized difference water index (NDWI) and normalized difference building index (NDBI) are used as downscaling factors. First, the relationship between low spatial resolution downscaling factor and low spatial resolution surface temperature is established using a random forest regression method. Then, the above relationship is applied to the scale factor of high spatial resolution to obtain the predicted value of high spatial resolution surface temperature, according to the scale invariance effect. The final downscaling result is obtained after the regression with the original low spatial resolution surface temperature.

9.3 Remote Sensing Inversion and Application of Urban Aboveground Biomass

Aboveground biomass (AGB) refers to the total amount of vegetation organic matter (dry weight) accumulated per unit area at a certain time, including the total amount of trunk, branches and leaves. AGB is an important indicator to not only measure the carbon sequestration capacity of vegetation but also evaluate the regional carbon balance. The accurate estimation of aboveground biomass is of great importance in the study of the earth's carbon cycle and global climate change.

Downloaded from www.worldscientific.com
by fac sciences de la terre universite annaba on 07/30/24. Re-use and distribution is strictly not permitted, except for Open Access articles.

Vegetation is characterized by its spectral reflection signals, which are different from the soil, water and other urban features. The responses of vegetation to electromagnetic wave are determined by its chemical and morphological characteristics, which are closely related to the development, health and growth conditions of vegetation. Between the visible and near-infrared bands (about 0.76 μm), the reflectivity of vegetation rises sharply, leading to the "red edge" phenomenon (Figure 9.6). Such shape rise in reflection represents the most notable feature of the plant curves. Many plant types present insignificant reflection differences in the visible light band but notable differences in the near-infrared band.

Vegetation index is a simple, effective and empirical measure of surface vegetation activities, which provides essential knowledge on vegetation health and coverage. As an effective remote sensing data processing method, the construction of VI has been widely used in land cover change detection, vegetation type identification, and biomass estimation.

Considering the commonly used vegetation biomass sensitivity index and the factors significantly affected by biomass change, combined with the band setting of commonly used optical satellite sensors, the spectral indexes and texture feature indexes are generally dominated (Table 9.2).

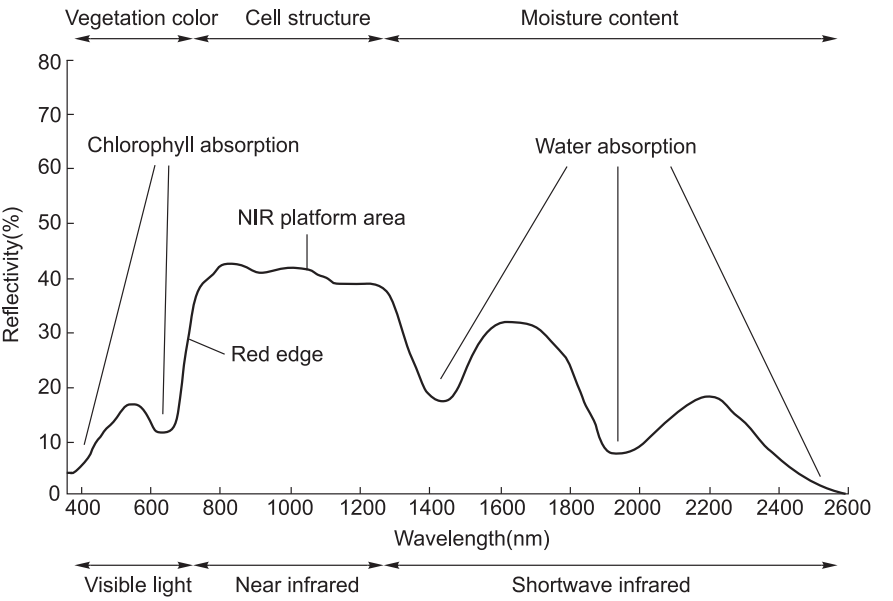

Figure 9.6 The vegetation spectral characteristic curve.

Downloaded from www.worldscientific.com
by fac sciences de la terre universite annaba on 07/30/24. Re-use and distribution is strictly not permitted, except for Open Access articles.

Table 9.2 The spectral and texture indexes and their formula.

Variable type	Variable	Description
Spectral band	B	Original image band, band i ($i = 1, 2, 3, 4$)
	G	
	R	
	NIR	
Spectral index	SR	Simple ratio vegetation index, $\frac{\text{NIR}}{R}$
	NDVI	Normalized difference vegetation index, $\frac{\text{NIR} - R}{\text{NIR} + R}$
	EVI	Enhanced vegetation index, $\frac{2.5 \times (\text{NIR} - R)}{1 + \text{NIR} + 6 \times R - 7.5 \times B}$
	SAVI	Soil-adjusted vegetation index, $(1 + 0.5)\frac{\text{NIR} - R}{\text{NIR} + R + 0.5}$
	MSAVI	Modified soil-adjusted vegetation index, $\text{NIR} + 0.5 - \sqrt{(\text{NIR} + 0.5)^2 - 2 \times (\text{NIR} - R)}$
	OSAVI	Optimized soil-adjusted vegetation index, $(1 + 0.16)\frac{\text{NIR} - R}{\text{NIR} + R + 0.16}$
	Cl_{green}	Green chlorophyll index, $\frac{\text{NIR}}{G} - 1$
	ARVI	Atmospherically resistant vegetation index, $\frac{\text{NIR} - (2 \times R - B)}{\text{NIR} + (2 \times R - B)}$
	VI_{Green}	Green vegetation index, $\frac{G - R}{G + R}$
Texture feature	ME	Mean, $\sum_{i,j=0}^{N-1} iP_{i,j}$
	HO	Homogeneity, $\sum_{i,j=0}^{N-1} i\frac{P_{ij}}{1 + (i - j)^2}$
	CON	Contrast, $\sum_{i,j=0}^{N-1} iP_{i,j}(i - j)^2$
	DI	Dissimilarity, $\sum_{i,j=0}^{N-1} iP_{i,j}\lvert i - j\rvert$

(*continued*)

Table 9.2 (*continued*)

Variable type	Variable	Description
	EN	Entropy, $\sum_{i,j=0}^{N-1} iP_{i,j}(-\ln P_{i,j})$
	VAR	Variance, $\sum_{i,j=0}^{N-1} P_{i,j}(1-\mu_i)$
	SM	Second moment, $\sum_{i,j=0}^{N-1} iP_{i,j}^2$
	COR	Correlation, $\sum_{i,j=0}^{N-1} i\frac{\sum_{i,j=0}^{N-1} ijP_{i,j}-\mu_i\mu_j}{\sigma_i^2\sigma_j^2}$

Where, $\mu_i = \sum_{i=0}^{N-1} i\sum_{j=0}^{N-1} P_{i,j}$; $\sigma_i^2 = \sum_{i=0}^{N-1}(i-\mu_i)^2\sum_{j=0}^{N-1} P_{i,j}$; $\sigma_j^2 = \sum_{j=0}^{N-1}(j-\mu_j)^2\sum_{j=0}^{N-1} P_{i,j}$.

The overall process of remote sensing inversion of urban aboveground biomass contains the following steps:

1. The aboveground biomass of the sample plot is calculated based on the aboveground biomass parameters of the field investigation in the urban area. The aboveground biomass of the typical sample area is estimated by using the variables such as the biomass of the sample plot and the altitude information extracted by the airborne LiDAR, and the aboveground biomass estimation model of the typical sample area based on the airborne LiDAR is established.
2. Sample data are extracted from the aboveground biomass estimated by airborne LiDAR, and the aboveground biomass in the urban area is estimated with the band reflectance, vegetation index and texture features extracted from high-resolution images.

After the establishment of the best inversion model of urban aboveground biomass, the thematic map of aboveground biomass distribution can be made, as shown in Figure 9.7, where an example of the urban aboveground biomass distribution in Hengqin, China, is presented.

Downloaded from www.worldscientific.com
by fac sciences de la terre universite annaba on 07/30/24. Re-use and distribution is strictly not permitted, except for Open Access articles.

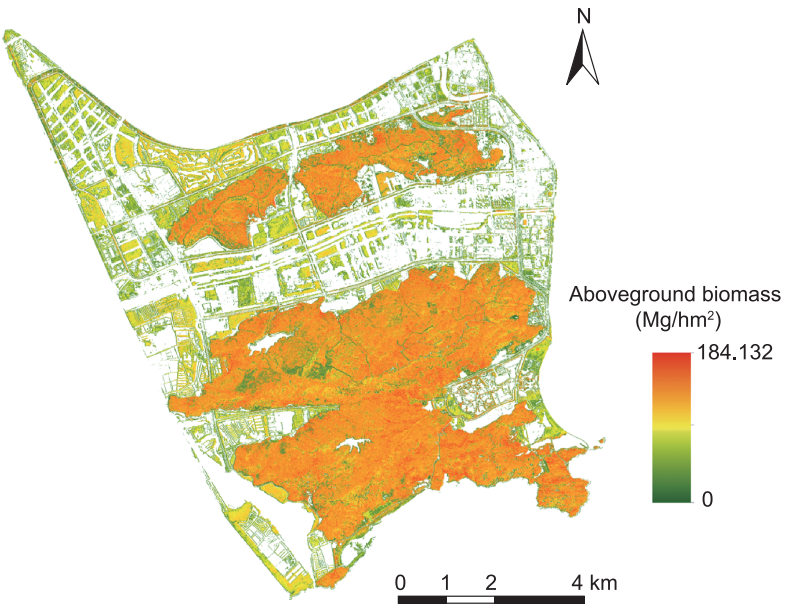

Figure 9.7 The thematic map of urban aboveground biomass distribution in Hengqin, China, in 2018.

Remote sensing techniques are able to provide observations that cover large geographical areas in a real-time and dynamic manner. The improvement of resolution enables high-precision urban aboveground biomass investigation. Through the combination of LiDAR data and optical data, various characteristic parameters with great correlation with aboveground biomass can be extracted. At the same time, using the sample observation data with selected spatially representative biomass samples, the urban aboveground biomass inversion model can be established to realize the biomass inversion of large regions.

9.4 Innovative Models and Methods in Remote Sensing Quantitative Monitoring of Cyanobacteria from Urban Lakes with Eutrophication

Eutrophication describes a phenomenon of water pollution caused by the high content of plant nutrients (e.g., nitrogen and phosphorus).

Downloaded from www.worldscientific.com
by fac sciences de la terre universite annaba on 07/30/24. Re-use and distribution is strictly not permitted, except for Open Access articles.

Downloaded from www.worldscientific.com
by fac sciences de la terre universite annaba on 07/30/24. Re-use and distribution is strictly not permitted, except for Open Access articles.

Eutrophication of urban lakes has become a severe issue, usually accompanied by the frequent outbreak of cyanobacteria bloom, which leads to the deterioration of water quality. In certain cases, it can deplete oxygen in the water and cause the death of fish. Cyanobacteria bloom has become the focus of lake eutrophication control all over the world. By monitoring and early warning of the occurrence of water blooms, its impact and loss can be reduced. Remote sensing technologies, characterized by large coverage, range, regular periodicity and low cost, have been largely adopted to provide timely information on the distribution of cyanobacteria bloom. The emergence of hyperspectral sensors and high spatio-temporal remote sensing sensors makes accurate early warning of cyanobacteria bloom possible. The recent years have seen great progress on the remote sensing monitoring of cyanobacteria blooms, which can be grouped into three categories: the inversion of chlorophyll concentration, phycocyanin concentration and cyanobacteria abundance.

Chlorophyll-a whose content is relatively stable and easy to measure manually, is a pigment rich in algae. Its concentration is an important index to reflect the degree of water eutrophication, contributing to the evaluation of phytoplankton biomass and primary productivity. However, due to the complex optical characteristics of the water body, the content of chlorophyll-a in a water body can be easily affected by various factors. Transcending traditional manual monitoring methods, remote sensing techniques can carry out real-time, dynamic and full-range monitoring.

The spectral characteristics of water are complex, which are determined by the light radiation scattering properties and absorbance of various optically active substances in water. The reflectance curve of pure water in the visible band follows a nearly linear pattern. When water contains other substances, its spectral reflectance curve tends to have valleys and peaks. Chlorophyll-a is an optically active substance. In water, the spectral reflection peaks vary due to the different concentrations of chlorophyll-a. The algal substances in the water body show absorption peaks in the blue-violet light band (0.420–0.50 μm) and red light band (0.675 μm). If the water body contains a large amount of chlorophyll-a, the strong absorption of chlorophyll-a leads to valleys in the reflectance curve in these two bands and peaks in the near-infrared band (0.70 μm). In conclusion, the basic principle of remote sensing monitoring of water chlorophyll-a lies in the fact that within a certain wavelength range, different chlorophyll-a concentration levels can lead to the significantly different reflectivity. By analyzing the reflection spectral

Downloaded from www.worldscientific.com
by fac sciences de la terre universite annaba on 07/30/24. Re-use and distribution is strictly not permitted, except for Open Access articles.

characteristics of the water surface with different chlorophyll concentrations, a relationship between chlorophyll-a concentration and water reflectivity can be constructed.

Because the optical properties of water are relatively complex, it is difficult to establish a universal and high-precision chlorophyll-a inversion model. At present, chlorophyll-a remote sensing inversion methods can be divided into three categories: empirical methods, semi-empirical/ semi-analytical methods and analytical methods.

The empirical method is to select the optimal band or band combination of remote sensing data synchronized with the measured data for statistical analysis, construct the correlation relationship and then retrieve the chlorophyll-a concentration. The main algorithms of empirical methods include the single-band model, band ratio model and neural network model.

The semi-empirical/semi-analytical method combines theoretical analysis and empirical statistical analysis to construct the inversion model. The classical representative algorithms of semi-empirical methods include the three-band method and reflection peak position method.

The analysis method is a physical model, which simulates the propagation process of the electromagnetic wave in water by describing the relationship between the irradiance ratio and water quality parameters, and establishes the relationship between the irradiance ratio and chlorophyll-a absorption coefficient and backscattering coefficient. The typical representative algorithm is the bio-optical model.

Phycocyanin (PC) is a phycobiliprotein. Cyanobacteria are the dominant algae species in water eutrophication, and PC is the characteristic pigment of cyanobacteria. Therefore, the concentration of PC can be used as a measurement to reflect the content of cyanobacteria in water, providing a new indicator for early warning of cyanobacteria bloom. Different from other algae, phycocyanin has an absorption peak at 620 nm. Thus, scholars all over the world aim to identify, monitor and quantitatively estimate cyanobacteria, taking advantage of this optical characteristic. In water environment monitoring, the concentration of PC can effectively reflect the levels of primary productivity and eutrophication. Therefore, the establishment of an effective PC inversion model is of great significance for rapid, real-time and dynamically quantitative monitoring of cyanobacteria biomass and eutrophication degree of lakes.

Cyanobacteria abundance refers to the proportion of cyanobacteria density to total algae density. Cyanobacteria is the dominant algae species in water

eutrophication. However, remote sensing monitoring of algae in the water is based on the measurement of chlorophyll-a, and PC cannot reflect whether cyanobacteria are the dominant algae species. Cyanobacteria bloom is usually a continuous process where algae biomass gradually accumulates in water. Before and after an outbreak of cyanobacteria bloom and during the bloom, the phytoplankton community continues to grow and the abundance of cyanobacteria gradually increases, leading to its dominant position. Therefore, understanding the abundance of cyanobacteria in water is of great significance for monitoring and providing early warning of cyanobacteria bloom. Remote sensing technology benefits the monitoring of the abundance of cyanobacteria, as it is able to provide real-time and dynamic measurement, reflect whether cyanobacteria are the dominant species and provide the temporal and spatial differences and change rules of cyanobacteria abundance distribution. PC is the characteristic pigment of cyanobacteria, and chlorophyll-a is the common pigment of planktonic algae. Theoretically, the ratio of PC concentration to chlorophyll-a concentration (PC : Chla) can characterize the abundance of cyanobacteria. Despite that, some scholars started to use the PC : Chla ratio as an indicator to reflect the proportion of cyanobacteria in planktonic algae. Whether the PC : Chla ratio can be used to represent the measured cyanobacteria abundance in water needs further verification.

Downloaded from www.worldscientific.com
by fac sciences de la terre universite annaba on 07/30/24. Re-use and distribution is strictly not permitted, except for Open Access articles.

Questions

1. What scenarios are the different remote sensing monitoring methods for the urban heat island effect suitable for?
2. What impacts do urban heat islands have on vegetation biomass?
3. Please summarize how to carry out remote sensing monitoring of lake eutrophication.

References

Chen Y, Li X, Shi P. 2002. Analysis of spatial pattern of thermal environment in Shanghai City. *Geographic Science*, 3: 317–323.

Englhart S, Keuck V, Siegert F. 2011. Modeling aboveground biomass in tropical forests using multi-frequency SAR data — A comparison of methods. *IEEE Journal of Selected Topics in Applied Earth Observations and Remote Sensing*, 5(1): 298–306.

Gallo K P, McNab A L, Karl T R, Brown J F, Hood J J, Tarpley J D. 1933. The use of a vegetation index for assessment of the urban heat island effect. *International Journal of Remote Sensing*, 14(11): 2223–2230.

Howard L. 2012. *The Climate of London: Deduced from Meteorological Observations*. New York: Cambridge University Press.

Liu G, Simis S G H, Li L, Wang Q , Li Y M, Song K S, Lyu H, Zheng Z B, Shi K. 2018. A four-band semi-analytical model for estimating phycocyanin in inland waters from simulated MERIS and OLCI data. *IEEE Transactions on Geoscience and Remote Sensing*, 56(3): 1374–1385.

Shao Z, Tang P, Wang Z Y, Saleem N, Yam S, Sommai C. 2020. BRRNet: A fully convolutional neural network for automatic building extraction from high-resolution remote sensing images. *Remote Sensing*, 12(6): 1050.

Voogt J A, Oke T R. 2003. Thermal remote sensing of urban climates. *Remote Sensing of Environment*, 86(3): 370–384.

Yang Y B, Li X L, Pan X, Zhang Y, Cao C. 2017. Downscaling land surface temperature in complex regions by using multiple scale factors with adaptive thresholds. *Sensors*, 17(4): 744.

Downloaded from www.worldscientific.com
by fac sciences de la terre universite annaba on 07/30/24. Re-use and distribution is strictly not permitted, except for Open Access articles.

This page intentionally left blank

Downloaded from www.worldscientific.com
by fac sciences de la terre universite annaba on 07/30/24. Re-use and distribution is strictly not permitted, except for Open Access articles.

Downloaded from www.worldscientific.com
by fac sciences de la terre universite annaba on 07/30/24. Re-use and distribution is strictly not permitted, except for Open Access articles.

Chapter 10

Prospects of Urban Remote Sensing Technologies and Applications

In the 20th century, one of the major advances of mankind is the realization of space-to-earth observation. Remote sensing observation can be carried out from the air and space, and the data and information obtained can be stored on computer networks in an efficient manner, largely benefiting the sustainable development of human society (Li and Shao, 2009). In just 50 years, remote sensing has been fully developed as an emerging interdisciplinary discipline. This chapter summarizes and envisions the developing directions of urban remote sensing technologies and applications.

10.1 The Developing Directions of Urban Remote Sensing Sensors

In recent years, remote sensing sensors have been designed with increasingly diversified spatial resolutions, refined sensor bands and increasingly broad application areas. We summarize the specific developing trends of remote sensing sensors as follows:

1. Increased applications of the wave spectrum and the emergence of new sensors such as hyperspectral, luminescent remote sensing and multi-angle SAR.

   Space-air-ground multi-platform hyperspectral sensors provide a feasible sensing approach to and data support for the fine distinguishment of various objects and materials. They have been widely used to support the construction of sponge cities, ecologically friendly cities and healthy cities.

Downloaded from www.worldscientific.com
by fac sciences de la terre universite annaba on 07/30/24. Re-use and distribution is strictly not permitted, except for Open Access articles.

The socio-economic activities of cities can be evaluated by night-light remote sensing. Since most nighttime visible light and human activities are closely linked, night-light remote sensing is able to obtain the urban economic and social dynamics and assess the urban economic and social development at a macro level.

Multi-angle SAR imaging can achieve a complete description and all-around imaging of the electromagnetic scattering characteristics of the target by fusing the target information under multiple angles (Ran *et al.*, 2016). Compared with single-angle conventional SAR, multi-angle SAR is characterized by its spatial diversity and by the increased amount of data samples. Multi-angle SAR effectively expands the spatial-spectral support area of the detected targets, avoids the target occlusion and overlay masking issues in conventional SAR imaging detection, and improves the classification and recognition capability of targets in complex urban scenes. By combining multi-carrier frequency, multi-waveform and multi-polarization technologies, multi-angle SAR can eventually realize multi-dimensional SAR imaging and detection. In addition, multi-angle SAR can synthesize the information at multiple observation angles and can solve the problems of target occlusion and overlay masking caused by traditional SAR due to terrain and observation angle limitations through certain signal processing and information fusion techniques. The comprehensive information and characteristics of targets obtained by multi-angle SAR lead to important practical values in urban target detection, target identification and classification, to list a few.

2. An integrated active–passive remote sensing sensor system is under development, aiming to provide better solutions for information acquisition of complex scenes of urban remote sensing in the near future.

10.2 New Application Fields of Urban Remote Sensing

The new application fields of urban remote sensing are introduced from seven aspects, which are earth observation service to earth observation brain, the observation of urban time-sensitive targets and events, remote sensing big data services, integration of communication, navigation and remote sensing, human observation, quantitative remote sensing and multi-factor monitoring.

Downloaded from www.worldscientific.com
by fac sciences de la terre universite annaba on 07/30/24. Re-use and distribution is strictly not permitted, except for Open Access articles.

1. From urban remote sensing earth observation data service to "earth observation brain" real-time information service.

   The original Earth Observation Satellite (EOS) System was proposed as a means to perceive the Earth, which later required human reprocessing and decision-making. What if we can combine the theoretical knowledge from brain science and cognitive science to upgrade the Earth observation Satellite System into an earth observation brain? Nowadays, various satellites (e.g., navigation satellites, remote sensing satellites and communication satellites) are just like the human eyes and ears. A system (like a brain) can be formed by integrating remote satellites, achieving intelligent processing of "eyes" and "ears" perception of the data to provide users with PNTRC functions — P (position) for location, N (navigation) for navigation route, T (time) for time, R (remote sensing) for remote sensing images, state and C (communication) for communication. The information on situational awareness generated by the earth observation "brain" can be sent to portable devices of users.

   The earth observation brain is an intelligent earth observation system that simulates brain perception and cognition processes and integrates measurement, calibration, target perception and cognition, and service users in a space-based spatial information network environment by combining knowledge from geospatial information science, computer science, data science, and brain and cognitive science (Li *et al*., 2017). In essence, the earth observation brain obtains spatial data information on Earth's surfaces through satellite constellations in the space, airships and aircraft in the air, and uses in-orbit image processing technology and on-satellite data analysis techniques to obtain useful knowledge that facilitates users' decision-making process, thus realizing real-time intelligent space-air-ground knowledge acquisition.

   A total of 200 remote sensing satellites and 300 communication satellites are expected in order to achieve global service. The service index can be as low as 5 min; that is, the required image target can be found within 5 min. The spatial resolution and navigation accuracy are expected to reach 0.5 m, and the in-orbit processing and communication time is less than 1 min before it reaches the user's cellphones. An earth observation brain can be built by developing the B2B, B2G and B2C intelligent services of air and space information and by realizing "one star with multiple uses, multi-star network, multi-network integration and intelligent services".

Downloaded from www.worldscientific.com
by fac sciences de la terre universite annaba on 07/30/24. Re-use and distribution is strictly not permitted, except for Open Access articles.

In the geospatial framework of digital cities, remote sensing data serve as an important urban spatio-temporal infrastructure that benefits the construction of smart cities, as they provide real-time information services for the city.

2. From the observation of urban surface to the observation of urban time-sensitive targets and events.

The traditional remote sensing platforms provide static remote sensing data of urban surfaces. However, cities contain a large number of pedestrians, vehicles and other moving targets. Thus, the dynamic observations and investigations of pedestrians and vehicles are of great significance to the development of cities. The static information of the ground surface acquired by the traditional remote sensing platform fails to provide the dynamic information of moving targets. The observation of moving targets requires the use of remote sensing sensors with high temporal resolution. With the rapid development of remote sensing sensors, video satellites, as well as UAVs, are able to provide urban monitoring in a dynamic manner, realizing the transition from static monitoring to dynamic monitoring of moving targets and events.

Video satellites tend to have high temporal resolution and high spatial resolution. Vehicles, ships and aircraft are the main motion targets of satellite video. The detection and tracking of moving targets based on satellite video greatly benefit the development of cities. Space-air-ground multi-platform video big data are expected to provide monitoring and early warning services for urban time-sensitive targets and events. Figure 10.1 shows the vessel detection and tracking services provided by the Jilin-1 video satellite.

Figure 10.1 Vessel detection and tracking based on Jilin-1 video satellite.

Downloaded from www.worldscientific.com
by fac sciences de la terre universite annaba on 07/30/24. Re-use and distribution is strictly not permitted, except for Open Access articles.

As an emerging type of remote sensing sensor, the UAV has become an important platform for spatial data collection given its various advantages such as high spatial resolution, real-time image transmission, low cost and high flexibility. In complex urban environments, pedestrians and vehicles are the major moving targets. UAV-based abnormal behavior detection can detect dangerous signals in the crowd in a timely manner to avoid sudden mass events. UAV platforms can also monitor the urban human, vehicle and logistics flows in real time. As shown in Figure 10.2, pedestrian detection by UAV allows real-time crowd counting. Figure 10.3 shows the UAV-based social distance index estimation, based on the real-time distance measurement between pedestrians.

3. Demand-oriented urban remote sensing big data services.

Remote sensing data belong to big data. The data are complex from spatial, temporal, multi-dimensional perspectives and contains spatial uncertainty. The expansion rate of urban remote sensing big data far exceed that of conventional transaction management type data, forming an ecological situation of big spatial data. Therefore, how to effectively fuse urban remote sensing big data and extract complementary information while eliminating redundant information is an urgent technical problem to be solved for urban remote sensing big data.

In stark contrast to the current ability to acquire high-resolution remote sensing data needed to serve from digital cities to wisdom construction, our remote sensing information processing ability is considerably limited.

Figure 10.2 Pedestrian detection based on UAV images.

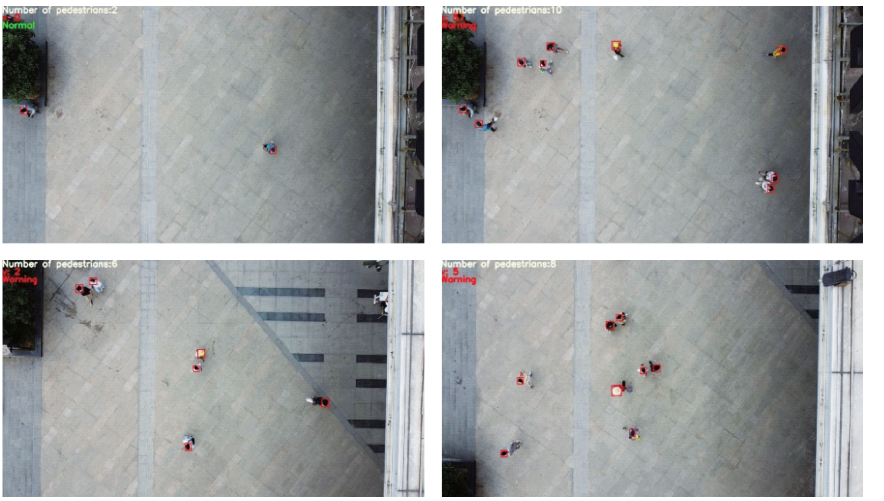

Figure 10.3 Estimation of social distance index based on UAV images.

The main bottleneck problems are that the existing remote sensing image analysis and massive data processing technologies are mainly designed for a single sensor, without considering the requirements of cooperative processing of multi-source heterogeneous remote sensing data. (i) It is difficult to realize the information extraction and unified expression of diversified remote sensing big data; (ii) it is difficult to meet the information retrieval demand of content-based multi-source heterogeneous data; and (iii) it is difficult to obtain the semantic cognition of scenes from diversified image data in an automatic manner, and the information utilization rate of remote sensing big data is low. A notable imbalance exists between remote sensing information processing technology and data acquisition capability. Such imbalance is described in the paradoxical circle of "big data, small information". Moreover, due to the large amount of accumulated data that have not been effectively utilized, the massive data require a considerable amount of storage space, leading to "data disaster". Urban remote sensing big data mining is to explore and excavate the laws of natural and social changes from urban remote sensing big data and provide auxiliary decision-making basis for various management and services.

The "spatio-temporal-spectral correlation" observation model provides a demand-oriented urban remote sensing observation approach. The multi-spectral, multi-scale, multi-angle and multi-temporal remote sensing data combined with machine learning methods mark the entrance

Downloaded from www.worldscientific.com
by fac sciences de la terre universite annaba on 07/30/24. Re-use and distribution is strictly not permitted, except for Open Access articles.

Downloaded from www.worldscientific.com
by fac sciences de la terre universite annaba on 07/30/24. Re-use and distribution is strictly not permitted, except for Open Access articles.

into the data model stage from statistical models and physical models, as urban remote sensing big data can better carry out urban surface parameter inversion and support resilient urban environment research. The data model of "large sample data set + complete parameter description ability" is used to replace the traditional physical model of "small sample data set + prior knowledge constraint". This change will certainly be a revolution of remote sensing inversion of land surface parameters in the era of remote sensing big data. Meanwhile, other types of big urban data that can serve the elements involved in urban environmental science research, such as atmosphere, vegetation, water quality, ground surface, ecology and urban socio-economic activities, can also be converted to the big data center of the city through various sensor networks. The increase of the sample knowledge and the improvement of the algorithm (e.g., the application of deep learning) lead to improved accuracy in urban monitoring, observation and analysis.

Urban remote sensing big data and spatial information are effectively integrated with hydrological data, and relevant factors reflecting the characteristics of urban subsurface production and confluence can be monitored (including the distribution of semi-permeable surface, permeable surface and impermeable surface, surface temperature, humidity and surface evaporation information). Remote sensing big data and other big data fusion can benefit in-depth urban hydrological analysis to obtain better knowledge in the hydrological processes and acquire disaster situational awareness. It is necessary to explore data fusion and data mining methods based on urban remote sensing big data and other urban big data, which can provide technical support for regular monitoring of urban socio-economic activities, feasible solutions for urban environmental sustainability monitoring and auxiliary decision-making services for enhancing urban resilience.

4. Integration of communication, navigation and remote sensing.

Under the guidance of the idea of network information system, the integrated development of communication, navigation and remote sensing can realize the integrated services of satellite remote sensing, satellite navigation, satellite communication and ground Internet and ground communication network, which can support all kinds of users in any place, any time and any terminal for fast, efficient, highly reliable and flexible access to information acquisition, high-precision positioning, navigation, timing and multimedia communication services.

To solve the application problem of the integration of communication, navigation and remote sensing using network information system, the key is to build a network connecting the existing satellite resources, and realize the barrier-free and fast transmission of all kinds of information. That is, with the integrated information network of air and ground as the backbone, all kinds of communication, navigation and remote sensing information can be accessed in the "five-in-one" of high orbit, medium orbit, low orbit, earth (sea) surface and underwater. Based on a number of ground information ports, the ground undertakes the functions of data aggregation, management, processing and distribution, application and so on, so as to construct a three-dimensional space-based information network consisting of satellites with different orbit heights and several ground-based nodes on the ground.

As shown in Figure 10.4, the fusion architecture of communication, navigation and remote sensing is based on the integrated information network of space and earth, which consists of a space-based backbone

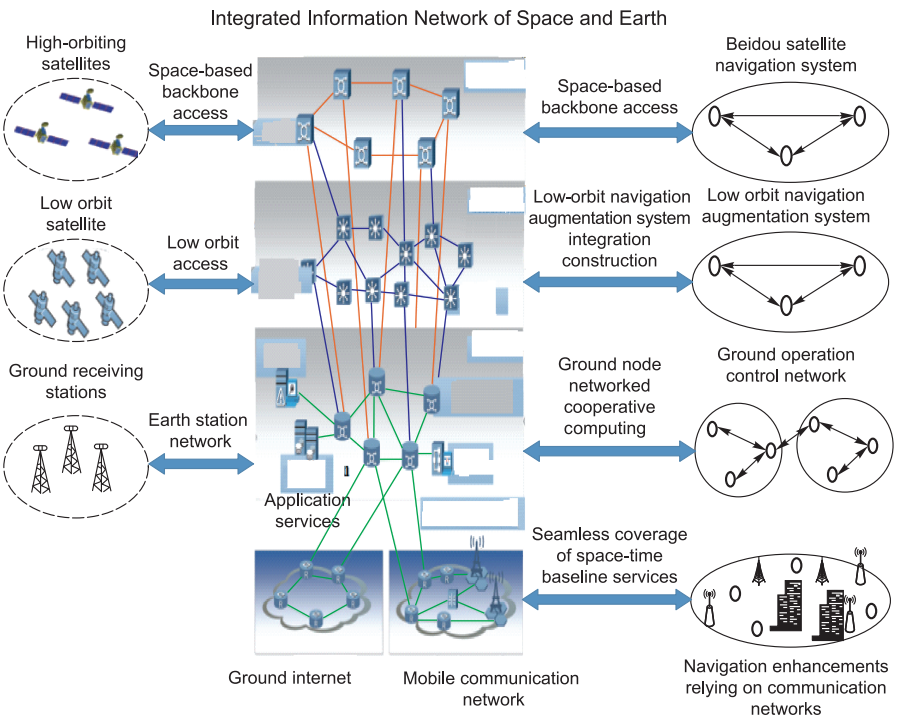

Figure 10.4 Architecture of the space–ground integrated communication and remote fusion (Zheng *et al.*, 2020).

Downloaded from www.worldscientific.com by fac sciences de la terre universite annaba on 07/30/24. Re-use and distribution is strictly not permitted, except for Open Access articles.

network, space-based access network and ground-based node network to form the foundation of the communication network covering space and earth, and the access to various communication networks is realized through the space-based inter-satellite link and the ground-based network interface.

The satellite navigation system with BeiDou as the core can access the integrated network through inter-satellite links and complete the forwarding of navigation signals with the coverage capability of the integrated information network between space and earth to achieve seamless coverage of navigation signals; low-orbit communication satellites carrying navigation augmentation payloads can achieve global coverage of navigation augmentation information. Figure 10.5 demonstrates seamless indoor and outdoor navigation providing high accuracy positioning.

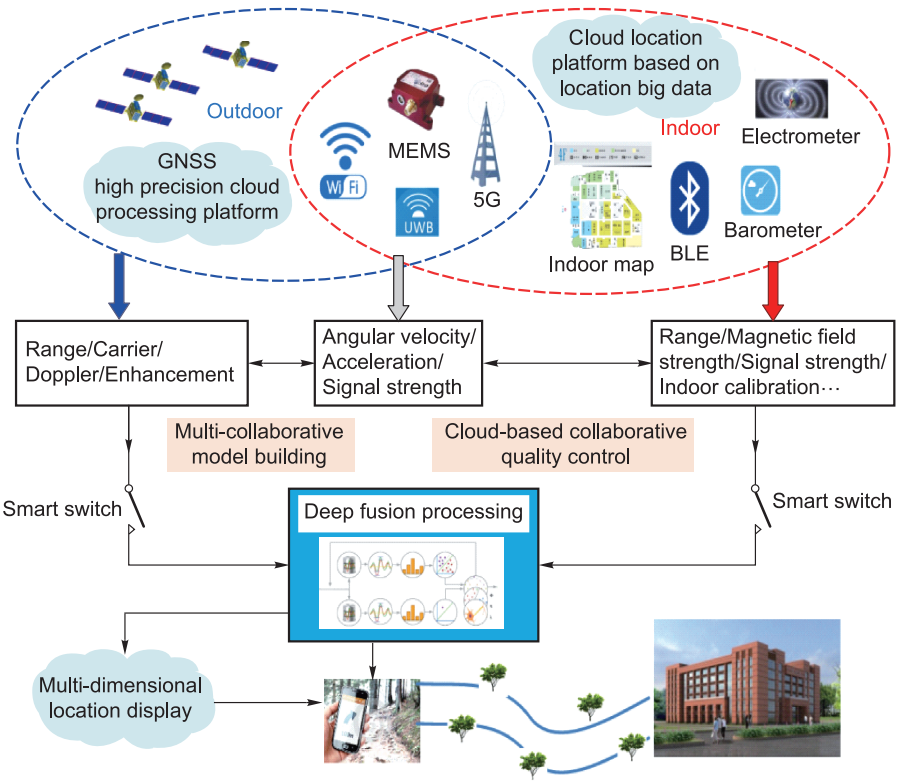

Figure 10.5 Seamless indoor–outdoor navigation architecture.
Source: Prof. Shi Chuang.

Downloaded from www.worldscientific.com
by fac sciences de la terre universite annaba on 07/30/24. Re-use and distribution is strictly not permitted, except for Open Access articles.

Downloaded from www.worldscientific.com
by fac sciences de la terre universite annaba on 07/30/24. Re-use and distribution is strictly not permitted, except for Open Access articles.

5. From Earth observation to human observation.

   We use sensors/remote sensors to detect the radiation or scattering and reflection characteristics of electromagnetic waves of objects, and the targets are extracted, judged, processed, analyzed and applied to realize the monitoring of induction telemetry and resource management on the earth's surface. In addition, based on ITS/mobile phone/social media and other carriers, the formation of social relations, spatio-temporal interaction activities, spatio-temporal movement trajectories and network activities of large-scale groups in physical and virtual space are detected. The essence of remote sensing observation on earth to observe people is the relationship between people and earth (Figure 10.6).

   Night-light remote sensing was analyzed for GDP, population, electricity energy consumption, carbon emissions, urban sprawl, urbanization and poverty. In addition, night-light remote sensing for war impact assessment reveals the spatial patterns of nighttime lights through clustering analysis of normalized multi-temporal nighttime light images to assess the human impact of the Syrian civil war. Moving from earth to human observations also includes other aspects, such as tracking urban mobility (traffic flow, pedestrian flow, etc.) and intelligent emergency platforms for traffic management (e.g. Wuhan).

6. From urban geometric remote sensing to quantitative remote sensing.

   Image correction mainly refers to radiation correction and geometric correction. Radiation correction includes sensor radiation correction, atmospheric correction, illumination correction of relic streaks and speckle determination and elimination. Geometric correction is to correct

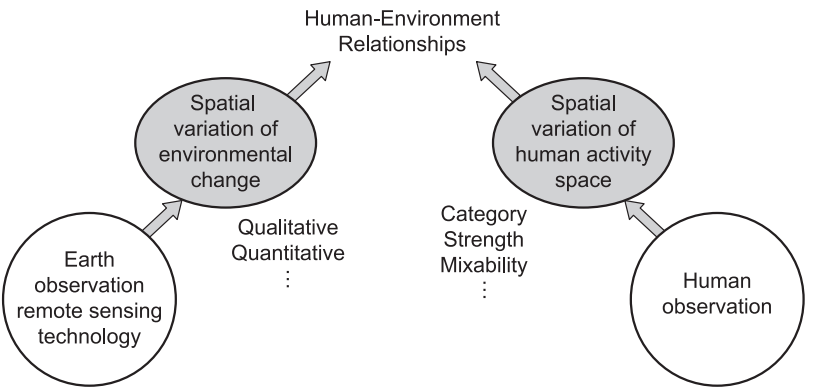

Figure 10.6 Remote sensing earth to human observation.

Downloaded from www.worldscientific.com
by fac sciences de la terre universite annaba on 07/30/24. Re-use and distribution is strictly not permitted, except for Open Access articles.

various geometric aberrations caused by the imaging process, including geometric coarse correction and geometric fine correction. Geometric coarse correction is to correct the causes of aberrations, and the satellite remote sensing data we get are generally processed by geometric coarse correction. Geometric refined correction is the geometric correction using ground control points, which is a mathematical model to describe the geometric distortion process of remote sensing images in a close way, and to determine several geometric distortion models using some corresponding points (ground control point data) between the standard image and the distorted remote sensing image. This model is then used for geometric distortion correction, which does not consider the specific causes of distortion formation, but only how to make use of the distortion model to correct the remotely sensed image. Geometric correction of remote sensing images is a prerequisite for directional remote sensing and quantitative remote sensing analysis.

Qualitative remote sensing is similar to map reading, by treating remote sensing images as special "pictures" and analyzing and processing them through methods such as computer image recognition and classification to get the knowledge we need. For example, simple land use classification, object-oriented segmentation and classification and monitoring changes are only qualitative classifications.

Quantitative remote sensing mainly refers to the study of techniques and methods for quantitative extraction of surface parameters from the electromagnetic wave signals of earth observation, which is different from the method of qualitative identification of features that relies only on empirical interpretation. The remote sensing information gives quantitative physical quantities and accurate spatial locations of surface materials in different wavelengths of electromagnetic waves. From this quantitative remote sensing information, certain geological or biological information can be quantitatively inferred or extrapolated by linking the remote sensing information to geological parameters through experimental or physical models. The physical, geographic, chemical and even biological state parameters about the target are obtained from the electromagnetic wave property parameters, so establishing some functional relationship between the measurable parameters and the target state parameters is a key step to realize the inversion of the target parameters, which we call modeling. Remote sensing models are generally classified into three types: (i) statistical models (i.e., empirical models),

Downloaded from www.worldscientific.com
by fac sciences de la terre universite annaba on 07/30/24. Re-use and distribution is strictly not permitted, except for Open Access articles.

(ii) physical models, and (iii) semi-empirical models. In addition, inversion and modeling are two different problems. Modeling is the problem of establishing a mathematical equation or a system of equations corresponding to a certain physical process, while inversion is like the problem of solving an equation or a system of equations, and obviously establishing an equation and solving an equation are two problems of different nature but closely related. The so-called inversion is based on the knowledge of the model, based on the cloud of measurable parameter values to invert the real-time state parameters of the target. To realize the inversion generally requires one to obtain a sufficient amount of information, which can be expressed in mathematical language as the number of independent equations must be equal to or greater than the number of unknown parameters.

7. From single-factor to multi-factor monitoring.

Previously, due to the limitation of remote sensing technology, the remote sensing data obtained were very limited, and the remote sensing observation of cities can often only obtain one factor or two factors, such as the vegetation status information of cities through the normalized difference vegetation index. In addition, due to the very limited research on cities, people's understanding of cities is usually described only by single-factor one-sided descriptions, which cannot provide a comprehensive and objective understanding of the changing conditions of cities.

With the rapid development of remote sensing technology and in-depth research, scholars found that the real situation of cities cannot be obtained from single factors only. So, multiple factors are used to monitor the city. Xu (2013) uses the principal component analysis technique to integrate four evaluation indexes of urban ecological environment condition, such as vegetation index, humidity component, surface temperature and building index, which can quantitatively evaluate and compare the ecological quality of cities and conveniently analyze the spatial and temporal dynamic changes. In the future, we can use the integration of air-space and space remote sensing to obtain more real-time factors to comprehensively and objectively monitor the complex urban background environment.

10.3 The Future Directions of Urban Remote Sensing

Urban remote sensing, as a multidisciplinary research field that incorporates remote sensing science and urban planning, has achieved rapid development in recent years. In the context of national new urbanization planning, ecological civilization and smart city construction, urban remote sensing faces emerging opportunities and challenges (Du, 2018). The rapid development of remote sensing data acquisition technology and the breakthrough in information processing theories and methods in the era of big data and artificial intelligence, on the other hand, provide strong support for urban remote sensing. Against such a background, opportunities, and challenges we highlight the developing trends of urban remote sensing as follows:

1. *Facing more important needs*: Urban remote sensing needs to support the needs of green, low-carbon, healthy and intelligent development of cities and the needs to dovetail with relevant national planning and key projects to investigate and solve the key problems. For example, the national new-type urbanization plan puts forward the overall planning of the urban spatial layout, promoting the appropriate mix of urban land functions and reasonably setting the normative requirements such as volume ratio, greening rate and ground penetration rate for land development and utilization in different functional areas. How to use remote sensing technology to assist the design and investigation of urban spatial function layout and calculate indicators that include volume rate, greening rate and ground penetration rate for land development and utilization requires new breakthroughs in data processing, information extraction, indicators design and model analysis.
2. *Using big data*: With the development of remote sensing data acquisition technology, multi-platform, multi-resolution and multi-observation remote sensing data are used to provide support for more objective and comprehensive investigations. In recent years, the combination of remote sensing data, social data, field observation data and statistical information has provided new developing momentum for urban remote sensing. With the development of big geographic data and big spatio-temporal data, the adoption of richer remote sensing, monitoring and surveying data is expected to become more popular. In particular, many institutions are providing more and more interpretation products. Using these remote

Downloaded from www.worldscientific.com
by fac sciences de la terre universite annaba on 07/30/24. Re-use and distribution is strictly not permitted, except for Open Access articles.

Downloaded from www.worldscientific.com
by fac sciences de la terre universite annaba on 07/30/24. Re-use and distribution is strictly not permitted, except for Open Access articles.

sensing products to carry out comprehensive analysis can greatly expand the research and application groups of urban remote sensing.

3. *Developing advanced methods*: The rapid development of remote sensing data acquisition provides abundant remote sensing images, and information processing technology is the key to extract useful information from them. On the one hand, the development of new theories and methods of artificial intelligence and machine learning (such as deep learning, migration learning and integrated learning) should be used in urban remote sensing image processing to improve the automation and intelligence of data processing while mitigating the issues of insufficient training samples and insufficient data quality. On the other hand, effective multi-source data fusion models and multiple information synthesis and analysis models need to be developed and deployed to achieve a comprehensive analysis of multi-source data and information for specific tasks. In addition, it is necessary to establish effective quantitative remote sensing models for surface parameters and develop more advanced new methods for parameter inversion in complex urban environments.
4. *Providing more comprehensive information*: Combined with the national new urbanization planning as well as other needs, urban remote sensing is expected to change from simply investigating dynamics of urban expansion and land uses to applications in social science domains, such as population estimation, energy consumption, economic analysis, environmental health evaluation, public safety and emergency management, further expanding to the ecological environment, habitat environment, thermal environment, environmental capacity, landscape ecology, ecological carrying capacity and ecological security. While promoting explanatory research on urban phenomena, patterns and functions, we need to conduct diagnostic research oriented to urban diseases, urban functions and urban evolution, further integrate the use of long-term remote sensing data to support the urban environmental health evaluation, risk prevention and control, and advance the goal of urban remote sensing to predictive and decision-making development.
5. *Achieving finer expressions*: Early urban remote sensing studies focused on extracting information that reflects urban structure, pattern and changes from remote sensing images. With the rapid development of quantitative remote sensing, quantitative description of urban ecological environment parameters based on remote sensing information has

Downloaded from www.worldscientific.com
by fac sciences de la terre universite annaba on 07/30/24. Re-use and distribution is strictly not permitted, except for Open Access articles.

become a new hotspot to realize the fine expression of geometric and physical attributes in both a qualitative and quantitative manner at different spatial resolutions. Urban remote sensing needs to provide not only thematic information in two-dimensional planes but also three-dimensional spatial expressions, such as three-dimensional urban modeling, ground subsidence analysis and geological disaster monitoring based on LiDAR, UAV remote sensing and tilt photography, to list a few. Furthermore, it is necessary to compound various geometric, physical and socio-economic information in three-dimensional space, investigate the evolutionary trends of natural processes and human activities in three-dimensional urban space and their resources and environmental responses, and realize more refined expressions of urban structures, patterns and functions.

6. *Serving a wider variety of objects*: Urban remote sensing studies should pay more attention to the connection with application objectives. In terms of objects to be investigated, besides typical cities as a research entity, urban clusters, towns and villages should also be paid more attention. In addition to the spatial scale, attention should also be paid to the temporal scale of urban remote sensing to achieve a comprehensive study of urbanization and resource environment response in terms of positioning, characterization and timing. As for service targets, emphasis should be attached to the precise docking with the needs of different urban departments and industries, providing products that can be interpreted, applied and supported for decision-making.

Questions

1. Please introduce the future directions of remote sensing sensors that can meet the needs of cities.
2. Give examples of new applications of remote sensing technology in sustainable urban development.
3. What information can real-time urban imagery services provide for emergency events in cities?
4. What role do video satellite images and night-light remote sensing images play in urban informationization?
5. Discuss the prospects of urban remote sensing applications.

References

Du P J. 2018. Progress and trends of urban remote sensing: Reading guidance for the special column on urban remote sensing. *Geography and Geo-Information Science*, 34(3): 1–4.

Li D R, Shao Z F. 2009. On the new geographic information era. *Science in China*, 39(6): 579–587.

Li D R. 2012. On Space-air-ground integrated earth observation network. *Journal of Geo-Information Science*, 14(4): 419–425.

Li D R, Shen X, Li D L, Li S X. 2017. On civil-military integrated space-based real-time information service system. *Geomatics and Information Science of Wuhan University*, 42(11): 1501–1505.

Li D R. 2016. Towards geospatial information science in of big data era. *Acta Geodaetica et Cartographica Sinica*, 45(4): 379–384.

Li D R, Li X. 2015. An overview on mining of nighttime light remote sensing. *Acta Geodaetica et Cartographica Sinica*, 44(6): 591–601.

Li D R, Wang M, Shen X, Dong Z P. 2017. From earth observation satellite to earth observation brain. *Geomatics and Information Science of Wuhan University*, 42(2): 143–149.

Li M X, John R T, Wu B F. 2010. Contributions to the global earth observation system of systems by China. *Journal of Remote Sensing*, 14(3): 571–578.

Ran D,Yin C B, Jia X. 2016. Research progress on multi-angle synthetic aperture radar imaging technology. *Journal of Equipment Academy*, 27(4): 86–92.

Xu H Q. 2013. A remote sensing urban ecological index and its application. *Acta Ecologica Sinica*, 33(24): 7853–7862.

Zheng Z Y, Xue Q H, Qiu L Y, Liu G, Li Q X. 2020. Discussion on integration application of communication navigation remote-sensing with the idea of network information system of system. *Journal of CAEIT*, 15(8): 709–714.

Downloaded from www.worldscientific.com
by fac sciences de la terre universite annaba on 07/30/24. Re-use and distribution is strictly not permitted, except for Open Access articles.

Downloaded from www.worldscientific.com
by fac sciences de la terre universite annaba on 07/30/24. Re-use and distribution is strictly not permitted, except for Open Access articles.

Index

3D change detection, 169
3D management platforms, 146
3D reconstruction, 129

A

aboveground, 206
active sensors, 3, 12
active–passive remote sensing, 222
AlexNet, 115
artificial intelligence, 234
automatic extraction, 119
automatic interpretation, 75

B

band-pass filter, 91
band-stop filter, 91
big data services, 225
building extraction, 123
building information model (BIM), 149

C

Canny method, 65
change detection, 153, 156, 158
chlorophyll, 216
classification, 167
classification datasets, 117
cloud detection, 84
collaborative observation, 5
color, 64
color infrared remote sensing, 44
comparison, 167
component replacement, 99
comprehensive information, 234
comprehensive optimization, 84
correlation coefficient, 159
crowdsourcing geographic data, 36
cultivated land, 175, 190
cyanobacteria, 216

D

deep learning, 168
dictionary learning, 103
digital aerial cameras, 32
digital three-dimensional models, 51
digital twin city, 133
direct interpretation signs, 63
downscaling methods, 211
dynamic monitoring, 179
dynamic monitoring system, 192

E

earth observation brain, 223
earth observation sensor network, 182, 184, 185
earth observation system, 28
eutrophication, 215
extraction method, 195

F

feature space, 61
filter, 101
fine 3D model, 131
finer expressions, 234

G

geological conditions, 197
global mapping project, 109
ground LiDAR, 137

H

high-pass filter, 91
high-resolution (HR), 9
homomorphic filter, 91
hue, 64
human observation, 230
hyperspectral data, 44
hyperspectral sensors, 221

I

image enhancement, 91
image fusion, 98
image interpretation, 57
image preprocessing, 83
image regression method, 160
image retrieval, 77
image segmentation, 164
impervious surface, 172, 188
InceptionNet, 115
indirect interpretation signs, 63
inertial measuring unit (IMU), 136
instance segmentation, 77
ISODATA, 110
iterative closest point (ICP), 143

K

K-means, 110

L

lake monitoring, 186
land cover and land use, 4
land cover type, 108
land cover/use, 172
level of detail (LOD), 134
lighting conditions, 53
low-pass filter, 91

M

manual tracking, 119
maximum likelihood classification, 113
MNDWI, 125
mobile mapping systems, 136
monitoring demands, 154
multi-angle SAR, 222
multi-factor monitoring, 232
multi-resolution analysis, 99
multi-spectral remote sensing, 43

N

natural resources, 185
NDWI, 125
network information system, 227
night-light, 222

O

object detection, 77
object-based change detection, 170
object-level change detection method, 164
onboard LiDAR, 135
overall accuracy, 158

P

passive sensors, 3, 12
pattern recognition, 62, 84
phycocyanin, 216
physical methods, 84
pixel-level change detection, 158
point-by-point change detection, 170
post-classification change detection, 166
practices, 172
producer accuracy, 157

Q

quality control strategy, 145
quantitative remote sensing, 230

R

radar images, 50
ratio method, 160
real scene 3D, 148
real-time high-resolution remote sensing, 32
reconstruction methods, 95

Downloaded from www.worldscientific.com
by fac sciences de la terre universite annaba on 07/30/24. Re-use and distribution is strictly not permitted, except for Open Access articles.

ResNet, 115
road extraction, 119

S

semantic segmentation, 77
semi-automatic extraction, 119
service targets, 235
shadow detection, 87, 89
shadow extraction, 89
sparse expression, 100
spatial filter enhancement, 91
spatial transformation, 91
spatial-spectral, 99
spectrum Space, 61
stereo image pair, 133
street view data, 141
super-resolution, 94, 95
supervised classification, 113
surface temperature, 48, 204

T

texture feature difference method, 162
texture reconstruction, 140
thermal infrared, 204
thermal landscape, 210
time series, 182
time-sensitive, 6
time-sensitive targets, 224
transform domain, 103

U

unmanned aerial vehicle (UAV), 14
unsupervised classification, 110
urban buildings, 38
urban change, 154
urban conditions, 194
urban ecological environment, 201
urban green space, 39
urban heat island (UHI), 202
urban lakes, 124
urban monitoring, 180
urban planning, 156, 191
urban roads, 38
urban situation monitoring, 194
urban vegetation, 204
urban water bodies, 40
user accuracy, 158

V

vehicle mobile measurement systems, 34
very high-resolution (VHR), 9
vggNet, 115
visual interpretation, 71
voluntary manner, 54

W

water bodies, 124
water radiation, 124
weighting, 103

Downloaded from www.worldscientific.com
by fac sciences de la terre universite annaba on 07/30/24. Re-use and distribution is strictly not permitted, except for Open Access articles.